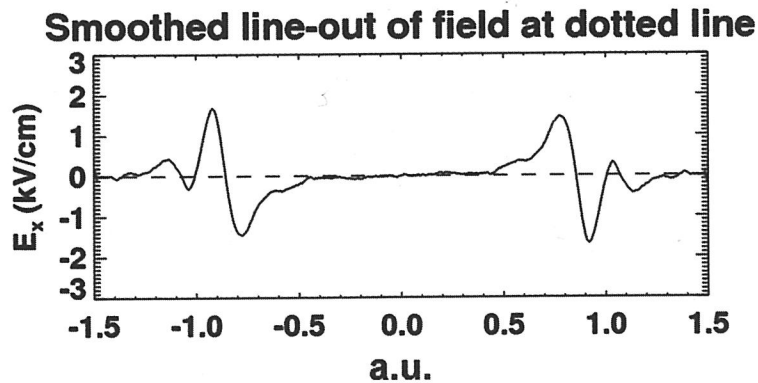
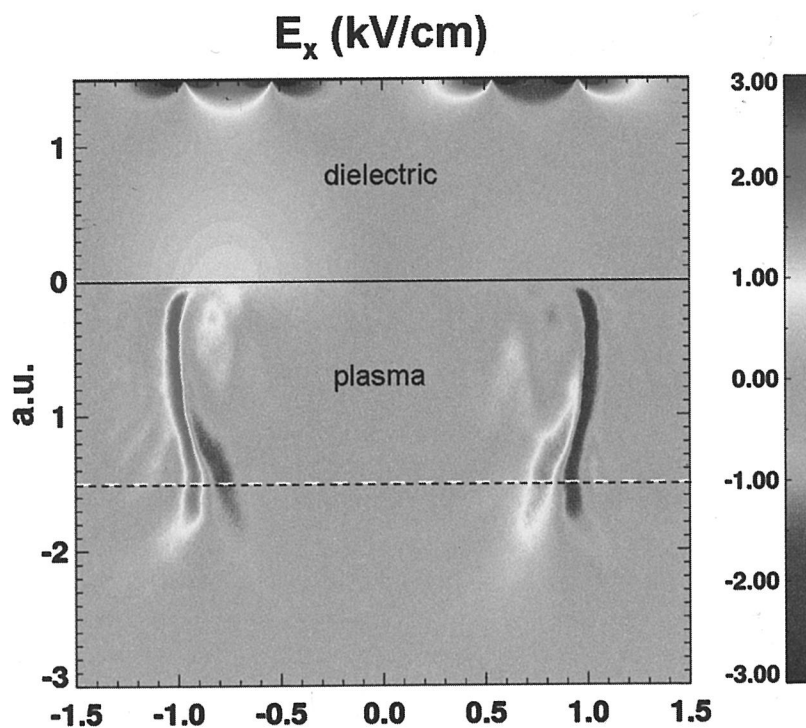


BULLETIN

OF THE AMERICAN PHYSICAL SOCIETY

62nd ANNUAL GASEOUS ELECTRONICS CONFERENCE

October 20–23, 2009
Saratoga Springs, New York



October 2009

Volume 54, No. 12

APS
physics

BULLETIN

OF THE AMERICAN PHYSICAL SOCIETY

Vol. 54, No. 12, October 2009

GEC Meeting 2009

TABLE OF CONTENTS

General Information	3
Special Sessions and Events	3
Workshop Sessions	3
GEC Sessions	3
Conference Format	4
Presentation Formats	4
GEC Student Award for Excellence	4
Registration	5
Banquet and Reception	5
Email and Other Business Services	5
Audio-Visual Equipment	5
Saratoga Springs	5
Dining Options	5
Call for Nominations for GEC General and Executive Committees	5
<i>GEC 2009 Executive Committee</i>	6
<i>Conference Secretary</i>	6
Sponsors and Exhibitors	7
Please Note	7

Epitome	8
Main Text	11
<i>Monday, October 19</i>	11
<i>Tuesday, October 20</i>	17
<i>Wednesday, October 21</i>	53
<i>Thursday, October 22</i>	64
<i>Friday, October 23</i>	94
Author Index	100
Floor Plans	At End of Issue

62nd Annual Gaseous Electronics Conference

October 20–23, 2009

Workshop on Advances in Kinetic Theory, Experiment and Modeling

October 19, 2009

Saratoga Springs, NY

GENERAL INFORMATION

Welcome to upstate New York and Saratoga Springs! You are coming to Irving Langmuir's backyard. Irving Langmuir lived, worked, and earned his Nobel laurels in nearby Schenectady 30 minutes south of Saratoga Springs. He spent much of his free time swimming, hiking, and skiing at Lake George and the Adirondack Mountains, 30 minutes north of Saratoga Springs.

The 62nd Gaseous Electronics Conference (GEC) of the American Physical Society is being held at the Saratoga Springs Hilton and Saratoga Springs City Center. The 2009 GEC will highlight current research in gaseous electronics. The conference program includes the GEC Foundation talk, several scientific special events, and several events that will commemorate the life and work of Irving Langmuir.

This year, the GEC and the accompanying workshop and events will present 51 invited talks, 153 oral and 188 poster presentations. The GEC will also give the "Student Award for Excellence" to the best student talk.

SPECIAL SESSIONS AND EVENTS

The GEC Executive Committee is pleased to announce that the GEC foundation talk will be presented by Professor David Graves of University of California, Berkeley. His talk, "When Low Temperature Plasmas Meet Surfaces" will be at 10:00 AM on Wednesday, October 21 in the Ballroom.

A one-day workshop titled "Advances in Kinetic Theory, Experiment and Modeling" will be held on Monday, October 19, 2009, one day before the start of the GEC.

The GEC has organized a special session on Plasma Aided Implantation, on Tuesday, October 20, 2009.

On Wednesday evening, October 21, 2009, the GEC will hold an offsite joint session (along with a tour and

reception) with the College of Nanoscale Science and Engineering, at the Albany Nanotech center.

Throughout the conference, you will be able to learn more about the life and work of Irving Langmuir. The Schenectady Museum will prepare an exhibition, and you will also be able to see a 60 minute documentary produced by his grandson, Roger Summerhayes. The Thursday banquet speaker, George Wise, GE historian, will give a talk titled "Irving Langmuir: Inventing Industrial Research."

Finally, the GEC is organizing two lunchtime tutorials. The first one, on Intellectual Property, hosted by Tokyo Electron, is held on Wednesday, October 21st. The second one, hosted by Tech-X Corp., will highlight their PIC code, VORPAL. This tutorial is held on Thursday, October 22nd.

WORKSHOP SESSIONS

OCTOBER 19, 2009

- | | |
|------------|--|
| Session AM | Opening Session, Role of Electron Kinetics, Swarms |
| Session BM | General Kinetic Models |
| Session CM | Data for Modeling and Modeling Example |
| Session DM | Electron Kinetics |

GEC SESSIONS

OCTOBER 20–23, 2009

- | | |
|-------------|--|
| Session EM | Reception |
| Session FT1 | Capacitively-Coupled Plasmas I |
| Session FT2 | Plasma Thrusters |
| Session FT3 | Laser Based Diagnostics at High Pressure |
| Session GT1 | Plasma Aided Implantation |
| Session GT2 | Actuators and Flow Control |

Session GT3	Low Pressure Plasma Diagnostics
Session HT1	Inductively Coupled Plasmas
Session HT2	DC, Pulsed, RF and Microwave Glows
Session HT3	Optical Diagnostics I
Session JT1	Sheaths
Session JT2	High Pressure Cold Plasmas and Arcs
Session JT3	Microplasmas and Jets
Session KTP	Poster Session I
Session LW1	Dusty and Negative Ion Plasmas
Session LW2	Atomic Data for Modeling
Session LW3	Lamps
Session MW	GEC Foundation Talk
Session NW	Business Meeting
Session PW1	Optical Diagnostics II
Session PW2	Heavy Particle Collisions with Atoms and Molecules
Session PW3	Laser Produced Plasmas Induced Breakdown and Applications of High Pressure Plasmas
Session QW	Joint GEC/CNSE Session including Reception and CNSE Tour
Session RR1	Biological and Emerging Applications of Plasma I
Session RR2	Charged Particle Molecule Collisions
Session SR1	Biological and Emerging Applications II
Session SR2	Electron and Positron Collisions with Atoms
Session SR3	Plasma-Surface Interactions
Session TR1	Materials Processing
Session TR2	Electron and Photon Interactions with Atoms and Molecules
Session TR3	Plasma Chemistry
Session URP	Poster Session II
Session VR	Banquet
Session WF1	Plasmas and Liquids
Session WF2	Electron Molecule Collisions
Session XF1	Microplasmas
Session XF2	Capacitively-Coupled Plasmas II

CONFERENCE FORMAT

Following the 61st GEC precedent, the first three days of the 62nd GEC will have three parallel sessions in Ballrooms 1, 2 & 3 of the Saratoga Hilton. The poster sessions will be held in Hall D of the adjoining City Center. For most of the conference duration (except on Monday and Tuesday morning), Hall D will also host the refreshment breaks, exhibitors, the registration desk, internet kiosk, etc.

PRESENTATION FORMATS

Papers that have been accepted for presentation are listed in the technical program. Invited papers are allotted 25 minutes, with 5 additional minutes for questions and discussion. Oral contributed presentations are allotted 12 minutes, with 3 additional minutes for questions. Poster sessions will be provided with 48" by 96" poster boards. Presenters may mount their posters anytime in the day upon which their presentation is scheduled. Poster materials must be removed at the close of the poster session.

GEC STUDENT AWARD FOR EXCELLENCE

The GEC Executive Committee will award a \$1000 prize for the best paper presentation by a student. Students must have been nominated by a professional member before being selected to present and compete for the award. Students competing for the award, in the order of their appearance in the program, are:

Jochen Waskoenig, Queens University Belfast,
 "Non-linear frequency coupling in dual radio-frequency atmospheric pressure plasmas," 9:00–9:15 AM, Tuesday, October 20, 2009, Session FT1: Capacitively-Coupled Plasmas I

Emilie Despia-Pujo, LPP - Ecole Polytechnique,
 "Global model of instabilities in low-pressure inductively coupled chlorine plasmas," 2:30–2:45 PM, Tuesday, October 20, 2009, Session HT1

Scott Wright, University of Michigan,
 "Microdischarge-based pressure sensors utilizing multiple cathodes for operation up to 1000°C," 4:00–4:15 PM, Tuesday, October 20, 2009, Session JT3

Aaron LaForge, Missouri University of Science & Technology, Rolla, Mo, "Single ionization of atomic Hydrogen by 75 keV proton impact," 2:15–2:30 PM, Wednesday, October 21, 2009, Session PW2

Joao Santos Sousa, LPGP, France, "Atmospheric pressure generation of singlet oxygen by arrays of microplasmas for DNA oxidation," 8:00–8:15 AM, Thursday, October 22, 2009, Session RR1

Caleb Nelson, University of Texas at Dallas, "Temperature impact on plasma-surface interactions in an FC plasma environment," 10:30–10:45 AM, Thursday, October 22, 2009, Session SR3

R.O. Jung, University of Wisconsin-Madison, "Electron excitation into the $Xe(5p^57p)$ configuration from the ground and $1s_5$ ($J=2$) metastable level," 11:30–11:45 AM, Thursday, October 22, 2009, Session SR2

REGISTRATION

The registration desk will be in the lobby of the Saratoga Hilton on Sunday, Monday and Tuesday morning. Thereafter, the registration desk will be in Hall D of the City Center. Registration will be available from 4:00–6:00 PM on Sunday afternoon and then beginning Monday at 7:30 AM and remaining available through most of the remainder of the conference. The on-site conference registration cost is \$450 for regular registration, \$225 for students and retirees and \$250 for a single day.

BANQUET AND RECEPTION

An opening reception will be held at 6:00 PM on Monday, October 20 in the Gallery of the Saratoga Hilton. The conference banquet will be held at 7:00 PM on Thursday, October 22nd in the Ballroom of the hotel. Tickets for the banquet are \$65 and available on-site through Tuesday Oct 20th. All conference attendees and guests are encouraged to attend.

EMAIL AND OTHER BUSINESS SERVICES

Internet access will be available in guest rooms for a fee and in the hotel business center. Services such as faxing and photocopying are also available in the hotel business center. An internet kiosk will be set up in the breaks and posters area in Hall D of the City Center.

AUDIO-VISUAL EQUIPMENT

Each conference room will be equipped with an LCD projector and laptop. If additional equipment is required, please contact the conference secretary. The laptops will accept files in Powerpoint and Acrobat formats, and read files from CD's and USB drives.

SARATOGA SPRINGS

A century ago, before the advent of air-conditioning, Saratoga Springs was the summer destination of well-to-do New Yorkers. Today it is the summer destination for the New York City Ballet, big-name music performers and their fans, and horse-racing fans. And at all times of the year, it is also the gateway to the Adirondacks Mountain and the Adirondack Park, the largest state-level protected area in the contiguous United States.

DINING OPTIONS

The Saratoga Hilton is in downtown Saratoga Springs. The downtown features restaurants, galleries, stores and bars, all within walking distance from the Saratoga Hilton.

CALL FOR NOMINATIONS FOR GEC GENERAL AND EXECUTIVE COMMITTEES

The GEC Executive Committee (ExComm) is the governing body of the GEC. It is the responsibility of the ExComm to oversee all aspects of the conference. This includes selection of meeting sites, budgetary decisions, selection of special topics and invited speakers, accepting and rejecting abstracts, and arranging of the program. The General Committee and the ExComm meet during the GEC, and the ExComm meets again during the summer to plan the program of the next GEC. There are numerous communications between members of the ExComm (usually e-mail) during the year to ensure the successful completion of their duties. We have been fortunate over the years to have a dedicated group of volunteers who have been willing to take on these very necessary roles.

The by-laws of the Gaseous Electronics Conference describe the process whereby members of the ExComm are elected. At the GEC Business Meeting (to be held on Wednesday, October 21, at 11:00 in the Ballroom), nominations are accepted for members of the GEC General Committee (GenComm).

The GenComm consists of the ExComm and six at-large members elected at the Business Meeting. The eligible voting membership of the GEC (defined as those attending the Business Meeting) elects six at-large members. The GenComm then meets to elect new members of the ExComm.

The ExComm membership consists of the Chair, Treasurer, Past-Secretary, Secretary, Secretary-elect, past or incoming Chair, and four at-large members. The Chair is a 4 year term (1 year incoming, 2 years Chair, and 1 year past-Chair), the Secretary is a 3 year term (1 year incoming, 1 year Secretary, 1 year past-Secretary), and all other ExComm members serve 2 years.

The location of future conferences is selected by the GenComm, from bids host the conference. The author of the winning bid is then elected to a 3 year term as Secretary that begins 2 years prior to the conference as Secretary-Elect. Bids to host the conference are encouraged and should be discussed with and submitted to the Chair.

The ExComm welcomes nominations, including self-nomination, for both the GenComm and the ExComm. Becoming a GenComm and/or ExComm member provides a unique opportunity to see both how the GEC is run and to influence its future direction by helping to define the programs and choosing future sites.

Please submit your nominations to the GEC Chair or any member of the ExComm. The ExComm also welcomes inquiries on hosting future GECs.

The GEC maintains a website at www.gec.org, which contains links to current and past conferences, as well as the governing Constitution and Bylaws of the conference.

GEC 2009 EXECUTIVE COMMITTEE

Bill Graham, Chair, Queens University Belfast

Klaus Bartschat, Treasurer, Drake University

Mirko Vukovic, Secretary, Tokyo Electron Ltd.

Peter Ventzek, Past-Chair, Lam Research

Pascal Chabert, Secretary-Elect, LPP,

Ecole Polytechnique

Larry Overzet, Past-Secretary, University of Texas,

Dallas

Dmitry Fursa, Curtin University

Masara Hori, Nagoya University

Eric Joseph, IBM T.J. Watson Research Center

Murtadha Khakoo, California State University

Tom Kirchner, York University

Don Madison, Missouri S&T

Thomas Miller, Boston College

Amy Wendt, University of Wisconsin-Madison

CONFERENCE SECRETARY

Mirko Vukovic

Tokyo Electron, US Holdings

255 Fuller Road, Suite 244

Albany, NY, 12203

Phone: 518-320-1948

Fax: 518-677-1664

Email: mirko.vukovicus.tel.com

GEC 2009 SPONSORS AND EXHIBITORS (TO PRINTING DATE)

Sponsors and Exhibitors allow the GEC Executive committee to provide many benefits to attendees including travel assistance and decreased registration fees for junior attendees.

The 62nd GEC has been fortunate to receive support from the following organizations (up to the time of publication.) In light of the exceptional economic downturn in 2009, the 62nd GEC is especially grateful for the continued support from the industry.

US Government agencies and laboratories:

The US Department of Energy

Sandia National Laboratories

The National Science Foundation

Company support:

Applied Materials

Novellus

Tokyo Electron

Exhibitors:

IOP Publishing

Tech X Corporation

Hidden Analytical

COMSOL Inc.

PLEASE NOTE

The APS has made every effort to provide accurate and complete information in this *Bulletin*. However, changes or corrections may occasionally be necessary and may be made without notice after the date of publication. To ensure that you receive the most up-to-date information, please check the meeting Corrigenda distributed with this *Bulletin*.

Epitome of the 62nd Gaseous Electronics Conference of the American Physical Society

7:45 MONDAY MORNING
19 OCTOBER 2009

AM **Kinetics Workshop:**
Opening Session, Role
of Electron Kinetics, Swarms
Mark Kushner, Toshiaki Makabe,
Sasa Dujko
Ballroom 1, Saratoga Hilton

10:00 MONDAY MORNING
19 OCTOBER 2009

BM **Kinetics Workshop:**
General Kinetic Models
Vladimir Kolobov, Igor
Kaganovich, Annemie Bogaerts,
Ralf Peter Brinkmann
Ballroom 1, Saratoga Hilton

13:30 MONDAY AFTERNOON
19 OCTOBER 2009

CM **Kinetics Workshop: Data for**
Modeling and Modeling Example
Stephen Buckman, Gorur Govinda
Raju, Laxminarayan Raja,
Detlef Loffhagen
Ballroom 1, Saratoga Hilton

16:00 MONDAY AFTERNOON
19 OCTOBER 2009

DM **Kinetics Workshop:**
Electron Kinetics
Steven Shannon, Chao Li,
Scott Baalrud
Ballroom 1, Saratoga Hilton

18:00 MONDAY EVENING
19 OCTOBER 2009

EM **Reception**
Gallery, Saratoga Hilton

8:00 TUESDAY MORNING
20 OCTOBER 2009

FT1 **Capacitively-Coupled Plasmas I**
Uwe Czarnetzki
Ballroom 1, Saratoga Hilton

FT2 **Plasma Thrusters**
Laxminarayan Raja
Ballroom 2, Saratoga Hilton

FT3 **Laser Based Diagnostics**
at High Pressure
Ballroom 3, Saratoga Hilton

10:00 TUESDAY MORNING
20 OCTOBER 2009

GT1 **Plasma Aided Implantation**
Michael A. Lieberman,
Mark Kushner
Ballroom 1, Saratoga Hilton

GT2 **Actuators and Flow Control**
Ballroom 2, Saratoga Hilton

GT3 **Low Pressure Plasma Diagnostics**
ChinWook Chung
Ballroom 3, Saratoga Hilton

13:30 TUESDAY AFTERNOON
20 OCTOBER 2009

HT1 **Inductively Coupled Plasmas**
Gerjan Hagelaar, Yuichi Setsuhara
Ballroom 1, Saratoga Hilton

HT2 **DC, Pulsed, RF and Microwave**
Glow
Ballroom 2, Saratoga Hilton

HT3 **Optical Diagnostics I**
Akihiro Kono, Peter Hakel
Ballroom 3, Saratoga Hilton

16:00 TUESDAY AFTERNOON
20 OCTOBER 2009

- JT1 **Sheaths**
 Ballroom 1, Saratoga Hilton
- JT2 **High Pressure Cold Plasmas
 and Arcs**
 Ballroom 2, Saratoga Hilton
- JT3 **Microplasmas and Jets**
 Ballroom 3, Saratoga Hilton

19:00 TUESDAY EVENING
20 OCTOBER 2009

- KTP **Poster Session I (7:00-9:00PM)**
 Hall D, Saratoga Springs
 City Center

8:00 WEDNESDAY MORNING
21 OCTOBER 2009

- LW1 **Dusty and Negative Ion Plasmas**
 Ballroom 1, Saratoga Hilton
- LW2 **Atomic Data for Modeling**
*Michael Brunger, Paul Johnson,
 Christopher Fontes*
 Ballroom 2, Saratoga Hilton
- LW3 **Lamps**
 Ballroom 3, Saratoga Hilton

10:00 WEDNESDAY MORNING
21 OCTOBER 2009

- MW **GEC Foundation Talk**
David Graves
 Ballroom 1-2-3, Saratoga Hilton

11:00 WEDNESDAY MORNING
21 OCTOBER 2009

- NW **Business Meeting**
 Ballroom 1-2-3, Saratoga Hilton

12:00 WEDNESDAY NOON
21 OCTOBER 2009

- 2W **Intellectual Property Tutorial**
Tug Yasar
 Whitney, Saratoga Hilton

13:30 WEDNESDAY AFTERNOON
21 OCTOBER 2009

- PW1 **Optical Diagnostics II**
Yi-Kang Pu
 Ballroom 1, Saratoga Hilton
- PW2 **Heavy Particle Collisions with
 Atoms and Molecules**
Allison Harris
 Ballroom 2, Saratoga Hilton
- PW3 **Laser Produced Plasmas Induced
 Breakdown and Applications of
 High Pressure Plasmas**
Todd Ditmire
 Ballroom 3, Saratoga Hilton

19:00 WEDNESDAY EVENING
21 OCTOBER 2009

- QW **Joint GEC/CNSE Session
 following CNSE Visit**
*Uwe Kortshagen, John Arnold,
 Magnus Bergkvist, J. Gary Eden,
 Edward M. Cupoli, Rikizo
 Hatakeyama, Timothy J. Dalton*
 NFS Auditorium, College of
 Nanoscale Science and Engineering

8:00 THURSDAY MORNING
22 OCTOBER 2009

- RR1 **Biological and Emerging
 Applications of Plasma I**
S.M. Rossnagel
 Ballroom 1, Saratoga Hilton
- RR2 **Charged Particle Molecule
 Collisions**
*Thomas Schlathoelter,
 Markus Schoeffler*
 Ballroom 2, Saratoga Hilton

10:00 THURSDAY MORNING
22 OCTOBER 2009

SR1 **Biological and Emerging Applications II**
Michael Kong
 Ballroom 1, Saratoga Hilton

SR2 **Electron and Positron Collisions with Atoms**
Danica Cvejanovic
 Ballroom 2, Saratoga Hilton

SR3 **Plasma-Surface Interactions**
Matthew Goeckner
 Ballroom 3, Saratoga Hilton

12:00 THURSDAY NOON
22 OCTOBER 2009

3R **VORPAL Tutorial**
Ed Case
 Whitney, Saratoga Hilton

13:30 THURSDAY AFTERNOON
22 OCTOBER 2009

TR1 **Materials Processing**
Jane P. Chang, Song-Yun Kang
 Ballroom 1, Saratoga Hilton

TR2 **Electron and Photon Interactions with Atoms and Molecules**
Bruno deHarak
 Ballroom 2, Saratoga Hilton

TR3 **Plasma Chemistry**
Biswa Ganguly, Masaharu Shiratani
 Ballroom 3, Saratoga Hilton

16:00 THURSDAY AFTERNOON
22 OCTOBER 2009

URP **Poster Session II (4:00-6:00PM)**
 Hall D, Saratoga Springs
 City Center

19:00 THURSDAY EVENING
22 OCTOBER 2009

VR **Banquet**
George Wise
 Ballroom 1-2-3, Saratoga Hilton

8:00 FRIDAY MORNING
23 OCTOBER 2009

WF1 **Plasmas and Liquids**
 Ballroom 1, Saratoga Hilton

WF2 **Electron Molecule Collisions**
Timothy Gay, Ann Orel
 Ballroom 2, Saratoga Hilton

10:00 FRIDAY MORNING
23 OCTOBER 2009

XF1 **Microplasmas**
J. Gary Eden
 Ballroom 1, Saratoga Hilton

XF2 **Capacitively-Coupled Plasmas II**
 Ballroom 2, Saratoga Hilton

SESSION AM: KINETICS WORKSHOP: OPENING SESSION, ROLE OF ELECTRON KINETICS, SWARMS
Monday Morning, 19 October 2009; Ballroom 1, Saratoga Hilton at 7:45; Zoran Petrovic, Institute of Physics, presiding

7:45

AM 1 Introduction and Welcome

8:15

AM 2 Controlling electron energy distributions for plasma technologies.*

MARK KUSHNER, *University of Michigan*

The basic function of low temperature plasmas in society benefiting technologies is to channel power into specific modes of atoms and molecules to excite desired states or produce specified radicals. This functionality ultimately depends on the ability to craft an electron energy distribution (EED) to match cross sections. Given electric fields, frequencies, gas mixtures and pressures, predicting EEDs and excitation rates can in large part be reliably done. The inverse problem, specifying the conditions that produce a given EED, is less well understood. Early strategies to craft EEDs include adjusting gas mixtures, such as the rare gas-Hg mixtures in fluorescent lamps, and externally sustained discharges, such as electron-beam sustained plasmas for molecular lasers. More recent strategies include spiker-sustainer circuitry which produces desired EEDs in non-self-sustained plasmas; and adjusting frequency in capacitively coupled plasmas. In this talk, past strategies for customizing EEDs in low pressure plasmas will be reviewed and prospects for improved control of plasma kinetics will be discussed using results from 2-dimensional computer models.

*Work supported by Semiconductor Research Corp., Tokyo Electron Ltd., Applied Materials Inc. and Department of Energy.

8:45

AM 3 Incorporating swarm data into plasma models and plasma surface interactions.

TOSHIAKI MAKABE, *Keio University*

Since the mid-1980s, modeling of non-equilibrium plasmas in a collisional region driven at radio frequency has been developed at pressure greater than \sim Pa. The collisional plasma has distinct characteristics induced by a quantum property of each of feed gas molecules through collisions with electrons or heavy particles. That is, there exists a proper function caused by chemically active radicals, negative-ions, and radiations based on a molecular quantum structure through short-range interactions mainly with electrons. This differs from high-density, collisionless plasma controlled by the long-range Coulomb interaction. The quantum property in the form of the collision cross section is the first essential through swarm parameters in order to investigate the collisional plasma structure and to predict the function. These structure and function, of course, appear under a self-organized spatiotemporal distribution of electrons and positive ions subject to electromagnetic theory, i.e., bulk-plasma and ion-sheath. In a plasma interacting with a surface, the flux, energy and angle of particles incident on a surface are basic quantities. It will be helpful to learn the limits of the swarm data in a quasi-equilibrium situation and to find a way out of the difficulty, when we predict the collisional plasma, the function, and related surface processes. In this talk we will discuss some of these experiences in the case of space and time varying radiofrequency plasma and the micro/nano-surface processes. This work is partly supported by Global-COE program in Keio University, granted by MEXT Japan.

9:15

AM 4 Recent advances in the kinetic theory of hydrodynamic and non-hydrodynamic charged particle swarms in gases.*

SASA DUJKO, *School of Engineering and Physical Sciences, James Cook University*

Recent developments in plasma processing technology using non-equilibrium plasma discharges have led to a resurgence of interest in the fundamental kinetic theory of charged particles in gases. In this work we outline the current status of both the hydrodynamic and non-hydrodynamic kinetic theory of charged particle swarms with the goal of reconciling the plasma and swarm literature. Three fundamental issues: (i) the temporal and spatial non-local behavior; (ii) the effects of magnetic fields and field orientations on the transport properties, and (iii) the duality in transport coefficients arising from non-conservative collisions (attachment/ionization), are discussed for electrons for certain model and real gases. Much research has been devoted to interpretation of transport data obtained under different experimental arrangements and their proper use in plasma models. Two complimentary techniques are employed: a multi term solution of Boltzmann's equation and Monte Carlo simulation technique, both adapted to consider the time-dependent hydrodynamic and steady state non-hydrodynamic conditions. New and significant numerical results are presented to highlight the rich and diverse range of kinetic phenomena observed in varying configurations of time-dependent electric and magnetic fields. We systematically study the origin and mechanisms for such phenomena, their sometimes paradoxical manifestations and possible physical implications which arise from their explicit inclusion into plasma models.

*The Australian Research Council and the MNTR project 141025.

SESSION BM: KINETICS WORKSHOP: GENERAL KINETIC MODELS

Monday Morning, 19 October 2009; Ballroom 1, Saratoga Hilton at 10:00; Mirko Vukovic, Tokyo Electron America, presiding

10:00**BM 1 Kinetic Modeling of Complex Plasma Equipment.**VLADIMIR KOLOBOV, *CFD Research Corporation*

Kinetics of electrons, ions and neutrals play an important role in industrial plasma systems. These systems are often characterized by complex geometries and require 2D and 3D models of varying resolution for realistic simulations of relevant processes. We will describe hybrid approach to modeling such systems using kinetic models for electrons and hydrodynamic (fluid) models for ion and neutral components. Kinetic modeling of electrons involves numerical solution of the Boltzmann equation or its derivatives. Using two-term spherical harmonics expansion in velocity space, the 6D Boltzmann equation can be reduced to a 4D Fokker-Planck (F-P) equation for the Electron Energy Distribution Function (EEDF), which depends of electron energy and spatial position. This equation can be conveniently solved using total electron energy (kinetic + potential) for a wide range of discharge conditions. Further simplifications are possible in the two extremes. At high gas pressures one can solve local F-P equation for the EEDF as a function of local electric field and plasma composition, and generate Look-Up-Tables (LUTs) for electron transport coefficients and rates of electron induced chemical reactions to be used in fluid models for electrons. The other extreme corresponds to a "nonlocal approach" where the EEDF depend solely on the total energy and does to depend explicitly on spatial position. We will describe the architecture of the F-P solver for electrons in the CFD-ACE+ software package and its application to simulations of low-pressure ICP, CCP, and DC discharges, as well as high-pressure micro-plasmas. The peculiarities of the EEDF formation in these systems, and the importance of nonlocal kinetic effects for the formation of striations, electron heating and macro-plasma parameters will be discussed. We will also discuss the limitations of the F-P approach and our current efforts to develop a full Boltzmann solver for simulations of fast (runaway) electrons and nonlocal electromagnetic phenomena in low-pressure RF discharges.

10:30**BM 2 Nonlocal collisionless and collisional electron transport in low temperature plasmas.***

IGOR KAGANOVICH,

The purpose of the talk is to describe recent advances in nonlocal electron kinetics in low-pressure plasmas. A distinctive property of partially ionized plasmas is that such plasmas are always in a non-equilibrium state: the electrons are not in thermal equilibrium with the neutral species and ions, and the electrons are also not in thermodynamic equilibrium within their own ensemble, which results in a significant departure of the electron velocity distribution function from a Maxwellian. These non-equilibrium conditions provide considerable freedom to choose optimal plasma parameters for applications, which make gas discharge plasmas remarkable tools for a variety of plasma applications, including plasma processing, discharge lighting, plasma propulsion, particle beam sources, and nanotechnology. Typical phenomena in such discharges include nonlocal electron kinetics, nonlocal electrodynamics with collisionless electron heating, and nonlinear processes in the sheaths and in the bounded plasmas. Significant progress in understanding the interaction of electromagnetic fields with real bounded plasma created by this field and the resulting changes in the structure of the applied electromagnetic field has been one of the major achievements of the last decade in this area of research [1-3]. We show on specific examples that this progress was made possible by synergy between full scale particle-in-cell simulations, analytical models, and experiments. In collaboration with Y. Raitsev, A.V. Khrabrov, Princeton Plasma Physics Laboratory, Princeton, NJ, USA; V.I. Demidov, UES, Inc., 4401 Dayton-Xenia Rd., Beavercreek, OH 45322, USA and AFRL, Wright-Patterson AFB, OH 45433, USA; and D. Sydorenko, University of Alberta, Edmonton, Canada. [1] D. Sydorenko, A. Smolyakov, I. Kaganovich, and Y. Raitsev, *IEEE Trans. Plasma Science* **34**, 895 (2006); *Phys. Plasmas* **13**, 014501 (2006); **14** 013508 (2007); **15**, 053506 (2008). [2] I. D. Kaganovich, Y. Raitsev, D. Sydorenko, and A. Smolyakov, *Phys. Plasmas* **14**, 057104 (2007). [3] V.I. Demidov, C.A. DeJoseph, and A.A. Kudryavtsev, *Phys. Rev. Lett.* **95**, 215002 (2005); V.I. Demidov, C.A. DeJoseph, J. Blessington, and M.E. Koepke, *Europhysics News*, **38**, 21 (2007).

*This work was supported by AFOSR through STTR contract.

11:00

BM 3 Modeling of low-temperature plasmas: some case studies of different modeling approaches.ANNEMIE BOGAERTS, *University of Antwerp*

In this talk, some examples will be given of different modeling approaches, used in our group. Special attention will be put on input data, needed for the models. As an example of fluid modeling, we will illustrate the detailed plasma chemistry in a DBD used for gas conversion purposes. In this model, a large number of different species (various molecules, radicals and ions, besides the electrons) are included, which can all react with each other. For all these species, transport coefficients need to be defined, as well as reaction (sticking) probabilities at the walls. Moreover, energy-dependent cross sections and thermal rate coefficients have to be defined for all the electron reactions and the heavy particle reactions, respectively. These data are typically not available for the more exotic plasma species, so that certain assumptions have to be made. The second example is for particle-in-cell – Monte Carlo collisions simulations, developed for magnetron discharges in argon/oxygen and argon/nitrogen gas mixtures, used for the reactive sputter-deposition of metal oxide and nitride layers. In this modeling approach, the behavior of the electrons, the various ions and energetic neutrals is described by Newton's laws, and their collisions are treated by the Monte Carlo procedure. Again, energy-dependent cross sections for the various collisions are required. The last example is for hybrid Monte Carlo – fluid modeling, based on the HPEM code developed by Kushner and coworkers. It is applied to an ICP in Ar/Cl₂/O₂, used for Si etching. Besides the plasma behavior, also the etching (and deposition) process is described, for which a large number of data (etch and sticking probabilities and sputter yields) are required. We try to obtain accurate values for these data by molecular dynamics simulations. Results of the latter simulation method will also be presented.

11:30

BM 4 The Linearized Kinetic Equation – A Functional Analytic Approach.*RALF PETER BRINKMANN, *Ruhr-University Bochum, Theoretical Electrical Engineering*

Kinetic models of plasma phenomena are difficult to address for two reasons. They i) are given as systems of nonlinear coupled integro-differential equations, and ii) involve generally six-dimensional distribution functions $f(\mathbf{r}, \mathbf{v}, t)$. In situations which can be addressed in a linear regime, the first difficulty disappears, but the second one still poses considerable practical problems. This contribution presents an abstract approach to linearized kinetic theory which employs the methods of functional analysis. A kinetic electron equation with elastic electron-neutral interaction is studied in the electrostatic approximation. Under certain boundary conditions, a nonlinear functional, the kinetic free energy, exists which has the properties of a Lyapunov functional. In the linear regime, the functional becomes a quadratic form which motivates the definition of a bilinear scalar product, turning the space of all distribution functions into a Hilbert space. The linearized kinetic equation can then be described in terms of dynamical operators with well-defined properties. Abstract solutions can be constructed which have mathematically plausible properties. As an example, the formalism is applied to the example of the multipole resonance probe (MRP). Under the assumption of a Maxwellian background distribution, the kinetic model of that diagnostics device is compared to a previously investigated fluid model.

*Support from the Federal Ministry of Education and Research is gratefully acknowledged.

SESSION CM: KINETICS WORKSHOP: DATA FOR MODELING AND MODELING EXAMPLE

Monday Afternoon, 19 October 2009; Ballroom 1, Saratoga Hilton at 13:30; Mark Kushner, University of Michigan, presiding

13:30

CM 1 Electron scattering data as the basis for kinetic models – what can we realistically provide, and how?*STEPHEN BUCKMAN, *CAMS, Australian National University*

It is unlikely that anyone would dispute the important role that the availability of accurate data can play in the modeling and simulation of low temperature plasmas. Fundamental measurements of collision processes, from the relatively simple (eg. elastic scattering) to the complex (eg. molecular dissociation) are critical to developing an understanding of discharge and plasma behaviour. While there has been a healthy relationship between the data users and data gatherers at meetings such as GEC for many years, there are often misunderstandings about the capabilities that reside in each of these areas, and how best to maintain and strengthen the communication between them. This paper will attempt to summarise those electron-driven processes that are accessible, in a quantitative sense, in modern scattering experiments. Advances in treating reactive and excited species will also be discussed, as will the potential to push our measurement technologies further. An inescapable conclusion is that the collision community can best contribute through a strategic alliance between experiment and theory. Theory should be benchmarked against experiment for those processes and targets that are accessible, and used wisely for those processes where experiment cannot contribute.

*Supported by the Australian Research Council.

14:00

CM 2 A New Scaling Law of Resonance in Total Scattering Cross Section in Gases.GORUR GOVINDA RAJU, *University of Windsor*

Electrical discharges in gases continue to be an active area of research because of industrial applications such as power systems, environmental clean up, laser technology, semiconductor fabrication etc. A fundamental knowledge of electron-gas neutral interaction is indispensable and, the total scattering cross section is one of the quantities that have been measured extensively. The energy dependence of the total cross sections shows peaks or resonance processes that are operative in the collision process. These peaks and the energies at which they occur are shown to satisfy a broad relationship involving the polarizability and the dipole moment of the target particle. Data on 62 target particles belonging to the following species are analyzed. (Eq 1) Rare gas atoms (Eq 2) Di-atomic molecules with combinations of polar, non-polar, attaching, and non-attaching properties Poly-atomic molecules with combinations of polar, non-polar, attaching, and non-attaching properties. Methods of improving the newly identified scaling law and possible application have been identified. 1 INTRODUCTION: Data on electron-neutral interactions are one of the most fundamental in the study of gaseous electronics and an immense literature, both experimental and theoretical, has become available since about the year 1920. [1-5]. In view of the central role which these data play in all facets of gas discharges and plasma science, it is felt that a critical review of available data is timely, mainly for the community of high voltage engineers and industries connected with plasma science in general. The electron-neutral interaction, often referred to as scattering in the scientific literature, is quantified by using the quantity called the total scattering cross section (Q_T , m^2). In the literature on cross section, total cross section and total scattering cross section are terms used synonymously and we follow the same practice. A definition may be found in reference [1]. This paper concerns scaling of total cross section of gases at resonance energy and the electron energy at which resonance occurs. The meaning of resonance is briefly explained in the following section. Here, we use the term scaling to relate the two quantities mentioned, namely, the resonance energy and the total cross section at that energy. Consistent with the definition of scaling, if the law proposed holds, one of the two quantities mentioned above may be calculated if the other is known. Such a method is very useful in gas discharge modeling and calculation of breakdown voltages, as more fully explained in the later section of the paper. 2 DESCRIPTION OF RESONANCE: A brief description of resonance phenomena in several types of target particles, viz., atomic, poly atomic, polar, non-polar phenomena are presented. 3 PREVIOUS SCALING LAWS: A common representation of a given characteristic with as few adjustable parameters as possible is generally known as the scaling law. The Paschen curve for breakdown voltage is such a familiar scaling law. With reference to cross sections several attempts have been made to obtain a scaling law, with varying degree of success. If the cross section-energy curve is qualitatively similar without having sharp peaks and oscillations, moderately successful scaling laws may be devised. For example, the ionization cross section- energy curves for most gases follow a general pattern. Several published scaling laws are discussed. 4 A NEW SCALING LAW AND DISCUSSION: In this work the author has compiled the resonance details for more than 60 gases that include the range from simple atoms to complex molecules that are polyatomic, dipolar, electron-attaching and isomers. The target particles exhibit a number of distinct features, as far as their total cross section variation with electron energy is concerned as already explained.

14:30

CM 3 Data needs for plasma modeling.LAXMINARAYAN RAJA, *The University of Texas at Austin*

Plasma discharge phenomena are governed by a complex interplay between electromagnetic field phenomena, gas-phase non-equilibrium chemistry, gas-phase species transport, and interactions of the gas species with surfaces including surface chemistry. A wide hierarchy of models is used to represent discharge phenomena. These models are essentially approximations to the Maxwell's equations coupled to the species Boltzmann equation or moments of the Boltzmann equation, with additional model representations for surface interactions. This talk will highlight the data needs to complete the model description of the plasma. Data requirements for species collision cross sections, species transport properties, reactive gas-phase chemistry, surface phenomena including secondary electron emission and surface chemistry will be discussed. Sources of this data ranging from experimental measurements to *ab initio* calculations will be described. Finally, dependence of solution accuracy of the plasma models on the uncertainty in the input data will be illustrated through examples.

15:00

CM 4 Kinetic modeling of gas discharges.DETLEF LOFFHAGEN, *INP Greifswald, Felix-Hausdorff-Str. 2, 17489 Greifswald, Germany*

Numerical modeling of gas discharge plasmas has gained growing importance for the basic understanding of plasma processes and dynamics as well as for the optimization of discharge parameters in plasma applications and the design of plasma reactors. Different modeling approaches are commonly utilized to describe theoretically the behavior of gas discharges. The present contribution focuses on modeling and analysis of non-isothermal plasmas by means of time- and space-dependent hybrid methods combining a hydrodynamic description of the plasma species with the solution of the inhomogeneous Boltzmann equation of the electrons. Recent progress in such hybrid modeling is reported and illustrated by means of results of the analysis of the spatiotemporal behavior of spatially one-dimensional glow discharge plasmas. The results make the pronounced nonlocal characteristics of the electrons understandable. The analysis demonstrates as well the applicability and the limits of current models. Perspectives of kinetic modeling are discussed.

SESSION DM: KINETICS WORKSHOP: ELECTRON KINETICS

Monday Afternoon, 19 October 2009; Ballroom 1, Saratoga Hilton at 16:00; Laxminarajan Raja, University of Texas at Austin, presiding

16:00

DM 1 Accurate reconstruction of non-Maxwellian electron energy distribution functions.*STEVEN SHANNON, *North Carolina State University*

Low temperature plasmas, particularly those used for materials processing, are likely to have electron energy distribution functions (EEDF's) that are non-Maxwellian. Analysis of Langmuir probe voltage-current (VI) characteristics using the Druyvesteyn relationship has provided researchers with a means of obtaining these distributions to study phenomena in areas ranging from plasma chemistry to RF heating. Two aspects of obtaining non-Maxwellian EEDF's with Langmuir probes are reviewed. The first is how to address the ill-posed nature of the integral Druyvesteyn problem to obtain an accurate representation of the actual EEDF. The second is how to incorporate non-Maxwellian distributions into more advanced probe models, specifically models that account for conditions where the bias sheath on a Langmuir probe approaches the physical extent of the probe itself, commonly referred to as the thick sheath approximation. In collaboration with Ahmed Elsaghir, North Carolina State University.

*This work is supported by the State of North Carolina and the NC General Assembly.

16:30

DM 2 3D hybrid simulations for run-away electrons from streamers.CHAO LI, *Centrum Wiskunde and Informatica, 1098XG Amsterdam*

X-ray and gamma ray bursts with quantum energies from hundreds of eV to tens of MeV have been observed in lightning and in long sparks in laboratory. In the lab, hard X-rays are observed during the streamer-leader phase. Therefore the generation of very energetic run-away electrons in streamers has to be investigated, and the consecutive generation of energetic photons through Bremsstrahlung. Following the precise electron energy distribution in the high field region of the streamer head requires a Monte Carlo approach. MC is also suited to study streamer branching triggered by particle fluctuations or streamer inception from few electrons. But a long streamer demands enormous computational power and storage while so-called super-particle methods create numerical artifacts. Fluid approximations, on the other hand, are computationally efficient in regions with large particle densities like the interior of a streamer finger. Therefore a hybrid model that couples fluid and particle model in suitable regions has been developed. The coupling needs a consistent description of the electron dynamics in particle and fluid model, especially in their buffer region. The consistency of the transport coefficients is studied both for swarms and for planar fronts. The fluid model has to be extended to include the non-local effects at the streamer ionization front. The 3D hybrid model can simulate long streamers while following the electron motion at the most active region. The correct prediction of run-away electrons requires reliable cross sections and differential cross sections, which is lacking in the energy range from tens of keV to MeV. We investigate the generation of run-away electrons and present how keV electrons are produced in a growing streamer. The work was performed together with U. Ebert, W. Hundsdorfer, W. Brok and J.J.A.M. van der Mullen.

17:00

DM 3 Kinetic Theory of Instability-Enhanced Collisional Effects.*SCOTT BAALRUD, *University of Wisconsin-Madison*

A generalization of the Lenard-Balescu collision operator is derived which accounts for the scattering of particles by instability amplified fluctuations that originate from the thermal motion of discrete particles (in contrast to evoking a fluctuation level externally, as is done in quasilinear kinetic theory) [1]. Emphasis is placed on plasmas with convective instabilities. It is shown that an instability-enhanced collective response results which can be the primary mechanism for scattering particles, being orders of magnitude more frequent than conventional Coulomb collisions, even though the fluctuations are in a linear growth phase. The resulting collision operator is shown to obey conservation laws (energy, momentum, and density), Galilean invariance, and the Boltzmann \mathcal{H} -theorem. It has the property that Maxwellian is the unique equilibrium distribution function; again in contrast to weak turbulence or quasilinear theories. Instability-enhanced collisional effects can dominate the physics of low-temperature plasmas. For example, this theory has been applied to two outstanding problems: Langmuir's paradox [2] and determining Bohm's criterion for plasmas with multiple ion species. Langmuir's paradox is a measurement of anomalous electron scattering rapidly establishing a Maxwellian distribution in gas discharges with low temperature and pressure. This may be explained by instability-enhanced scattering in the plasma-boundary transition region (presheath) where convective ion-acoustic instabilities are excited. Bohm's criterion for multiple ion species is a single condition that the ion fluid speeds must obey at the sheath edge; but it is insufficient to determine the speed of individual species. It is shown that an instability-enhanced collisional friction, due to streaming instabilities in the presheath, determines this criterion.

[1] S.D. Baalrud, J.D. Callen, and C.C. Hegna, *Phys. Plasmas* **15**, 092111 (2008).

[2] S.D. Baalrud, J.D. Callen, and C.C. Hegna, *Phys. Rev. Lett.* (to appear June 2009); preprint UW-CPTC 09-4 at www.cptc.wisc.edu.

*This material is based upon work supported under a NSF Graduate Research Fellowship and by U.S. DoE Grant No. DE-FG02-86ER53218.

SESSION FT1: CAPACITIVELY-COUPLED PLASMAS I

Tuesday Morning, 20 October 2009; Ballroom 1, Saratoga Hilton at 8:00; Amy Wendt, University of Wisconsin, presiding

Invited Papers

8:00

FT1 1 The electrical asymmetry effect in capacitive discharges.UWE CZARNETZKI, *Institute for Plasma and Atomic Physics, Ruhr-University Bochum, 44780 Bochum, Germany*

One of the major demands in plasma processing has always been the independent control of ion energy and ion flux. Dual-frequency capacitive discharges with one low and one typically an order of magnitude higher frequency are one of the concepts presently applied in industry. However, recent investigations have shown that there is in fact a coupling between the two frequency components that limits independent control by the two RF powers. Here, a novel concept is introduced based on the electrical asymmetry effect (EAE) that provides simple and stable control of ion energy and flux in an almost ideally independent way [1]. Also here two RF frequencies are applied but with the second frequency being exactly the second harmonic of the first and with a fixed but controllable phase. This phase is the control parameter for the ion energy that changes approximately linearly with the phase. Geometrically symmetric discharges can be made effectively asymmetric with one electrode showing a higher sheath potential than the other. Choosing the proper phase allows then to reverse the situation or to make the discharge symmetric. In geometrically asymmetric discharges the wall potential can be raised or lowered. When tuning the phase, the flux stays approximately constant and its absolute value can be set with the RF amplitudes. The concept of the EAE is developed and analyzed by 1) an analytical model, 2) a hydrodynamic and Monte-Carlo (MC) simulation, 3) a self consistent PIC/MC simulation, and 4) an experimental verification in a laboratory experiment. All four approaches show excellent agreement and confirm the above advantages. The technique has found successful application already in an industrial reactor for large area solar cell production (Leybold Optics). Compared to the standard single frequency case at 13.56 MHz the silicon deposition rate was easily more than doubled and the homogeneity improved. [1] Brian G. Heil, U. Czarnetzki, R. P. Brinkmann, T. Mussenbrock, *JPhysD: Appl. Phys.* 42, 165202 (2008)

Contributed Papers

8:30

FT1 2 Experimental investigations of the Electrical Asymmetry Effect*

JULIAN SCHULZE, EDMUND SCHUENDEL, DIRK LUGGENHOELSCHER, UWE CZARNETZKI, *Ruhr-University Bochum* ZOLTAN DONKO, *Hungarian Academy for Science* In 2008 a method to generate a variable DC self bias even in geometrically symmetric capacitively coupled radio frequency (CCRF) discharges was proposed theoretically [1]. If the discharge is operated at a fundamental frequency and its second harmonic, it has been predicted that the resulting DC self bias can be adjusted by the phase angle between the applied voltage harmonics. A PIC simulation demonstrated that this Electrical Asymmetry Effect (EAE) allows separate control of the energy and flux of ions at the electrode surfaces. Here the EAE and the related separate control of ion energy and flux is investigated experimentally in a geometrically symmetric CCRF discharge operated at 13.56 MHz and 27.12 MHz with variable phase shift between the harmonics in argon at different pressures. The DC self bias, the energy as well as the flux of ions at the grounded electrode are measured. The experimental results verify the theoretical predictions and show that ion energy and flux can be controlled separately. The EAE is optimized by choosing low and high frequency voltage amplitudes that yield the strongest relative DC self bias. [1] Heil B G et al. 2008 *J. Phys. D* 41 165202

*Funding: DFG (GRK1051) and Hungarian Fund for Scientific Research

8:45

FT1 3 Dual-frequency capacitive radiofrequency discharges: Effect of low-frequency power on electron density and flux*

JEAN-PAUL BOOTH, GARRETT CURLEY, *LPN DRAGANA MARIC, Institute of Physics, Zemun, Serbia* JEROME BREDIN, PASCAL CHABERT, *LPP* Dual-frequency capacitively-coupled etch reactors using Ar/fluorocarbon/O₂ mixtures are widely employed for etching of dielectric films for integrated circuit manufacture. We have measured the ion flux to the wall and the center electron density (using a microwave hairpin resonator) as a function of 2 and 27 MHz power (W₂ and W₂₇) in a modified industrial etch reactor. In Ar/O₂ discharges both flux and density increase progressively with both W₂ and W₂₇, and the flux/density ratio remains constant, in accordance with simple electropositive transport theory. The high plasma densities observed can be attributed to the large secondary electron emission coefficient of oxidized Si. In Ar/C₄F₈/O₂ mixtures flux and density are again increased by both W₂ and W₂₇. However, the electron density is much lower, and the ratio flux/density is not constant, reaching very high values for high W₂/W₂₇ ratios. The reasons for this will be discussed in terms of negative ion production and plasma chemistry.

*We thank Lam Foundation for financial support.

9:00

FT1 4 Non-linear frequency coupling in dual radio-frequency atmospheric pressure plasmas*

JOCHEN WASKOENIG, TIMO GANS, *Centre for Plasma Physics, Queens University Belfast, BT7 1NN Belfast, Northern Ireland, UK* Dual frequency operation provides additional control over power coupling and ionization mechanisms in radio-frequency driven atmospheric pressure plasmas. The tailored electron dynamics allows manipulation of mode

transitions and plasma chemistry. Numerical simulations, benchmarked against experiments using phase resolved optical emission spectroscopy, reveal that plasma ionization, and associated mode transitions, are governed through frequency coupling in the dynamics of the plasma boundary sheath. Ionization in low-power mode is determined by the non-linear coupling of electron heating and the momentary local plasma density. Ionization in high-power mode is driven by electron avalanches during phases of transient high electric fields within the boundary sheath. The transition between these distinctly different modes is controlled by the total voltage of both frequency components. Under certain conditions it is observed that plasmas operated in helium with small admixtures of oxygen can contain significant densities of negative ions influencing the sheath dynamics and creating transient double layers.

*Support: Science and Innovation Award by EPSRC.

9:15

FT1 5 EEDf of the DC+RF Hybrid Etcher: Simulation and Measurement LEE CHEN, LIN XU, MERRITT FUNK, *Tokyo Electron America* The DC+RF Hybrid is a RF-capacitively coupled plasma etcher with RF applied to the wafer electrode and a high-negative DC voltage on the opposite electrode 3cm away. Secondary electrons from the DC electrode are accelerated by sheath and form ballistic electrons. Gridded energy analyzers are placed behind the RF electrode for EEDf measurements. Experiment's pressure-range varies from 30mt to 70mt with DC-voltage up to -1kV. EEDf reveals, (1) Maxwellian bulk, (2) ballistic electrons with energy corresponding to the applied DC-voltage, (3) a continuum from Maxwellian to the ballistic electron peak, (4) middle-energy electrons with distinct energy-peak. Measured EEDf qualitatively agree with PIC numerical experiments. The energy of the distinct middle-energy peak seems to depend on the sheath thickness and varies from $\sim 40\text{eV}$ to 300eV . While ballistic electrons' finite collisions contribute to the continuum, other non-negligible channel such as Landau-damped e^- -beam plasma waves, should be considered. The distinct middle-energy peak could be resulted from Landau damping of a strong plasma wave of a specific wave number. The energy range of middle-energy peak is favorable in sustaining ionization, rendering the necessity of heating the Maxwellian bulk for a similar level of ionization.

SESSION FT2: PLASMA THRUSTERS

Tuesday Morning, 20 October 2009

Ballroom 2, Saratoga Hilton at 8:00

Ane Aanesland, CNRS - Ecole Polytechnique, presiding

Contributed Papers

8:00

FT2 1 Optical Measurement of a Microwave-excited Miniature Plasma Source for Micro Propulsion YOSHINORI TAKAO, TAKESHI TAKAHASHI, SHUNSUKE KITANISHI, KOJI ERIGUCHI, KOUICHI ONO, *Department of Aeronautics and Astronautics, Kyoto University* Reducing the scale of propulsion systems is of critical importance for microspacecraft. This paper is concerned with an application of microplasmas to a microthruster. The microthruster consists of a cylindrical micro-

plasma source 10 mm in length and 1.5 mm in inner diameter and a conical Laval micronozzle 1.0 mm in length with a throat diameter of 0.2 mm. The microplasma source produces hot Ar plasmas by 2 - 11 GHz microwaves in the pressure range from 5 to 50 kPa at input powers below 6 W; and the micronozzle converts such high thermal energy into directional kinetic energy as a supersonic jet. The gas/rotational temperature and the plasma electron density were measured by adding a small amount of N_2 and H_2 , respectively, and then fitting the experimental data to theoretical calculations. Plasma diagnostics showed that the electron density and rotational temperature obtained were $10^{19} - 10^{20} \text{ m}^{-3}$ and 700 - 1000 K, respectively, in the range of Ar gas flow rate from 10 to 70 sccm at input powers of 3 and 6 W.

8:15

FT2 2 Particle-in-cell simulation for the acceleration channel of a Hall thruster* HAE JUNE LEE, *Pusan National University*

The Hall electric thruster is an electric propulsion device that allows a high specific impulse compared with chemical thrusters, and thus is very useful for a small satellite. A two-dimensional particle-in-cell simulation with Monte-Carlo Collision (MCC) has been developed to investigate the discharge in the acceleration channel of a stationary plasma thruster. The dynamics of electrons and ions under the magnetic field are calculated at the time scale of electrons. Xenon neutrals are injected from the hall in the anode and experience elastic, excitation, and ionization collisions with electrons and are scattered by ions. These collisions are simulated by using an MCC model. The neutral particle motion is coupled with the plasma dynamics in the simulation. Investigated are the effects of magnetic field profiles, gas pressure, electron current density, and the applied voltage. The simulation method for the external circuit equation is also discussed.

*Supported by a Korea Research Foundation grant funded by the Korean Government (Ministry of Education & Human Resources Development (MOEHRD), KRF-2007-331-D00182.

8:30

FT2 3 Effects of the cathode electron emission on transient phenomena in magnetized thruster discharge* YEVGENY RAITSES, JEFFREY B. PARKER, NATHANIEL J. FISCH, *Princeton Plasma Physics Laboratory*

Large-amplitude, low-frequency, discharge current oscillations invariably occur in the Hall thruster discharge. These discharges are characterized by magnetized electrons and unmagnetized ions. The oscillations are thought to result from various ionization mechanisms [1]. A rotating potential perturbation, called a spoke, is observed to propagate in the $\mathbf{E} \times \mathbf{B}$ direction for certain magnetic field topologies of the thruster discharge, including both cylindrical and annular configurations [2, 3]. We show that increasing the cathode electron emission curiously suppresses both the rotating spoke and the low frequency oscillations. This effect correlates with a change in the local V-I characteristics of the plasma discharge. In particular, in the regime with the enhanced electron emission, there are no plasma regions with negative differential resistance, which are normally observed for the self-sustained operation of the thruster discharge. [1] S. Barral and E. Ahedo, *Phys. Rev. E* **79**, 046401 (2009). [2] G. S. Janes and R. S. Lowder, *Phys. Fluids* **9**, 1115 (1966). [3] Y. Raitses, A. Smirnov and N. J. Fisch, *Phys. Plasmas* **16**, 057106 (2009).

*This work was supported by the AFOSR and the US DOE under contract No. DE-AC02-09CH11466.

8:45

FT2 4 Electrode Polarity Effects in Direct Current Glow Discharges for Supersonic Flow Control SHANKAR MAHADEVAN, LAXMINARAYAN RAJA, *The University of Texas at Austin* Computational simulations of air glow discharge plasma in the presence of supersonic flow are presented. The glow discharge model is based on a self-consistent, multi-species, continuum description of the plasma. A finite-rate air chemistry model with 11 species is validated against experiments from the literature at $p=600$ mTorr. The validated air plasma model is then used to study the effect of the surface plasma on $M=3$ supersonic flow at freestream pressure 18 Torr and the corresponding effects of the

flow on the discharge structure. The Navier-Stokes equations are solved on the entire computational domain, and the plasma equations are solved on a smaller subdomain consistent with the typical length-scale of the glow discharge. Results indicate that O^- can have comparable concentrations to electrons in the pressure range 1-20 Torr. The peak gas temperature from the computations is found to be 1420 K with the surface plasma alone, and 1180 K in the presence of supersonic flow with the cathode located upstream with respect to the flow direction. The effect of placing the cathode downstream with respect to the flow direction is investigated. For the case studied in this work the primary effect of the plasma on the supersonic flow is volumetric heating.

Invited Papers

9:00

FT2 5 Microdischarge plasma thrusters for small satellite propulsion.
LAXMINARAYAN RAJA, *The University of Texas at Austin*

Small satellites weighing less than 100 kg are gaining importance in the defense and commercial satellite community owing to advantages of low costs to build and operate, simplicity of design, rapid integration and testing, formation flying, and multi-vehicle operations. The principal challenge in the design and development of small satellite subsystems is the severe mass, volume, and power constraints posed by the overall size of the satellite. The propulsion system in particular is hard to down scale and as such poses a major stumbling block for small satellite technology. Microdischarge-based miniaturized plasma thrusters are potentially a novel solution to this problem. In its most basic form a microdischarge plasma thruster is a simple extension of a cold gas micronozzle propulsion device, where a direct or alternating current microdischarge is used to preheat the gas stream to improve to specific impulse of the device. We study a prototypical thruster device using a detailed, self-consistent coupled plasma and fluid flow computational model. The model describes the microdischarge power deposition, plasma dynamics, gas-phase chemical kinetics, coupling of the plasma phenomena with high-speed flow, and overall propulsion system performance. Unique computational challenges associated with microdischarge modeling in the presence of high-speed flows are addressed. Compared to a cold gas micronozzle, a significant increase in specific impulse (50 to 100 %) is obtained from the power deposition in the diverging supersonic section of the thruster nozzle. The microdischarge remains mostly confined inside the micronozzle and operates in an abnormal glow discharge regime. Gas heating, primarily due to ion Joule heating, is found to have a strong influence on the overall discharge behavior. The study provides a validation of the concept as simple and effective approach to realizing a relatively high-specific impulse thruster device at small geometric scales.

SESSION FT3: LASER BASED DIAGNOSTICS AT HIGH PRESSURE

Tuesday Morning, 20 October 2009

Ballroom 3, Saratoga Hilton at 8:00

Timo Gans, Queen's University Belfast, presiding

8:00

FT3 1 Dynamics of dielectric barrier discharge in non-uniform gas composition investigated by laser spectroscopic measurements KEIICHIRO URABE, *Department of Electronic Science and Engineering, Kyoto University* YOSUKE ITO, JOON-YOUNG CHOI, OSAMU SAKAI, KUNIHIDE TACHIBANA, It is well known that stable and glow dielectric barrier discharge (DBD) at atmospheric pressure is observed using helium gas and AC high voltage of kHz-order frequency. We have investigated the discharge mechanisms of DBDs from a view point of the spatiotemporal distributions of excited species measured by laser spectroscopic methods. In this presentation, we will show convincing arguments about the discharge model of the DBD especially having the non-uniformity of gas composition. As a DBD plasma source for atmospheric pressure processes, we have investigated an atmospheric pressure plasma jet (APPJ) using helium gas flow in ambient air, and this plasma source can be regarded as

the DBD near the boundary interface of helium gas and ambient air. In this APPJ, we observed spatiotemporal distributions of excited species density inside the helium gas channel, using laser absorption spectroscopy and laser induced fluorescence, to measure the densities of helium metastable atom (2^3S_1 state) and nitrogen ion ($X^2\Sigma_g^+$ state) respectively. To study the influence of nitrogen gas contamination on the discharge profile of DBD, we have also applied CO_2 -laser heterodyne interferometry to measure the special distribution of electron density in parallel-plate DBD.

8:15

FT3 2 Electric field measurements in near-atmospheric pressure nitrogen and air based on a four-wave mixing scheme SARAH MUELLER, *Institute for Plasma and Atomic Physics, Ruhr-Universitaet Bochum* TSUYOHITO ITO, *Frontier Research Base for Young Researchers, Osaka University* KAZUNOBU KOBAYASHI, *Center for Atomic and Molecular Technologies, Osaka University* DIRK LUGGENHOELSCHER, UWE CZARNETZKI, *Institute for Plasma and Atomic Physics, Ruhr-Universitaet Bochum* SATOSHI HAMAGUCHI, *Center for Atomic and Molecular Technologies, Osaka University* Electric field induced coherent Raman scattering (E-CRS) measurement is a promising technique for measuring electric fields in high-pressure environments and was first demonstrated with hydrogen molecules. In this study, we have demonstrated electric field mea-

measurements by using nitrogen molecules. Two pulsed ns laser beams (532 nm and 607 nm) are employed for the measurement. In nitrogen molecules those two laser beams together with the electric field induce a coherent IR signal at a wavelength of 4.29 μm . In our current experimental setup, the minimum detectable field strength in open air is about 100 Vmm^{-1} , which is sufficiently small compared with the average field present in typical microdischarges. No further knowledge of other gas/plasma parameters such as the nitrogen density is required for the measurement. Further details on the techniques as well as measurement results in microdischarges will be presented.

8:30

FT3 3 Argon microplasma diagnostics by diode laser absorption NAOTO MIURA, JUN XUE, JEFFREY HOPWOOD, *Tufts University* Argon kinetic gas temperature and line integrated resonance state ($1s_4$) density in argon microplasma at 1-760 Torr were estimated by diode laser absorption. A 900 MHz microstrip split ring resonator (MSRR) was used as the microplasma generator. An argon atomic transition at 810.4 nm ($1s_4-2p_7$) was chosen as the absorption line. The wavelength of a single-mode laser diode was tuned by changing the diode case temperature. The absorption line was scanned by modulating the laser driving current. The laser output was collimated and passed through a 0.5 mm hole drilled between the MSRR electrodes where the microplasma was sustained. The absorption profile was fit with a Voigt function. The gas temperature was estimated from the broadening, and the line integrated density of the argon resonance state ($1s_4$) was obtained from the integral of the absorption profile. The line integrated densities of argon $1s_4$ were $1.7 \times 10^{15} \text{ m}^{-3} \text{ m}$ at 1 Torr and $1.4 \times 10^{15} \text{ m}^{-3} \text{ m}$ at 760 Torr with 1W of input power. The visually observed length of plasma decreased from 1 cm at 1 Torr to a few hundred microns at 760 Torr. The measured gas temperature increased from 350 K at 1 Torr to 750 K at 760 Torr. The microplasma was also simulated using a fluid model, which will be compared with experimental measurements.

8:45

FT3 4 Dissociation profiles of oxygen in a capacitively coupled atmospheric pressure discharge NIKOLAS KNAKE, DANIEL SCHRÖDER, VOLKER SCHULZ-VON DER GATHEN, JÖRG WINTER, *Ruhr-Universität, Bochum* The creation of atomic oxygen in a capacitively coupled jet type discharge is investigated using spatially resolved xenon calibrated TALIF and OES. The discharge is a planar jet type 13.56MHz rf device of $1 \times 1 \text{ mm}^2$ discharge cross section and an electrode length of 40 mm using a 1.4 slm helium base gas flow containing a small amount of molecular oxygen being dissociated in the discharge. The spatial build up of the dissociation profiles along the first few millimeters of the discharge channel is investigated as well as the inter electrode distribution. Studies on the variation of transmitter power, gas flux and gas mixture were performed in the plasma itself, the effluent and the transition area from plasma to effluent. To get an insight into the production and destruction processes of the oxygen molecules, it is a prerequisite to understand the atomic density build up in the plasma and the decay especially inside the transition region between core plasma and effluent. Even several milli-

meters outside the discharge in the effluent atomic oxygen can be found with densities up to some 10^{14} cm^{-3} . This project is supported by the DFG in the framework of "FOR1123," "SCHU-2353/1," and the "Research School der Ruhr-Universität Bochum."

9:00

FT3 5 Determination of Absolute Number Densities of OH Radicals in an Atmospheric Microwave Plasma Jet Using Cavity Ringdown Spectroscopy* CHUJI WANG, NIMISHA SRIVASTAVA, *Mississippi State University* THEODORE S. DIBBLE, *State University of New York College of Environmental Science and Forestry* MSU TEAM,†SUNY-ESF COLLABORATION, Identification and quantification of reactive plasma species in the downstream part of an atmospheric plasma jet remain less explored; and how far a reactive species can exist in the downstream and its formation mechanism remain little known. The objective of this work was to employ the UV-cavity ringdown spectroscopy technique to explore how far OH radicals can exist in the downstream zone of a small-scale (3 - 12 mm) atmospheric argon microwave plasma jet. We report on observation of the OH radicals existing in far downstream of the plasma jet column. The "far" downstream is characterized by the ratio of the distance from the jet orifice to the length of the jet column. In this work, the far downstream is referred to as the location, where the ratio is > 3 . Absolute number densities of the OH radicals in the far downstream part as well as in the jet column were measured. Discussion of the source of the OH radicals is also given.

*Supported by National Science Foundation, grant # CTS-0626302.

†cw175@msstate.edu

9:15

FT3 6 Collective Thomson Scattering Diagnostics of Laser Produced Plasmas for EUV Light Sources KENTARO TOMITA, YASUHISA HYAKUTA, KOTA OHARA, KIICHIRO UCHINO, *Kyushu University* UCHINO LABORATORY TEAM, Extreme ultraviolet (EUV) lights are going to be used for semiconductor lithography after the 32 nm half-pitch technology node. For EUV light sources, high density (electron density $n_e = 10^{24} - 10^{26} \text{ m}^{-3}$) and high temperature (electron temperature $T_e = 10 - 30 \text{ eV}$) plasmas should be generated using Xe or Sn atoms. In order to produce required EUV lights efficiently, plasma parameters such as n_e , T_e and averaged ionic charge \bar{Z} should be optimized. We have tried to apply the LTS measurement to EUV plasmas. When we use a visible laser as a probing laser, the LTS spectra from the EUV plasmas are in the collective regime. The spectrum of the collective Thomson scattering consists of an ion term and an electron term. Taking account of the strong background radiation from the plasma, we determined to measure the ion term, for which we could expect enough SN ratios against the background radiation. One problem to measure the ion term is that the spectral resolution of 10 pm is needed, and the other problem is that the intense wall-scattered laser lights easily overwhelm the ion spectra. In order to overcome these problems, we constructed a newly designed LTS measurement system whose spectral resolution and stray light rejection were enough to resolve fine feature of the ion term.

SESSION GT1: PLASMA AIDED IMPLANTATION

Tuesday Morning, 20 October 2009; Ballroom 1, Saratoga Hilton at 10:00; Svetlana Radovanov, Varian Semiconductor, presiding

Invited Papers

10:00

GT1 1 Sheath dynamics and energetic particle distributions on substrates.MICHAEL A. LIEBERMAN, *UC Berkeley*

The energy and angular distributions (EAD's) of energetic particles arriving at a substrate determine crucial plasma processing characteristics; thus knowledge and control of the EAD's are vital for nanoelectronics design and fabrication during scale-down to the ultimate 4–6 nm transistor gate lengths over the next 15 years. We review the history and state-of-the-art of measurements, simulations, and analyses of ion, fast neutral, and ballistic electron EAD's. Ion measurements have been made using electrostatic energy analyzers, cylindrical mirror analyzers, and retarding grid analyzers, often now coupled with quadrupole mass spectrometers to compare different ions in the same discharge. The state-of-the-art for capacitive rf sheaths has advanced greatly since the first observation of a bi-modal ion energy distribution (IED) over 50 years ago. More recently, measurement techniques and models have been developed to determine fast neutral distributions. Monte Carlo, and particle-in-cell simulations with Monte Carlo collisions (PIC-MCC) have been used to study IED's since the late 1980's. Recently, PIC-MCC simulations were used to obtain ballistic electron EAD's. Analytical models of the IED for collisionless rf sheaths have emphasized the role of τ_i/τ_{rf} , the ratio of ion transit time across the sheath to rf period, with separate models for the low and high frequency regimes. Various simplifications and bridging models now exist. For collisional rf sheaths, the important role of λ_i/s , the ratio of ion-neutral mean free path to sheath width, in modifying the collisionless bi-modal IED was demonstrated in the early 1990's. Surface charging effects on insulating substrates are important for low frequency rf discharges or for pulsed transient sheaths; the latter are found during plasma ion implantation processes. Analytical models of the IED for plasma ion implantation have been extended to insulating surfaces and compared with experimental results.

10:30

GT1 2 Multi-frequency, finite-wavelength and dc-augmentation effects in large area capacitive sources.*MARK KUSHNER, *University of Michigan*

The scaling of high frequency, multi-frequency capacitively coupled plasmas (CCPs) to large areas has many challenges. It has been well established that electromagnetic (EM) effects become increasingly more important as the frequency of excitation increases while the diameter of the substrate also increases. The complexity of the system increases with the addition of dc-augmentation. Although much has been learned about EM effects, scaling laws are difficult to develop because the discharge characteristics are functions of the frequency dependence of the conductivity, the response of the electron energy distribution (EED) to the electric fields that penetrate into the plasma, the geometry of the reactor, gas mixture, pressure and dc augmentation power. In the case of multi-frequency excitation, the coupling of low and high frequencies through surface waves and through the bulk plasma is also an issue. In this talk we will discuss results from a computational investigation of multi- and high- frequency (up to 200 MHz) excitation of CCPs having diameters up to 450 mm, with and without dc augmentation. The model used in this study includes a full time-domain solution of Maxwell's equations that enables investigation of coupling between frequencies. A Monte Carlo simulation is used to predict EEDs as a function of position and ion energy distributions to the substrate. Gas mixtures (e.g., Ar and Ar/CF₄), pressures (10 mTorr to 100 mTorr) and geometry (gap size) are investigated. Methods to minimize EM effects will be discussed by using variable conductivity and shaped electrodes; and segmented electrodes in which the electrical path from the generator to any point in the plasma is made as consistent as possible.

*Work supported by Semiconductor Research Corp., Tokyo Electron, Applied Materials and Department of Energy.

Contributed Papers

11:00

GT1 3 Self-Regulation Plasma Doping for 2D and 3D devices

BUNJI MIZUNO, *Ultimate Junction Technologies Inc.* UJT LAB TEAM, Plasma Doping has been industrialized for DRAM application. On the other hand, for 3D application, conformal and shallow doping for tri-gate and side-wall doping for fins are required to form junctions on the side-walls. This requirement is quite difficult to be realized by conventional ion implantation (II) or cluster II. Plasma doping (PD) has been proposed as a candidate for

this requirement. Relatively better conformality was achieved such as the ratio of the top to the side resistivity of fin is 1.4 by PD and 1.08 by VPD or ALD. In addition, sputter erosion for fins was the most significant issue in case of PD. We have been proposed SRPD as a technique to solve the less conformality of II and the less controllability of conventional PD, VPD and ALD. We present New Self-Regulation Plasma Doping (nSRPD) with B₂H₆/He plasma that has been developed to provide precisely controllable ultra-shallow junctions for planar FET and conformal junctions for 3D structures. Manufacturing level of process controlla-

bility ($< 1\%$ on dose) and advantage on the devices of nSRPD has been achieved with FinFETs and planar pMOSFETs. This nSRPD has been developed on commercially available and production worthy plasma platform.

11:15

GT1 4 Advanced Dopant Profile Control for Plasma Doping Processes LUDOVIC GODET, VSEA SHU QIN, *Micron Technology, Inc.* ZIWEI FANG, G.D. PAPASOULIOTIS, TIMOTHY MILLER, VIKRAM SINGH, SVETLANA RADOVANOV, VSEA After intense research and development of plasma doping systems, successful application in low energy ion implantation has been demonstrated. Plasma doping enables new fabrication options for advanced CMOS and non-planar devices. Understanding plasma-surface interactions during plasma implantation is critical for successful development of new applications. During plasma immersion ion implantation, ionized species present in the plasma are extracted and implanted into the wafer, and, in addition, many other physical mechanisms, such as deposition, etching and sputtering, are competing in parallel. The dopant profile into the substrate results from contributions of all these mechanisms. By optimizing plasma composition and balancing deposition, etching and sputtering of the implanted surface, the dopant profile can be modified from typical surface peaked to retrograde/Gaussian profile. In this study, we report on the dopant profile optimization using ion mass spectrometry.

11:30

GT1 5 One-Step, Non-Contact Pattern Transfer by Direct-Current Plasma Immersion Ion Implantation DIXON T.K. KWOK, PAUL K. CHU, *City University of Hong Kong* A one-step non-contact pattern transferring method is demonstrated. Clear non-identical images with well-defined boundaries are simultaneously transferred to a substrate by -15 kV plasma immersion ion implantation through a patterned metal mask. The metal mask is 6 cm away from the substrate and no lens system is necessary for the pattern transfer. To avoid diversification of compensating ions, the electric field must be smoothed out by the fine mesh overlapping on top of the metal mask. Complex patterns with micrometer size line-widths can be transferred onto a silicon wafer by placing the metal masks 4 mm away from the wafer. Scanning electron microscopy (SEM) discloses that by negatively biasing the metal mask, ions coming from a hole with a diameter of 200 micrometers in the mask can be confined to a smaller region of 100 micrometers. The ion focusing effect is confirmed by two-dimensional multiple grid particle-in-cell (PIC) simulation.

11:45

GT1 6 Transport Coefficients for Electrons in BF₃ ZORAN L.J. PETROVIC, ZELJKA NIKITOVIC, *Institute of Physics OLIVERA SASIC, Faculty of Transport and Traffic Engineering ZORAN RASPOPOVIC, VLADIMIR STOJANOVIC, Institute of Physics SVETLANA RADOVANOV, Varian Semiconductor Equipment Associates* We use the available cross section data [1] for electron impact on BF₃ supplemented by newly calculated cross sections for total scattering, electronic excitation and ionization [2]. Monte Carlo simulation was applied to perform calculations of transport coefficients as well as rate coefficients in DC and RF electric fields. Since BF₃ has a high threshold for attachment a presence of some of the F or F₂ radicals would affect the prop-

erties of plasma significantly. Thus we have supplemented the cross section set by the cross section data for the two radicals and made calculations for different abundances. In addition calculations in crossed electric and magnetic (ExB) fields have been made together with calculations for time resolved coefficients ($E(t) \times B(t)$). We discuss the differences between the original and new cross section set and try to discuss how these will affect the operation of discharges used for ion implantation. [1] S. Biagi, 2005 unpublished. [2] M. Vranic, J. Varhambia, M. Radmilovic, J. Tennyson, Z. Lj. Petrovic 2009 to be published.

SESSION GT2: ACTUATORS AND FLOW CONTROL
Tuesday Morning, 20 October 2009
Ballroom 2, Saratoga Hilton at 10:00
David Smith, General Electric, presiding

10:00

GT2 1 Thrust Enhancing Designs for single DBD Plasma Actuators SONG GUO, UWE KORTSHAGEN, *University of Minnesota* Dielectric Barrier Discharge (DBD) plasma actuator can be used for the separation control of the air foil applications, whose performance is directly related to the thrust which is generated during the discharge. To obtain more efficient performance, designs which can produce more thrust than the conventional single DBD plasma actuator were made by exploring the asymmetry of the discharge and introducing a semi-conductive layer on the top of the dielectric surface. Direct thrust measurement proved that the new designs can increase the thrust by 70% compared to the traditional plasma actuator, when operated on the same input voltage and discharge frequency. Measurement also showed evidence that by increasing the conductivity of the semi-conductive layer, the thrust will increase.

10:15

GT2 2 Experimental investigations of a simple DBD-based flow actuator YACINE BABOU, ANNA-ELODIE KERLO, SEBASTIEN PARIS, *The von Karman Institute for Fluid Dynamics* Optical, electrical and effectiveness measurements of a single dielectric-barrier discharge (DBD)-based flow actuator operating in ambient quiescent air will be presented. actuator is constituted by two thin alumina foil electrodes asymmetrically displayed on both sides of a dielectric (MACOR) plate (~ 50 cm²) and powered by an AC sinus high frequency (~ 10 kHz) high voltage (~ 10 kV peak-peak). The experiments were done for a wide range of configurations and operating conditions. The current in the electrical circuit is constituted of a periodic contribution and of short pulses of few ns related to streamers propagation. Thermodynamic state was characterized by means of conventional optical emission spectroscopy technique. A typical gas temperature of 295 K is obtained with the N₂ second positive system rotational bands, whereas vibrational temperature is about 2500 K. The induced flow velocity and the produced thrust were gauged by means of simple techniques and are respectively of order 1 m/s and 0.1 g. Unsteady operations and applications to realistic situations will be presented.

10:30

GT2 3 Separation control using plasma actuator: Simulation of plasma actuator* MEENAKSHI MAMUNURU, DOUGLAS ERNIE, TERRY SIMON, UWE KORTSHAGEN, *University of Minnesota* We have simulated dielectric barrier discharge in atmospheric pressure air on a two dimensional domain approximating the plasma actuator geometry. The applied voltage to the exposed electrode is a nanosecond range Gaussian pulse with amplitude of 3.5 kV. When a positive pulse was applied, the plasma was intense. A higher thrust was obtained in the downstream direction. When a negative pulse was applied, a weaker plasma and smaller thrust in the opposite direction were seen. The charge accumulation on the dielectric, and the streamer formation process were seen to be drastically different for both the cases. The component of thrust acting perpendicularly down on the actuator surface was seen to be larger than the force in parallel direction for both discharges. We have examined the importance of including photoionization in the air chemistry. A thin semi-conducting layer on the dielectric would drain the charge after a discharge cycle and prevent the occurrence of a reverse discharge, and enhance the time averaged thrust in the downstream direction. We have included a thin conducting layer on the dielectric in our simulations and obtained preliminary results.

*This work was supported by NASA Cooperative Agreement NNX07AB94A.

10:45

GT2 4 Simulations of Thermal Phenomena in Nanosecond Pulsed Plasma Discharged in Supersonic Flows DOUG BREDEN, LAXMINARAYAN RAJA, *University of Texas, Austin* The use of nanosecond repetitively pulsed plasmas to ignite and sustain ignition and combustion in supersonic flows has shown promise in recent years. While it is known that radicals produced by the plasma are the primary drivers for enhancing combustion, there is some uncertainty concerning whether radical production is due primarily to electron-impact dissociation or thermal dissociation. We use a self-consistent, multi-species plasma solver is coupled with a compressible Navier-Stokes fluid solver to simulate the temperature field and radical number densities for an H_2-O_2 mixture and pure argon. Temperature increases of $\sim 100-1000$ K occur in the cathode near-field region for both mixtures where the electron temperature peaks at ~ 40 eV in H_2-O_2 and ~ 20 eV in argon for voltages of -1000 V and -400 V respectively. Radical production of O, H and OH is observed to occur in streamers separate from thermal heating regions. O radicals are seen with number densities as high as 10^{21} cm^{-3} , H densities on the order of 10^{19} cm^{-3} and OH radicals densities of 10^{17} cm^{-3} . From these results, it can be concluded that radical production is due primarily to electron-impact dissociation in the streamers, while thermal effects are due to electron-joule heating in the cathode sheath.

11:00

GT2 5 Three electrode-design and semiconducting barriers to enhance the thrust of plasma actuators* SONG GUO, TERRY SIMON, DOUGLAS ERNIE, UWE KORTSHAGEN, *University of Minnesota* The deposition of surface charge on the dielectric barrier of a plasma actuator plays a central role in its performance. While surface charge deposition is necessary in order to prevent the formation of an arc or spark discharge, it inevitably causes an undesired reverse plasma pulse as soon as the high voltage is disengaged from the powered electrode. This reverse plasma pulse has been observed to lead to an almost complete cancellation of the forward and reverse thrust in nanosecond pulse driven actuator

experiments. We are here investigating two schemes to drain the surface charge between half cycles of an applied sinusoidal high voltage signal. A third electrode in combination with high voltage diodes is used to drain surface charge to this electrode during one half cycle. A semiconducting layer is employed to further allow the flow of surface charge to this electrode. The combination of these two measures leads to a 70% enhanced thrust compared to the traditional two-electrode actuator using a dielectric barrier.

*This work was supported by NASA Cooperative Agreement NNX07AB94A.

11:15

GT2 6 Two-dimensional fluid simulation of a plasma actuator* MEENAKSHI MAMUNURU, TERRY SIMON, DOUGLAS ERNIE, UWE KORTSHAGEN, *University of Minnesota* We have developed a two-dimensional time-dependent fluid model for a plasma actuator based on a dielectric barrier discharge in atmospheric pressure air. The voltage applied to the exposed electrode is a nanosecond Gaussian pulse. When a positive pulse was applied, an intense plasma is formed. Significant thrust was obtained in the downstream direction. When a negative pulse was applied, a weaker plasma and smaller thrust in the opposite direction were seen, leading to a net force in downstream direction when averaged over both positive and negative pulses. The charge accumulation on the dielectric, and the streamer formation process were drastically different for both cases. We also examined the importance of including photoionization in the air chemistry, which overall leads to a smoothing out of the plasma gradients. A thin semiconducting layer on the dielectric was included in order to test the hypothesis that surface charge deposited during the leading edge of a voltage pulse would be drained and that a reverse plasma pulse on the falling edge of the pulse can be minimized. Preliminary results for including a semiconducting layer will be presented.

*This work was supported by NASA Cooperative Agreement NNX07AB94A.

11:30

GT2 7 Numerical and Experimental Investigations of Plasma Actuators Based on Magnetogasdynamics CHIRANJEEV KALRA, SOHAIL ZAIDI, MIKHAIL SHNEIDER, RICHARD MILES, *Princeton University* Numerical and experimental studies were conducted of magnetically driven DC surface plasma discharges. Their application to supersonic boundary layer control is investigated, specifically the shockwave-turbulent boundary layer interaction problem and the induced separation control is shown. This interaction causes incoming boundary layer thickening and localized pressure loads and high heating rates. In the case of scramjet engine inlet this results in reduced effective cross-section and loss of thrust and efficiency. Magnetogasdynamic flow control is achieved by generating a plasma column close to the wall in boundary layer and dragging the gas close to the wall using Lorentz force due to perpendicular (to flow direction as well as current) magnetic field. The surface plasma column appears as a transverse "arc" between two slightly diverging electrodes which is driven by $j \times B$ forces so that it sweeps the gas near the surface in the separated region or the recirculation zone, either in the downstream direction or in the upstream direction. Depending on the direction of Lorentz force, separation bubble is either induced in the boundary layer or the shockwave induced bubble is reduced in intensity and probably eliminated. It is shown that these interactions between the plasma and the recirculation zone are non-thermal in nature.

SESSION GT3: LOW PRESSURE PLASMA DIAGNOSTICS

Tuesday Morning, 20 October 2009; Ballroom 3, Saratoga Hilton at 10:00; John Boffard, University of Wisconsin, presiding

Invited Papers**10:00****GT3 1 Plasma diagnostics using floating harmonics method and recent results in processing plasmas.**CHINWOOK CHUNG, *Hanyang University*

Recently, a floating harmonics method for processing plasma has been developed [1]. When a sinusoidal voltage is applied on a probe at a floating potential, the current flowing through the probe has many harmonics due to the nonlinearity of sheath. From the harmonic current components, plasma densities and electron temperatures can be found. There are many advantages of this method such as relative low voltages (a few V), good time resolution (\sim msec), no perturbation (no net current), immune to rf interference, strong to contamination on probes. In this presentation, some improvement of this method and some measurements in various processing plasma reactors (SF₆, CF₄, N₂, Ar, etc) as well as relevant physics will be given. Electron energy distribution function (EEDF) measurement based on the harmonic method and refinement technique for the EEDF will be given. A 2D wafer type probe array for 2D plasma density profile was developed and 2D plasma density profiles in an ICP at various conditions will be presented. [1] MH Lee, SH Jang and CW Chung, *J. Appl. Phys.*, **101**, 033305 (2007)

Contributed Papers**10:30****GT3 2 Evaluation of Advanced Algorithms to improve EEDF extraction from Langmuir Probe data Using Tikhonov Regularization Methods**

A. EL SAGHIR, C. KENNEDY, S. SHANNON, NCSU B. PATHAK, J. ALEXANDER, K. NORDHEDEN, *University of Kansas* EEDF extraction from Langmuir probe data is ill-posed due to the integral relationship between the EEDF and probe current. Curve fitting of data and reconstruction of the integral problem using regularization address this to some extent, with regularized solutions offering an advantage in EEDF accuracy over curve fitting. However, both methodologies have limitations in their ability to extract accurate EEDF's over a wide energy range for moderate signal noise. The limitations confronting regularization can be summarized in over and under regularization. Over regularization captures the high energy portion of the distribution at the expense of the low energy; and vice versa with under regularization. Advanced reconstruction algorithms using weighting and iteration are studied in order to overcome such limitations. Weighting factors scale the regularized conditioning with respect to energy to decouple the regions of interest. Iterative techniques modify the regularizer and conditioning matrix to converge on an optimal solution. To illustrate this point, the reconstruction of EEDF's from probe data taken in an electronegative RF discharge is studied. The non-Maxwellian EEDF generated by this system shows many of the challenges in EEDF reconstruction for low temperature plasmas.

10:45**GT3 3 Impedance Characteristics of the Plasma Absorption Probe**

YOHEI YAMAZAWA, *Tokyo Electron AT LTD.* The plasma absorption probe (PAP) is a diagnostics for determination of spatially resolved electron density.¹ PAP has attracted considerable interest because of its applicability in a reactive plasma. The simple structure of the probe allows us a robust measurement

while the mechanism of the absorption is complicated and there are still some uncertainty.² In this study, we focus on the frequency characteristics of the impedance instead of the absorption spectrum. An electromagnetic field simulation reveals that there is only one parallel resonance in the impedance characteristics even in a case there are many peaks in absorption spectrum. Thus, the impedance characteristics provide a clue to understanding the mechanism.

¹H. Kokura, et al., *Jpn. J. Appl. Phys.* **38** 5262 (1999).²M. Lapke, et al., *Appl. Phys. Lett.* **90**, 121502 (2007)**11:00****GT3 4 Diagnostics of RF magnetron sputtering plasma for synthesizing transparent conductive Indium-Zinc-Oxide film***

TAKAYUKI OHTA, MARI INOUE, NAOKI TAKOTA, *Wakayama University* MASAFUMI ITO, *Meijo University* YASUHIRO HIGASHIJIMA, *NU System Co., Ltd.* HIROYUKI KANO, *NU EcoEngineering Co., Ltd.* SHOJI DEN, KOJI YAMAKAWA, *Katagiri Engineering Co., Ltd.* MASARU HORI, *Nagoya University* Transparent conductive Oxide film has been used as transparent conducting electrodes of optoelectronic devices such as flat panel display, solar cells, and so on. Indium-Zinc-Oxide (IZO) has been investigated as one of promising alternatives Indium Tin Oxide film, due to amorphous, no nodule and so on. In order to control a sputtering process with highly precise, RF magnetron sputtering plasma using IZO composite target was diagnosed by absorption and emission spectroscopy. We have developed a multi-micro hollow cathode lamp which can emit simultaneous multi-atomic lines for monitoring Zn and In densities simultaneously. Zn and In densities were measured to be 10^9 from 10^{10} cm⁻³ at RF power from 40 to 100 W, pressure of 5Pa, and Ar flow rate of 300 sccm. The emission intensities of Zn, In, InO, and Ar were also observed.

*This work was partly supported by the Knowledge Cluster Initiative (the Second Stage)-Tokai Region Nanotechnology Manufacturing Cluster-from MEXT in Japan.

11:15

GT3 5 Origin of electrical changes occurring at plasma etching endpoint MARK SOBOLEWSKI, DAVID LAHR, *NIST* When a plasma etch consumes one layer and exposes an underlying layer, changes are detected in measured electrical parameters, such as impedance magnitude, phase, and dc self-bias voltage. Consequently, these electrical signals are useful for endpoint detection. However, the mechanisms responsible for the observed electrical changes are not well understood. To investigate these mechanisms, we performed experiments and numerical modeling of CF₄/Ar plasma etches of thermal silicon dioxide films on silicon substrates, in an rf-biased, inductively coupled plasma reactor. A wave cutoff probe was used to measure the plasma electron density as a function of time during etching. As the etch breaks through the oxide and exposes the underlying silicon, changes in the gas-phase densities of etch products and reactants cause the electron density to increase. This increase (and an accompanying increase in ion current) has a large effect on the measured electrical signals. Using a numerical model and measurements made at varying bias frequencies, the effect of changes in electron density can be distinguished from smaller effects caused by other parameters that vary at endpoint, including the electron temperature, average ion mass, and the ion-induced emission of electrons from the wafer surface. In addition to explaining the experimental results, the model provides predictions, over a wide range of conditions, for the sensitivity and reliability of the electrical endpoint signals.

11:30

GT3 6 Behavior of hydrogen atoms in plasma enhanced chemical vapor deposition of microcrystalline silicon film YUSUKE ABE, SHO KAWASHIMA, *Nagoya University* KEIGO TAKEDA, MAKOTO SEKIN, MASARU HORI, *Nagoya University*, *JST-CREST* Microcrystalline silicon ($\mu\text{c-Si}$) thin film grown by low temperature plasma enhanced chemical vapor deposition (PECVD) is an attractive material for applications in large area electronics and optoelectronics especially on flexible plastic substrates. In the PECVD processes for the $\mu\text{c-Si}$ film formation, conditions with high pressure (1 Torr \sim) and high H₂-dilution of SiH₄ are widely appropriated. Hence, the role of H atoms is very

important to fabricate highly crystallized $\mu\text{c-Si}$ film, however their behavior in the gas phase has not been clarified yet. In this study, we measured the absolute density and translational temperature of H atoms in a very high frequency capacitively coupled plasma (VHF-CCP) source at high pressure by using vacuum ultraviolet laser absorption spectroscopy (VUVLAS). The VHF power and the flow rate of SiH₄/H₂ gas were fixed at 500 W and 5/495 sccm, respectively. The pressure was varied from 0.5 Torr to 7 Torr. The absolute density increased $4.1 \times 10^{12} \text{ cm}^{-3}$ to $9.0 \times 10^{12} \text{ cm}^{-3}$ and translational temperature increased from 500 to 1600 K with increasing pressure.

11:45

GT3 7 Tomographic diagnostics of nonthermal plasmas NATALIA DENISOVA, *Institute of Theoretical & Applied Mechanics* In the previous work [1], we discussed a "technology" of tomographic method and relations between the tomographic diagnostics in thermal (equilibrium) and nonthermal (nonequilibrium) plasma sources. The conclusion has been made that tomographic reconstruction in thermal plasma sources is the standard procedure at present, which can provide much useful information on the plasma structure and its evolution in time, while the tomographic reconstruction of nonthermal plasma has a great potential at making a contribution to understanding the fundamental problem of substance behavior in strongly nonequilibrium conditions. Using medical terminology, one could say, that tomographic diagnostics of the equilibrium plasma sources studies their "anatomic" structure, while reconstruction of the nonequilibrium plasma is similar to the "physiological" examination: it is directed to study the physical mechanisms and processes. The present work is focused on nonthermal plasma research. The tomographic diagnostics is directed to study spatial structures formed in the gas discharge plasmas under the influence of electrical and gravitational fields. The ways of plasma "self-organization" in changing and extreme conditions are analyzed. The analysis has been made using some examples from our practical tomographic diagnostics of nonthermal plasma sources, such as low-pressure capacitive and inductive discharges. [1] Denisova N. Plasma diagnostics using computed tomography method // IEEE Trans. Plasma Sci. 2009 37 4 502.

SESSION HT1: INDUCTIVELY COUPLED PLASMAS

Tuesday Afternoon, 20 October 2009; Ballroom 1, Saratoga Hilton at 13:30; Hirotaka Toyoda, Nagoya University, presiding

Invited Papers

13:30

HT1 1 Electron heating in inductive discharges.*

GERJAN HAGELAAR, *LAPLACE, Université de Toulouse*

Radio-frequency inductive discharges are used to sustain plasma in negative ion sources for neutral beam injection [W. Kraus et al 2002 Rev. Sci. Instrum. 73, 1096] currently under development for the ITER fusion experiment. To accompany the experimental development, a comprehensive numerical model is being developed, describing the main physical principles of these sources self-consistently: inductive coupling and electron heating in the source drivers, magnetised plasma transport in the source body, negative ion extraction across a magnetic filter, low-density neutral flow and depletion by the plasma, chemistry of negative ion creation in the volume and at the surface, etc. In this presentation we discuss the principles and modelling of the inductive electron heating in these sources. In particular, we propose a simple method to describe the anomalous skin effect through a fluid equation for electron momentum including a viscosity term with an effective viscosity coefficient. We also discuss the effects of the static and radio-frequency magnetic fields on the inductive coupling and the consequences for the plasma properties.

*This work is supported by the ANR (National Research Agency) under contract BLANC08-2_310122, by the ITER Federation, and by the French Atomic Energy Commission (CEA).

14:00

HT1 2 Production and Control of Inductively-Coupled Plasmas with Multiple Low-Inductance Antenna Modules for Large-Area and Low-Damage Processes of Next-Generation Devices.*YUICHI SETSUHARA, *Osaka University, JST, CREST*

Large-area and low-damage processing of materials is of key importance for fabrication of devices including flat panel displays, thin-film photovoltaic cells and flexible electronics or electronics on polymers. In particular, organic-inorganic hybrid materials are expected as a key materials system for next-generation devices. For successful development of next-generation devices, it is of great significance to develop plasma process technologies capable of reducing plasma damage in order to achieve ultra-fine control of organic-inorganic interface without suffering degradations of organic layer. Furthermore, for enhancement of production efficiency and/or cost reduction in fabrication of these devices, it is significant to develop meters-scale/ultra-large area uniform plasma reactor. In enlargement of source size exceeding a meter, however, plasma distributions hence processing profiles become inherently non-uniform primarily due to non-uniform power deposition profile caused by standing-wave effects. In order to overcome these constraints, plasma generation and control technologies have been developed with low-inductance antenna (LIA) modules to sustain inductively-coupled RF discharge [1,2]. High-density plasma productions to attain plasma densities $10^{11} - 10^{12} \text{ cm}^{-3}$ have been demonstrated with simultaneous achievement of reduced sheath-edge potential (as low as or less than 5 eV) and capabilities in active control of the plasma profiles have also been exhibited by adjusting power deposition profiles over large area. Furthermore, plasma-enhanced deposition of silicon films showed low-temperature (200 deg.C) formation of micro-crystalline silicon films due to sufficiently reduced damage during deposition. [1] Y. Setsuhara, T. Shoji, A. Ebe, S. Baba, N. Yamamoto, K. Takahashi, K. Ono, and S. Miyake, *Surf. Coat. Technol.* **174-175**, 33 (2003). [2] Y. Setsuhara, K. Takenaka, A. Ebe and K. Nishisaka, *Plasma Process. Polym.* **4**, S628 (2007).

*This work was supported partly by JST, CREST and Global COE program (Material, Osaka Univ.).

Contributed Papers

14:30

HT1 3 Global model of instabilities in low-pressure inductively coupled chlorine plasmas EMILIE DESPIAU-PUJO, PASCAL CHABERT, *LPP - Ecole Polytechnique* Experimental studies have shown that low-pressure inductive discharges operating with electronegative gases are subject to instabilities near the transition between capacitive (E) and inductive (H) modes. A global model, consisting of two particle balance equations and one energy balance equation, has been previously proposed to describe the instability mechanism in $\text{SF}_6/\text{ArSF}_6$ [1]. This model, which agrees qualitatively well with experimental observations, leaves significant quantitative differences. In this paper, the model is revisited with Cl_2 as the feedstock gas. An alternative treatment of the inductive power deposition is evaluated and chlorine chemistry is included. Old and new models are systematically compared. The alternative inductive coupling description slightly modifies the results. The effect of gas chemistry is even more pronounced. The instability window is smaller in pressure and larger in absorbed power, the frequency is higher and the amplitudes of oscillations are reduced. The feedstock gas is weakly dissociated ($\approx 16\%$) and Cl_2^+ is the dominant positive ion, which is consistent with the moderate electron density during the instability cycle. [1] M.A. Lieberman, A.J. Lichtenberg, and A.M. Marakhtanov, *Appl. Phys. Lett.* **75** (1999) 3617

14:45

HT1 4 A control-oriented self-consistent model of an inductively-coupled plasma BERNARD KEVILLE, MILES TURNER, *NCPST, Dublin City University* PRECISION STRATEGIC RESEARCH CLUSTER TEAM, An essential first step in the design of real time control algorithms for plasma processes is to determine dynamical relationships between actuator quantities such as gas flow rate set points and plasma states such electron

density. An ideal first principles-based, control-oriented model should exhibit the simplicity and computational requirements of an empirical model and, in addition, despite sacrificing first principles detail, capture enough of the essential physics and chemistry of the process in order to provide reasonably accurate qualitative predictions. This presentation describes a control-oriented model of a cylindrical low pressure planar inductive discharge with a stove top antenna. The model consists of equivalent circuit coupled to a global model of the plasma chemistry to produce a self-consistent zero-dimensional model of the discharge. The non-local plasma conductivity and the fields in the plasma are determined from the wave equation and the two-term solution of the Boltzmann equation. Expressions for the antenna impedance and the parameters of the transformer equivalent circuit in terms of the isotropic electron distribution and the geometry of the chamber are presented.

15:00

HT1 5 Effects of RF-bias power on plasma parameters in a low gas pressure inductively coupled plasma HYO-CHANG LEE, MIN-HYONG LEE, CHIN-WOOK CHUNG, *Department of Electrical Engineering, Hanyang University* Remarkable changes of the electron temperature and the plasma density by increasing bias power were observed in low gas pressure inductively coupled plasma (ICP) by the measurement of electron energy distribution function (EEDF). As the bias power increases, the electron temperature increased with accompanying the evolution of the EEDF from bi-Maxwellian to Maxwellian distribution. However, a different trend of the plasma density was observed with a dependence on the ICP powers. When the ICP power was relatively small and therefore the discharge is in E mode, the plasma density increased considerably with the bias power, while slight decrease of the plasma density was observed when the discharge is in H mode. The change of the plasma density can be explained by the balance between total power absorption and power dissipation.

15:15

HT1 6 Low-pressure inductive gas discharges in Ar, Kr, He and Ar+Hg mixture NATALIA DENISOVA, *Institute of Theoretical & Applied Mechanics* REVALDE GITA, SKUDRA ATIS, *Institute of Atomic Physics and Spectroscopy, University of Latvia* This paper presents results of theoretical and experimental investigations of high-frequency (HF) inductive gas discharges in Ar, Kr, He and Ar+Hg mixture in the pressure area of 0.1-10 Torr. The HF inductive discharges are known as effective sources of spectral lines. Our estimations predict that due to the skin-effect, high-frequency inductive discharge should have more high line intensity if compare with a DC discharge in the related conditions. The intensities of the Ar, Kr, He and Hg spectral lines in visible region are measured at a wide range of gas pressures varying the HF generator current. Tomographic reconstructions of spatial profiles of emitting mercury atoms in Ar+Hg discharge are performed. A stationary self-consistent model of high-frequency inductive discharge is developed including detailed kinetics of the excited atomic states. Based on the developed model, the spatial profiles of atoms in excited levels and emission properties of the discharge plasma are calculated. The detailed comparative analysis of the experimental and theoretical curves has been performed. We make the conclusion that numerical results are in good agreement with the experimental data. The obtained results - dependencies of the line intensities versus gas pressure and HF generator current - are discussed.

SESSION HT2: DC, PULSED, RF AND MICROWAVE GLOWS

Tuesday Afternoon, 20 October 2009

Ballroom 2, Saratoga Hilton at 13:30

Siva Kanakasabapathy, IBM, presiding

13:30

HT2 1 Temporal variation of plasma density in atmospheric-pressure pulsed-microwave plasma* HIROTAKE TOYODA, HAIPENG YANG, TATSUO ISHIJIMA, *Nagoya University* Atmospheric pressure plasma is often produced by pulsed mode at a power duration less than a few tens μs so as to suppress transition from non-equilibrium to equilibrium plasma. Taking account for the time scale of plasma density increase (a few to 10 μs) after the plasma ignition, the plasma density is considered to be strongly time-dependent during the pulsed atmospheric pressure plasma. In this study, temporal variation of H_{β} spectra in atmospheric-pressure pulsed-microwave plasma is investigated by a gated optical multichannel analyzer (OMA) to give insight into the temporal variation of plasma density as well as the electric field. From the H_{β} line-width measurements for different polarizations, i.e., polarization parallel and perpendicular with respect to the applied electric field, contribution of Stark splitting due to external electric field is discriminated from the measured H_{β} line width. Line broadening due to the Stark splitting is clearly observed immediately after the plasma ignition, suggesting that the externally applied field penetrates into the plasma at this stage and that such influence must be subtracted for the precise plasma density measurement by Stark broadening.

*Part of this work is supported by Grant-in-Aid from MEXT, Japan.

13:45

HT2 2 The rf Micro-Hollow Device P.D. MAGUIRE, C.M.O. MAHONY, J. GREENAN, *NIBEC University of Ulster* T. GANS, D. O'CONNELL, W.G. GRAHAM, *CPP Queens University Belfast* The rf Micro-Hollow Device (rfMHD) is a new micro-plasma source with which we aim to provide sub 10 micron plasmas and densities $> 10^{22}\text{m}^{-3}$. Applications include targeted processing for electronic & bio-materials, gas sensors and light sources. The micron-scale dimensions and near atmospheric pressure operation give new physics at turn on and during steady state operation. RfMHDs of 25 microns diameter have been demonstrated[1]; they ignite readily and operate stably at powers less than 10W. The rfMHD device will be introduced and its operation described. Results from electrical and optical measurements & their analysis will be presented. Potential processes contributing to ignition & sustainment will be discussed. The prospects of operating with smaller source diameters & the science required to describe operation at these reduced scales will be addressed. The rfMHD will be presented in the context of biomedical applications currently of interest to this centre. [1] Mahony, Gans, Graham, Maguire & Petrovic, 2008 *Appl Phys Lett* 93 011501

14:00

HT2 3 Discharge mechanisms and spatial evolution of the EEDF in a microwave surface-wave plasma JIANPING ZHAO, RON BRAVENEC, MERRITT FUNK, LEE CHEN, *Tokyo Electron America, Inc.* TOSHIHISA NOZAWA, *Tokyo Electron Technology Development Institute, Inc.* TOKYO ELECTRON AMERICA, INC. TEAM, TOKYO ELECTRON TECHNOLOGY DEVELOPMENT INSTITUTE, INC. COLLABORATION, Microwave surface-wave discharges can be used to produce large-area high-density plasmas which diffuse toward the wafer region. Therefore, a quiescent, uniform, and low temperature Maxwellian plasma exists in the wafer region. Because of these advantages, we need to understand electron heating and power absorption mechanisms in the discharge region and the spatial evolution of plasma parameters in the plasma volume. The plasma source we use consists of a radial line slot antenna (RLSA) which transmits 2.45 GHz microwaves into a large quartz resonator which then couples to the plasma. Electron energy distribution functions (EEDF's) of a nitrogen plasma are measured using Langmuir probes. The EEDF's are analyzed using a novel curve fitting method that assumes electrons in the plasma consist of two Maxwellian distributions and a drifting Maxwellian that models a beam component. The relative populations and magnitudes of these electron components vary with vertical location in the plasma volume as well as with pressure and power. Measurements and 2-D particle-in-cell simulations of the EEDF are presented.

14:15

HT2 4 The Presence of Normal Modes Above a Capacitive Plasma Applicator WALTER GEKELMAN, *UCLA Plasma Physics* MICHAEL BARNES, *Intevac Corporation* STEVEN VINCENA, PATRICK PRIBYL, *UCLA Plasma Physics* Normal modes of standing waves in the plasma potential have been observed over the entire surface of a dual-frequency capacitive applicator immersed in an inductively-generated rf glow discharge. An emissive probe used to measure the plasma potential is located 0.95 cm above the applicator and moved by a two-dimensional drive system. The heater current to the probe is switched off during the 100 μs measurement to eliminate uncertainties due to the heater voltage. V_p is mapped at 208 spatial locations and digitized at 1 GHz. An electrically floating probe is located 1.84 cm above

the center of applicator to afford a means to generate correlation functions for the detection of waves in the low temperature plasma. The observed normal modes in potential can be expressed as summations of Bessel functions much as the vibrational modes in circular membranes and plates. The modes are most likely excited by the oscillations of the plasma-sheath interface including harmonic oscillations arising from the nonlinear mechanisms governing the sheath dynamics. As the frequency is increased, the order of the normal modes is postulated to increase as these modes are likely determined by the impedance terminating conditions on the chamber surfaces.

14:30

HT2 5 Gas Temperature Measurement in a Glow Discharge Plasma KENNETH SLONEKER, *Electronic Development Labs Inc.* NIRMOL PODDER, WILLIAM E. MCCURDY, SHI SHI, *Dept. of Math & Physics, Troy University* In this study a relatively inexpensive quartz protected thermocouple is used to measure the gas temperature in the positive column of a glow discharge plasma. For simplicity a K-type thermocouple is used to interpret the gas temperature from the sensor voltage at pressures from 0.5 Torr to 15 Torr and discharge currents from 5 mA to 120 mA. Gas temperature is investigated as a function of the gas pressure at fixed discharge currents and as a function of discharge current at fixed gas pressures in three different gas species (Ar, N₂, and He). An infinite cylinder model is used to compute the average gas temperature of the discharge from joule heating and gas thermal conductivity. The model and measurement data agree within 1% to 10% depending on plasma parameters. Data for all three gases have a similar quasi-linear increasing error as compared to the model.

14:45

HT2 6 Ar glow discharge – benchmark for state-of-art modeling NICOLAI DYATKO, *TRINITI, Troitsk, Russia* IGOR KOCHETOV, *Kintech Lab, Moscow, Russia* ANATOLII NAPARTOVICH, *TRINITI, Troitsk, Russia* TIMOTHY SOMMERER, *GE Research Laboratory, US* Ar glow discharge is well studied and can serve as a reference for modeling of discharges in chemically inert gases. Paper reviews experimental works and summarizes progress in the theoretical investigation of the discharge. Special attention is focused on the new theoretical and experimental data of the elementary processes and sensitivity of the calculated plasma parameters to the uncertainty of the elementary processes and type of the chosen model. It was shown that such effects as gas rarefaction and nonuniform distribution of the plasma species affect essentially on the plasma parameters and should be taken into account for correct description of discharge constriction.

15:00

HT2 7 Silicon oxide permeation barrier coating of PET bottles and foils SIMON STEVES, MICHAEL DEILMANN, PETER AWAKOWICZ, *INSTITUTE FOR PLASMA TECHNOLOGY, RUHR UNIVERSITY BOCHUM TEAM*, Modern packaging materials such as polyethylene terephthalate (PET) have displaced established materials in many areas of food and beverage packaging. Plastic packing materials offer are various advantages concerning production and handling. PET bottles for instance are non-breakable and lightweight compared to glass and metal containers. However, PET offers poor barrier properties against gas permeation. Therefore, the shelf live of packaged food is reduced. Permeation of gases can be reduced by depositing transparent plasma polymerized silicon oxide (SiO_x) barrier coatings. A microwave (2.45 GHz) driven low pressure plasma reactor is developed based on a modified Plasmaline antenna to treat PET foils or bottles. To increase the barrier properties of the coatings furthermore a RF substrate bias (13.56 MHz) is applied. The composition of the coatings is analyzed by means of Fourier transform infrared (FTIR) spectroscopy regarding carbon and hydrogen content. Influence of gas phase composition and substrate bias on chemical composition of the coatings is discussed. A strong relation between barrier properties and film composition is found: good oxygen barriers are observed as carbon content is reduced and films become quartz-like. Regarding oxygen permeation a barrier improvement factor (BIF) of 70 is achieved.

15:15

HT2 8 Transverse Gas Flow RF Slab Discharge Generator of Singlet Delta Oxygen for Oxygen-Iodine Laser ANDREY IO-NIN, YURII KLIMACHEV, OLEG RULEV, LEONID SELEZNEV, DMITRY SINITSYN, *Lebedev Physical Institute of Russian Academy of Sciences* IGOR KOCHETOV, ANATOLY NAPARTOVICH, *TRINITI LEBEDEV PHYSICAL INSTITUTE OF RUSSIAN ACADEMY OF SCIENCES TEAM, TRINITI TEAM*, Results of experimental and theoretical study of singlet delta oxygen (SDO) production in transverse gas flow RF slab discharge for an electric discharge oxygen-iodine laser are presented. The electric discharge facility operating in both pulse-periodic and CW mode was manufactured: gas flow duct including multi-path cryogenic heat exchanger, dielectric slab channel, and slab electrode system incorporated in the channel for RF discharge ignition. Experiments on SDO production in transverse gas flow RF discharge were carried out. SDO production depending on gas mixture content, gas mixture, gas flow velocity, low-frequency modulation of RF power and RF discharge power was experimentally studied. It was shown that SDO yield increased with gas pressure decrease, gas flow deceleration and helium dilution of oxygen at the same input power. CW RF discharge was demonstrated to be the most efficient for SDO production at the same averaged input power of RF discharge. SDO yield was demonstrated to be not less than 10 percent.

SESSION HT3: OPTICAL DIAGNOSTICS I

Tuesday Afternoon, 20 October 2009; Ballroom 3, Saratoga Hilton at 13:30; Marc Schaepekens, Momentive Performance Materials, presiding

*Invited Papers***13:30****HT3 1 Laser Thomson scattering diagnostics of low-temperature plasmas.**AKIHIRO KONO, *Nagoya University*

Laser Thomson scattering (LTS) is the light scattering by free electrons and one can derive electron density and energy distribution from the intensity and profile of a light scattering spectrum. To apply LTS technique to diagnostics of low-temperature plasmas, one needs to detect narrow (\sim a few nm) and extremely weak light scattering spectra against orders-of-magnitude stronger background stray scattering. This difficulty has been overcome by the development of a triple grating spectrograph [1], which produces a light scattering spectrum on its output focal plane with the stray component highly suppressed (10^{-6}) with the aid of an internal spatial filter. Imaging detection of the spectrum with a gated ICCD camera with photon-counting-level sensitivity enables one to carry out measurements within a reasonable time. The technique has been applied to a number of cases where a conventional Langmuir probe method is difficult to use, including measurements of EEDF near the plasma-dielectric interface in a surface wave plasma (where strong microwave field interferes with the probe), high spatial resolution measurements for atmospheric pressure microdischarge, etc. Other applications of the LTS measurement system could be negative ion density measurements (with the aid of laser photodetachment effect) and Raman scattering measurements, giving local gas temperature and local gas species concentration. To make reliable LTS measurements, one should be careful about electron production due to multiphoton ionization caused by strong laser field in the focal region. Direct measurements of multiphoton ionization yields for various gas species indicate that metastable rare-gas atoms are ionized with a high probability and even ground-state atoms and molecules are ionized with a probability exceeding the ionization degree of the plasma under study, depending on the gas species, plasma conditions, and laser focusing conditions, which should be controlled to minimize the laser perturbation. [1] Kono and Nakatani, *Rev. Sci. Instrum.* 71 (2000) 2716.

*Contributed Papers***14:00****HT3 2 Two-dimensional mapping of electron densities and temperatures using laser-collisional fluorescence**

EDWARD BARNAT, KRAIG FREDERICKSON, *Sandia National Laboratories* We discuss the application of the laser-collisional induced fluorescence technique to produce two-dimensional maps of both electron densities and electron temperatures in a helium plasma. A collisional-radiative model is used to describe the evolution of electronic states after laser excitation. We discuss generalizations to the time dependant results that are used to simplify data acquisition and analysis. Calibration of the predictions made by the model is achieved using an cw rf discharge that is periodically perturbed via a high voltage pulse. We then demonstrate the capability of the technique by producing images of electron density and temperature of the sheath region formed around a biased electrode.

14:15**HT3 3 Absorption spectroscopy diagnostics of a dual-frequency capacitive dielectric etch tool using Ultraviolet Light-Emitting Diodes***

JEAN-PAUL BOOTH, *LPP, CNRS/Ecole Polytechnique, France* JEROME BREDIN, *LPP* Dual-frequency capacitively-coupled etch reactors using Ar/fluorocarbon/O₂ mixtures are widely employed for etching of dielectric films for integrated circuit manufacture. CF₂ radicals play an important role in the gas-phase and surface chemistry controlling etching and polymer deposition, and their density can be measured by UV absorption via the A-X band (230-270 nm). Previously Xe arc lamps have been used as the light source, but they are rather unstable, limiting the sensitivity of the technique, as well as being cumbersome and relatively expensive. We have successfully replaced the Xe arc with UV light-emitting diodes. The CF₂ density was determined as a function of gas composition and power in a modified 2 + 27MHz commercial etch reactor operating in Ar/C₄F₈/O₂. The CF₂ density decreases rapidly as the O₂/C₄F₈ ratio is increased, and increases with RF power at both frequencies, but is most affected by 27 MHz power. There is speculation that CF₂ may play an important role in the creation and destruction of F- negative ions. However, we did not find any simple correlation between CF₂ density and electro-negativity.

*We wish to thank the Lam Foundation for financial support.

Invited Papers

14:30

HT3 4 Integration of PIC simulations and magnetic-sublevel atomic kinetics for plasma polarization spectroscopy.PETER HAKEL, *University of Nevada, Reno*

Interactions of high-intensity ultrashort-duration laser pulses with matter often result in the creation of highly non-equilibrium plasmas. Electrons and other particles can be accelerated to high velocities and can be very directional. Studies of such anisotropic plasmas are important both from the fundamental research point of view and also because of their relevance to such problems as fast ignition. In this work we study some aspects pertaining to the spectroscopic modeling of anisotropic plasmas. We investigate the possible diagnostic value of polarized line emissions driven by energetic plasma particles. We build on our previous experience with magnetic sublevel atomic kinetics models for polarized line emissions [1,2]. In particular, we discuss the details of constructing more accurate sublevel models that incorporate results of PIC simulations [3] of laser-matter interactions and the formation of directed energetic particles. New analytic expressions for the calculations of sublevel collisional atomic rates are given and their performance evaluated. These techniques make the calculation of collisional rates more accurate and realistic than before. Finally, we discuss the degrees of polarization of selected spectral lines and their sensitivity to the details of the particle distributions. [1] P. Hakel et al., *Phys. Rev. A* 76, 012716 (2007). [2] P. Hakel et al., *Phys. Rev. E* 69, 056405 (2004). [3] Y. Sentoku and A. J. Kemp, *J. Comput. Phys.* 227, 6846 (2008).

Contributed Papers

15:00

HT3 5 Diagnostic based Modelling for Determination of Absolute Atomic Oxygen Densities in Cold Atmospheric Pressure Plasmas STEPHAN REUTER, KARI NIEMI, LUCY M. GRAHAM, JOCHEN WASKOENIG, TIMO GANS, *Queen's University Belfast* The present study introduces a novel diagnostic technique for the determination of absolute atomic oxygen densities in rf atmospheric pressure plasmas, which combines easy to apply optical emission spectroscopy (OES) with a relatively simple 1D numerical simulation. Atomic oxygen ground state densities are determined from the intensity ratio of the $\lambda = 750.4$ nm argon and the $\lambda = 844$ nm atomic oxygen line. The effective excitation rate coefficients k_g^* of the upper $Ar(2p^1)$ and $O(3p^3P)$ states, adequately describing the time and space integrated optical emission measurements, are calculated on basis of the time and space averaged EEDF from the numerical simulation. The method is applied on a low temperature rf-driven atmospheric pressure plasma jet operated in helium with small admixtures of oxygen and argon. The results were confirmed by reliable independent two-photon laser-induced fluorescence measurements.

15:15

HT3 6 Nonlinear Zeeman Spectroscopy of Nitric Oxide in Strong Magnetic Field* ANDREI KOTKOV, ANDREI IONIN, YURII KLIMACHEV, ANDREI KOZLOV, *P.N. Lebedev Physical Institute of RAS* In our experiments the Zeeman splitting of several rotational-vibrational spectral lines of nitric oxide in pulsed magnetic field up to 14 T was measured with frequency-tunable CO-laser. We developed computational model for calculation of Zeeman splitting in different orders of perturbation theory for nitric oxide molecules. We took into account nonlinear Zeeman splitting in third order of perturbation theory only when the comparison demonstrated a satisfactory agreement between the experimental and calculated data on time histories of measured and calculated absorption coefficients in pulsed magnetic field. Our study demonstrated that nonlinear Zeeman spectroscopy of nitric oxide could measure a strong magnetic field up to 15T in plasma.

*This research was supported by RFBR (Project 07-02-01400a).

SESSION JT1: SHEATHS

Tuesday Afternoon, 20 October 2009

Ballroom 1, Saratoga Hilton at 16:00

Eric Joseph, IBM T.J. Watson Research Center, presiding

16:00

JT1 1 Different models of the plasma-sheath transition RIE-MANN KARL-ULRICH, *Ruhr-University Bochum* The space charge formation in the boundary layer of a quasi-neutral plasma is strongly influenced by the contribution of slow ions. As a consequence, the structure of the plasma-sheath transition depends in detail on the way how slow ion production is accounted for in the applied modeling approach. The "intermediate scale" connecting plasma sheath is therefore different (i) in fluid analysis, (ii) in kinetic analysis with cold ion source, and (iii) in kinetic analysis with hot ion source. We discuss the different models and present convenient analytical approximations for the cases (i) and (ii). The approximations supplement corresponding sheath approximations published previously [1]. The case (iii) is not solved until now. We derive the appropriate scaling and discuss the inherent difficulties. [1] K.-U. Riemann, *Plasma Sources Sci. Technol.* 18, 014007 (2009)

16:15

JT1 2 Collisional Friction Enhanced by Two-Stream Instabilities Determines the Bohm Criterion in Plasmas With Multiple Ion Species* S.D. BAALRUD, C.C. HEGNA, J.D. CALLEN, *University of Wisconsin-Madison* Ion-ion streaming instabilities are excited in the presheath region of plasmas with multiple ion species if the ions are much colder than the electrons. Streaming instabilities onset when the relative fluid flow between ion species exceeds a critical speed, ΔV_c , of order the ion thermal speeds. Using a generalized Lenard-Balescu theory that accounts for instability-enhanced collective responses [1], one is able to show the instabilities rapidly (within a few Debye lengths) enhance the collisional friction between ion species far beyond the contribution from Coulomb collisions alone. This strong frictional force determines the relative fluid speed between species. When this condition is combined with the Bohm criterion generalized for multiple ion species, the fluid speed of each ion species is determined at the

sheath edge. For each species, this speed differs from the common "system" sound speed by a factor that depends on the species concentration and ΔV_e . [1] S.D. Baalrud, J.D. Callen, and C.C. Hegna, *Phys. Plasmas* **15**, 092111 (2008).

*This material is based upon work supported under a National Science Foundation Graduate Research Fellowship (S.D.B) and by U.S. Department of Energy Grant No. DE-FG02-86ER53218.

16:30

JT1 3 Experimental test of the Baalrud's model for ion loss from a two-species plasma* NOAH HERSHKOWITZ, CHISHUNG YIP, *University of Wisconsin - Madison* Recent experiments have shown that ions in plasmas containing two ion species reach a common velocity at the sheath-presheath boundary [1]. A new theory [2] suggest that collisional friction between the two ion species enhanced by two stream instability dominates the drift velocity of each ion species near the sheath edge but also suggest that there are differences in ion the velocity at the sheath-presheath boundary given by $\sqrt{1/2\alpha(v_{th1}^2 + \alpha v_{th2}^2)}$. This suggests that significant differences in velocity will occur as the relative concentration varies. We report the first experimental test of this model. We measure ion velocity distribution functions (ivdfs) near sheath edge in an Argon/Xenon plasma as a function of the concentration ratios. The relative concentration of the two ion species is determined by the Ion Acoustic Wave phase velocity measurements, the ivdfs are determined by Laser Induced Florescence, the electron temperature is measured by Langmuir probe and the plasma potential is measured by emissive probe. [1] Lee, D; Hershkowitz, N; Severn, GD. *Appl. Phys. Lett.* **91**, 041505 (2007) [2] S.D. Baalrud, J.D. Callen, and C.C. Hegna, GEC 2009

*Work supported by the DoE grant no. DE-FG02-97ER54437.

16:45

JT1 4 Field-enhanced Auger emission of electrons from metals B. EISMANN, *Univ Toulouse A.V. PHELPS, JILA, U. of Colorado and NIST* L.C. PITCHFORD, *CNRS and Univ Toulouse* The electric field strength, E , at the cathode surface in microdischarges operating at high pressures is predicted to reach some 100 kV/cm. In this context, the objective of our work is to evaluate the influence of a high surface field on the ion-induced secondary electron emission coefficient from metal surfaces. Our starting point is the classical theory of Hagstrum (*Phys. Rev.*, **96**, 336, 1954), which we extended to include an electric field in the calculation of the probability for electron ejection following Auger neutralization of an incident ion. Among the various effects considered, the Schottky effect is by far the most important, and the secondary electron emission coefficient can be well approximated analytically as a constant (Hagstrum's original theory) plus a term depending on square root of E . The latter term is relatively more important for higher work function metals, and it is independent of

the nature of the incoming ion. For argon ions incident on a tungsten surface, the calculated secondary electron emission coefficient is almost constant for $E < 100$ kV/cm and thereafter increases from 0.05 to 0.08 for a factor of 50 increase in E .

17:00

JT1 5 Ion Flux Formation in 2 MHz Capacitive Discharge at Different Gas Pressures* IRINA SCHWEIGERT, *Institute of Theoretical and Applied Mechanics, Russian Academy of Sciences INSTITUTE OF THEORETICAL AND APPLIED MECHANICS, RUSSIAN ACADEMY OF SCIENCES TEAM*, We have studied the ion energy and angular distribution functions in a 2 MHz capacitive discharge in argon using 1D and 2D Combined Particle in Cell Monte-Carlo Collision simulations. We found that secondary electrons produced by ion bombardment from the electrodes make important contribution to the ionization at higher gas pressure. Calculations showed that the ion flux on the electrode is very sensitive to the plasma parameters. However, the ion angular distribution function weakly responds to a change of the gas pressure. For the given voltage amplitude the ions can have larger energy at higher gas pressure. The explanation of this phenomenon was found. For these conditions, variation of the sheath width can change the regime of ion motion.

*This work was supported by the RFBR grant (08-02-00833a).

17:15

JT1 6 Charge separation in a magnetized plasma-sheath-lens EUGEN STAMATE, *Risoe DTU, Technical University of Denmark* Most of plasma processing technologies are based on radical-assisted ion-induced surface-modification where ions accumulate energy in the sheath, and then strike the surface modifying its properties in a desirable way. Plasma-sheath-lens is a three-dimensional potential distribution of customized shape, formed by the space charge surrounding a biased electrode-insulator interface. The discrete and modal focusing effects have been revealed for this type of electrostatic structures formed in plasma [1] and several applications including sheath thickness evaluation, negative ion detection and extraction of positive or negative ion beams have been developed. A non-magnetized plasma-sheath-lens act as a kinetic energy separator, but it is not mass sensitive. However, a magnetized plasma-sheath-lens exhibits mass separation, so that ions of different mass will impact the electrode at different locations on the biased electrode surface. The mass spectrum can be measured as the radial distribution of the ion current density over the plasma-sheath-lens's electrode. Relevant fluid and particles simulations of the magnetized plasma-sheath-lens structures and ion trajectories within them are presented for different plasma parameters and magnetic field configurations. Practical aspects linked to the development of a new type of mass spectrometers are also investigated.[1] E. Stamate and H. Sugai, *Phys. Rev. Lett.* (2005) **94**, 125004

SESSION JT2: HIGH PRESSURE COLD PLASMAS AND ARCS

Tuesday Afternoon, 20 October 2009

Ballroom 2, Saratoga Hilton at 16:00

Patrick Pedrow, Washington State University, presiding

16:00

JT2 1 Nanosecond Repetitively Pulsed Discharges in Air at Atmospheric Pressure – Experiment and Theory of Regime Transitions* DAVID PAI, DEANNA LACOSTE, CHRISTOPHE LAUX, *Ecole Centrale Paris* LABORATOIRE EM2C UPR288 TEAM, In atmospheric pressure air preheated from 300 to 1000 K, the Nanosecond Repetitively Pulsed (NRP) method has been used to generate corona, glow, and spark discharges. Experiments have been performed to determine the parameter space (applied voltage, pulse repetition frequency, ambient gas temperature, and inter-electrode gap distance) of each discharge regime. Notably, there is a minimum gap distance for the existence of the glow regime that increases with decreasing gas temperature. A theory is developed to describe the Corona-to-Glow (C-G) and Glow-to-Spark (G-S) transitions for NRP discharges. The C-G transition is shown to depend on the Avalanche-to-Streamer Transition (AST) as well as the electric field strength in the positive column. The G-S transition is due to the thermal ionization instability. The minimum gap distance for the existence of the glow regime can be understood by considering that the applied voltage of the AST must be lower than that of the thermal ionization instability. This is a previously unknown criterion for generating glow discharges, as it does not correspond to the Paschen minimum or to the Meek-Raether criterion.

*We acknowledge the financial support of the ANR-IPER project.

16:15

JT2 2 Electron-Beam Generated Air Plasma Measurements: Effect of Reduced Electric Field* ROBERT VIDMAR, ANUSHA UPPALURI, *University of Nevada, Reno* KENNETH STALDER, *Stalder Technologies and Research* Measurements of electron density and momentum-transfer collision rate are discussed for plasma generated by an electron beam in air from 1 mT to 636 T as a function of the reduced electric field. A 100 keV electron source operating at a few mA is used to ionize air. A 10 GHz in-phase and quadrature microwave detector measures the electron number density and momentum-transfer collision rate. Optical emissions at 391.4 nm from N_2^+ provide an estimate of volumetric ionization profile along the microwave propagation path. Grids in the air-plasma test cell provide a means of imposing a reduced electric field, while the electron beam ionizes air. Results are discussed in the context of electron density as a function of reduced electric field and pressure.

*This material is based on research sponsored by the Air Force Research Laboratory, under agreement numbers FA9550-05-1-0087 and FA9550-07-1-0021.

16:30

JT2 3 Surrogate Models of Electrical Conductivity in Air NICHOLAS BISEK, MARK KUSHNER, IAIN BOYD, *University of Michigan* JONATHAN POGGIE, *US Air Force Research Laboratory* Accurately determining the electrical conductivity of a gas is essential when estimating its electromagnetic effects. These effects are important in ionized flows, a condition typically ob-

served in hypersonics because the high kinetic energy partially ionizes the gas as it passes through a strong shock or in regions where plasma-based control devices increase and/or utilize existing ionized flows-fields. Several existing semi-analytic electrical conductivity models are investigated and found to be deficient for the range of conditions present in a representative hypersonic flow that could benefit from these plasma-based technologies. This work utilizes surrogate modeling techniques to develop a general model (response surface), of solutions to Boltzmann's equation, an exact method which uses an extensive list of real collision cross-section data to determine the electrical conductivity of weakly ionized air. The optimal surrogate model, along with existing semi-analytic models, are coupled to a 3D flow solver in order to simulate hypersonic flow around a representative geometry that is utilizing a plasma-based flow control device. This effort helps quantify the importance of using a highly accurate electrical conductivity model (the surrogate model) and provides a framework for modeling solutions to Boltzmann's equation for a flow-field with arbitrary species.

16:45

JT2 4 Role of Matching Network Design in Excitation of Atmospheric Plasmas CAMERON MOORE, SCOTT HERES, CARL ALMGREN, GEORGE COLLINS, *Colorado State University* Recent refinements in the design and operation of atmospheric pressure plasmas are presented, specifically that there are advantages possible specific to match network design and selection of components. We show that a more thorough examination of an entire atmospheric plasma system which accounts for systemic compatibility leads to improvements. We present a simple example which considers electrode specifics (sizes, spacings) during selection of match network topology and match network component types and values.

17:00

JT2 5 Numerical simulation of anode activity under action of high-current vacuum arc LIJUN WANG, SHENLI JIA, DINGGE YANG, KE LIU, LIUHO WANG, *State Key Laboratory of Electrical Insulation and Power Equipment* ZONGQIAN SHI, Anode activity is critical for success or failure of vacuum interrupters when arc current attains to a certain limiting value. Based on anode activity model, anode thermal process under action of high-current arc column is simulated. Simulation results show that for sinusoid current, anode surface temperature firstly increases rapidly, then decreases slower. With the increase of heat flux density to anode, anode surface temperature will be increased. The maximal value of anode surface temperature appears near 7ms moment. Simulation results also are compared with experimental results.

17:15

JT2 6 Investigation on the voltage characteristic of vacuum arc under different axial magnetic field distributions ZONGQIAN SHI, XIAOCHUAN SONG, SHENLI JIA, XINTAO HUO, LIJUN WANG, *Xi'an Jiaotong University* APPLIED PLASMA GROUP OF XI'AN JIAOTONG UNIVERSITY TEAM, Axial magnetic field (AMF) is widely used in vacuum interrupters as an effective arc control technique. In this paper, the voltage characteristic of vacuum arc under different AMF distributions is investigated. Experiments with arc current of 10kA (RMS) and gap distance of 6-26mm were conducted with five pairs of specially designed electrodes generating conventional bell-shaped AMF profile and different saddle-shaped AMF distributions. Arc column

and cathode spot images were photographed by a high speed digital camera with exposure time of 2 microseconds. The average amplitude and high-frequency oscillation of arc voltage was analyzed based on the light intensity at different positions of arc column, and the dynamic and distribution of cathode spots. Experimental results indicate that saddle-shaped AMF can control vacuum arc much more efficiently than bell-shaped AMF, particularly, at large gap distance.

SESSION JT3: MICROPLASMAS AND JETS

Tuesday Afternoon, 20 October 2009

Ballroom 3, Saratoga Hilton at 16:00

Leanne Pitchford, CNRS - Universite Paul Sabatier, presiding

16:00

JT3 1 Microdischarge-based pressure sensors utilizing multiple cathodes for operation up to 1000°C SCOTT WRIGHT, YOGESH GIANCHANDANI, *University of Michigan* High temperature pressure sensors have uses in numerous industrial sectors including gas turbine engines, coal boilers, internal combustion engines, and oil/gas exploration machinery. Microdischarges are well-suited for high-temperature operation because of the inherently high temperatures of the ionized species that sustain them. This work describes sensors that operate by measuring the change, with pressure, in the spatial current distribution of pulsed DC microdischarges. The spatial current distribution is determined from the current in two cathodes, with different interelectrode spacing, and the differential current is treated as the output. At low pressures, current favors the farthest cathode while at high pressures, the opposite occurs. Two versions of the sensors are reported. The first type uses 3-D arrays of horizontal bulk metal electrodes embedded in quartz substrates with electrode diameters of 1–2 mm and 50–100- μm interelectrode spacing. These devices were operated in nitrogen over a range of 10–2000 Torr, at temperatures as high as 1000°C. The maximum measured sensitivity was 5420 ppm/Torr, while the temperature coefficient of sensitivity was as low as -550 ppm/K. Sensors of the second type use planar electrodes and have active areas as small as 0.13 mm² with a maximum sensitivity of 9800 ppm/Torr.

16:15

JT3 2 Spatial and Temporal Properties of Radiation for Various Electrode Configurations in Arrays of Glass Microchannel Plasma Devices S.H. SUNG, H.C. LEE, A.G. BERGER, S.-J. PARK, J.G. EDEN, *University of Illinois at Urbana Champaign* Asymmetric and symmetric structures of microchannel plasma devices having different channel width of 50 – 200 μm are fabricated on 0.4 mm thick sodalime glass substrate. The aspect ratio – channel length to width – has been obtained up to 500. All microplasmas are stable and well confined for several gas pressures of 200 – 700 Torr, and gas mixtures including ambient air. The

examination for spatially-resolved emission shows the tendency that peak intensity increases with increasing pressure. The peak emission intensity for 100 μm wide channel plasmas is doubled while increasing pressure from 200 to 600 Torr, but it also depends on geometrical factors. The temporal radiation in 300 – 800 nm for various pressures also shows different feature when the microdischarge is driven by AC source. It will be reported that the effect of electrode configuration on the properties of microplasmas.

16:30

JT3 3 Parabolic Cross-Sectional Al₂O₃ Microcavity Devices: Volume Dependent Plasma Characteristics Optimization JE KWON YOON,*BRIAN P. CHUNG,[†]YEON JOON MOON,[‡]SUNG-JIN PARK,[§]J. GARY EDEN,^{||} *University of Illinois at Urbana-Champaign* Parabolic cross-sectional microcavity arrays having as small as 80 μm apertures have been reported [1]. As an electrode, ~ 100 μm thick aluminum foil is used and wet chemical processes can reduce the thickness of the electrode as thin as 20 μm , varying the volume of the plasma. Due to the controllable electrode height and the electrochemical method introduced previously, dynamic range of aspect ratio from 0.2 to 2.2 can be provided. Plasma volumes from 1.3 to 6.9 pm³ are evaluated while the diameters of apertures are kept constant. Plasma characteristics such as Paschen's curve and emission spectrums in Ne and Ne/Xe are investigated below 700 torr. This study can be applied to devices for display. [1] K. S. Kim, T. L. Kim, J. K. Yoon, S.-J. Park, and J. G. Eden, *Appl. Phys. Lett.*, 94, 011503, 2009.

*Graduate Student

[†]Undergraduate Student

[‡]Undergraduate Student

[§]Adjunct Associate Professor

^{||}Lab Director and Professor

16:45

JT3 4 Investigations of plasma bullets formed in a non-thermal plasma jet in air JULIEN JARRIGE, ERDINC KARAKAS, ASMA BEGUM, MOUNIR LAROUCI, *Laser & Plasma Engineering Institute, Old Dominion University* Recent studies have shown that low temperature atmospheric pressure plasma jets are formed by the propagation of small plasma bullets traveling at very high velocities in ambient air. However, the propagation mechanisms are still not well understood. In this paper we report experimental investigations of plasma bullets dynamics. The plasma jet was generated by a dielectric barrier discharge reactor fed with pure Helium. The discharge was driven by high voltage (4-10 kV) short rise time (nanoseconds) pulses at frequencies up to 10 kHz. ICCD camera was used to determine the evolution of the velocity during the different propagation stages of the plasma bullet. Optical Emission Spectroscopy (OES) of the different reactive species (N₂^{*}, N₂⁺, He*) show that the bullet is ring shaped. The active species are mainly formed at the interface between He flow and ambient air. Fluid dynamics simulation was used to study the influence of He flow rate on propagation characteristics, and the results were compared to experimental data. It was found that the HV pulse width and the mole ratio of air in the He flow plays a major role in the extinction of the bullet.

17:00

JT3 5 Measurements of the propagation velocity of an atmospheric pressure plasma plume by various method* XINPEI LU, *College of EEE, HUST* Z. XIONG, Q. XIONG, Y. XIAN, C. ZOU, W. GONG, J. LIU, F. ZOU, Z. JIANG, J. HU, Y. PAN, COLLEGE OF EEE, HUST TEAM, The propagation behavior of atmospheric pressure plasma plumes has recently attracted lots of attentions. In this paper, five different methods are used to measure the propagation velocity of an atmospheric pressure plasma plume. The first method, called the "current method," obtains the propagation velocity of the plasma plume by measuring the currents carried by the plasma plume at different positions. The second method, called "voltage method," obtains the plume propagation velocity by measuring the voltage at different positions along the plasma jet with a voltage divider. The third method, called "charge method," which significant interferes with the plume propagation, estimates the plume propagation velocity by measuring the charges deposited on the surface of a quartz tube. The fourth method, which is noninterference method, obtains the plume propagation velocity by capturing the dynamics of the plasma plume with an ICCD camera. Finally, the fifth method, estimates the plume propagation velocity based on the temporal optical emission intensity measurement of selected species by using a spectroscopy. The experimental results show that plasma plume velocities obtained from the five methods have reasonable agreement with each other.

*This work is supported by the National Natural Science Foundation (Grant No. 10875048) and the Chang Jiang Scholars Program, Ministry of Education, People's Republic of China.

SESSION KTP: POSTER SESSION I

Tuesday Evening, 20 October 2009

Hall D, Saratoga Springs City Center at 19:00

KTP 1 GLOWS: DC, PULSED, RF, MICROWAVE, INDUCTIVE, OTHERS

KTP 2 Radial Structure of Normal and Abnormal Modes of the DC glow discharge VALERIY LISOVSKIY, NADIYA KHARCHENKO, VLADIMIR YEGORENKOV, *Kharkov National University, 4 Svobody sq., Kharkov, 61077, Ukraine* As is known dc glow discharge can burn in normal and abnormal modes. The aim of our work was to study the radial distribution of plasma density in both modes. Experiments were performed in the nitrogen pressure range $p = 0.1 - 2$ Torr and the dc voltage range $U < 600$ V. It is shown that in the normal mode the discharge occupies only a part of the cathode area and the current density radial profile has a maximum at the center of the discharge spot and then it goes down rapidly to the border of the spot. With the dc current increasing the radial current density profile becomes broader and its maximum value higher. The maximum value of the current density approaches a constant "normal" value before the transition of the discharge from the normal to the abnormal mode. In the abnormal mode the radial current density has almost a uniform profile across the electrode surface and the average current density increases with the dc current increasing.

KTP 3 Consequences of the local-mean-energy and the local-field approximation on the similarity parameters of abnormal glow discharges* GORDON K. GRUBERT, MARKUS M. BECKER, DETLEF LOFFHAGEN, *INP Greifswald, Felix-Hausdorff-Str. 2, 17489 Greifswald, Germany* The local-mean-energy approximation and the local-field approximation are commonly applied to include the electron properties like transport and rate coefficients into a hydrodynamic description of gas discharge plasmas. Both the approaches base on the solution of the stationary, spatially homogeneous Boltzmann equation for the electron component, but the consequences of these approaches differ drastically. In particular, the similarity parameters of abnormal glow discharges can be used to illustrate the applicability of both the approximations. Additionally, the influence of rough and extended reaction kinetics has been studied. The analysis of discharges in argon and oxygen as representatives of rare and reactive gases, respectively, leads to the conclusion that the local-mean-energy approximation is to be strongly recommended for the application to hydrodynamic descriptions of discharge plasmas.

*This work is supported by the Deutsche Forschungsgemeinschaft within the SFB TR 24.

KTP 4 Line intensities in nitrogen low-pressure microwave discharges L.L. ALVES, V. GUERRA, *IPFN/IST, Lisbon, Portugal* C. LOPEZ, J. COTRINO, *ICMSE/CSIC, Sevilla, Spain* This paper analyzes the intensity of radiative transitions in nitrogen low-pressure (0.3-0.5 Torr) microwave (2.45GHz) discharges, using both optical emission spectroscopy (OES) measurements and a 0D non-equilibrium kinetic model. The latter solves the homogeneous and stationary electron Boltzmann equation, coupled to the rate balance equations for the $N_2(X, v=1-45)$ vibrationally excited states, the $N_2(A^3\Sigma_u^+, B^3\Pi_g, C^3\Pi_u, a^1\Sigma_u, a^1\Pi_g, w^1\Delta_u, a^1\Sigma_g^+)$ electronic states, the $N(^4S, ^2D, ^2P)$ atomic states, and the $N_2^+(X,B)$ and N_4^+ molecular ions. The plasma is produced by a surface-wave discharge, within an 8mm diameter quartz tube, at ~ 55 W power and ~ 100 mm axial length. The rotational (gas) temperature of the nitrogen plasma ($\sim 300-600$ K) is experimentally determined from measurements of the band transition with the first positive system [FPS, $N_2(B)-N_2(A)$]. Comparison between simulations and measurements for the line intensity ratio R of the first negative system [FNS-00, $N_2^+(B, v=0)-N_2^+(X, v=0)$ at 391.4 nm] to the second positive system [SPS-25, $N_2(C, v=2)-N_2(B, v=5)$ at 394.3 nm] are used to estimate the electron density ($\sim 10^{11} \text{ cm}^{-3}$) and temperature ($\sim 3\text{eV}$). We discuss the calculation of R using different model approximations, analyzing its evolution with variations in the working parameters: electron density, gas pressure, and gas temperature.

KTP 5 Characterization of Electrical Discharges inside the Electron Sheath YEONG-SHIN PARK, DA-HAE CHOI, *Seoul National University* KYUNG-JAE CHUNG, *Samsung Electronics Co.* YONG-SEOK HWANG, *Seoul National University* Electron sheath which occurs in front of a small positively biased electrode immersed in pre-existing plasma has been investigated by focusing on the onset voltages of the breakdown in the electron sheath. A model for electron sheath is established and thickness of the sheath is provided. The calculated electron sheath thickness is verified by Langmuir probe diagnostics and particle-in-cell simulation. Outbreak voltages of the breakdown in the electron sheath are gauged at various pressures and powers. Regarding the plasma as a cathode, biased electrode as an anode and electron sheath

thickness as a discharge gap respectively, one-dimensional breakdown model is suggested. Applying Townsend's criteria of DC discharge to this breakdown model, a nonlinear equation for breakdown voltages is derived. Comparison of model-based numerical calculations to experimental results shows a good agreement between them.

KTP 6 Investigation of a medium-pressure Xe discharge in pulsed mode MYKHAYLO GNYBIDA, DETLEF LOFFHAGEN, DIRK UHRLANDT, *INP Greifswald, Felix-Hausdorff-Str. 2, 17489 Greifswald, Germany* The pulsed positive column in xenon plasmas at conditions of the contracted discharge has been studied by means of a time- and radial-dependent fluid model. The self-consistent model comprises the particle balance equations for the relevant species, the balance equation of the mean electron energy and the heavy particle temperature in the plasma, the Poisson equation for the radial space-charge potential, and a current balance determining the axial electric field. About 80 collision processes as well as 12 radiative processes are included in the collisional-radiative model. The electron transport and rate coefficients have been applied in dependence on the mean energy of the electrons, heavy particle temperature and ionization degree. Model calculations have been carried out for xenon plasmas in a discharge tube with an inner diameter of 6.5 mm at currents between 60 and 150 mA and pressures from 10 to 50 Torr. The main features of the pulsed xenon discharge at medium pressure are discussed. The results have been compared with experimental data of the axial electric field and of excited xenon atom densities. The agreement is well for the electric field. The model results reproduce the significant increase of low-lying (metastable and resonance) atomic levels densities in the afterglow phase of the pulse, which has also been observed in the experiments.

KTP 7 Long-path breakdown in micro-discharges NIKOLA SKORO, DRAGANA MARIĆ, GORDANA MALOVIĆ, ZORAN LJ. PETROVIĆ, *Institute of Physics, Belgrade, Serbia* We report results of our studies of the influence of long-path breakdown to the shape of Paschen curves in micro-discharges. It has often been postulated that any departure from the rapidly rising left hand side of the Paschen curve is an indication of field emission effects with little attention being paid to a possibility of the long path breakdown. For that purpose, we designed complex electrodes that facilitate the long-path breakdown in the left branch of the Paschen curve. Along with the measurements of the breakdown voltages, we recorded emission profiles with ICCD camera, in order to follow the exact path of the discharge. Diameter of the electrodes in our experiment was 2 mm, while the electrode gap was between 500 microns and 1 millimetre. Our results show that the long-path breakdown leads to the shape of the left branch of the Paschen curve, which is either flat or broadened to the lower pd -s. Quite often, this shape has been incorrectly attributed to the breakdown of the Paschen law even in standard dimension discharges. We have confirmed that when long path breakdown is possible the left hand side remains more or less constant as long as the effective d is not the minimal gap and has enough room to increase. Simulations indicate that when field emission is important the voltage continues to drop rapidly towards smaller pd .

KTP 8 Particle-in-cell simulations of electron transport in complex shape dc discharges* ALEX V. KHRABROV, IGOR D. KAGANOVICH, YEVGENY RAITSES, *Princeton Plasma Physics Laboratory, Princeton, NJ, USA* VLADIMIR I. DEMIDOV, *UES Inc., 4401 Dayton-Xenia Rd., Beavercreek, OH 45322, USA* DMYTRO SYDORENKO, *University of Alberta, Edmonton, Canada* A region of dc discharge near cathode, or negative glow, exists in very nonequilibrium state. Three distinct groups of electrons play different roles in discharge self-organization [1]: 1) fast electrons from cathode produce ionization; 2) very cold trapped electrons make up the plasma density; and 3) intermediate electrons conduct the current. These non-equilibrium conditions provide considerable freedom to choose optimal plasma parameters for many applications by controlling electron energy distribution function (EEDF). The EEDF modification is achieved by making use of additional biased electrodes or cathode voltage forms in afterglow [2]. We have performed particle-in-cell simulations in 1 and 2D geometry to demonstrate possible control of EEDF. [2] V.I. Demidov, C.A. DeJoseph, and V. Ya. Simonov, *Appl. Phys. Lett.* **91**, 201503 (2007).

*This work was supported by AFOSR through STTR contract.

KTP 9 Coupled plasma and gas dynamics in pulsed microplasmas MANISH JUGROOT, *Royal Military College of Canada* There is a great interest in understanding plasmas in small spaces as the complexity of micro-technology systems increases. A self-consistent model of plasma and neutral gas dynamics is applied to pulsed atmospheric microplasmas in helium. Fluid equations of the self-consistent and time-dependant model are described with emphasis on the close coupling among plasma, neutral gas and the electric field. The microplasmas are studied from an initial cloud and both continuous and recurring voltage pulses are investigated. Gas heating and neutral depletion initiation are observed, highlighting the close interaction between neutral gas and charged species in governing the evolution of the microplasmas.

KTP 10 Models of H_{α} Doppler emission profiles from low-pressure, hollow-cathode discharges in hydrogen A.V. PHELPS, *JILA, University of Colorado and NIST* Calculated Doppler profiles are compared with experiment for the H_{α} line excited in collisions of fast atoms, ions, molecules, and electrons with H_2 in low-pressure, high-voltage hollow-cathode hydrogen discharges. We test the proposal of Lavrov and Mel'nikov¹ that their observation of fast $H(n=3)$ moving away from the cathode is the result of acceleration of H^- and its subsequent collisions with H_2 . Our recent model² is extended to include the kinetics of H^- . Because the cathode fall is mostly outside the cylindrical cathode, the cathode is approximated as a nearly transparent planar electrode with an unknown area for reflection of fast H atoms and for production of H^- . Calculated Doppler profiles are compared with emission measurements parallel to the tube axis for their wide range of pressures. Using experimental H^- yields, the calculated H^- contribution to the H_{α} wing is significantly smaller than that caused by H atoms reflected by the cathode and comparable with the noise in the measured data.

¹B. P. Lavrov and A. S. Mel'nikov, *Optics and Spectrosc.* **79**, 842 (1995).

²A. V. Phelps, *Phys. Rev. E* **79**, 066401 (2009).

KTP 11 Factors of Local Plasma Heating near a Target during Pulse Rise Time JAE-MYUNG CHOE, GON-HO KIM, *Seoul National University* Factors to heat plasmas during a rise time of pulse on the electrode covered by plasmas are explained. When pulse applies to the target, electrons with energy of several tens eV are detected at an early time. Different from secondary electrons, they can be measured only while sheath expands by a pulse rise and ionized locally near the target. They cause increase of bulk plasma before secondary electrons do and the amount of generated plasmas is larger than the latter, which critically enhances ion flux to the target and blocks sheath expansion at the very beginning of pulse rise. From the measured energy and generation time, gained energy is proportional to a sheath speed expanding from the target and the mechanism can be explained by a Stochastic heating. Experiments are performed in Ar plasma with a pulse voltage of several kV and time-transient and spatial electron energy distributions processed by Wavelet transform algorithm are analyzed for the explanation.

KTP 12 Properties of a differentially pumped constricted hollow electrode plasma source* SHANTANU KARKARI, *National Center for Plasma Science and Technology, Dublin City University, Collins Avenue, Dublin 9, Ireland* MUBARAK MUJAWAR, *National Center for Plasma Science and Technology, Dublin City University, Dublin 9, Ireland* The neutral beam injection heating system for ITER requires uniform, high density hydrogen plasma source for the negative hydrogen ion production at 0.3 Pa. In this paper we present a pulsed-dc discharge using a differentially pumped constricted hollow electrode acting as anode and distributed parallel plates acting as cathode. Preliminary investigation shows higher discharge current and lower sustenance voltage by reducing the effective area of the constricted anode. The plasma outside the parallel plates is found to be highly uniform. The electron temperature between the parallel plates is higher than in the bulk plasma which is suitable for the production of negative ions.

*This project is funded by the Enterprise Ireland grant TD/07/335 and EURATOM Association DCU Fusion grant FU07-CT-2007-00052.

KTP 13 Low-pressure plasma discharge of Ar/N₂/CO₂ ternary mixture* GERARDO GARCIA-COSIO, *Facultad de Ciencias, UNAM* MANUELA CALIXTO-RODRIGUEZ, HORACIO MARTINEZ, *Instituto de Ciencias Fisicas, UNAM* A low-pressure DC plasma discharge sustained in a 1.6%Ar-2.7%N₂-95.3%CO₂ ternary mixture is studied. This plasma was generated in the total pressure range of 0.5 to 8.7 Torr, power of 6.3 W and with 12 l/min flow rate of gases. The diagnostic has been made by optical emission spectroscopy (OES) using a spectrometer and the determination of electron temperature was obtained by the measurements with a Langmuir double Probe. The species observed in the plasma mixture were CO₂, CO₂⁺, CN, CO, CO⁺, O₂, O₂⁺, N₂, N₂⁺, NO, C⁺, Ar, and Ar⁺. The electron temperature was found to be of 10.63 eV, and the ion density in the order of 10¹⁰cm⁻³.

*The authors are grateful to A. Bustos, A. González, R. Bustos, O. Flores and José Rangel for technical assistance. This research was partially sponsored by DGAPA IN-105707-3, CONACyT 41072-F.

KTP 14 Influence of the Walls on the Formation of a DC Glow Discharge* VLADIMIR DEMIDOV, *West Virginia University* YEVGENY BOGDANOV, *SPbSU* STEVE ADAMS, *AFRL* ANATOLY KUDRYAVTSEV, *SPbSU* 2D simulations of a DC glow discharge with a cold cathode in argon have been performed for various radii of the discharge tube. It is shown that the loss of the charged particles to the walls can significantly affect plasma parameters as well as properties of the cathode sheath. The longitudinal dimensions of the Negative Glow and Faraday Dark Space depend on the transverse loss of the charge particles and are not consistently predicted with a 1D model. The common assumption that the cathode sheath can be analyzed independently of the plasma also may not be valid. The transverse inhomogeneity of the plasma leads to a change in the current density distribution over the cathode surface. The thickness of the cathode sheath can vary with radial distance from the discharge axis, even for the case of negligible radial loss of the charge particles. The 2D model results provide an analysis of the conditions of applicability of the 1D model.

*This work was supported by the AFOSR.

KTP 15 Positive point-to-plate corona discharge as influenced by different nitrogen pressure AASIM A. AZOOZ, *Department of Physics, College of Science, Mosul University, Iraq* SABAH I. WAIS, *Department of Physics, Kurdistan region, Duhok University, Iraq* An empirical formula for IV characteristics in the nitrogen pressure ranged between ($P_o-2.5P_o$) is presented for a point-to-plate electrode corona discharge. Fast automatic data acquisition system is built to acquire the experimental data of the corona current and voltage and to determine the corona inception voltage. Three values of inception current ($I_o = 0.1, 0.5, \text{ and } 1.0 \mu\text{A}$) are used to demonstrate that the minimum observed inception current gives more accurate inception voltage, for which the exponent n of a general formula $I=A(V-V_o)^n$ has been optimized. The experimental investigation discloses that the inter-electrode separation S and the gas pressure have the strongest influence on both the dimensional parameter A and the corona inception voltage V_o . Of all potentially influential factors, a new empirical formula relating corona current, corona inception voltage, inter-electrode separation and gaps pressure is reached.

KTP 16 Super Hot Hydrogen Atoms in Microwave Plasmas EDGAR FELIZARDO, ELENA TATAROVA, FRANCISCO DIAS, M LINO DA SILVA, CARLOS FERREIRA, *IPFN - IST, Portugal* BORIS GORDIETS, *Lebedev Physics Institute, Moscow* IPFN - IST, PORTUGAL TEAM, LEBEDEV PHYSICS INSTITUTE, MOSCOW, RUSSIA COLLABORATION, "Super hot" (with kinetic energy in the range 4 - 8 eV) and "hot" (kinetic energy ~ 0.3 eV) hydrogen atoms were detected throughout the volume of a surface wave (500 MHz) generated H₂ plasma column, at pressure $p = 0.01$ mbar, from the analysis of the H _{β} , H _{γ} , H _{δ} and H _{ϵ} emission line profiles. The profiles were found to evolve from single Gaussian to bi-Gaussian towards the column end. Population inversion between the levels 5 \rightarrow 4 and 6 \rightarrow 4 was detected from the measured relative intensities of transitions within the Balmer series. The Doppler temperatures corresponding to the H _{β} , H _{γ} , H _{δ} , H _{ϵ} line broadening are much higher than the rotational temperature, as measured from the hydrogen molecular Fulcher- α band (350 - 500 K), and than the wall temperature (300 - 450 K). At pressure $p = 0.2$ mbar, "super hot" atoms were not detected while "hot" atoms are present. It has also been found that

the kinetic temperature of excited H ($n = 4-7$) atoms, as determined from the fitting of the spectral lines with a single Gaussian profile, increases with the upper level principal quantum number. These experimental results are analyzed in the framework of a kinetic model, which accounts for the generation of three groups of atoms.

KTP 17 Instability-driven ionization in a low-pressure helium discharge T.P. HUGHES, M.M. HOPKINS, P.S. CROZIER, J.J. BOERNER, *Sandia National Laboratories* We have carried out modeling of a plane-parallel low-pressure helium discharge with a thermionic cathode. Initially, ionization is due to direct-impact of cathode-emitted electrons on the neutral atoms. When a sufficient density of trapped electrons is established, a strong electron-plasma two-stream instability develops which heats the trapped electrons. The ionization rate is then enhanced by the hot electrons and by the collective fields of the instability. We present results showing the effect of neutral density and applied voltage on the V-I characteristics of the discharge.

KTP 18 Development of a compact, versatile electron beam source* S.G. WALTON, *Plasma Physics Division, Naval Research Laboratory* C.D. COTHRAN, *Global Strategies Group (North America)* R.F. FERNSLER, W.E. AMATUCCI, R.A. MEGER, *Plasma Physics Division, Naval Research Laboratory* The operating characteristics of a high-energy electron beam source are described. Electrons are extracted from a hollow cathode plasma and then accelerated by anode located downstream from the cathode. The anode to cathode surface area ratio is less than the root of the electron to ion mass ratio such that an electron sheath forms at the anode; a bias on this anode then accelerates the electron flux into a beam. A magnetic field assists the beam collimation. Paschen breakdown in the few Torr range at 500V initiates the hollow cathode plasma, and typical continuous operation requires less pressure and applied voltage. Varying the hollow cathode current allows direct control of the beam current, while the bias on the accelerating anode determines the beam energy. Beams at up to 5kV and 80mA have been produced with this device. Critical component designs for stable operation in both CW and pulsed operation are discussed.

*This work was supported by the Office of Naval Research.

KTP 19 CORONAS, BREAKDOWN, AND SPARKS

KTP 20 DC Breakdown of Low Pressure Gas in Long Tubes VALERIY LISOVSKIY, VERONIKA KOVAL, VLADIMIR YEGORENKOV, *Kharkov National University, 4 Svobody sq., Kharkov, 61077, Ukraine* We studied the dc breakdown of low pressure nitrogen in the pressure range $p = 0.1 - 2$ Torr. The measurements were performed in the tube of radius $R = 4$ mm, whereas the inter-electrode gap values varied in the range $L = 2 - 250$ mm. The conventional Paschen law was shown to hold in short discharge tubes for which $L/R \leq 1$. At $L/R > 1$ the increase of the inter-electrode distance shifts the breakdown curves $U(p)$ to higher breakdown voltage values U and lower gas pressure ones (larger products of gas pressure and inter-electrode distance pL). The breakdown curve minima lie on the same straight line. At L/R

> 10 increasing L makes the dc breakdown curves to shift to higher U values, their minima being observed almost at the same gas pressure value. Perhaps the electrons escaping to the tube walls due to diffusion perturb the electric field distribution and affect the development of the gas breakdown.

KTP 21 Modelling of a breakdown phenomena in dual-frequency discharges MARIJA RADMILOVIC-RADJENOVIC, BRANISLAV RADJENOVIC, *Institute of Physics* Gas breakdown represents the first step in generation of plasma and therefore is one of the most fundamental processes. In large scale systems, the experimentally observed Paschen law has been successfully explained by the Townsend theory. This paper contains the results of the detailed simulation studies of low-pressure gas breakdown in dual-frequency rf discharges in argon. Calculations were performed by using a Particle-in-cell/Monte Carlo collisions (PIC/MCC) code with the secondary emission model adjusted to include the energy dependence of the secondary electron yield at large separations. The obtained simulation results represents breakdown voltage curves that dictate the breakdown voltage for a particular gas as a function of the pd product for dual-frequency discharges in argon.

KTP 22 Control of the energy deposited in a high voltage nanosecond discharge and combustion triggering in $N_2/O_2/C_3H_8$ mixtures at atmospheric pressure NICOLAS MOREAU, SABRINA BENTALEB, *PHD student* PIERRE TARDIVEAU, *doctor* CHRISTIAN POSTEL, FRANÇOIS JORAND, *engineer* STEPHANE PASQUIERS, *doctor* The energy control in a point to plane corona discharge induced in dry air under nanosecond scale high overvoltage is investigated. The spatial behaviour of the discharge is described by CCD imaging coupled to energy measurements. The energy is modified by varying the voltage and the pulse duration. In previous works we obtained a diffuse regime and a streamer regime are obtained below 3 bar, and a leader-like regime above. In the diffuse regime, the discharge constricts in the point-plane axis when the energy increases while intensification of the emission can be observed on one or more filaments in the streamer one. The energy can be controlled till a pulse duration limit greater for the streamer regime than for the diffuse one. Below this duration limit, the current pulse ends with the voltage pulse. Difficulties appeared to control the energy in the leader-kind regime. The combustion triggering of $N_2/O_2/C_3H_8$ mixtures by one pulse and the flame propagation are studied at 1 bar. The diffuse regime disappears in mixtures with C_3H_8 and the discharge is a filamentary one. Combustion always triggers near the tip with a lower energy deposited limit of a few millijoules.

KTP 23 On the mechanism of the cathode erosion in negative corona discharge ALEXEY PETROV, RAVIL AMIROV, IGOR SAMOYLOV, *Joint Institute for High Temperatures RAS DEPARTMENT 3.3 OF PLASMA TEAM*, Negative corona discharge was investigated in atmospheric pressure air and SF_6 in Trichel pulse and glow mode in point-to-plane electrode configuration. As a cathode pointed carbon, copper and aluminum pins with tip size 0.02-1 mm were used. It is found that negative corona causes the erosion of cathode surface in form of nanometer-size craters and fissures. Observed etching may be explained in terms of microexplosive process. This process is initiated by interaction of the cathode surface with the cathode-directed ionization wave. This wave is registered as a Trichel pulse. Local electric field of

the head of wave gives rise to the field emission from the cathode surface which initiates microexplosion due to Joule heating. It is assumed that a single Trichel pulse causes the ejection of an erosion fragment from the cathode surface and current on the cathode surface runs through the cross-section of elementary erosion fragment. The value of Trichel pulse action integral which depends on the cathode current density and pulse duration and serves as a criterion of micro-explosion is $10^9 \text{ A}^2\text{s/cm}^4$. Hence the conclusion has been made that erosion of the cathode in Trichel pulse mode of negative corona was caused by microexplosive processes. General erosion picture of the cathode surface depends on the discharge dynamics. Correlation between discharge dynamics, erosion picture and Trichel pulse parameters was found.

KTP 24 CAPACITIVELY COUPLED PLASMAS

KTP 25 Sputter processes in capacitively coupled multi frequency discharges STEFAN BIENHOLZ, EGMONT SEMMLER, PETER AWAKOWICZ, AEPT INSTITUTE FOR PLASMA TECHNOLOGY TEAM, In material processing applications capacitively coupled plasmas have been of great importance over several years. For plasma deposition processes single frequency capacitively coupled discharges only play a minor role due to rather low deposition rates. In contrast a higher electron density, hence a higher ion flux can be achieved in magnetron coaters, which accordingly leads to significantly higher deposition rates. However, disadvantages such as limited target exploitation or restricted usage of non-conductive or magnetic targets are still present. In this contribution we propose a multi frequency driven capacitive discharge to combine the major advantages of both processes with respect to large scale applications. Whereas high electron densities and therefore a high ion flux can be achieved by using very high frequencies (VHF = 60-90 MHz), an additional lower frequency (HF = 1-14 MHz) gives a certain control over the ion bombarding energy. However complex frequency coupling limits the separated tunability.

KTP 26 PIC simulations of electrically asymmetric dual frequency capacitive RF discharges* ZOLTAN DONKO, *Hungarian Academy for Science* JULIAN SCHULZE, EDMUND SCHUENGEL, UWE CZARNETZKI, *Ruhr-University Bochum* A geometrically symmetric dual frequency capacitively coupled RF discharge operated in argon at 13.56 MHz and 27.12 MHz with variable phase shift between the driving voltage waveforms is investigated by a 1d PIC simulation. Due to the Electrical Asymmetry Effect (EAE) a variable DC self bias is generated as a function of the phase shift, that allows efficient separate control of ion energy and flux at the electrodes. An analytical model demonstrates why the ion flux does not depend on the phase shift. The quality of this separate control is found to be better compared to conventional dual frequency discharges operated at substantially different frequencies, where limitations due to frequency coupling occur. The EAE is optimized by choosing optimum amplitudes of

the low and high frequency voltage waveforms. For the first time non-linear self excited plasma series resonance (PSR) oscillations are observed in geometrically symmetric discharges. The PSR oscillations and non-linear electron resonance heating (NERH) are turned on and off depending on the electrical discharge asymmetry controlled by the phase shift between the driving frequencies.

*Funding: DFG (GRK1051) and Hungarian Fund for Scientific Research

KTP 27 3D simulation of a radio-frequency driven microplasma jet* TORBEN HEMKE, THOMAS MUSSENBROCK, RALF PETER BRINKMANN, *Institute for Theoretical Electrical Engineering, Ruhr-Universitaet Bochum* An increasing number of microplasma sources were developed in the last few years. These sources differ in geometries, single or array discharge configurations, DC or RF discharges, and the used chemistry - depending on the underlying application. In this paper we concentrate on a radio-frequency driven microplasma jet (referred to as the μ -APPJ) invented by Schulz-von der Gathen and co-workers. The μ -APPJ with an electrode gap of 1 mm is driven at 13.56 MHz (approx. 10 W), typical chemistry consists of He with addition of less than 1% molecular oxygen. To study the μ -APPJ in 3D we use a commercial computational fluid dynamics code (CFD-ACE+). We treat the electrons kinetically to build a look-up table for its transport coefficients and include a HeO_2 reaction chemistry scheme. We discuss basic insights into the fundamental mechanisms of the μ -APPJ. Finally we present a brief discussion of the results of the 3D simulation compared with a simplified analytical model.

*This work is supported by the Research Group FOR 1123 "Physics of microplasmas" founded by the German Research Foundation DFG.

KTP 28 Charge dynamics in electrically asymmetric dual frequency capacitive RF discharges* JULIAN SCHULZE, EDMUND SCHUENGEL, UWE CZARNETZKI, *Ruhr-University Bochum* ZOLTAN DONKO, *Hungarian Academy for Science* Charge dynamics in electrically asymmetric, geometrically symmetric dual frequency capacitively coupled RF discharges operated at 13.56 MHz and 27.12 MHz with variable phase shift between the driving voltage waveforms is investigated experimentally as well as by a PIC simulation and analytical models. Via the Electrical Asymmetry Effect a variable DC self bias is generated as a function of the phase shift. Differences between the DC self bias resulting from simulation/experiment and analytical/fluid models at small phase angles are explained by the charge dynamics within one low frequency RF period (not taken into account in the models). Depending on phase shift and pressure the excitation at the powered electrode is stronger or weaker compared to the grounded electrode (asymmetric excitation). The excitation dynamics is different at high (100 Pa) and low pressures (3 Pa): at low/high pressure the excitation is asymmetric at phase shifts of strong/weak DC self bias, respectively. This dynamics is understood in the frame of a simple analytical model.

*Funding: DFG (GRK1051) and Hungarian Fund for Scientific Research.

KTP 29 Modeling of capacitively coupled radio-frequency discharges in nitrogen* L. MARQUES, C.D. PINTASSILGO, L.L. ALVES, *IPFN/IST, Lisbon, Portugal* G. ALCOUFFE, G. CERNOGORA, *LATMOS/UVSQ, Verrières le Buisson, France* This paper reports the modeling of capacitively coupled radio-frequency discharges (13.56 MHz) in pure nitrogen, produced within a cylindrical parallel-plate reactor, similar to a GEC reference cell surrounded by a lateral grounded grid, at 0.2-3 mbar pressures and 5 -30 W coupled powers. This reactor is used to simulate, at laboratory scale, the N_2/CH_4 chemistry of Titan's atmosphere. We have used a 2D, time-dependent fluid-type code to describe the transport of electrons and positive ions N_2^+ and N_4^+ in the reactor, coupled to a 0D kinetic code for N_2 . The fluid code solves the charged particle and the electron mean energy transport equations, coupled to Poisson's equation for the RF electric potential. The kinetic code solves the electron Boltzmann equation and the rate balance equations of 45 vibrationally excited states and 7 electronically excited states of the N_2 molecule, yielding a set of electron transport parameters and rate coefficients for the charged particle production and destruction. Model results are compared to measurements of the self-bias potential, the average electron density, and the line intensities of the FNS(0-0) [$N_2^+(B,0)-N_2^+(X,0)$] and of the SPS(0-2) [$N_2(C,0)-N_2(B,2)$].

*Work supported by a PICS Cooperation Program (FCT-CNRS).

KTP 30 Effect of the relative phase of the driving sources on heating of dual frequency capacitive discharges DENNIS ZIEGLER, JAN TRIESCHMANN, THOMAS MUSSENBRÖCK, RALF PETER BRINKMANN, *Ruhr University Bochum* The influence of the relative phase of the driving voltages on heating in asymmetric dual frequency capacitive discharges is investigated. Basis of the analysis is a recently published global model [1] extended by the possibility to freely adjust the phase angles between the driving voltages. In recent publications it was reported that nonlinear electron resonance heating (NERH) drastically enhances dissipation at moments of sheath collapse due to plasma series resonance (PSR) excitation [2]. This work shows that depending on the relative phase of the driving voltages, the total number and exact moments of sheath collapse can be influenced. In case of a collapse directly being followed by a second collapse ("double collapse") a substantial increase in dissipated power, well above the reported growth due to a single PSR excitation event per period, can be observed. [2] T. Mussenbrock, R. P. Brinkmann, M. A. Lieberman, A. J. Lichtenberg, and E. Kawamura, *Phys. Rev. Lett.* **101**, 085004 (2008)

KTP 31 Improving plasma density uniformities at VHF/UHF operating frequencies using a scalable, multielectrode, VHF/UHF plasma source* DAVID O'FARRELL, *Dublin City University / Phive Plasma Technologies* SHANE LINNANE, CEZAR GAMAN, *Dublin City University* BERT ELLINGBOE, *Dublin City University / Phive Plasma Technologies* At VHF/UHF operating frequencies significant electrode voltage non-uniformities develop over even modestly sized electrodes leading to plasma density non-uniformities. This has frustrated the use of higher operating frequencies in larger area PECVD processes despite the potential for increased deposition rates and improved film quality. A scalable, multi-electrode, VHF/UHF plasma source is described that enables high frequency large area operation without plasma non-uniformities. Plasma uniformity data is presented over a series of powers, pressures and operating frequencies.

*Funded by Enterprise Ireland.

KTP 32 Frequency Agile Tuning For Plasmas Excited Using RF SCOTT HERES, MICHAEL KABALA, CARL ALMGREN, CAMERON MOORE, GEORGE COLLINS, *Colorado State University* Frequency agile tuning, while commonly used at GHz range, presents a number of difficulties for realization at frequencies in the 10's of MHz. We describe methods to achieve frequency agile tuning to perform controllable impedance matching and discuss methods by which tuning ranges may be further broadened.

KTP 33 Computational Optimization of Magnetically Enhanced CCP Plasma Uniformity for Disk Etch Applications VLADIMIR KUDRIAVTSEV, WENLI COLLISON, HUONG NGUYEN, PAT WARD, MICHAEL BARNES, *Intevac* MARK KUSHNER, *University of Michigan* Discrete track recording (DTR) is currently the most perspective way of nanomanufacturing of hard disk magnetic media. Using lithography and plasma etch steps it forms patterned narrow gaps. In this study we optimize magnetron plasma chamber uniformity to enable optimal plasma etch process. We have utilized HPEM plasma model to investigate CF_4 capacitively coupled single frequency plasma enhanced with static magnetic field, and analyze radial plasma uniformity near disk surface. Results will be discussed for the spatial dependence of plasma density, ion and radical fluxes (CF_x , F) as a function of chamber height, electrode to magnet distance and overall strength of magnetic field. Plasma density distribution and shape of visible plasma emissions are largely controlled by the shape of magnetic field lines. We were able to show in this study that full plasma model is required and use of only of the static magnetic field model is grossly insufficient and can lead to incorrect results. Through the use of computational model we have found optimal combination of governing parameters that control plasma uniformity across the disk, which was improved from 26% down to 4%. Using these parameters production plasma etch chamber was build and experimental studies further confirmed computational results.

KTP 34 Spatially resolved modeling of the plasma series resonance excitation in capacitively coupled plasmas SCHABNAM NAGGARY, DENNIS ZIEGLER, MARTIN LAPKE, THOMAS MUSSENBRÖCK, RALF PETER BRINKMANN, *Ruhr University Bochum* MICHAEL KLICK, *Plasmetrex GmbH Berlin* It is widely acknowledged that the excitation of the plasma series resonance can be important for the heating of capacitively coupled plasmas. This holds particularly for the asymmetric case. Fundamental studies on this phenomenon has recently been performed by means of various nonlinear global models. However, it has been shown that only a spatially resolved model can describe the complete fine structure of the very complex nonlinear dynamics. [1] In this paper we discuss the excitation of the plasma series resonance using a spatially resolved model of an asymmetric capacitive discharge. It allows for a realistic geometry as well as for a simplified but self-consistent sheath model. [1] T. Mussenbrock and R.P. Brinkmann, *Plasma Sources Sci. Technol.* **16**, 377 (2007).

KTP 35 INDUCTIVELY COUPLED PLASMAS

KTP 36 Analytical modeling of the anomalous skin effect and negative power absorption in low pressure plasmas THOMAS MUSSEN BROCK, MARTIN LAPKE, THOMAS EISENBARTH, Ruhr University Bochum RALF PETER BRINKMANN, Ruhr University The theory of the anomalous skin effect and related phenomena in a bounded low pressure plasma (below 1 Pa) is discussed. In this particular regime the relation between the high frequency current density and the electric field is nonlocal. To describe the situation, Maxwell's equations have to be coupled self consistently with Boltzmann's equation. In this paper we present an analytical, self-consistent solution to the one-dimensional problem of a plane wave propagating from the left half space into the right half space filled with a bounded homogeneous plasma. Particularly, we discuss phase mixing and negative power absorption, and finally the effect of the finite thermal velocity of electrons on the field distribution and the power deposition.

KTP 37 2D Axisymmetric Simulation of an Inductively/Capacitively Coupled Plasma Reactor* EMI KAWAMURA, MICHAEL A. LIEBERMAN, DAVID B. GRAVES, University of California, Berkeley, CA 94720 We use the commercial finite elements simulation package COMSOL to simulate a 2D axisymmetric TCP reactor. The simulation consists of four basic parts: an EM model, a Plasma Fluid Model, a Sheath Model, and a Gas Flow Model. For a pure argon plasma, the simulations were completed in less than an hour on a typical desktop machine with a 2GHz CPU and 4GB of memory. The EM model includes both inductive and capacitive coupling of the rf energy from the source coils to the target plasma via a dielectric window. The Plasma Fluid Model solves the time-dependent plasma fluid equations for the ion continuity and electron energy balance. The Sheath Model models an actual vacuum sheath of variable thickness with a fixed-width sheath of variable dielectric constant. The Gas Flow model solves for the steady state pressure, temperature and velocity of the neutrals. By varying the model parameters (e.g., pressure, input power, source coil configuration, chamber height), we observe the effect on the plasma (e.g., uniformity, density, capacitive coupling).

*We gratefully acknowledge support from Lam Research Corporation.

KTP 38 Additional planar antenna effect on the ferromagnetic core inductively coupled plasma JIN YOUNG BANG, CHIN WOOK CHUNG, Hanyang University The side type ferrite inductively coupled plasma (ICP) with 400 kHz driving frequency suitable for the next generation processing in large areas was recently developed in our previous work [1]. In this ICP, the plasma density at the edge of the chamber is higher than the center at high pressure because the plasma generation by heated electrons is localized at the edge and hardly diffuses to the center. In this paper, in order to improve the uniformity of the plasma density by increasing the ionization around center, a planar antenna whose driving frequency is 13.56 MHz was installed on the top of the chamber. The synergy effect was observed when the plasma was generated by two sources, and the uniformity could be controlled by apply-

ing only small power compared with that of the ferrite ICP to the additional planar antenna. [1] Kyeonghyo Lee, Youngkwang Lee, Sungwon Jo, Chin Wook Chung and Valery Godyak, Plasma Sources Sci. Technol., 17, 015014 (2008)

KTP 39 Analysis of the environmental ramifications of an SF₆/O₂ etch using simulation JAMES MUNRO, Quantemol JONATHAN TENNYSON, STEPHEN HARRISON, University College London DANIEL BROWN, Quantemol Sulfur Hexafluoride (SF₆) is a processing gas that is used industry-wide in a range of processes for the dry etching of silicon. However, the performance and efficiency of different processes and machines can vary widely. Through simulation we can gain significant insight into the optimization problem and provide a low cost means for further development. SF₆ is very bad for the environment with a Greenhouse Warming Potential that is 22,000 times that of CO₂. Therefore it is vital that SF₆ is used sparingly and efficiently in every process. Simulation can help to find ways of remediating harmful waste gases and optimize the process for typical processing goals (e.g. etch rate, uniformity) as well as improving SF₆ consumption efficiency and other environmental measures. Here we present an full chamber 2D simulation of an SF₆/O₂ silicon etch process, building upon previous calculations of SF₆ plasma chemistries using Quantemol-P (J.J. Munro and J. Tennyson, J. Vacuum Sci. Tech. A, 26, 865). Etch rate, pressure and power trends along with chamber wide contour plots of gas-phase species concentrations and fundamental plasma properties are considered.

KTP 40 Experimental observation of the transition from non-local to local kinetics in inductively coupled plasmas HYONCHANG LEE, MIN-HYONG LEE, CHIN-WOOK CHUNG, Hanyang university The transition from nonlocal to local kinetics was observed through the spatially resolved measurements of electron energy distribution functions in inductively coupled plasmas. As gas pressures increase, the spatial profiles of the effective electron temperatures (T_{eff}) from the electron energy distribution functions changed dramatically from hollow shapes to flat shapes. With further increases in gas pressure, the T_{eff} had saddle-shaped profiles with the highest T_{eff} in the vicinity of an antenna coil. These changes in the radial profiles of the T_{eff} show a transition of the electron kinetics from nonlocal to local regimes. This transition occurred when the electron energy relaxation lengths became smaller than the antenna half size.

KTP 41 Measurement of the total energy lost per electron-ion lost in argon, helium and oxygen inductively coupled plasmas JU-HWAN KU, YOUNG-KWANG LEE, SEUNG-JU OH, CHIN-WOOK CHUNG, Hanyang University The total energy lost per electron-ion pair lost was measured at various gases (Ar, O₂, He, Ar/O₂, Ar/He) and in the pressure range of 5–50 mTorr in an inductively coupled plasma. A floating harmonics method [1] was used to measure the electron temperatures and ion fluxes at the chamber wall. The absorbed power was determined by measuring the antenna resistance and current. The total energy lost were determined from a power balance equation of a global model. The measured of the total energy lost per electron-ion pair ranged from 80 V to 250 V for Ar and from 70 V to 90 V for He, respectively. In molecular gas, it ranged from 250 V to 2300 V for O₂ plasma due to additional collisional energy losses. The measured total energy lost decrease with absorbed power and increase with pressure. In mixture discharges, the total energy lost rapidly increase

with mixing ratio of oxygen in Ar/O₂ plasma while the total energy lost slightly decrease with mixing ratio of helium in Ar/He plasma. These experimental results were consistent with theoretical ones. [1] M. H. Lee, S. H. Jang, C. W. Chung, J. Appl. Phys. 101, 033305 (2007).

KTP 42 Investigation of electron energy distribution function in a weak magnetic field in solenoidal inductive discharge YEONG-KWANG LEE, JU-HWAN KU, CHIN-WOOK CHUNG, *Hanyang University* Plasma parameters such as electron temperatures, plasma densities, and dc plasma potential in the vicinity of electron cyclotron resonance (ECR) in the solenoidal inductive argon discharge have been investigated by observing electron energy distribution function (EEDF). Langmuir probe method system was built to study the EEDF dependencies on the radial position and rf driving frequency. The measurement was performed on the bulk plasma under range of weak dc magnetic field (0 - 20 G) at low pressure and power. In this study, the changes in the radial profile of the plasma parameters with respect to the varying the magnetic field was discussed. It was experimentally verified that no effective electron temperature maximum appear at ECR condition due to the characteristics of the local electron kinetics, while plasma density maximum appears at different magnetic field. Furthermore, the measured dc plasma potential largely increases with the rf driving frequency. These results are also compared with that of the typical planar inductive discharge [1] C.W. Chung, S. S. Kim, and H.Y. Chang, Phys. Rev. E 69, 016406 (2004)

KTP 43 The effects of magnetic field on the plasma parameters in a planar inductively coupled plasma etch system* JAE-CHUL JUNG, JAE HYUN SONG, WAN SOO KIM, KI-WOONG WHANG, *Seoul National University, Daehak-dong, Kwanak-gu, Seoul, Korea* PLASMA LABORATORY TEAM, In this paper, magnetic field effects on a planar inductively coupled plasma etch system were studied, in which the magnetic field was applied by the use of the permanent magnets in order to obtain a uniform, high density plasma with a large diameter (≥ 150 mm) at low gas pressure (≤ 10 mTorr). Plasma parameters were measured by the double Langmuir probe and the power transfer efficiency by the impedance analyzer. Coupling mode conversion from the C- to L-mode was observed to result in big changes in the plasma density. When the magnetic field is applied, the density at the center linearly increased with the input power, and then a sharp increase in plasma density could be observed at a certain input power level which connects to a plasma density hysteresis loop. The plasma density increase with the decrease of RF power once the density jump occurred. Electron temperatures at the outer region became low after the mode transition, but the peak density increase by about 4 times. When the magnetic field configuration is optimized, the uniformity of density and temperature improved with the application of magnetic field.

*This work was supported by the system IC2010 project.

KTP 44 OTHER PLASMA TOPICS

KTP 45 Real time model based control of an inductively coupled plasma BERNARD KEVILLE, MILES TURNER, *NCPST, Dublin City University* PRECISION STRATEGIC RESEARCH CLUSTER TEAM, Process yield in many plasma assisted processes may be improved significantly by real time, closed loop control of certain plasma species. This presentation describes a control algorithm for the closed loop control of a low pressure, inductively coupled plasma simulation. The simulation consists of a global model of the plasma chemistry coupled to an equivalent circuit. The equivalent circuit incorporates an impedance matching box and a model of power coupling from the antenna into the plasma which has been derived from the wave equation and the two term solution to the Boltzmann equation. In addition, mass flow controller models and gas flow transport delays are included. This work indicates how a control algorithm may be determined from a control-oriented model of the process (model-based control) in order to guarantee a robustly stable closed loop response. In general, process parameters such as wall sticking coefficients are difficult to estimate and may change over time and process measurements may be noisy and indirect. This work will indicate how an optimal state estimator may be used to improve estimates obtained from noisy data and how such estimates may be used to adapt the control algorithm in real time in order to guarantee process stability despite changes in process parameters.

KTP 46 MAGNETICALLY-ENHANCED PLASMAS: ECR, HELICON, MAGNETRON, OTHERS

KTP 47 2D PIC simulations for an EN discharge with magnetized electrons and unmagnetized ions MICHAEL A. LIEBERMAN, EMI KAWAMURA, ALLAN J. LICHTENBERG, *University of California, Berkeley, CA 94720* We conducted 2D particle-in-cell (PIC) simulations for an electronegative (EN) discharge with magnetized electrons and unmagnetized ions, and compared the results to a previously developed 1D (radial) analytical model of an EN plasma with strongly magnetized electrons and weakly magnetized ions [1]. In both cases, there is a static uniform applied magnetic field in the axial direction. The 1D radial model mimics the wall losses of the particles in the axial direction by introducing a bulk loss frequency term ν_L . A special (desired) solution was found in which only positive and negative ions but no electrons escaped radially. The 2D PIC results show good agreement with the 1D model over a range of parameters and indicate that the analytical form of ν_L employed in [1] is reasonably accurate. However, for the PIC simulations, there is always a finite flux of electrons to the radial wall which is about 10 to 30% of the negative ion flux. [1] G. Leray, P. Chabert, A.J. Lichtenberg and M.A. Lieberman, J. Phys. D, accepted for publication 2009.

KTP 48 High speed images and electrical measurements of drift waves in magnetized microdischarges TSUYOHITO ITO, *Osaka University* MARK CAPPELLI, *Stanford University* High speed images and electrical measurements from $E \times B$ discharges in micro-scale magnetically confined plasmas are presented. The image sequences depict strong and highly-ordered drift waves and underlying smaller-scale turbulence near the plasma edge, with characteristic length scales larger than the electron cyclotron radius. The measured phase velocity of the large scale disturbances is in good agreement with that for classic density-gradient driven isothermal drift waves. Propagating azimuthal waves of mode numbers $m = 3-5$ are clearly present in the image sequences, with mode excitation and mode frequency found to be dependent on discharge voltage. The experiments are compared to simple theory for drift-wave dispersion, and are found to be in good quantitative agreement. Dispersion characteristics extracted from the images are also compared to a limited set of measurements taken using Langmuir probes and segmented electrodes. These studies suggest that such magnetically confined microdischarges may provide a useful test-bed for simulations of plasma confinement and turbulence in plasmas of moderate ion temperature.

KTP 49 Time-resolved plasma parameters in HiPIMS discharges with titanium target* MARTIN CADA, PETR ADAMEK, STEPAN KMENT, PETR VIROSTKO, ZDENEK HUBICKA, *Institute of Physics of the ASCR, v.v.i.* The paper deals with time-resolved measurement of electron effective temperature, electron density, plasma and "floating" potential in High Power Impulse Magnetron Sputtering (HiPIMS) system equipped with 2" in diameter titanium target. The Langmuir probe was placed 70 mm from the target face and below the racetrack. The pressure of argon in a chamber was kept at 0.3 Pa, 2 Pa and 20 Pa. The temporal resolution of the Langmuir probe acquisition system reveals that T_e decreases during pulse ON time approximately linearly for pressure 0.3 Pa and exponentially-like for pressures 2 and 20 Pa. The steady value of T_e was approximately 0.4 eV for all the pressures. The maximal value was ~ 2.2 eV and ~ 0.6 eV for pressures 20 Pa, 2 Pa and 0.3 Pa respectively. Furthermore, the local maximum in T_e at the end of the voltage pulse is observed only for working gas pressure 2 Pa. During the pulse OFF time we observed exponential-like decay of the electron temperature for all the pressures. The plasma density demonstrates steep increase during pulse ON time. For pressures 2 Pa and 20 Pa, the plasma density reaches the maximal value at time 25 μs and 70 μs after turn off of the plasma pulse. After that we observed recombination-like plasma decay followed by ambipolar diffusion.

*This work was supported by projects KJB100100805, KJB100100707 and KAN301370701 by the Grant Agency of the ASCR and by project 202-09-P159 by the Grant Agency of the Czech Republic.

KTP 50 Transport in low-temperature magnetized plasma with significant ionization rate LAURENT LIARD, ANE AANESLAND, JEAN-LUC RAIMBAULT, PASCAL CHABERT, *Laboratoire de Physique des Plasmas, Ecole Polytechnique, France* STEPHANE MAZOUFFRE, ICARE, CNRS, Orleans, France PLASMAS FROIDS TEAM, ICARE COLLABORATION, In low-temperature plasma used for microelectronics, the ionization fraction remains sufficiently small (around 10^{-4}) for the neutral density to stay uniform in the reactor. However, with high electronic density reactor, such as helicons or ICP's, the ionization fraction can be significant, reaching 10^{-2} . This fraction

may even reach 10 % in plasma thrusters. Theoretical works have shown that when the electronic pressure, $ne_k B T_e$, reaches the same range than the neutral pressure, $nn_k B T_n$, a neutral depletion at the center of the discharge occurs. In this poster, experimental study of this phenomenon is presented: Aanesland *et al.* and O'connell *et al.* have measured the ground state density of xenon atoms using TALIF. Their results confirm that the neutral density obtains a minimum at the center of the discharge. Moreover, time resolved measurements of TALIF shows that this phenomenon gathers two different phenomena with their own time scale. Space resolved measurements of the argon metastable temperature have also been performed to estimate the influence of gas heating in neutral depletion, and compared with previous theoretical work.

KTP 51 Fluid modeling of a high power positive column: Competitive effects of magnetic field and neutral depletion LAURENT LIARD, JEAN-LUC RAIMBAULT, PASCAL CHABERT, *Laboratoire de Physique des Plasmas, Ecole Polytechnique, France* PLASMAS FROIDS TEAM, Transport phenomena in low temperature plasmas only need charged particles dynamics to be considered when the ionization fraction is small. However, recent reactor discharges such as ICP's and helicon allow high ionization rate, which changes drastically the transport dynamics. Recently, several authors included neutral dynamics in classical low-temperature discharge models and showed that, when electronic ($ne_k B T_e$) and neutral ($nn_k B T_n$) pressure are on the same range, neutrals are pushed away from the discharge centre, resulting in neutral depletion effects. In this paper, we add to the neutral depletion model an axial magnetic field. Exact numerical solutions of the fluid model are found, but we also derive an approximate analytical solution. Densities spatial profiles, electronic temperature and edge-to-center ratio are presented as a function of the magnetic field amplitude. On one hand, the presence of the magnetic field confines the plasma and so limits the diffusion of charged species to the wall. This goes against the neutral depletion effect. But on the other hand, the electronic density in a helicon discharge is strongly dependant of the magnitude of the magnetic field, which in turns tends to increase the depletion effect at fixed power.

KTP 52 Magnetic Electron Filtering by Fluid Models for the PEGASES Thruster GARY LERAY, PASCAL CHABERT, *LPP-Ecole Polytechnique-CNRS* ALLAN LICHTENBERG, MICHAEL LIEBERMAN, *EECS-UC Berkeley* The PEGASES thruster produces thrust by creating positive and negative ions, which are then accelerated. To accelerate both type of ions, electrons need to be filtered, which is achieved by applying a static magnetic field strong enough to magnetize the electrons but not the ions. A 1D fluid model with three species (electrons, positive and negative ions) and an analytical model are proposed to understand this process for an oxygen plasma with $p = 10$ mTorr and $B_0 = 300$ G [1]. The resulting ion-ion plasma formation in the transverse direction (perpendicular to the magnetic field) is demonstrated. It is shown that an additional electron/positive ion loss term is required. The solutions are evaluated for two main parameters: the ionizing fraction at the plasma center ($x = 0$), n_{e0}/n_g , and the electronegativity ratio at the center, $\alpha_0 = n_{n0}/n_{e0}$. The effect of geometry and magnetic field amplitude are also discussed. [1] Leray G, Chabert P, Lichtenberg A J and Lieberman M A, *itJ. Phys. D: Appl. Phys., Plasma Modelling Cluster issue*, to appear (2009)

**KTP 53 HELICON, MAGNETRON
AND OTHER PLASMA SOURCES**

KTP 54 Measurements of low-frequency plasma potential fluctuations in the near-field of a coaxial Hall plasma discharge indicating azimuthal waves ANDREW SMITH, MARK CAPPELLI, *Stanford University* Space and time-correlated measurements of floating potential, plasma potential, and electron temperature are made throughout much of the near-field region of a coaxial Hall plasma discharge using an emissive probe synchronized to quasi-coherent fluctuations in discharge current. We utilize an emissive probe to examine the mean (time-averaged) and low-frequency structure of these properties within a Hall discharge accelerator that operates at relatively low power. The results of our comprehensive set of measurements (covering more than 1800 spatial points) show that these properties exhibit complex structure (in particular the plasma potential and electron temperature) at frequencies on the order of the so called "breathing mode" ionization instability often seen in these types of discharges. Most notably, the plasma potential appears to fluctuate in a helical fashion, resembling tilted drift-waves rotating about the central axis. The spectrum of the near-field property fluctuations indicates a peak near 25 kHz (the same as the breathing mode), with subsidiary broad peaks out to ~ 100 kHz. The observed azimuthal rotation of the plasma potential is opposite the imposed $E \times B$ direction with an azimuthal velocity of ~ 1800 m/s. This complex time-dependent structure may impact electron transport properties, possibly accounting for the current flow in this region.

**KTP 55 DIELECTRIC BARRIER DISCHARGES,
DISPLAYS**

KTP 56 Voltage slew rate dependence of plasma excitation in 10-200 Torr argon-nitrogen gas mixture DBD FENG LIU, GEORGE HUANG, *Center for Advanced Power and Energy Conversion, Department of Mechanical and Materials Engineering, Wright State University* BISWA GANGULY, *Air Force Research Laboratory* Argon-nitrogen gas mixture dielectric barrier discharge (DBD) excited by short (rising time ~ 20 ns) and long (rising time ~ 100 ns) 3 to 6 kV high-voltage pulses was investigated in the pressure range of 10-200 Torr. Time resolved spectra of Ar ($2P_1-1S_2$), Ar⁺ ($4P-4D^o$), N₂ ($C^3\Pi_u - B^3\Pi_g$), and N₂⁺ ($B^2\Sigma_u^+ - X^2\Sigma_g^+$) were recorded while the applied voltage kept constant during measurements; the influence of different applied voltages and nitrogen concentration on the observed spectra were also obtained. Mean electron energies, T_e , were derived from the ratio of the measured emission intensities by comparing excitation rates calculated using BOLSIG+ code, assuming a Maxwellian EEDF. The T_e of short-pulse excited DBD was in the range of 6-8 eV and it decreased by about 0.5 eV for lower voltage slew rate excitation under the same experimental conditions. The pulsed DBD plasma processes with different slew rate were analyzed based on the dependence of observed emission spectra and T_e on the discharge operating parameters. The discharge voltage, current and power deposition were also estimated from applied voltage and current measurements.

KTP 57 ABSTRACT WITHDRAWN
KTP 58 HIGH PRESSURE GLOW DISCHARGES

KTP 59 Numerical study of discharge progress and characteristics in Microhollow Cathode Discharge* GUANGQING XIA, *Dalian University of Technology* GENWANG MAO, MAOLIN CHEN, *Northwestern Polytechnical University* The two-dimensional numerical model for Microhollow cathode discharge (MHCD) consists of the continuity equations for electron and ion and Poisson's equation. The model considers the drift-diffusion approximation for the flux of electron and ion and accounts for the mean electron energy dependence of the ionization rate. In the numerical study, two molybdenum foils with 100 μm thickness are stacked on an alumina foil with 250 μm thickness. The ports with the hole diameter 100 μm are drilled. The discharge occurs in argon with the pressure 100 Torr. The computation results show the potential profile, electron density, ion density and electron temperature distribution. The potential contour shows that the axial electric field is dominant at the discharge initialization and then the radial electric field becomes very important as the forming of the cathode sheath. The results indicate the temporal dynamic behavior of MHCD with the electron density of order 10^{19}m^{-3} , electron temperature of several to tens of eV. The peak electron/ion density occurs near the region of the cathode and the dielectric as well as near the anode at the discharge initialization, then localizes along the centerline of the hollow near the cathode. Most of the model predictions are in agreement with experimental data for MHCD under the similar conditions.

*This work was supported by China Scholarship Council (CSC).

KTP 60 Spectroscopic investigations of an atmospheric pressure singlet oxygen plasma source JOAO SANTOS SOUSA, *LPGP, CNRS-UPS, 91405 Orsay, France and IPFN, IST, 1049-001 Lisboa, Portugal* GERARD BAUVILLE, BERNARD LA-COUR, PASCAL JEANNEY, LIONEL MAGNE, VINCENT PUECH, *LPGP, CNRS-UPS, 91405 Orsay, France* Microcathode sustained discharges (MCSD) offer the possibility to produce DC non-thermal plasmas at high gas pressure. The remarkable stability of MCSD has allowed us to operate glow discharges, free from the glow-to-arc transition, in He/O₂/NO mixtures, at atmospheric pressure, with low values of E/N [1]. As a result, these MCSD can efficiently generate large amounts of O₂(1D) and O₃, which makes them very useful for many biological applications [2]. From optical measurements we deduced the gas temperature, the O density profiles, the O₃ spatial distribution, and the yield of O₂(1D). The gas temperature in the MCSD was determined from the high resolution spectra of O₂ atmospheric band at 760 nm. The O density profiles were measured by Two-photon Absorption Laser Induced Fluorescence spectroscopy, while the O₃ density distributions have been obtained by UV absorption spectroscopy. The density of the O₂(1D) was evaluated from IR emission at 25cm downstream from the MCSD. The effect of different parameters such as gas flows and mixtures, and discharge current are discussed in the study. [1] J.S. Sousa et al., *Appl. Phys. Lett.* 93, 011502 (2008) [2] J.S. Sousa et al., these proceedings.

KTP 61 Modeling of the spatiotemporal behavior of an argon glow discharge at atmospheric pressure MARKUS M. BECKER, DETLEF LOFFHAGEN, *INP Greifswald* The spatiotemporal behavior of gas discharges is described by means of a fluid model which comprises the coupled set of balance equations for the densities of electrons, ions and neutral particles, the electron energy balance equation as well as Poisson's equation for the electric potential. This system of equations is numerically solved using a stabilized finite element method. The discharge voltage required for the solution of Poisson's equation is determined from the solution of the external electric circuit equations taking into account the time-dependent capacity and resistance of the plasma. In the present contribution first results related to an argon plasma at atmospheric pressure in a discharge configuration designed to generate small homogeneous high-pressure glow discharges¹ are presented. Main features of the temporal evolution of the discharge, which can be divided into Townsend, ignition, quasi-steady-state and recombination phase, are discussed. It is found that the cathode-fall thickness and current density in the quasi-steady state are of the order of the values given by the similarity laws for normal glow discharges.

¹W. Böttcher et al., *Appl. Phys. B* 54 (1992) 295

KTP 62 Fluid modeling of a microwave micro-plasma at atmospheric pressure* J. GREGORIO, *IPFN/IST, Lisbon, Portugal* C. BOISSE-LAPORTE, *LPGP/UPS, Orsay, France* L.L. ALVES, *IPFN/IST, Lisbon, Portugal* This paper presents the modeling of an argon micro-plasma produced by microwaves (2.45 GHz) at atmospheric pressure. The study uses a 1D stationary fluid-type code that solves the transport equations for electrons, positive ions, and the electron mean energy, together with Poisson's equation for the space-charge electrostatic field, Maxwell's equations for the electromagnetic excitation field and the gas thermal energy equation (ions are assumed to be in thermal equilibrium with the neutral gas). The model uses a simple kinetic scheme for Ar that includes the ground state, a lumped Ar(4s) excited state, and the Ar⁺ and Ar₂⁺ ionization states. The main features are: (i) the existence of combined kinetic-transport features, affecting the populations of both ions species (with similar densities); (ii) a strong decrease in the near-wall values of the electron mean energy, leading to a reduction in the production / destruction rates of Ar(4s) by electron impact, and causing its main production channel, near the wall, to become the electron dissociative recombination of Ar₂⁺; (iii) a self-consistent profile of the gas temperature with a small axis-to-wall variation (~ 70K).

*Work supported by the FCT under Grant No. SFRH/29294/2006 and Project PTDC/FIS/65924/2006.

KTP 63 Microwave micro-plasma sources at atmospheric pressure* J. GREGORIO, O. LEROY, P. LEPRINCE, C. BOISSE-LAPORTE, *LPGP/UPS, Orsay, France* L.L. ALVES, *IPFN/IST, Lisboa, Portugal* This paper studies two linear resonator sources, which use a continuous 2.45 GHz microwave excitation to produce stable micro-plasmas, in air and in argon, at atmospheric pressure. In both sources, "large" volume micro-plasmas (~ 10⁻⁴-10⁻² cm³) are produced and sustained within the 50-200 μm gap delimited by two metal electrodes (with either 6 mm or 14 mm in length), placed at the open-end of a microstrip-like planar transmission line. The excitation can use "high" powers (~ 50 W), for long periods, without visible damages of the electrodes, even in air discharges. Particular attention is given to the design

and optimization of the sources (in terms of frequency tuning and power coupling), using both simulations and experiments. OES diagnostics allow deducing the rotational, vibrational and excitation gas temperatures, and the electron density (using Stark broadening measurements of the H_β line-emission profile). Both sources have similar quality factors (~ 15), yielding high-density (~ 10¹⁴ cm⁻³), non-equilibrium micro-plasmas, with rotational temperatures (~ 600-1500 K) much lower than vibrational and excitation temperatures (~ 4500-6000 K).

*Work supported by the FCT under Grant No. SFRH/29294/2006 and Project PTDC/FIS/65924/2006.

KTP 64 Comparison of different fluid models for the atmospheric pressure DC glow microdischarge in helium* ANATOLY KUDRYAVTSEV, EUGENE BOGDANOV, KIRILL KAPUSTIN, ALEXANDER CHIRTSOV, *St. Petersburg State University, Russia* One- and two-dimensional self-consistent fluid simulations of a DC microdischarge in helium at atmospheric pressure were performed. The plasmachemical model used includes five atomic and two molecular excited levels of helium and more than 80 reactions between them. Comparison of simulation results obtained by using this reaction set both with approach of Maxwellian and non-Maxwellian EDF with results from previous papers is presented. Simulations predict main observed properties of DC glow discharge, including formation of the normal current density when discharge occupies only part of cathode (the normal glow discharge). Gas heating was found to play an important role in shaping discharge profiles both in the cathode sheath and plasmas. Basic plasma properties such as density of charged and excited particles, electron and gas temperatures, electric field profiles etc. appeared to depend on choice of reaction set and EDF shape.

*Work partially supported by RFBR grants 09-02-01194 and 09-02-91225.

KTP 65 Modeling of a microwave plasma torch* L.L. ALVES, *IPFN/IST, Lisbon, Portugal* R. ALVAREZ, *ICMSE/CSIC, Sevilla, Spain* L. MARQUES, *IPFN/IST, Lisbon, Portugal* S.J. RUBIO, A. RODERO, M.C. QUINTERO, *Dep. Fis/UCO, Cordoba, Spain* This paper presents simulation results for a microwave plasma torch (MPT, at 2.45 GHz). The particular device under study couples the MPT (connected to a coaxial waveguide) to a cylindrical reactor chamber, where it produces helium plasma at atmospheric pressure. The study gives a 2D description of the MPT-reactor system, based on an electromagnetic model (that solves Maxwell's equations adopting a time-harmonic description, to calculate the distribution of the EM fields and the average power absorbed by the plasma) and a hydrodynamic model (that solves the Navier-Stokes' equations for the flowing neutral gas, to calculate the distribution of velocities, mass density, pressure, and temperature within the reactor). Model results, such as the power transmission coefficient and the gas temperature, are particularly dependent on the reactor dimensions, the electron density and temperature, and the gas input flow. Comparison between simulations and measurements reveals common variation trends, with changes in the reactor height, for the power reflected by the system, and yield a qualitative agreement for the axial profile of the gas rotational temperature.

*Work supported by the FCT under Project PTDC/FIS/65924/2006.

KTP 66 Characterization of a Martian Simulated Discharge*

DERETH DRAKE, SVETOZAR POPOVIC, LEPOSAVA VUSKOVIC, *Department of Physics, Old Dominion University* We performed a detailed characterization of a Martian simulated discharge at Mach 2.15. Supersonic flow was generated using a convergent-divergent nozzle upstream of the discharge region. Gases were premixed in the stagnation chamber at room temperature by adding 2.75% N₂ and 1.55% Ar to pure CO₂. A cylindrical microwave cavity was used to sustain a discharge in the mixture in the pressure range of 100-600 Pa. Optical emission and absorption spectroscopy were used to determine excited state populations and electron temperature from the Ar spectra. The gas temperature and electron density were determined from the CO Ångstrom bands and N₂ C³Π_u-B³Π_g system, respectively. Results were compared with a kinetic model that included adequate concentrations of CO₂, N₂, and Ar, along with CO, O₂, and NO, in the discharge mixture.

*Supported by NASA Langley Research Center and NASA Marshall Space Flight Center.

KTP 67 Numerical Simulations of Atmospheric Pressure Discharge using Three-dimensional Fluid Model

MUHAMMAD M. IQBAL, MILES M. TURNER, *NCPST, DCU* We elaborate the three-dimensional numerical simulations of uniform and filamentary atmospheric pressure discharge in the parallel-plate dielectric barrier geometry with symmetric boundary conditions. The analysis of spatio-temporal species distribution demonstrates that the different discharge regimes are distinguished with their distinctive properties in the uniform glow and filamentary discharges. The spatial profile of electron density along with surface charge density enhances the understanding of a breakdown pulse for the quarter of a cycle. The temporal evolution of current density exhibits that it increases from 20 to 50 KHz, start decreasing and follows an approximate stable path at higher frequencies. The emergence of filaments is analyzed in the lower frequency regime, which explains the precise internal details of their temporary shapes and patterns during the growth and decay phases of filamentary atmospheric pressure discharge. The noticeable structures of filaments are marked at lower frequencies prominently than higher frequencies because the filaments coalesce and form a uniform distribution of discharge plasma at higher frequencies. The movement of filaments is examined with the slice distributions of electrons, which illuminate the path and constricted part of electron density inside the filaments.

KTP 68 Characterisation of Sub-Millimetre Plasmas

J. GREENAN, C.M.O. MAHONY, P.D. MAGUIRE, *NIBEC University of Ulster* D. MARIC, *Belgrade, Institute of Physics* High pressure molecular gas hollow cathode (HC) plasmas have potential biomedical applications[1,2]. Issues however remain with geometries presented by realistic applications. Here we investigate the electrical & optical characteristics of such a geometry, a 2 mm diameter HC with a variable precisely positioned anode cathode gap. We present HC electrical measurements including static IV, Paschen curves & other derived scaling characteristics eg j/p^2 [3] for various gases (inert and molecular), pressures (> 100 mTorr) & gaps (< 1 mm). Analysis of these discharge characteristics sheds light on the HC effect in our sub-mm geometries, including instabilities, oscillations & self-pulsing. Investigations of electron distribution & gas temperature via optical emission spectroscopy are under way; plasma density may also be attainable. Other studies include molecular gas dissociation and detection of NxOy &

other molecular gases via FTIR spectroscopy using optics developed for point source plasma measurement. [1] McLaughlin et al 2008 *Diamond & Related Mat* 17 873 [2] Mariotti et al 2004 *PSST* 13 207 [3] Petrovic et al 2008 *J Phys D* 41 194002

KTP 69 Interactions between atmospheric pressure plasma jets

QAIS TH. ALGWARI, COLM O'NEILL, DEBORAH O'CONNELL, *Queen's University Belfast* CENTRE FOR PLASMA PHYSICS TEAM, Cold atmospheric pressure plasmas offer a unique environment for treatments of soft materials. Here we investigate the possibility of exploiting the interaction of two or more atmospheric pressure plasma jets for increased control and manipulation. The interaction zone itself offers the possibility of a more controllable gentle environment for delicate treatments. The interaction between two counter-streaming atmospheric pressure plasma jets is investigated. The individual plasmas are formed inside a glass tube between two ring electrodes surrounding the tube and driven using a kHz excitation frequency. Gas is supplied between the two electrodes and this design produces significant plasma jets (few centimeters) at both the powered and grounded electrode side. The emission from these jets, while continuous to the naked eye, of a time scale of micro-seconds emits discrete plasma pockets (from both the grounded and powered electrode side). The dynamics of the interaction between these plasma pockets is presented.

KTP 70 Unconfined cylindrical RF discharge at atmospheric pressure

YVONNE SUTTON, *The Open University* GEORGE NAIDIS, *Russian Acad Sci, Joint Inst High Temp, Moscow* PETER JOHNSON, *The Open University* JON MOORE, *B & W Group Ltd, UK* DAVID SHARP, NICHOLAS BRAITHWAITE, *The Open University* Electrical and optical data for a vertical arc discharge sustained at 325 kHz in atmospheric pressure, ambient air have been compared with a fluid model based on the dominant collision processes in nitrogen-oxygen mixtures. This particular non-equilibrium discharge, has been used as an acoustic source; the present analysis is of the unmodulated RF arc. For a 15 mm long, 20 mA discharge, observations and the model reveal that the gas temperature is about 3000 K, the axial field is ~ 100 kV m⁻¹ and the electron density is $\sim 2 \times 10^{17}$ m⁻³; the column radius is ~ 1 mm in terms of optical emission, but the gas temperature width is about three times broader.

KTP 71 Characterization of microplasmas and nanoplasmals in ambient and above atmospheric pressure liquids and gases

DAVID STAACK, ADITYA CHITRE, *Texas A&M Mechanical Engineering* DC glow discharges, DC corona discharges, and nanosecond pulsed corona discharges are investigated in various high density liquids and gases. The discharges are characterized by microscopic visualization, voltage-current measurements, and optical emission spectroscopy. The plasmas are investigated with regards to their small feature size, high energy density properties, discharge scaling laws, and instabilities. For operation in gases above atmospheric pressure the DC glow microplasma discharges behave as pressure scaled version normal glow discharges though there are significant temperature effects and the ionization overheating instability becomes more prevalent at higher pressures. Energy densities in the plasmas may range to as high as 10²⁶ J/m³ in pulsed and transient high density discharges. Temperatures range from near ambient to thermal plasma conditions depending on increasing with operating density and pulse duration. In pulsed

high energy density operation in liquids and high pressure gases a short (~ 50 ns) transition from non-thermal to thermal regime is observable. For operation in liquids and very high pressure gases discharge features ~ 200 nm in size are apparent leading to the possibility of direct write nanofabrication by PECVD and plasma etching techniques using such nanoplazmas.

KTP 72 Structure of a micro hollow cathode discharge in the normal regime at medium pressure range in pure argon CLAUDIA LAZZARONI, PASCAL CHABERT, ANTOINE ROUSSEAU, *CNRS-Ecole Polytechnique* NADER SADEGHI, *CNRS LABORATOIRE DE PHYSIQUE DES PLASMAS TEAM, LABORATOIRE DE SPECTROMETRIE PHYSIQUE TEAM*, A microplasma is generated in the $400 \mu\text{m}$ diameter micro hole of a molybdenum-alumina-molybdenum sandwich (MHCD type) at medium pressure (30-300Torr) in pure argon. Experiments are performed during the normal regime, when the plasma is not only confined in the hole but also expands on the cathode backside. Imaging and emission spectroscopy allows the discharge structure to be studied and is used to infer the electronic density in the micro-hole via the Stark broadening of the H_{β} line. We find strong maxima of the plasma emission in the vicinity of the sheath edge. To explain some of the experimental observations, we use a one dimensional transport model to obtain the radial evolution of the charged-particles densities and fluxes. The result of this model is used as an input parameter of a sheath-model which allows the sheath thickness to be calculated as a function of pressure. The sheath size variation with pressure is well correlated with the maxima of plasma emission.

KTP 73 THERMAL PLASMAS: ARCS, JETS, SWITCHES, OTHERS

KTP 74 Experimental study of vacuum arc with different electrode materials DINGGE YANG, SHENLI JIA, LIJUN WANG, LIUHUO WANG, ZONGQIAN SHI, The material of electrodes is essential to affect the characteristics of vacuum arcs and the interruption performance of vacuum circuit breakers. In order to clarify the effect of electrode material on arc appearance and breaking capacity, experiments of cup-shaped axial magnetic field electrodes made of Cu and Cu70Cr30 were conducted respectively in a detachable vacuum chamber, with arc current varying from 5kA to 25kA (rms). The diameter of the electrodes is 58mm and the gap distance was fixed at 10mm in the experiments. The appearances of arc column, cathode surface and anode activities were recorded by a digital high-speed camera and the arc voltage was measured by a high-voltage probe of oscilloscope. The photos of contact surface erosion after experiments were also given. The experimental results of Cu electrodes were compared with those of Cu70Cr30 electrodes, the differences of the two kinds of vacuum arcs were given and those influencing the breaking capacity were also illustrated.

KTP 75 Structure and expansion characteristics of laser ablation tin plasma into a vacuum QIUSHI ZHU, JUNZABURO YAMADA, NOZOMU KISHI, TOMONAO HOSOKAI, MASATO WATANABE, AKITOSHI OKINO, KAZUHIKO HORIOKA, EIKI HOTTA, *Tokyo Institute of Technology* The structure and expansion characteristics of the plasma plume produced by laser ablation of a bulk tin target in vacuum have been investigated. A Q-switched Nd: YAG laser with 1064 nm wavelength, 5 ns pulse width, and the order of 10^{11} W/cm² power density was employed to create ablation plasma. Time-of-flight (TOF) measurements using a movable Faraday cup were conducted to study the velocity distributions of the tin ions in the ablation plume. The results exhibited triple-peak structure of the TOF spectra: two groups of fast ions with the mean velocity of ~ 100 km/s and ~ 60 km/s respectively, and a dominating slow ion group with the velocity less than 50 km/s. By fitting the velocity spectrum of the slow ion group with shifted-Maxwell-Boltzmann distribution, a multimodal structure with three distinct velocity distributions attributed to the ions with different charge states was obtained. The evolution dynamics of the Sn I and Sn II in the erosion tin plasma plume were compared using the optical emission lines. The results displayed different plume shapes of Sn I and Sn II due to different contributing factors towards the expansion dynamics; the drift velocity of Sn II in the plasma plume was in good agreement with the TOF results of the Faraday cup experiment.

KTP 76 Two-temperature modeling of a magnetically rotating arc MARGARITA BAEVA, DETLEF LOFFHAGEN, DIRK UHRLANDT, *INP Greifswald, Felix-Hausdorff-Str. 2, 17489 Greifswald, Germany* A three-dimensional, two-temperature MHD model of a DC plasma torch has been developed to study the behavior of a magnetically rotating arc in argon at atmospheric pressure. The torch consists of a 10 mm long rod-type cathode with a diameter of 3 mm surrounded by a 25 mm long hollow anode with a diameter of 10 mm. The arc is supplied by a current of 200 A. Without external axial magnetic field a heavy particle temperature T_h of about 14000 K and 8000 K is obtained near the cathode tip and downstream in the plume, respectively. Significant temperature differences between the electron temperature T_e and T_h up to a factor of 1.4 are found in the arc fringes. When applying an external axial magnetic field of 0.04 T, the high temperature plasma inside the torch is retracted axially and expanded radially. It is involved in rotation due to the Lorentz force and a backflow appears in front of the cathode close to the axis. The inflow and backflow gases impinge onto the anode. T_e and T_h are about 18000 and 13500 K, respectively, at maximum. The T_e profile gets broader than that of T_h . Both profiles are prolonged towards the anode. A similar behavior is observed for the arc power density and the electron density distribution.

KTP 77 Microwave Argon Plasma Torch EDGAR FELIZARDO, *IPFN - IST, Portugal* MARIANA PENCHEVA, EVGENIA BENOVA, *St. Kliment Ohridski University of Sofia* FRANCISCO DIAS, ELENA TATAROVA, *IPFN - IST, Portugal* IPFN - IST, PORTUGAL TEAM, ST. KLIMENT OHRIDSKI UNIVERSITY OF SOFIA TEAM, A theoretical and experimental investigation of a microwave (2.45 GHz) Argon plasma torch driven by a surface wave is presented. The theoretical model couples in a self-consistent way the wave electrodynamics and the electron and heavy particle kinetics. The set of coupled equations includes: Maxwell's equations, the electron Boltzmann equation,

including electron-electron collisions, and the particle balance equations for electrons, excited atoms (4s, 4p, 3d, 5s, 5p, 4d, 6s), and atomic (Ar^+) and molecular ions (Ar_2^+). The input parameters of the model are: gas pressure (760 Torr), plasma radius ($R = 0.75$ cm), dielectric permittivity ($\epsilon_d = 4.0$) and tube thickness ($d = 0.15$ cm) as well as the measured axial profile of the gas temperature (3500 K - 1500 K). The latter was determined from measurements of the rotational temperature of the OH molecular band in the range 306 - 315 nm. Phase and amplitude sensitive recording provides the data for the axial wavenumber and wave attenuation coefficient. The wavenumber decreases along the generated plasma torch. The electron density (N_e) axial profile as determined from measurements of H_β Stark broadening is in agreement with the theoretical one.

KTP 78 Wave Driven Ar-N₂-H₂ Plasma J. HENRIQUES, F.M. DIAS, E. TATAROVA, C.M. FERREIRA, IPFN, INSTITUTO SUPERIOR TÉCNICO, 1049-001 LISBOA, PORTUGAL TEAM, An experimental investigation of the spatial structure of an Ar-N₂-H₂ plasma torch is presented. A surface wave induced microwave (2.45 GHz) plasma torch is created using a conventional, surfaguide based set-up. A cylindrical, fused quartz discharge tube (with internal and external radii $R_1 = 7.5$ mm and $R_2 = 9.0$ mm, respectively) is filled by an Ar(78%)-N₂(20%)-H₂(2%) gas mixture at atmospheric pressure. A spectroscopic imaging system able to couple the plasma-emitted radiation into a SPEX 1250M spectrometer, equipped with a nitrogen cooled CCD camera, was used to measure 2D(r,z) profiles of emission intensities and line profiles. Abel inversion has been applied to derive the radial profiles from the side-on measurements. The H_β line profiles have been measured to determine the corresponding Doppler temperature and the electron density. The measurements are well fitted by Voigt profiles, whose Gaussian and Lorentzian components have been deconvoluted. In this way, hyperthermal hydrogen atoms have been detected. The measured Doppler temperatures (5,000–8,000 K) are higher than the rotational temperature by a factor of about 2. The 2D map of the electron density (5×10^{12} – 5×10^{13} cm⁻³) was also obtained. Acknowledgement- This work was supported by the Fundação para a Ciência e a Tecnologia, Ministério da Ciência, Tecnologia e Ensino Superior, Portugal

KTP 79 LIGHTING PLASMAS: GLOWS, ARCS, FLAT PANELS, NOVEL SOURCES, OTHERS

KTP 80 UV Discharge Lamp on Distilled Water Vapor SVETLANA AVTAEVA, *Kyrgyz-Russian Slavic University* ANDRIJ GENERAL, *Institute of Electron Physics NAS Ukraine* Recently interest in sources of ultra-violet (UV) radiation in a wavelength range of 200-400 nm has increased. Therefore we have created a source of spontaneous, incoherent UV radiation on distilled water vapor excited by the low-pressure capacitive discharge (1 Torr). Spectral, temporary and energy characteristics of the spontaneous UV radiation source have been experimentally studied. In addition the electron energy distribution function (EEDF), the mean electron energy, electron transport coefficients, rate constants of elastic and inelastic electron collisions with atoms and electron energy losses have been theoretically calculated with help of the program Bolsig+. Results of the theoretical calculation are used for optimizing radiative characteristics of the radiation source. Advantages of the created lamp based on the low-pressure capacitive discharge on water vapor are: 1) inexpensive and ecologically safe working medium on the basis of hydroxyl radicals; 2) absence of electrodes in a gas-discharge zone that allows to hope for significant increasing their useful operation resource, in comparison with lamps of glow or other discharges; 3) simplicity of the lamp construction.

KTP 81 A study on the influence of operating circuit on the position of emission point of fluorescent lamp TADAO UETSUKI, YUKI GENBA, *Tsuyama National College of Technology* TAKASHI KANDA, *Panasonic Electric Works Ltd.* High efficiency fluorescent lamp systems driven by high frequency are very popular for general lighting. Therefore it is very beneficial to be able to predict the lamp's life before the lamp dying, because people can buy a new lamp just before the lamp dying and need not have stocks. In order to judge the lifetime of a lamp it is very useful to know where the emission point is on the electrode filament. With regard to a method for grasping the emission point, it has been reported that the distance from the emission point to the end of the filament can be calculated by measuring the voltage across the filament and the currents flowing in both ends of the filament. The lamp's life can be predicted by grasping the movement of the emission point with operating time. Therefore it is very important to confirm whether the movement of the emission point changes or not when the operating circuit is changed. The authors investigated the difference in the way the emission points moved for two lamp systems which are very popular. One system had an electronic ballast having an auxiliary power source for the heating cathode. Another system had an electronic ballast with no power source, but with a capacitor connected to the lamp in parallel. In this presentation these measurement results will be reported.

KTP 82 A study on the ignition characteristics of inductively coupled electrode-less lamp TADAU UETSUKI, MASAO FUJITA, *Tsuyama National college of Technology* MOTOHIRO SAIMI, HIDENORI KAKEHASHI, *Panasonic Electric Works Ltd.* Almost twenty years have passed since the first electrode-less lamp operated at 13.56MHz was put on the market. Since then, it has come to be expected that the lumen output and the efficiency of these lamp systems would be improved. The present electrode-less lamp system operated at 135kHz has higher efficiency and output than the high pressure mercury lamp system which is very popular in the market. However, the ignition mechanism of the electrode-less lamp has not yet been completely worked out. To grasp the ignition voltage and time is very important for designing this lamp system, because these influence the cost of the system. The authors investigated how to reduce the ignition time. With regard to the ignition for magnetic coupled electrode-less lamp, it was reported that there are theoretically two types of ignition, E-discharge and H-discharge. However, the definition of the ignition actually is regarded as the time when the H-discharge occurs. The authors observed the starting state of the electrode-less lamp and found that the performance of the circuit influenced the transition from E- discharge to H- discharge. The large current is necessary for the smooth transition from E- discharge to H- discharge right after the E- discharge occurs.

KTP 83 A study on the relationship between CCFL's characteristics and gas pressure TADAU UETSUKI, NAOKI AOYAMA, *Tsuyama National college of Technology* YUJI TAKEDA, HIDETOSHI YANO, *Harison Toshiba Lighting Corp.* OSAMU FUKUMASA, *Ube National College of Technology* A continuous improvement in the lumen output and efficacy of the cold cathode fluorescent lamps (CCFLs) used for the backlight of LC-TV's is always expected. The lumen output and efficacy can be improved by controlling the electric field intensity by changing gas pressure. Therefore it is very important to grasp the relationship between the CCFL's characteristics and gas pressure. The authors investigated the influence of gas pressure on the cathode fall voltage (CFV) and the electric field intensity of the positive column. The measurement results show mainly three points. The first is that the CFV of the Ne-Ar lamp reaches a minimum at 5.3kPa, while the CFVs of the Ne-Ar-Hg lamps decrease with a rise in gas pressure monotonously. This difference is caused by the variation of the sheath thickness arising from the presence of the mercury. The second point is that the CFV of the Ni-electrode lamp is higher than the Mo-electrode lamps' whether the mercury is present or not. This is caused by the difference of gamma coefficients between Ni and Mo. The third point is that the electric field strength increases with a rise in gas pressure whether the mercury is present or not. This is caused by the increase of the elastic collision loss between electrons and atoms.

KTP 84 UV Discharge Lamp on Alcohol Vapor SVETLANA AVTAEVA, *Kyrgyz-Russian Slavic University* ANDRIJ HENERAL, *Institute of Electron Physics* The non coherent sources of UV radiation based on safe and nontoxic gaseous mixtures have good aspects for different applications. The paper reports about experimental investigations of the high voltage capacitive discharge in alcohol vapor. The time-integrated emission spectra have been studied in the wavelength interval from 200 to 400 nm at alcohol vapor pressure of 1 Torr. In the spectra the most intensive bands were vibrational bands of the $CO(b \rightarrow a)$ transition with heads at 283.3 (0-0), 297.7 (0-1), 313.4 (0-2), 330.5 (0-3) and

349.3 nm (0-4). The (0-2) band of CO molecules superimposes with (0-0) and (1-1) vibrational bands of the $CH(C\{to X\})$ transition with Q -heads at 314.49 and 315.66 nm on the long wavelength side and with bands of OH radicals with intensity maximums at 308.1 and 309.2 nm ($A \rightarrow X$ transition) on the short wavelength side. No other radiating species were detected. The emitting surface area of the lamp is 220 cm^2 , average output power of the UV radiation is 70 mW and the estimated efficiency is 0.2%. This source of UV radiation can be applied in photochemistry, in medicine, for disinfection of medical tools, in ecology and for purification and disinfection of water from different pathogenic microorganisms.

KTP 85 Study of the 222 nm KrCl emission produced by nanosecond pulsed arrays of microdischarges VIRGINIE MARTIN, GERARD BAUVILLE, BERNARD LACOUR, VINCENT PUECH, *LPGP, CNRS-UPS, Orsay, France* Microdischarges operating in DC mode have been widely used for producing VUV emission from rare-gas excimers. However for biological applications, pulsed UV sources emitting in the range 200-280 nm (DNA absorption band) are required. They can be obtained from exciplex molecules produced in discharges operating in rare-gas halogen mixtures. Up to now, DBD's have been mainly used to generate these emissions. However, the use of arrays of microdischarges could be very advantageous due to a simpler geometry, a reduced operating voltage and the possibility of higher power loading. The present paper reports results obtained from arrays of microdischarges powered, in Kr/Cl₂ mixtures, by nanosecond pulsed discharges operating at high repetition frequency. It will be shown that, without individual resistive ballasting, the nanosecond pulsed mode allows the simultaneous ignition of all microdischarges. As a result, an intense emission at 222 nm is obtained. Weak emissions from Cl₂* at 258 nm and from krypton at 762 nm are also detected. The influence, on the intensity of these emissions, of the different experimental parameters: total pressure, chlorine concentration, energy per pulse and repetition rate frequency, was studied and the conditions allowing the optimization of the 222 nm will be reported.

KTP 86 Modeling and simulation of emitter effects at cathodes in high intensity discharge lamps* ANDRE BERGNER, FRANK SCHARF, JUERGEN MENTEL, *Ruhr University Bochum, Germany* The temperature of tungsten cathodes in high intensity discharge lamps may be kept down by reducing the work function ϕ . This can be accomplished by an atomic dipole layer on the electrode surface made of a certain emitter material, e.g. thorium. If the emitter material is deposited by an ion current, ϕ will be reduced mainly in the center of the arc attachment area. This local reduction may cause a constricted arc attachment, called emitter spot. The power balance of the arc cathode can be simulated using the power flux density and current density as boundary conditions [1]. Both are functions of ϕ and the local cathode surface temperature. The emitter spot is simulated in accordance with experimental results [2] by a superposition of transfer functions for $\phi = 4.55$ eV and $\phi < 4.55$ eV, weighted in dependence on temperature. [1] S. Lichtenberg et al. *Phys. D: Appl. Phys.* **38** (2005) 3112-3127. [2] G. Kühn et al., *Phys. Rev. E* **75**, 016406 (2007).

*Supported by Deutsche Forschungsgemeinschaft GK1051.

KTP 87 Investigation of Ce-emitters in high intensity discharge lamps* CORNELIA RUHRMANN, MICHAEL WESTERMEIER, JENS REINELT, PETER AWAKOWICZ, JUERGEN MENTEL, *Ruhr-University Bochum, Germany* The improvement of lifetime is a particular interest of actual research into HID lamps. It can be achieved by a reduction of the temperature of the lamp electrodes being accomplished by the so called "emitter effect." It is generated by an atomic monolayer of certain emitter elements (e.g. Ce, Dy) on the tungsten electrode surface by which the work function is reduced. By means of a special optical absorption spectroscopy setup - presented in an accompanying contribution - the absorption coefficient of resonance lines is measured and the ground state atom density of the respective emitter material is determined within the plasma. Spatial and phase resolved measurements of Ce-densities and associated electrode temperatures in special research HID lamps will be presented for low and high frequencies. An emitter effect is observed not only in the cathodic but also in the anodic phase. At high frequencies the effect of the emitter material on the electrode temperature converges in both phases due to the inertia of the Ce-atoms and ions.

*Supported by Philips Lighting NL, the DFG (GK 1051) and the RUB Research School.

KTP 88 Ab initio based calculation of emission properties of Ar-AlCl₃ glow discharge MAXIM DEMINSKY, BORIS POTAPKIN, STANISLAV UMANSKII, ALEXANDER ZAITSEVSKII, *Kintech Lab, Moscow, Russia* DAVID SMITH, *GE Global Research, Niskayuna, US* DARRYL MICHAEL, TIMOTHY SOMMERER, *GE Global Research, Niskayuna, US* Emission properties of Ar-AlCl₃ DC glow discharge were calculated using "Chemical Workbench" VIBRAKIN code in frame work of quasi 1D model. Unknown properties of atoms and molecules were calculated from first principles. Potential energy curves of Al_xCl_y⁻ negative ions were performed by approximate quadratic coupled cluster (AQCC) and SCF methods. Potential energy curves, transition dipole moments of neutral species Al_xCl_y were calculated based on many-body multipartitioning perturbation theory (MPPT). These data are used for evaluation of the cross sections of the electron impact dissociative attachment and vibrational excitation for AlCl₃ and fragments of its decomposition. The cross sections of the electron impact excitation of electronic states of atoms and molecules are evaluated in frame work modified Born approximation with taking into account electron exchange. Based on calculated properties of molecular ions, the rate parameters of thermal ion-molecular reactions of molecular ions conversion were calculated. The calculation results present dependencies of the electron energy balance and the emission efficiency as a function of the plasma parameters.

KTP 89 Non Empirical Calculation of Emission Properties of Xe:Cl₂:Ar Glow Discharge MAXIM DEMINSKY, *Kintech Lab, Moscow, Russia* IRINA CHERNYSHEVA, ALEXANDER ELETSKII, IGOR KOCHETOV, ANDREI ZAITSEVSKII, BORIS POTAPKIN, *Kintech Lab, Moscow, Russia* DARRYL MICHAEL, DAVID SMITH, TIMOTHY SOMMERER, *GE Global Research, Niskayuna, US* Emission properties of the Xe:Cl₂:Ar DC glow discharge have been calculated using the kinetic code VIBROKIN. Potential energy curves for the ground and excited states and the electronic transitions strengths of XeCl excimer molecule are calculated ab initio within the quasirelativistic many-electron intermediate Hamiltonian approach; the relativity is introduced through the relativistic pseudo-potentials of atomic cores.

The cross section of the harpooning reaction responsible for formation of XeCl excimer molecule is evaluated on the basis of the asymptotic method. The similar approach was also applied for estimation of the cross section for quenching the XeCl excimer molecule and metastable Xe atoms by Cl₂ molecule. The electron impact excitation cross sections for the mixture components as well as the Cl₂ dissociation cross section were calculated using modified Born approximation, taking into account electron exchange. The calculation results present dependencies of the electron energy balance and the excimer emission efficiency as a function of the reduced electrical field strength, electron number density and gas mixture composition.

KTP 90 Parametric study of the breakdown of high intensity discharge lamps filled with xenon* MARTIN WENDT, MANFRED KETTLITZ, DETLEF LOFFHAGEN, *INP Greifswald, Felix-Hausdorff-Str. 2, 17489 Greifswald, Germany* SILKE PETERS, *PTB, Bundesallee 100, 38116 Braunschweig, Germany* A parametric study of model results on the breakdown of high intensity discharge lamps filled with xenon at pressures between 0.1 and 5 bar is presented. The results are compared with experimental measurements of voltage and current waveforms obtained for voltage rates of increase from 5 mV/ns to 100 V/ns. Specially designed lamps ensure a volume breakdown of the gas. The time-dependent, spatially one-dimensional model comprises the Poisson equation, electron energy balance and species continuity equations using the drift-diffusion approximation for the fluxes. The set of equations is solved on an inhomogeneous grid using the cubic interpolated propagation scheme with an adaptive time step. The electron transport parameters were used as function of the local mean electron energy. They were determined by solving the homogeneous Boltzmann equation. The breakdown voltages obtained by the model increase with growing pressure and voltage rate and are in good agreement with the experiments. A cathode-directed ionization front is found whose velocity increases with rising voltage rate and falling pressure.

*This work was supported by the BMBF project with FKZ 13N8604.

KTP 91 Ultra High Luminance and Luminous Efficacy Mercury-free Flat Fluorescent Lamp* IN WOO SEO, BYUNG JOO OH, JAE-CHUL JUNG, KI-WOONG WHANG, *Seoul National University* We proposed a new Mercury-free Flat Fluorescent Lamp (MFFL) as a flat light source which can be used as an alternative of conventional line-type Cold Cathode Fluorescent Lamp (CCFL) containing Mercury. The MFFL using dielectric barrier discharge with Ne-Xe gas mixtures has a pair of the parallel-running main electrodes covered by dielectric layer in a 40x40 mm size of the emission area as a unit cell. A new electrode structure and optimized driving methods have been adopted to make an effective glow discharge which shows a wide driving voltage margin. In order to realize the high luminance and luminous efficacy MFFLs, we optimized the phosphor profile to enlarge the surface area. The MFFL with the new phosphor profile shows a very wide luminance range from 2,600 to 17,000 nit with the corresponding luminous efficacy from 66 to 32.5 lm/W. The results were obtained with the color coordinate of the phosphor to be around (0.25, 0.23), which is required for LCD backlights. The work to realize improved luminance and luminous efficacy MFFLs with the color coordinate (0.32, 0.32) for daylight lighting is in progress.

*This work was supported by Samsung Electronics Co., LTD. LCD Division.

KTP 92 Rapid estimates of plasma emission spectra from any atomic species DAVID SMITH, TIM SOMMERER, *GE Research, USA* A method has been developed and implemented to provide rapid estimates of emission spectra from plasmas in atomic gases. Results from these calculations have been validated against experimental data for species with both sparse (Sn) and dense (Zr) emission spectra. The calculation relies on two profound assumptions on the atomic-plasma kinetics, namely a modified Boltzmann distribution of the excited-state densities accounting for a non-Maxwellian distribution, and a general expression for radiation trapping. The atomic density and excitation temperature are the input variables; the excitation temperature includes an additional scaling function to simulate the inelastic depletion of high-energy electrons. The model has been applied to identify Sb, Ge, Ga, Sn, Pt, and Mg as the most promising atoms for germicidal sources (excluding Hg). Additionally it has used to select species and gas phase densities of additives to avoid arc constriction in plasmas where most of the radiation comes from atoms with dense emission spectra.

KTP 93 PLASMA PROPULSION AND AERODYNAMICS

KTP 94 Performance prediction of a novel microplasma thruster with microhollow cathode discharge* GUANGQING XIA, *Dalian University of Technology* GENWANG MAO, *Northwestern Polytechnical University* The gas heating of microhollow cathode discharge (MHCD) is found to have a strong relation with overall discharge behavior in the theoretical and experimental investigation. It provides crucial understanding to support the application and preliminary design of MHCD plasma thruster. The hot gas heated is expanded through a Laval-type converging-diverging micro-nozzle to produce thrust. With the MHCD hole diameter 100 μm and at the pressure 50~750 Torr, input power 0.15~2 W and mass flow rate 0.15~1.5 mg/s, the thrust produced by this kind of propulsion system is preliminary expected to be in the range of several tens to several thousands μN and the specific impulse is evaluated on the order of 600~1000 N·s/kg when using argon while on the order of 3000 N·s/kg using helium as the propellant gas. From the main performance of the MHCD plasma thruster, it can be applied as a new microplasma propulsion system for attitude control and station keeping of nano-satellites.

*This work was supported by China Scholarship Council (CSC).

KTP 95 A multi-fluid 2-D simulation of a co-axial Hall plasma discharge AARON KNOLL, MARK CAPPELLI, *High Temperature Gasdynamics Laboratory, Stanford University* A multi-fluid 2-D simulation of a co-axial E x B plasma discharge is presented, resolving the azimuthal dynamics leading to the growth and saturation of high-frequency (0.5 - 10 MHz) azimuthally-propagating fluctuations. The simulation accounts for finite-rate ionization kinetics, with associated losses of particles and energy to the bounding ceramic walls. These discharges are typical of Hall thruster plasma accelerators, which are increasingly being used in space propulsion applications. The simulations presented are for full scale thrusters that operate in the 1 kW power levels, capturing the entire azimuthal domain. The simulations focus on the role played by these fluctuations in establishing the cross-field electron current in regions of relatively strong magnetic fields (50-200 Gauss). The time-average predictions for plasma properties are in qualitative

and quantitative agreement with experiments, and the findings seem to be supportive of the experimental results that indicate that high frequency fluctuations may be more important at defining electron current at lower discharge voltages, where the azimuthal electron shear is small.

KTP 96 V-I Characteristics and Power Measurements in Asymmetric Dielectric Barrier Discharges* DMITRY OPAITS, MIKHAIL SHNEIDER, RICHARD MILES, *Princeton University* SERGEY MACHERET, *Lockheed Martin* Dielectric barrier discharge (DBD) plasma actuators for flow control have been under extensive studies for the last decade. It is usually driven by a sinusoidal voltage profile at up to 20 kHz frequency, although some other voltage profiles, such as square, triangular, and positive and negative sawtooth, were also used and in some cases demonstrated an improvement in performance. A voltage profile consisting of nanosecond pulses added to bias voltage was also found to be effective in generating wall jets. It was also shown that if the dielectric is coated with a semiconductive material the actuator can be driven by dc voltage only. This work will present V-I characteristics and power consumption of the plasma actuators driven by various voltage profile, including sinusoidal in wide range of frequencies, nanosecond pulses and dc, and compare their efficiency.

*This work is supported through a grant from NASA Glenn under David Ashpis (contract number: NNX07AC02A).

KTP 97 Particle Simulation of a Micro ICP Plasma Source for Miniature Ion Thruster YOSHINORI TAKAO, KOJI ERIGUCHI, KOUICHI ONO, *Department of Aeronautics and Astronautics, Kyoto University* There has recently been an ongoing trend toward decreasing the mass, dimension, and overall complexity of spacecraft. Propulsion systems are no exception. We have developed an electrothermal-type microthruster so far, which can produce a relatively high thrust, and have investigated the thrust performance with an experimental and numerical approach. On the other hand, a microthruster with a high specific impulse, such as ion thruster, is also required. The micro ion thruster presented here uses a cylindrical micro ICP with a flat spiral coil for its ion source, the inner radius and the length of which are 3 mm and 6 mm, respectively. To investigate the plasma characteristics of the source, we have developed a particle simulation model (PIC/MC: Particle-in-Cell/Monte Carlo) for Ar gas as a propellant. The simulation results showed that the electron density obtained was $\sim 10^{17} \text{ m}^{-3}$ at an Ar gas pressure of 4 mTorr with an absorbed power of 10 mW, producing a thrust of 50 μN and specific impulse of 7000 s.

KTP 98 Analysis of a new Extraction Aperture for the Non-ambipolar Electron Source* JESSE GUDMUNDSON, NOAH HERSHKOWITZ, *University of Wisconsin-Madison* LUTFI OKSUZ, *Suleyman Demirel University* The Nonambipolar Electron Source (NES) is a radio frequency plasma-based electron source that does not rely on electron emission at a cathode. All electrons are extracted at an electron sheath through a biased ring and all ions are lost radially to a separately biased cylindrical graphite Faraday shield. Plasma density increases and electron confinement at the ring improves by the addition of an axial magnetic field. An electromagnet in the original NES has been replaced by a NdFeB magnet array. Approximately 30% of the electron current was extracted using the magnet array. The remainder was lost to the ring

while the electromagnet provided 90% extraction efficiency. A disk with a concentric hole has replaced the ring and the hole diameter was varied to improve extraction efficiency. The disk was separated from the cylinder to prevent shorting between them and sputtering of graphite on the insulator between the ring and the cylinder seen previously. Plasma potential, plasma density, electron temperature, and electron energies in the plume measurements as well as time resolved ICCD camera images of the plume will be discussed.

*Work supported by DOE Grant No. DE-FG02-97ER54437.

KTP 99 Wall material effect on electron transport in Hall thruster discharge* YEVGENY RAITSES, LEONID DORF,[†] IGOR KAGANOVICH, NATHANIEL J. FISCH, *Princeton Plasma Physics Laboratory, Princeton, NJ, USA* DMYTRO SYDORENKO, *University of Alberta, Edmonton, Canada* Plasma-wall interaction is studied for annular Hall thruster configurations, in which collisionless plasma is bounded by channel walls made of ceramic and graphite materials with different secondary electron emission (SEE) properties [1]. Plasma properties and discharge characteristics are measured for different discharge voltages at the same magnetic field [2]. It is shown that the electron cross-field mobility in the thruster with ceramic walls is higher than in the thruster with graphite walls. Results of analytical modeling [3] and particulate-in-cell simulations [4] demonstrate that this effect is a consequence of higher SEE of ceramic materials. [1] Y. Raitses, D. Staack, A. Dunaevsky and N. J. Fisch, *J. Appl. Phys.* 99, 036103 (2006). [2] Y. Raitses, A. Smirnov, D. Staack, and N. J. Fisch, *Phys. Plasmas* 13, 014502 (2006). [3] I. Kaganovich, Y. Raitses, D. Sydorenko and A. Smolyakov, *Phys. Plasmas* 14, 057104 (2007). [4] D. Sydorenko, A. Smolyakov, I. Kaganovich, and Y. Raitses, *Phys. Plasmas* 13, 014501 (2006).

*This work was supported by the US DOE under contract No. DE-AC02-09CH11466.

[†]Present address: Applied Materials, Santa-Clara, CA, USA.

KTP 100 Time resolved Schlieren imaging of DBD actuator flow fields CYRUS NOURGOSTAR, LUTFI OKSUZ, NOAH HERSHKOWITZ, *University of Wisconsin Madison* Schlieren imaging methods measure the first derivative of density in the direction of a knife-edge spatial filter. It has been used extensively in aerodynamic research to visualize the structure of flow fields. With a single barrier planer dielectric barrier discharge (DBD) actuator, Schlieren images clearly show the absence of significant vertical air flow normal to the surface, and no more than few millimeters thick induced boundary layer flow. A gated intensified CCD camera along with a Schlieren system can not only visualize the flow field induced by the actuator, but also temporarily resolve the images of the flow and plasma field. Our time resolved images with triangular applied voltage waveforms indicate that several separate discharge regimes occur during positive and negative going half cycles of single and double barrier DBD actuators. Time resolved Schlieren imaging of both single and double barrier DBDs with different applied waveforms, discharge parameters and electrode geometries reveal important information on the induced flow structure.

KTP 101 Nonequilibrium Supersonic Flow Field Measurements in a Mach 5 Plasma Wind Tunnel MUNETAKE NISHIHARA, KEISUKE TAKASHIMA, NAIBO JIANG, WALTER LEMPET, IGOR ADAMOVICH, J. WILLIAM RICH, *The Ohio State University* The effect of molecular energy transfer in non-equilibrium gas dynamic flows on supersonic/hypersonic flow field is studied using a Mach 5 nonequilibrium plasma wind tunnel. The tunnel uses a high pressure (0.5-1.0 atm) stabilized glow discharge in its plenum to load energy into internal molecular modes. The electric discharge system incorporates a repetitive nanosecond pulse discharge which weakly ionizes the flow and transverse DC discharge to load power into the vibrational energy mode of nitrogen. Translational temperature of the flow in the discharge remains low, 350-400 K, while vibrational temperature of nitrogen is up to 2,000 K. Vibration-translation (V-T) relaxation of nitrogen downstream of the discharge is accelerated by injecting hydrogen into the flow. The effect of partial vibrational relaxation of nitrogen on a shock wave stand-off distance in front of a cylinder model in a Mach 5 flow is studied by schlieren imaging and by NO Planar Laser-Induced Fluorescence (PLIF) using a pulse burst laser operating at a pulse repetition rate of 20 kHz.

KTP 102 DUSTY PLASMAS

KTP 103 Ion-acoustic solitons in multi-components dusty plasmas AMANDEEP SINGH BAINS, TARSEM SINGH GILL, *Department of Physics, Guru Nanak Dev University, Amritsar 143005* We have considered a hot dusty plasma system containing ions, electrons, positrons and negatively charged dust to study the solitary potential structures. Using reductive perturbation method, the Kadomtsev-Petviashvili (KP) equation has been derived. We have studied the characteristics of ion-acoustic solitary waves associated with negative/positive potential. The nonlinearity and dispersion coefficients are the function of positron to electron density ratio, dust density parameter, ion temperature and ratio of positron to electron temperature. It is observed that the amplitude and width of the solitary potential structures change with the variation of these parameters. We have explored the parametric regime for which the different type of negative/positive solitary potential structures exists.

KTP 104 Some Basic Experiments on Dusty Plasma with Negative Hydrogen Ions Generation* BIPUL KUMAR SAIKIA,[†]S.S. KAUSIK, B. KAKATI, *Centre of Plasma Physics, IPR, Nazirakhat, Tepesia, Sonapur, Kamrup-782402, Assam India* M. BANDYOPADHYAY, *Institute for Plasma Research, Bhat, Gandhinagar, Gujarat-383428, India* Some parametric studies like the effect of discharge current, plasma temperature and working pressure on the charging of dust grains in hot cathode discharge plasma will be presented. The designing concepts of a novel experiment to produce negative hydrogen ions from Cesium coated dust particles and related preliminary studies with dust particles in hydrogen plasma will be presented. The aim of producing negative hydrogen ions is to devise the possibility of using such negative ions in Neutral Beam Injection Heating of Tokamak plasma. **Refs:** S.S. Kausik, M.Chakraborty, P. Dutta, M. Kakati and B.K. Saikia, *Phys. Lett. A* 372, 860 (2008)

*Institute for Plasma Research, Bhat, Gandhinagar-382428, India

[†]Corresponding Author

KTP 105 NEGATIVE ION PLASMAS**KTP 106 ABSTRACT WITHDRAWN****KTP 107 WORKSHOP ON ADVANCES IN THE KINETIC DESCRIPTION OF LOW-TEMPERATURE PLASMAS: APPLICATIONS TO MODELING AND SIMULATION**

KTP 108 Study of the electron kinetics in abnormal dc glow discharges in oxygen by a multiterm approach and Monte Carlo simulations* GORDON K. GRUBERT, DETLEF LOFFHAGEN, *INP Greifswald, Felix-Hausdorff-Str. 2, 17489 Greifswald, Germany* The nonequilibrium properties of the electron component in gas discharge plasmas determine decisively the behavior of the whole discharge. These properties are commonly determined by solving the electron Boltzmann equation using a multiterm approximation of the Legendre polynomial expansion of the electron momentum distribution function or by performing Monte Carlo simulations. For comparative kinetic studies of spatially inhomogeneous plasmas, consistent conditions at the spatial margins of the discharge arrangement are required. Extended boundary conditions at the electron emitting cathode are represented, which are adequate for the direct comparison of multiterm Boltzmann equation calculations and Monte Carlo simulations. First results for dc discharges in oxygen at conditions typical of abnormal glow discharges are discussed. The excellent agreement between the results of both the independent kinetic approaches verifies the extended boundary conditions deduced.

*This work is supported by the Deutsche Forschungsgemeinschaft within the SFB TR 24.

KTP 109 Verification of high voltage rf capacitive sheath models with particle-in-cell simulations YING WANG, *Dept. of Nuclear Engineering, University of California, Berkeley CA 94720* MICHAEL LIEBERMAN, *Dept. of Electrical Engineering and Computer Science, University of California, Berkeley CA 94720* JOHN VERBONCOEUR, *Dept. of Nuclear Engineering, University of California, Berkeley CA 94720* Collisionless and collisional high voltage rf capacitive sheath models were developed in the late 1980's [1]. Given the external parameters of a single-frequency capacitively coupled discharge, plasma parameters including sheath width, electron and ion temperature, plasma den-

sity, power, and ion bombarding energy can be estimated. One-dimensional electrostatic PIC codes XPDP1 [2] and OOPD1 [3] are used to investigate plasma behaviors within rf sheaths and bulk plasma. Electron-neutral collisions only are considered for collisionless sheaths, while ion-neutral collisions are taken into account for collisional sheaths. The collisionless sheath model is verified very well by PIC simulations for the rf current-driven and voltage-driven cases. Results will be reported for collisional sheaths also. [1] M. A. Lieberman, *IEEE Trans. Plasma Sci.* 16 (1988) 638; 17 (1989) 338 [2] J. P. Verboncoeur, M. V. Alves, V. Vahedi, and C. K. Birdsall, *J. Comp. Phys.* 104 (1993) 321 [3] J. P. Verboncoeur, A. B. Langdon and N. T. Gladd, *Comp. Phys. Comm.* 87 (1995) 199

KTP 110 On Application of Transport Coefficients in Plasma Modelling Z. LJ. PETROVIC, S. DUJKO, Z. NIKITOVIC, D. MARIC, G. MALOVIC, *Institute of Physics Belgrade* R.E. ROBSON, R.D. WHITE, *James Cook University Townsville* In this paper we review recent developments in the transport theory as developed to deal with the so-called swarm experiments. We analyze where and how such results can affect the outcome of the plasma models [1]. In principle it is well understood that modeling of plasmas requires representing a large number of processes, and for a large group of these one does not know all the pertinent physical processes and even more so there is a general shortage of data. In that respect insisting on purity in the representation of the charged particle, in particular electron transport seems unnecessary. Nevertheless we wish to draw attention that neglecting some aspects of electron transport may lead to neglecting some important aspects of physics. We wish to draw attention to proper representation of the transport in crossed electric and magnetic fields, differences between flux and bulk transport properties under appreciable influence of non-conservative processes, temporal development of transport coefficients, anisotropy of diffusion and anomalous longitudinal diffusion when field changes direction and many more. Finally we wish to draw attention that plasma models should be benchmarked against basic swarm test models to verify how adequate the representation of some processes is. The stage of development of plasma models has reached such sophistication that perhaps requires that all aspects should be developed at the best available level. [1] RE Robson et al. *Rev. Modern Phys.* 77 (4) (2005) 1303.

KTP 111 Verifying Unmatter by Experiments, More Types of Unmatter, and a Quantum Chromodynamics Formula FLORENTIN SMARANDACHE, *University of New Mexico, Gallup Campus* As shown, experiments registered unmatter: a new kind of matter whose atoms include both nucleons and anti-nucleons, while their life span was very short, no more than 10^{-20} sec. Stable states of unmatter can be built on quarks and anti-quarks: applying the unmatter principle here it is obtained a quantum chromodynamics formula that gives many combinations of unmatter built on quarks and anti-quarks.

SESSION LW1: DUSTY AND NEGATIVE ION PLASMAS
 Wednesday Morning, 21 October 2009
 Ballroom 1, Saratoga Hilton at 8:00
 Lawrence Overzet, University of Texas at Dallas, presiding

8:00

LW1 1 Numerical simulations of a nanodusty RF plasma*
 STEVEN GIRSHICK, PULKIT AGARWAL, *University of Minnesota* The nucleation, growth, charging and transport of nanoparticles in a low-pressure RF plasma have profound effects on the plasma. In previous work we developed a numerical model for the spatiotemporal evolution of the plasma-nanoparticle system. The model simulates a one-dimensional parallel-plate capacitively-coupled plasma. It includes solutions to electron and ion population balance equations, and Poisson's equation for the electric field, models stochastic particle charging, and self-consistently solves the aerosol general dynamic equation, including particle size- and charge-dependent coagulation (including the effect of image potentials), and particle transport by electrostatic forces, Brownian diffusion, ion drag and thermophoresis. In the present work this model is used to explore the effect of system parameters on the nanoparticle and plasma behavior. Parameters studied include pressure, temperature and temperature distribution, applied voltage and gas flow rate. In addition we examine the behavior of the system at long times, when particles are pushed by ion drag out of the center of the plasma, opening a void that allows fresh nucleation.

*This work was partially supported by the U.S. National Science Foundation under grant CBET-0756315.

8:15

LW1 2 Model and experimental evidence of heating of nanoparticles in low-pressure silane plasmas* FEDERICO GALLI, UWE KORTSHAGEN, *University of Minnesota* Recently we developed a nanoparticle-plasma charging-heating model which included the effect of collisions between ions and neutrals in proximity of the particles and showed that for pressures of a few Torr a charge distribution that is less negative than collisionless orbital motion limited theory is obtained. The model also predicted the nanoparticle temperature distribution and morphology (amorphous or crystalline) to be a function of ion density. To support the theory a batch plasma reactor was used to nucleate, grow and crystallize silicon nanoparticles. The nanoparticle size distribution and morphology were characterized using transmission electron microscopy, x ray diffraction and Raman light scattering. Experimental results indeed show a strong correlation between crystallinity and ion density, here measured with time and space resolution using a capacitive probe technique. The use of a simple floating potential probe method is also presented. The probe traces show distinctive features belonging to a nucleation and growth phase and a successive diffusional loss phase. A simple theoretical model is proposed to explain probe measurements as a function of the other plasma properties.

*This work is supported by the National Science Foundation under grant CBET-0500332.

8:30

LW1 3 Formation of ion-ion plasmas and ion beams in continuously rf generated plasmas ANE AANESLAND, LARA POPELIER, PASCAL CHABERT, *LPP, Ecole Polytechnique* Ion-ion plasmas can offer useful advantages in a variety of applications where neutral or quasi-neutral beams are used, some examples are charge-free etching, neutral beam injections for fusion or for electric propulsion. For many electronegative gases the cross sections are such that ionizing collisions (creating positive ions) are dominating at high electron temperatures while electron attachment dominates at low Te (creating negative ions). Hence, ion-ion plasmas are therefore generally formed in the afterglow of electronegative plasmas or in the periphery of magnetized electronegative plasmas; in both cases the ion-ion plasma is formed where or when the electron temperature drops and efficient electron attachment can occur. The ion density in the ion-ion plasma region drops generally by a factor of ten or more, compared to the regions where electrons are present. This density decrease is catastrophic for the efficiency of any application using ion-ion plasmas. We demonstrate here that by tailoring Te and by injecting the electronegative gas in both a high and a low Te region can efficiently produce ion-ion plasmas. Grid-less extraction and acceleration of ions from an ion-ion plasma, by biasing the bulk plasma to large positive or negative voltages, is being investigated. Results from this experimental investigation will be reported here.

8:45

LW1 4 A global (volume averaged) model of the chlorine discharge JON TOMAS GUDMUNDSSON, EYTHOR GISLI THORSTEINSSON, *University of Iceland* A global (volume averaged) model is developed for the chlorine discharge using a revised reaction set [1]. The model is applied to explore both a steady state and pulsed modulated discharge. Various calculated plasma parameters are compared to measurements found in the literature, showing a good overall agreement. The reaction rates for the various reactions are evaluated in the pressure range 1 – 100 mTorr. In particular we explore the dissociation process as well as the creation and destruction of the negative ions Cl^- . The mechanism for Cl creation is complex, although electron impact dissociation dominates with roughly 50 – 60 % contribution, dissociative electron attachment is also of importance and mutual neutralization is an important contributor to the production of Cl atoms at higher pressures. The electronegativity increases rapidly with decreasing dissociation fraction since the Cl^- ions are created entirely by dissociative electron attachment, predominantly from $\text{Cl}_2(v = 0)$ but $\text{Cl}_2(v > 0)$ has upto 14 % contribution at 100 mTorr. The negative ion Cl^- is lost almost entirely through mutual neutralization with Cl_2^+ , but Cl^+ has a significant contribution at low pressure. Furthermore, dilution by argon was explored. Dilution by argon increases the electron temperature and the density of Cl^+ ions significantly. [1] E. G. Thorsteinsson and J. T. Gudmundsson, *Plasma Sources Science and Technology*, submitted 2009

9:00

LW1 5 Negative ion temperature in a low-pressure oxygen ICP discharge DEREK MONAHAN, MILES TURNER, *Dublin City University* The primary reaction mechanism leading to the formation of negative ions under typical oxygen discharge conditions is dissociative attachment of molecular O_2 . Though unable to absorb significant energy from the applied rf field these ions are formed "hot," acquiring kinetic energy from the local ambipolar field and via the process of chemical dissociation. However, their negative

charge and large mass (relative to the electrons) means they are confined to the discharge bulk and "cooled" efficiently in elastic collisions with the background gas. Thus, one commonly assumes that the effective negative ion temperature, T_- , is in approximate equilibrium with the background gas temperature, T_g . In our ICP-like oxygen plasma simulations, we observe a notable increase in T_- as the $O_2(a^1\Delta_g)$ metastable density is increased. We attribute this increase in effective temperature to an increase in the destruction rate of the negative ions and conclude that, in a sufficiently destructive plasma environment, T_- may exceed T_g considerably.

9:15

LW1 6 Time averaged negative ion density measurements in a reactive pulsed DC magnetron using the eclipse photodetachment method ROBERT DODD, SHAODON YOU, PAUL BRYANT, JAMES BRADLEY, *University of Liverpool* Using Langmuir probe assisted laser photodetachment technique time averaged negative ion density in the bulk plasma of a reactive

pulsed DC magnetron has been determined. Experimental results are shown for various oxygen / argon gas mixtures (0 - 100%), applied power (300 - 600 W), magnetron frequency (5 - 100 kHz) and total discharge pressure (2 - 25 mTorr). Laser photodetachment measurements showed the O^- ion to dominate over O_2^- . The maximum ratio of the negative ion to electron density, α , was found to be 0.2, weakly electronegative plasma ($\alpha < 1$). Variation of the operating parameters showed clear trends in the negative ion densities with maximums observed with increasing power (at 318 W) and oxygen partial pressure (30% O_2). With variation of operating parameters clear trends in α were seen. For instance, with increasing magnetron power α was found to decrease from 0.2 to 0.01. This trend was accompanied by a steady rise in the electron density. This observation was attributed to the enhanced detachment (destruction) rate of O^- ions as the energy of secondary electrons from the cathode increased with increased target voltage. These new results show significant concentrations of negative ions are present in the bulk magnetron plasma when operated in argon / oxygen gas mixtures during pulsed DC sputtering.

SESSION LW2: ATOMIC DATA FOR MODELING

Wednesday Morning, 21 October 2009; Ballroom 2, Saratoga Hilton at 8:00; Dmitry Fursa, Curtin University of Technology, presiding

8:00

LW2 1 Electron impact excitation data for modeling planetary atmospheres and cometary comae.

MICHAEL BRUNGER,* *ARC Centre for Antimatter-Matter Studies, Flinders University*

Measurements were undertaken of electron impact cross sections for vibrational and electronic excitation of NO. Incorporation of these in models showed that electron impact excitation produced a proportion of the (1 → 0) emissions near 5.3 μm in aurora. A study of the role of electronically excited N_2 in the production of nitric oxide, using new compilations of the relevant cross sections, showed that electron-impact excitation is significant. A compilation of recent experimental and theoretical cross sections for electron impact excitation of vibrational modes in CO_2 was undertaken and applied in an updated calculation of electron cooling rates in the atmosphere of Mars. These rates were found to be substantially larger in the very cold part of the Martian upper atmosphere, giving a possible explanation for why that region was measured to be colder than expected from modeling. Recent theoretical cross sections for electron-impact excitation of the $A^1\Pi$ state of CO were shown to be consistent with recent laboratory measurements. They were then applied in a simulation of the Fourth Positive emissions from CO in comet Hale-Bopp. It was found that the electron-impact excitation component is substantial, with implications for one estimate of the abundance of CO in the comet.

*Collaborator: Laurence Campbell

8:30

LW2 2 Electron-molecule processes relevant to planetary atmospheres.*

PAUL JOHNSON, *Jet Propulsion Laboratory*

Electron-molecule collisions play an important role in the nitrogen-rich upper atmospheres of Titan, Triton, and Earth. Modeling these processes requires accurate laboratory data. To this end, measurements and analyses of recent electron impact excitation experiments with molecular nitrogen are presented. Absolute excitation cross sections for transitions from the $X^1\Sigma_g^+(v''=0)$ to the $C^3\Pi_u$, $E^3\Sigma_g^+$, $a''^1\Sigma_g^+$, $b^1\Pi_u$, $c_3^1\Pi_u$, $o_3^1\Pi_u$, $b'^1\Sigma_u^+$, $c_4^1\Sigma_u^+$, $G^3\Pi_u$ and $F^3\Pi_u$ states are determined from electron energy loss measurements, integrated over a broad range of scattering angles, with incident electron energies ranging from 13 eV to 100 eV. Vibrationally resolved excitation of the $C^3\Pi_u(v')$ state for the $v'=0, 1, 2, 3$, and 4 levels will also be discussed, which indicates non-Franck-Condon behavior below roughly 30 eV. Results from rotationally resolved electron-impact induced VUV emission measurements will also be discussed. Of particular interest is the predicted variation of predissociation yield with increasing rotational quantum number. This is expected to introduce additional temperature dependencies to atmospheric models. Preliminary results of vibrationally resolved excitation functions for electron impact induced emissions of the Lyman-Birge-Hopfield (LBH) band system will be presented. Finally, we will discuss an investigation into e^-H_2 processes related to the Jovian and Saturnian aurora as well as the recently identified atomic hydrogen plume on Saturn.

*Support from NASA's Planetary Atmospheres and Outer Planets Research Programs is gratefully acknowledged.

9:00

LW2 3 Atomic Data Needs for Modeling Supernova Light Curves.*CHRISTOPHER FONTES,[†] *Los Alamos National Laboratory*

The modeling of supernovae requires the application of knowledge from a wide range of numerical and physical disciplines. The requisite expertise includes hydrodynamics, radiation transport, nuclear physics and atomic physics. Recently, there has been increased interest in improving the number and quality of supernova observations, as exemplified by missions such as NSF's Large Synoptic Survey Telescope (LSST) and NASA/DOE's Joint Dark Energy Mission (JDEM). In support of these missions, the corresponding modeling efforts are also being expanded. In this talk, the role of atomic data is discussed as it pertains to the modeling of radiation emitted by supernovae. The Los Alamos OPLIB opacity database has previously been used in this context to provide atomic opacities for modeling plasmas under local thermodynamic equilibrium (LTE) conditions. The Los Alamos suite of atomic physics codes is currently being used to explore options for providing non-LTE atomic physics data in order to model plasmas under more complicated conditions.

*This work was performed under the auspices of the U.S. Department of Energy by Los Alamos National Laboratory under Contract No. DE-AC52-06NA25396.

[†]In collaboration with J. Colgan, J. Abdallah, Jr., C.L. Fryer and A.L. Hungerford.

SESSION LW3: LAMPS

Wednesday Morning, 21 October 2009

Ballroom 3, Saratoga Hilton at 8:00

Tim Sommerer, GE Corporate Research Center, presiding

8:00

LW3 1 Plasma Efficiency and Losses for pulsed Xe Excimer DBDs at high Power Densities MARK PARAVIA, MICHAEL MEISSER, WOLFGANG HEERING, *Light Technology Institute, University Karlsruhe* The UV water disinfection for example needs efficient lamps with high power densities. Xe₂⁺ dielectric barrier discharges (DBDs) with phosphor coating can be used due to plasma efficiencies up to 60 % at pulsed electrical power densities of 0.04 W/cm² [1]. The power density can be increased by pressure or (operation) frequency. However, the plasma efficiency declines with frequency. We present measurements of the radiant flux for pulsed DBDs made of fused silica as function of pressure and frequency. By calculation of optical losses the plasma efficiency is estimated to be 52 % at 0.07 W/cm² but decreases to 34 % at 0.8 W/cm². The maximum frequency is pressure dependent and limited due to change-over from homogeneous into filamented mode. In comparison we measured the gas gap voltage and internal plasma current of a pulsed planar DBD for general lighting [2]. This comparison makes it possible to explain the frequency dependence of plasma efficiency and radiant flux. Due to the high frequency the remaining charge density is increased and the discharge becomes a glow discharge. For that reason the typical peak current during ignition drops and explains the declined efficiency by glow phase losses. [1] Beleznai, S., et al., *JPhysD*, 41 (2008) [2] Paravia, M., et al., GEC, Dallas, 2008

8:15

LW3 2 Optical absorption spectroscopy with an UHP-lightsource – an effective diagnostic method for Dy- and Ce-emitters in high intensity discharge lamps* MICHAEL WESTERMEIER, CORNELIA RUHRMANN, JENS REINELT, PETER AWAKOWICZ, JUERGEN MENTEL, *Ruhr-University Bochum, Germany* The so called "emitter effect" of elements like dysprosium and cerium is used to lower the work function and thereby the temperature of tungsten electrodes in HID lamps. A

special setup for absorption spectroscopy was developed to measure the density of particles within the lamp plasma consisting mainly of a backlight realized by a powerful ultra high pressure (UHP) lamp and a 1D-imaging spectrograph. It allows a direct measurement of the absorption profiles of Dy ($\lambda = 625.91$ nm) and Ce ($\lambda = 577.36$ nm) resonance lines within the lamp plasma. From these the ground-state atom density of Dy or Ce can be determined independently of the plasma temperature. Phase resolved measurements of the Dy-density and corresponding electrode temperatures in a ceramic HID lamp will be presented for low and high frequency operation. The results will be compared with measurements at lamps doped with Ce given in an accompanying poster and interpreted by the emitter effect.

*Supported by Philips Lighting NL, the DFG (GK 1051) and the RUB Research School.

8:30

LW3 3 First principle based calculation of emission properties of positive column of Ar-SnI₂ glow discharge MAXIM DEMINSKY, *Kintech Lab, Moscow, Russia* MARIA TUDOROVSKAIA, *RRC Kurchatov Inst., Moscow, Russia* IRINA CHERNYSHEVA, BORIS POTAPKIN, *Kintech Lab, Moscow, Russia* DARRYL MICHAEL, DAVID SMITH, TIMOTHY SOMMERER, *GE Global Research, Niskayuna, US* Possibility of replacement of mercury, an environmental hazard, by non-toxic elements in gas discharge lamps is intensively investigated now. Gases of metal halides are regarded as candidates of non-equilibrium source of emitters (metals) in glow discharge plasma. The model of glowing discharge in Ar/SnI₂ plasma is built using multilevel approach [1] for calculation of the cross sections and rate constant of electron collision with the metal halides. Sensitivity analysis shows, that dissociative attachment is one of the most important processes in that electronegative medium and directly influences on steady state parameters of glow discharge plasma. Optimization of the discharge parameters and conclusion about maximal light emission efficiency is performed. [1] itAdamson S. et al. *J. Phys. D: Appl. Phys.* 2007. V.40. P.3857

8:45

LW3 4 Application of coronal model for the emission properties calculations: Ti, Sc and Hg MAXIM DEMINSKY, IRINA CHERNYSHEVA, ALEXANDER ELETSKII, VALERII ASTAPENKO, BORIS POTAPKIN, *Kintech Lab, Moscow, Russia* The purpose of present paper is the theoretical study of titanium atoms emission properties in Ar : Ti and Sc gas mixture under glow discharge conditions. The electronic structure of neutral Ti is extremely rich containing a large number of energy levels. For this reason it is practically impossible to develop state-to-state kinetic model, which is usually used for such kind of studies. To overcome this difficulty the model was applied, which is usually known as "coronal" model. The populations of radiative states and emission power are computed using known cross sections for the excitation of these states and transition probabilities. Electron concentration and electric field strength are determined in self-consistent manner from electron energy balance equation and given value of discharge current. In fact, the applicability and reliability of "coronal" model is not rather obvious. To clarify the situation test studies were performed for Hg atom, which has relatively simple electronic structure. The calculations were made for Ar : Hg gas mixture under glow discharge conditions using two different approaches: "coronal" model and state-to-state kinetic model. The comparison of obtained results shows that "coronal" model may be used for the quantitative estimations of the emission properties.

9:00

LW3 5 Progress on Radiative Transition Probabilities in Neutral Cerium J.J. CURRY, *NIST, Gaithersburg, USA* Cerium is a rare-earth atom that is currently used in energy-efficient metal-halide lamps because of its rich visible emission spectrum. More than 20,000 lines have been observed and classified for neutral cerium in the wavelength range of 340 nm to 1 μm (Bill Martin, unpublished). We recently derived more than 500 absolute transition probabilities from existing experimental data (*J. Phys. D: Appl. Phys.* 2009). Lawler and Den Hartog at the University of Wisconsin have made measurements that are expected to produce a few thousand transition probabilities. These advances, however,

leave the data situation far short of what is needed to simulate an accurate global emission spectrum in numerical models of metal-halide lamps containing cerium. One possibility for closing this gap is through atomic structure calculations. Although it may be difficult for calculations to match the accuracy of measurements for any given transition, the global spectral distribution produced with calculated transition probabilities may still be satisfactory. For such a large number of lines, calculations may be the only realistic way to produce a reasonably complete set of data. We will discuss our recent atomic structure calculations of neutral cerium with the Cowan code based on a parametric fit of calculated energy level values to experimental values.

9:15

LW3 6 Breakdown characteristics of xenon HID Lamps* NATALIA BABAEVA, *University of Michigan* AYUMU SATO, NANU BRATES, KOJI NORO, *Universal Lighting Technologies, Inc.* MARK KUSHNER, *University of Michigan* The breakdown characteristics of mercury free xenon high intensity discharge (HID) lamps exhibit a large statistical time lag often having a large scatter in breakdown voltages. In this paper, we report on results from a computational investigation of the processes which determine the ignition voltages for positive and negative pulses in commercial HID lamps having fill pressures of up to 20 atm. Steep voltage rise results in higher avalanche electron densities and earlier breakdown times. Circuit characteristics also play a role. Large ballast resistors may limit current to the degree that breakdown is quenched. The breakdown voltage critically depends on cathode charge injection by electric field emission (or other mechanisms) which in large part controls the statistical time lag for breakdown. For symmetric lamps, ionization waves (IW) simultaneously develop from the bottom and top electrodes. Breakdown typically occurs when the top and bottom IWs converge. Condensed salt layers having small conductivities on the inner walls of HID lamps and on the electrodes can influence the ignition behavior. With these layers, IWs tend to propagate along the inner wall and exhibit a different structure depending on the polarity.

*Work supported by Universal Lighting Technologies, Inc.

SESSION MW: GEC FOUNDATION TALK

Wednesday Morning, 21 October 2009; Ballroom 1-2-3, Saratoga Hilton at 10:00; Bill Graham, Queen's University Belfast, presiding

10:00

MW 1 When Low Temperature Plasmas Meet Surfaces.
DAVID GRAVES, *University of California at Berkeley*

Low temperature plasmas are virtually always bounded by surfaces. Charged particles from the plasma recombine and are emitted at walls; plasma species exchange mass, momentum and energy with walls; the plasma electrostatic potential is referenced to wall potential; energetic and often chemically reactive charged and neutral species from the plasma impact surfaces and reflect, embed, diffuse and desorb back to the plasma; dust particle nuclei may be created at surfaces and ejected into the plasma; and surface erosion and re-deposition often dramatically alter plasma neutral composition and temperature. In this talk, I will present an overview of plasma-surface interactions with an emphasis on elements of what the gaseous electronics community has learned during the last several decades, and including some thoughts on new directions and opportunities.

SESSION NW: BUSINESS MEETING

Wednesday Morning, 21 October 2009; Ballroom 1-2-3, Saratoga Hilton at 11:00; Bill Graham, Queen's University Belfast, presiding

SESSION 2W: INTELLECTUAL PROPERTY TUTORIAL

Wednesday Noon, 21 October 2009; Whitney, Saratoga Hilton at 12:00

12:00

2W 1

TUG YASAR, *Tokyo Electron, U.S. Holdings*

SESSION PW1: OPTICAL DIAGNOSTICS II

Wednesday Afternoon, 21 October 2009

Ballroom 1, Saratoga Hilton at 13:30

Akihiro Kono, Nagoya University, presiding

Contributed Papers

13:30

PW1 1 Plasma diagnostic over prominent oxygen triplets

VLADIMIR MILOSAVLJEVIC, *NCPST-School of Physics, DCU, Dublin, Ireland & Faculty of Physics, University of Belgrade, Serbia* ALBERT R. ELLINGBOE, STEPHEN DANIELS, *NCPST-School of Physics, DCU, Dublin, Ireland* The plasma chemistry of fluorocarbon-oxygen-argon discharges and its influence on prominent oxygen triplets are presented. We investigate a cascade dependence of energy levels of the three oxygen triplets to the 777 oxygen triplet. The 777 triplet is very important for the measurement of atomic oxygen in low pressure plasmas, since the 777.417 nm spectral line is frequently used for actinometry. A carbon rich emission spectrum also has an influence on emission of the oxygen triplet spectral lines by including new lines, as well changing the spectral line shapes of existing oxygen lines. There is a link between emission of a couple atomic carbon lines (around wavelength 601 nm) and the oxygen spectral lines from 777 triplets. The experiments were performed in an Radio Frequency (RF) dual-frequency discharge chamber from Lam Research "EX-ELAN^{registered}," with drive frequencies 2MHz and 27MHz. Working gases are Ar-O₂-C₄F₈ mixtures, the total pressure was varied from 2 to 6 Pa. The RF powers of the lower frequency generator were varied from 0 to 600 W, and for the higher frequency generator the power was varied from 0 to 1200 W. Optical observations were carried out using a high resolution spectrometer with an ICCD camera and a low resolution spectrometer.

13:45

PW1 2 Determination of escape factors for the 811.53 nm argon atomic line

CHRISTIAN SCHARWITZ, TOSHIAKI MAKABE, *Faculty of Science and Technology, Keio University* MAKABE TEAM, As discussed in a previous study [Appl. Phys. Lett. 92 (2008), 071501] it is of interest for the determination of the density of low-energy electrons in Ar-plasmas to perform optical emission spectroscopy (OES) on the atomic transition line of Ar(2p9) to Ar(1s5) at 811.53 nm. For the metastable level Ar(1s5) a high population density is expected and radiation trapping is a challenge for these measurements. Radiation trapping is typically treated with so-called escape factors. To evaluate escape factors for the 811.53 nm Ar line, in our recent work two measurement methods are applied to inductively coupled plasmas. Based on the technique by [J. Phys. D 41 (2008), 065206] one of the methods is developed in such a way that the radiation trapping will have no impact, the other method is affected by the radiation trapping. The analysis of the results of both methods is used to evaluate the escape factors. The obtained escape factors will be presented and the results help to enhance the analysis of the OES measurements. This work is supported by a Grant-in-Aid for the Global COE Program operated at Keio University from MEXT Japan.

14:00

PW1 3 Color Schlieren Imaging for Plasma Diagnostics

ARLEN WARD, *Covidien Energy-based Devices* IL GYO KOO, ZENG-QI YU, GEORGE COLLINS, *Colorado State University* The value of color schlieren imaging is demonstrated for thermal analysis and fluid dynamics of plasmas in liquid and atmospheric environments. Temperature and density changes of the fluids allow for dynamic visualization of the plasma plume during the interactions. Video Schlieren techniques will be presented to compare and contrast the impact of plasma application to tissue proxy gels in both environments.

Invited Papers

14:15

PW1 4 Using C-R models to determine electron density and temperature in discharges containing rare gases.*YI-KANG PU, *Department of Engineering Physics, Tsinghua University, Beijing, People's Republic of China*

Electron density n_e and electron temperature T_e are important parameters for describing the plasma discharges. In many cases, the rare gases are used as a feed gas or added as a trace gas in low-temperature discharges. The intensity ratio of their optical emissions can be used to determine these parameters nonintrusively by using simple collisional-radiative models (C-R model) describing the kinetics of the excited levels. In this presentation, some simple C-R models for optical diagnostics are reviewed. Kinetic regimes, with different dominant processes, are identified for the Paschen 2p, 3p, 4p and 5p levels. One can then select proper excited levels to determine the plasma parameters according to the operation conditions. For example, for a low-pressure Ar/Xe inductive discharge, the $2p_1$ and $2p_5$ levels of Ar and Xe are in the corona regime, with the electron impact excitation from the ground state being dominant. Rate of this process is sensitive to the electron energy. As a result, line-ratios of Ar and Xe are used to give T_e . To obtain n_e , line-ratios of argon 3p, 4p and 5p levels are used, due to the significant electron impact transfer processes on these levels. This technique has been applied for a capacitive discharge containing Ar/Xe/CF₄. Similar method can be used for atmospheric-pressure nonequilibrium discharges to obtain the electron density. For example, for an argon microwave microplasma, the $2p_1$, $2p_3$ and $2p_6$ levels are found to be in the high-pressure nonequilibrium regime, with both the electron-impact and atom-collision processes being important. This provides a strong dependence of the line-ratios on n_e . T_e and n_e obtained from this technique are compared with that from other methods, such as the Langmuir probe and the Stark broadening method. Satisfactory agreement is obtained. The uncertainties and limitations of the line-ratio technique are also discussed.

*In collaboration with Xi-Ming Zhu, Department of Engineering Physics, Tsinghua University, Beijing, People's Republic of China.

Contributed Papers

14:45

PW1 5 Validation of Atomic Data Using a Plasma Discharge*DIRK DODT, ANDREAS DINKLAGE, *Max-Planck-Institut fuer Plasmaphysik, EURATOM Association, Greifswald, Germany*KLAUS BARTSCHAT, OLEG ZATSARINNY, *Drake University*

Using a neon discharge as a well-assessed reference, we demonstrate how such an arrangement can be employed to validate atomic data for discharge modeling. Specifically, a collisional-radiative-model of a neon DC discharge was set up using a set of structure and collision data from a semirelativistic *B*-spline *R*-matrix calculation [1], and the electron-energy distribution function of the plasma was determined from the spectroscopic measurement [2]. Since the model covers almost the entire visible spectrum, considering a large number of emission lines and all collisional coupling mechanisms enabled us to thoroughly test the consistency of the modeled excited-state populations. Inconsistencies, which appear as correction factors for rate coefficients, were extracted by means of Bayesian probability theory. Despite its limitations, the sensitivity of the approach was sufficient to provide critical information about the collision data, especially in cases where standard cross-section measurements using merged electron and atom beams are difficult to perform. The present approach thus complements experimental techniques to test theoretical predictions. [1] O. Zatsarinny and K. Bartschat, *J. Phys. B* **37**, 2173 (2004). [2] D. Dodt *et al.*, *J. Phys. D* **41**, 205207 (2008).

*Supported by the DFG (Germany) and the NSF (USA).

15:00

PW1 6 Optical plasma diagnostics: understanding the Ar emission spectrum*JOHN B. BOFFARD, R.O. JUNG, CHUN C. LIN, A.E. WENDT, *University of Wisconsin-Madison* Optical emission spectroscopy (OES) provides a simple, non-invasive method of learning about many important plasma parameters (e.g. electron temperature, number densities). Measurements of Ar

spectra in the 350-1200 nm wavelength range made on an inductive coupled plasma system under a range of operating conditions are compared to calculated emission spectra based on a radiation model that combines an electron energy distribution function (eedf) and number densities of ground state and Ar($3p^5 4s$) atoms with experimentally measured electron-impact excitation cross sections. Comparisons of the experimental and calculated spectra provide a quantitative assessment of the role of many processes in shaping the emission spectrum and thereby demonstrate how OES results can be utilized to extract plasma parameters. Examples include using radiation trapping of the $1s_x - 2p_y$ emission array to measure metastable densities which are compared to white-light absorption measurements; using electron-induced collisional de-excitation of the $5p_5$ level to measure electron density; and using variations in cross sections for excitation from the ground and metastable levels into $3p_x$ levels to obtain information on the electron temperature and shape of the eedf.

*Supported by NSF grant CBET-0714600.

15:15

PW1 7 Plasma diagnostics by optical emission spectroscopy on argon and comparison to Thomson scatteringD.L. CRINTEA, U. CZARNETZKI, *Institute for Plasma and Atomic Physics, Ruhr-University Bochum, 44780 Bochum, Germany*S. IORDANOVA, I. KOLEVA, *Faculty of Physics, Sofia University, 5, J. Bourchier Blvd., BG-1164 Sofia, Bulgaria*D. LUGGENHÖLSCHER, *Institute for Plasma and Atomic Physics, Ruhr-University Bochum, 44780 Bochum, Germany*

A novel optical emission spectroscopy (OES) technique for the determination of electron temperatures and densities in low-pressure argon discharges is compared to Thomson scattering (TS). The emission spectroscopy technique is based on the measurement of certain line ratios in argon and a collisional-radiative model (CRM) including metastable transport. The investigations are carried out in a planar inductively coupled neutral loop discharge over a wide

range of pressures, $p = 0.05 \text{ Pa} - 5 \text{ Pa}$. The discharge is operated in pure argon at a frequency of $f = 13.56 \text{ MHz}$ and powers varied between $P = 1 \text{ kW}$ and 2 kW . Both diagnostics, OES and TS, are applied in parallel. Electron densities and temperatures obtained by both diagnostic techniques are compared. Further, absolute

numbers of the metastable densities are derived. Excellent agreement is found throughout if depletion of the neutral gas density by increase of the gas temperature and electron pressure is included in the CRM. Electron pressure is the dominant depletion mechanism at gas pressures $p \leq 0.1 \text{ Pa}$ and rf powers $P > 1 \text{ kW}$.

SESSION PW2: HEAVY PARTICLE COLLISIONS WITH ATOMS AND MOLECULES
 Wednesday Afternoon, 21 October 2009; Ballroom 2, Saratoga Hilton at 13:30; Murtadha Khakoo,
 California State University, Fullerton, presiding

Invited Papers

13:30

PW2 1 Projectile Interactions and Electron Correlation in Four-Body Collisions.

ALLISON HARRIS, *Missouri University of Science and Technology*

The few-body problem is one of the most fundamental unsolved problems in physics, and arises from the fact that the Schrödinger equation is not analytically soluble for more than two mutually interacting particles. As a result, theory must resort to approximations, the validity of which are determined by comparison with experiment. There has been much work done on the three-body problem, and in many cases, theory and experiment agree very well. Recent advancements in experimental techniques and computing capabilities now allow for the study of more complicated collision systems, such as four-body collisions. The simplest four-body problem is a charged particle collision with a helium atom, in which both atomic electrons change state. This type of collision can result in many different outcomes, such as double excitation, excitation-ionization, double ionization, transfer-excitation, transfer-ionization, and double charge transfer. Many body interactions will be discussed in the context of several different four-body processes.

Contributed Papers

14:00

PW2 2 Fully Differential and Double Differential Cross Sections for Single Ionization of H₂ by 75 keV Proton Impact*

UTTAM CHOWDHURY, MICHAEL SCHULZ, DON MADISON, *Missouri S&T* We have calculated 3DW-EIS (3 body distorted wave – Eikonal initial state) fully differential cross sections (FDCS) and doubly differential cross sections (DDCS) for single ionization of H₂ by 75 KeV proton impact. Previously published DDCS (differential in the projectile scattering angle and integrated over the ejected electron angles) have found pronounced structures at relatively large angles which were interpreted as an interference resulting from the two-center potential of the molecule. We will investigate the source of these interference effects in the FDCS and examine how interference at the fully differential level can be still observable at the double differential level.

*Work supported by the NSF under grant 0757749.

14:15

PW2 3 Single Ionization of Atomic Hydrogen by 75 keV Proton Impact*

AARON LAFORGE, KISRA EGODAPITIYA, JASON ALEXANDER, MICHAEL SCHULZ, *Dept. of Physics, Missouri University of Science & Technology, Rolla, Mo* AHMAD HASAN, *Dept. of Physics, UAE University, Abu Dhabi, United Arab* MARCELLO CIAPPINI, *Institute of High Performance Computing, Singapore* MURTADHA KHAKOO, *Dept. of Physics, California State University, Fullerton, CA* Doubly differential cross sections (DDCS) for single ionization of atomic hydrogen and triple differential cross sections (TDCS) for ionization of molecular hydrogen by 75 keV proton impact have been measured and calculated as a function of the projectile scattering angle and energy loss for the first time. In the case of atomic hydrogen, the data were compared to three theoretical models, each with a dif-

ferent treatment of the nuclear-nuclear interaction. Surprisingly, this comparison reveals that a classical treatment of the nuclear-nuclear interaction is in best agreement with the experimental data. Also, for $v_{e|} \sim v_{proj}$ the “post-collision interaction” (PCI) between the ejected electron and the outgoing projectile ion has a significantly larger effect on the angular distributions of the DDCS than theoretically predicted.

*Funded by the National Science Foundation.

14:30

PW2 4 Structures in triply differential cross sections*

JOSEPH MACEK, *University of Tennessee and Oak Ridge National Laboratory* Triply differential cross sections present the momentum distribution $P(k)$ of electrons ejected from matter by particle impact. These distributions are used to extract insights about dynamical processes. Unusual, non-smooth, features play important roles in identifying essential features of the atomic dynamics. Our work has found a new source of structure in momentum distributions, namely, vortices in the time-dependent wave function for the dynamical system. We show that these vortices are formed when angular momentum is transferred from relative to internal motion. This angular momentum is normally thought to reside in bound states, however, it can also be carried by electrons ejected from target species. In the latter case the non-zero angular momentum is associated with regions where the electron distribution vanishes. Such regions have “holes” in the triply differential cross sections, thus giving rise to new, unexpected structures in electron momentum distributions. We illustrate these structures by calculations of triply differential cross sections for proton and electron impact on atomic species.

*J. H. M. acknowledges support from the Chemical Science, Geosciences and Biosciences Division, Office of Basic Energy Sciences, Office of Science US Department of Energy under Grant No. DE-FG02-02ER15283.

14:45

PW2 5 Electron Capture in Slow Collisions of Si⁴⁺ With Atomic Hydrogen* D.C. JOSEPH, J.P. GU, B.C. SAHA, *Department of Physics, Florida A&M University* In recent years the charge transfer involving Si⁴⁺ and H at low energies has drawn considerable attention both theoretically and experimentally due to its importance not only in astronomical environments but also in modern semiconductor industries. Accurate information regarding its molecular structures and interactions are essential to understand the low energy collision dynamics. Ab initio calculations are performed using the multireference single- and double-excitation configuration-interaction (MRD-CI) method to evaluate potential energies. State selective cross sections are calculate using fully quantum and semi-classical molecular-orbital close coupling (MOCC) methods in the adiabatic representation. Detail results will be presented in the conference.

*Supported by NSF CREST project.

15:00

PW2 6 A nonperturbative quantum mechanical approach to ion-molecule collisions TOM KIRCHNER, *Department of Physics and Astronomy, York University, Toronto, Ontario M3J 1P3* TOBIAS SPRANGER, *Institut fuer Theoretische Physik, TU Clausthal, D-38678 Clausthal-Zellerfeld, Germany* HANS JÜRGEN LÜDDE, *Institut fuer Theoretische Physik, Goethe-Universitaet, D-60438 Frankfurt, Germany* A nonperturbative quantum mechanical approach to ion-molecule collisions is presented. Its key ingredients are an expansion of the initially populated molecular orbitals in terms of a single-center basis and a spectral representation of the molecular Hamiltonian. Effectively, the approach amounts to a separation of molecular geometry and collision dynamics and offers the possibility to use well-established ion-atom methods with relatively minor modifications.

We apply this rather general approach to ion-water-molecule collisions and calculate cross sections for electron transfer and ionization at impact energies from the few-keV to the few-MeV regime. Different geometries are considered, and the variation of the results with respect to the orientation of the molecule is studied. To compare results with experimental data and other calculations we average the orientation-dependent parts of the Hamiltonian over the three standard Euler angles. This short cut is, of course, an approximation, but first results indicate that it yields reliable total cross sections.

15:15

PW2 7 Testing theoretical ion-atom interaction potentials by precise measurements of gas-phase ionic mobilities RAINER JOHNSEN, *University of Pittsburgh* LARRY VIEHLAND, *Chatham University* TIMOTHY WRIGHT, *University of Nottingham* In a collaborative effort, we have recently tested itab-initio interaction potentials for the ion-atom pairs O⁺-He, O⁺-Ne, O⁺-Ar, He⁺-Ne, and Ne⁺-He by comparing experimental ionic mobilities to those derived from the computed potentials (T. Wright and co-workers) in conjunction with ion transport theory (L. A. Viehland and co-workers). The computed mobilities were then compared to selected-ion drift-tube measurements carried out in the lab of R. Johnsen. Generally, the magnitude and E/n dependences of the calculated mobilities agree with their measured values sufficiently well (within a few percent) to be used with confidence in applications such as discharge modeling, but more accurate mobility measurements (at the 1% or better level) are needed to test for finer details of the interaction, e.g. effects arising from spin-orbit coupling, curve crossings, and the spin state of the ion. Improvements in the experimental apparatus are in progress. We will also present preliminary results on the He⁺-Ar ion-atom pair, for which no previous mobility measurements are available.

SESSION PW3: LASER PRODUCED PLASMAS INDUCED BREAKDOWN AND APPLICATIONS OF HIGH PRESSURE PLASMAS

Wednesday Afternoon, 21 October 2009; Ballroom 3, Saratoga Hilton at 13:30; Matthew Goeckner, University of Texas at Dallas, presiding

Invited Papers

13:30

PW3 1 Intense laser-driven cluster plasma production of fusion neutrons.

TODD DITMIRE, *University of Texas at Austin*

This abstract not available.

Contributed Papers

14:00

PW3 2 Triggering Excimer Lasers by Photoionization from Corona Discharges* ZHONGMIN XIONG, *University of Michigan* THOMAS DUFFEY, DANIEL BROWN, *Cymer, Inc.* MARK KUSHNER, *University of Michigan* High repetition rate ArF (192 nm) excimer lasers are used for photolithography sources in microelectronics fabrication. In highly attaching gas mixtures, preionization is critical to obtaining stable, reproducible glow discharges. Photoionization from a separate corona discharge is one technique for preionization which triggers the subsequent electron avalanche between the main electrodes. Photoionization triggering of an ArF excimer laser sustained in multi-atmosphere

Ne/Ar/F₂/Xe gas mixtures has been investigated using a 2-dimensional plasma hydrodynamics model including radiation transport. Continuity equations for charged and neutral species, and Poisson's equation are solved coincident with the electron temperature with transport coefficients obtained from solutions of Boltzmann's equation. Photoionizing radiation is produced by a surface discharge which propagates along a corona-bar located adjacent to the discharge electrodes. The consequences of pulse power waveform, corona bar location, capacitance and gas mixture on uniformity, symmetry and gain of the avalanche discharge will be discussed.

*Work supported by Cymer, Inc.

14:15

PW3 3 Laser Induced Avalanche Ionization in Gases with REMPI or Femtosecond Pre-Ionization MIKHAIL SHNEIDER, RICHARD MILES, *Princeton University* Results of a theoretical study regarding the minimal requirements for the first pre-ionizing pulse to initiate avalanche ionization and essential gas heating by the second pulse are presented. The problem of minimal gas component density for the REMPI (Resonance Enhanced Multi-Photon Ionization) pre-ionization with subsequent avalanche ionization in a bulk gas is explored on the basis of the theoretical model developed for the Ar:Xe mixture, where during the initial portion of the pulse (3+1) REMPI of Ar atoms starts the ionization, which subsequently continues to grow with an avalanche in the buffer Xe gas [1]. Note, that this method of plasma generation at intensities much lower than required for breakdown is very close to one considered in Ref. [2] with femtosecond pre-ionizing laser pulse. Scaling parameters for gas mixtures, laser pulse shape, focusing and frequency are studied. Possible applications for improving of the detection sensitivity of Radar REMPI diagnostic technique and laser initiated ignition are discussed. 1. M.N. Shneider, Z.Zhang, R.B. Miles, *J.Appl.Phys.* **104**, 023302 (2008); 2. Z. Henis, G. Milikh, K. Papadopoulos, A. Zigler, *J.Appl.Phys.* **103**, 103111 (2008)

14:30

PW3 4 X-Ray Induced Breakdown in Air with High Reduced Electric Field* ROBERT VIDMAR, ANUSHA UPPALURI, *University of Nevada, Reno* An X-ray pulse was used to initiate breakdown of laboratory air at a high reduced electric field in a parallel plate geometry. The X-ray pulse is from 100 ns to several ms in duration and originates from a 100 keV electron beam operating at a few mA. The X-ray pulse is shown to represent a volumetric ionization rate in air and the count rate from an X-ray detector is related to the volumetric ionization rate. An air-chemistry code is used to model the temporal change in electron density as a function of volumetric ionization rate and reduced electric field. Measurements of X-ray induced breakdown demonstrate the sensitivity of systems that operate with high reduced electric field to pulsed ionizing radiation.

*This material is based on research sponsored by the Air Force Research Laboratory, under agreement numbers FA9550-05-1-0087 and FA9550-07-1-0021.

14:45

PW3 5 Diffuse coplanar surface barrier discharge – basic properties and its application in surface treatment of nonwovens* DUSAN KOVACIK, JOZEF RAHEL, JANA KUBINCOVA, ANNA ZAHORANOVA, MIRKO CERNAK, *Department of Experimental Physics, Faculty of Mathematics, Physics and Informatics, Comenius University, Mlynska dolina, 842 48 Bratislava, Slovakia* In recent years, low temperature atmospheric pressure plasma surface treatments have become a hot topic because of the potential of fast and efficient in-line processing fabrication without expensive vacuum equipment. A major problem of atmospheric pressure treatment in air is insufficient treatment uniformity because, particularly at the higher plasma power densities, the air plasma has the tendency of filamentation and transition into an arc discharge. Diffuse coplanar surface barrier discharge (DCSBD) plasma source has been developed to overcome these problems. This type of discharge enables to generate mac-

roscopically homogeneous thin (~ 0.3 mm) plasma layer with power density of some 100 W/cm^2 practically in any gas without admixture of He. It was found that the ambient air plasma of DCSBD is capable to make lightweight polypropylene nonwoven fabrics permanently hydrophilic, without any pinholing and with low power consumption of some 1 kWh/kg .

*This research was supported by the Slovak Research and Development Agency under the contract APVV-0485-06.

15:00

PW3 6 Characterization of Atmospheric Pressure DC Negative Corona Discharges for Thin Film Deposition* DION ANTAO, ALEXANDER FRIDMAN, BAKHTIER FAROUK, *Drexel University* The applicability of DC corona discharges with their lower temperatures and uniformity is investigated for the deposition of thin films. The deposition is done at atmospheric pressure and room temperature, which lowers the facility cost as no vacuum or low pressure facilities are required and also enables continuous processing rather than batch processing. We report on our studies the operating regimes and the structures of DC negative corona discharges for a point to plate electrode configuration for thin film deposition. Traditionally DC coronas have been operated at extremely low currents. By modifying the circuit, we have been able to operate the DC corona at higher currents without breakdown. We operated the DC negative corona discharge in new regimes where a stable and diffuse glow has been observed near the anode surface. This diffuse glow is observed in air and methane containing discharges. The discharge is characterized by voltage-current diagnostics. Optical emission spectroscopy (OES) is used to obtain spatially resolved temperature measurements. The DC negative corona discharge has been observed to deposit films on the anode surface. The deposition of films and particles on the anode surface has introduced the possibility of using corona discharges as a novel method of materials deposition or surface modification at atmospheric pressure.

*The work reported is supported by the US National Science Foundation under grant DMII-0423409.

15:15

PW3 7 Measured Current Distribution Functions Describing an Array of High Voltage Needles Operating in the Avalanche and Streamer Modes ERIK WEWLINGER, PATRICK PEDROW, MANUEL GARCIA-PEREZ, SU HA, OSCAR MARIN-FLORES, MARVIN PITTS, *Washington State University* It is hypothesized that cold plasma processing of small oxygenated molecules present in bio-oil will reduce coking in a catalytic steam reformer. The cold plasma reactor will be placed upstream of the reformer and will consist of an array of needles held at a DC voltage in the 5-10 kV range. The distribution of current pulses on each needle will be measured for gas mixtures consisting of varying amounts of argon, water, methanol, oxygen, and carbon dioxide. The small oxygenated hydrocarbon molecules from bio-oil can be reduced to hydrogen and synthesis gas by the catalytic steam reformer. However, the steam reforming of these oxygenated hydrocarbon molecules has a high tendency of coke formation. In this work, catalyst coking will be reduced by integrating the atmospheric pressure cold plasma reactor. Studying how distribution functions for elements in a small array (< 10 needles) "interact" will facilitate design of larger needle arrays that can be used for the commercial processing of biofuels.

SESSION QW: JOINT GEC/CNSE SESSION FOLLOWING CNSE VISIT
Wednesday Evening, 21 October 2009; NFS Auditorium, College of Nanoscale Science and Engineering at 19:00; Eric Joseph, IBM T.J. Watson Research Center, presiding

19:00

QW 1 Plasma synthesis of silicon nanocrystal inks for low-cost photovoltaics.*

UWE KORTSHAGEN, *University of Minnesota*

Silicon is the most widely used material in the microelectronics and photovoltaics industry. Currently it is used in one of two forms: as wafers of single- or polycrystalline material or as CVD deposited thin film material. In this presentation, we discuss an alternate route to forming silicon thin films from solution on flexible substrates. Silicon nanocrystals are formed in a nonthermal plasma. By adding dopant precursors, p- and n-doped as well as intrinsic crystals can be formed. Organic ligands can be attached in the plasma such that nanocrystals become soluble in organic solvents. These "nanocrystal inks" can be used to form silicon films with ultra-low-cost printing or coating techniques. Film properties of silicon-ink processed films will be discussed. Proof-of-concept demonstrations of solar cells produced from silicon inks will be presented.

*This work was supported by NSF under grants MRSEC DMR-0819885, NIRT CBET-0506672, CMMI-0556163.

19:25

QW 2 Plasma Processing for Advanced Interconnects.

JOHN ARNOLD, *IBM Research at Albany Nanotech*

As the critical dimensions of interconnects for advanced semiconductor devices have entered the sub-100nm regime, the interactions of materials with their processing environments have become increasingly important. Modern ultralow-k (ULK) dielectric materials are particularly sensitive to damage caused by exposure to electrons, ions, reactive neutrals and UV radiation during their deposition, patterning, and characterization. This presentation will follow the "plasma processing life cycle" of a typical ULK film sample, from deposition through etching and metallization. Particular attention will be paid to damage of the film during etching and the associated structural characterization. Trends of plasma damage with dielectric constant and composition will be described. Finally, the long-term outlook for patterning ULK films to the "end of the roadmap" will be discussed.

19:50

QW 3 Biomacromolecule immobilization and self-assembled monolayer chemistry on atomic layer deposited metal oxide materials.

MAGNUS BERGKVIST, *College of Nanoscale Science and Engineering, University at Albany - SUNY*

Many biotechnology applications involve interfacing proteins, DNA and other macromolecules to non-biological material surfaces acting as supports. Support materials employed for this purpose span the periodic table and range from polymeric membranes/hydrogels to metals and ceramics, for example gold and hydroxyapatite. Lab-on-a-chip and other sensing/detection applications based on lithography and semiconductor technology typically rely on alkanethiol and organosilane chemistry to immobilize biological material to gold and silica. While successful in many instances, organosilane chemistry offers limited options for orthogonal chemistry and often results in multilayer film buildup. Self-assembly on gold is straight forward but gold is often undesirable from a device perspective. Recent developments in atomic layer deposition (ALD) allow fabrication of high quality thin films of alumina and high-k oxide materials that are compatible with clean room operations and are interesting emerging materials for integrated optical, electronic and biological applications. Here we will show alternative self-assembly chemistries on ALD materials for biological immobilization than those used on gold/silica and also demonstrate direct biological interfacing to high-K materials for potential use in bioscreening and detection.

20:15

QW 4 Opportunities at the Confluence of Microplasma and Nanomaterials.

J. GARY EDEN, *University of Illinois at Urbana-Champaign*

More than a decade ago, plasma science ventured into the mesoscopic realm with low temperature, nonequilibrium plasmas confined to cavities having a characteristic dimension (d) below $50 \mu\text{m}$. today, the lower limit for microplasma dimensions is $d^3L \sim 10 \mu\text{m}$ but experiments in which d approaches $1 \mu\text{m}$ are expected in the near future. Several previous microplasma devices have exploited nanomaterials and nanostructures to realize new functionality. This presentation will briefly describe past efforts to integrate microplasmas with nanomaterials and/or nanodevices. A few thoughts regarding exciting opportunities in merging nanoelectronics or nanoptics with $\leq 1\text{-}10 \mu\text{m}$ microplasmas will be offered.

20:40

QW 5 The CNSE Public-Private Partnership Paradigm: A Driver for New York State and U.S. Educational, Research and Economic Excellence in the 21st Century.EDWARD M. CUPOLI, *College of Nanoscale Science and Engineering, University at Albany - SUNY*

The College of Nanoscale Science and Engineering (CNSE) of the University at Albany-SUNY is the first college in the world dedicated to education, research, development, and deployment in the emerging disciplines of nanoscience, nanoengineering, nanobioscience, and nanoeconomics. Envisioned and developed as a bold and unique educational, technological and business paradigm, the CNSE model has produced outcomes that are both significant and unparalleled: preparation of a highly educated, highly skilled workforce that is critical to driving opportunity and growth at all levels; acceleration of nanoscale research and development that is vital to advancing the commercialization of cutting-edge technologies and applications; and, generation of unmatched high-tech investment and job creation that are serving to foster a positive economic and societal impact throughout New York State, while also enhancing national competitiveness in the global innovation economy of the 21st century. In less than a decade of operation, CNSE has become a globally recognized entity. CNSE's Albany NanoTech Complex is the most advanced research enterprise of its kind at any university in the world: a \$5 billion, 800,000-square-foot complex that continuously attracts corporate partners from around the world, offers students a one-of-a-kind academic experience, and educates society on the implications of advances in nanotechnology. CNSE's Albany NanoTech houses the only fully-integrated 300mm wafer, computer chip pilot prototyping and demonstration line within 80,000 square feet of Class 1 capable cleanrooms. More than 2,500 scientists, researchers, engineers, students, and faculty work on site at CNSE's Albany NanoTech, with a network of global corporate partners that includes more than 250 leading nanotechnology companies, such as IBM, AMD, GlobalFoundries, SEMATECH, Toshiba, ASML, Applied Materials, Tokyo Electron, Vistec Lithography and Atotech, among many others.

21:05

QW 6 Effects of Plasma-Ion Irradiation on Structures and Properties of Carbon Nanotubes.RIKIZO HATAKEYAMA, *Department of Electronic Engineering, Tohoku University*

Nanocarbons of carbon allotropes have drawn great attention due to their high potential for unique properties and a variety of applications. Since carbon nanotubes among them are furnished with one-dimensional hollow inner-nanospaces, various kinds of atoms and molecules are possible to be injected into the nanospaces based on plasma nanotechnology, which could lead to innovative functionalization of the pristine ones. For that purpose original approaches using nanoscopic plasma processing mainly in ionic plasmas have been performed in order to develop SWNT(single-walled carbon nanotube)-, and DWNT(double-walled carbon nanotube)-based materials with novel functions corresponding to nano electronic and biological applications, where positive and negative ions with their energies and fluxes controlled are irradiated to immersed substrates coated with the pristine carbon nanotubes. Consequently, we have innovatively created various kinds of charge-/spin-exploited atoms and molecules encapsulated SWNTs and DWNTs. Finally, their electronic, magnetic, and optical properties are intensively investigated using a configuration of field effect transistor (FET) and a SQUID magnetometer. As a result, we have for the first time realized air-stable semi-conducting pn control, formed nano structures with magnetic semiconductor and ultimate air-stable nano pn-junctions, found distinct characteristics of negative differential resistance, and observed photoinduced electron transfer phenomena upon the encapsulated SWNTs and DWNTs.

21:30

QW 7 Leveraging Microelectronics Research to Enable A Smarter Planet.TIMOTHY J. DALTON, *IBM T. J. Watson Research Center*

Over the course of the last fifty years, the microelectronics industry has made tremendous strides in the development and manufacturing of ever more complex integrated circuits (IC). These circuits have typically been applied to the information technology (IT) industry and have driven improvements in the computational power per dollar of many orders of magnitude. Part of the "toolbox" of skills acquired to produce integrated circuits is the ability to form desired patterns at ever decreasing sizes. The minimum controllable feature size has been reduced by six orders of magnitude (from millimeters to nanometers) during the last fifty years. With feature sizes rapidly approaching 10nm, the conventional silicon IC industry is nearing a threshold with the end of conventional silicon scaling approaching. Research today focuses on new device structure to replace the CMOS FET as the engine of the IT industry. A very exciting research area today is the concept of taking the skill-set acquired from IC research, development, and manufacturing, and applying those skills into new domains where they can enable a "smarter planet." These new domains include areas such as energy, water, and health care / life sciences. All of these are outside of the traditional IT focus for microelectronics research, yet, the new "smarter planet" domains may form the basis for future industries. This presentation will look at the evolution of IBM's research model and focus, shifting from one solely focused on IT, to one that compliments IT research with Smarter Planet domains.

SESSION RR1: BIOLOGICAL AND EMERGING APPLICATIONS OF PLASMA I
Thursday Morning, 22 October 2009
Ballroom 1, Saratoga Hilton at 8:00
Deborah O'Connell, Queen's University Belfast, presiding

Contributed Papers

8:00

RR1 1 Atmospheric pressure generation of singlet oxygen by arrays of microplasmas for DNA oxidation JOAO SANTOS SOUSA, *LPGP, CNRS-UPS, 91405 Orsay, France and IPFN, IST, 1049-001 Lisboa, Portugal* GERARD BAUVILLE, BERNARD LACOUR, VINCENT PUECH, *LPGP, CNRS-UPS, 91405 Orsay, France* MICHEL TOUZEAU, *LTM, CNRS-UJF-INPG, 38054 Grenoble, France* JEAN-LUC RAVANAT, *CEA, Inac, SCIB/LAN CEA-UJF, 38054 Grenoble, France* Recently, we demonstrated [1] that Micro-Cathode Sustained Discharges (MCSD) can be very effective for producing large amounts of $O_2(a^1\Delta)$ at atmospheric pressure. In the present work, we show that $O_2(a^1\Delta)$ densities higher than $3 \times 10^{16} \text{ cm}^{-3}$ can be produced by arrays of MCSD operating at atmospheric pressure in He/ O_2 /NO mixtures, resulting in $O_2(a^1\Delta)$ fluxes above 30 mmol/h. The effect of different parameters such as gas flows and mixtures, discharge current and array geometry are discussed. Arrays of MCSD, allowing the production at atmospheric pressure of $O_2(a^1\Delta)$ and O_3 densities between 10^{13} and 10^{16} cm^{-3} , with an easily tunable ratio, appear to be very useful tools to study in details the reactivity of these reactive oxygen species with DNA constituents. Experiments were conducted showing that Adenine, Thymine and Cytosine constituents are effectively oxidized by O_3 , while $O_2(a^1\Delta)$ only reacts with 2'-deoxyguanosine (dGuo). A more detailed study on the reactivity of $O_2(a^1\Delta)$ and O_3 with aqueous DNA solutions is in progress. [1] J.S. Sousa et al., *Appl. Phys. Lett.* **93**, 011502 (2008)

8:15

RR1 2 Role of Plasma Discharge in Division of Prostatic Tissue ARLEN WARD, CARL ALMGREN, *Covidien Energy-based Devices* ZENG-QI YU, *Colorado State University* JOE SARTOR, *Covidien Energy-based Devices* GEORGE COLLINS, *Colorado State University* During the treatment of benign prostatic hyperplasia electrical energy is used to separate prostatic tissue and remove it as a urinary obstruction. This surgical procedure is often

Invited Papers

9:00

RR1 5 Measuring DNA through a Nanopore Fabricated Using Plasma Processing Technology. S.M. ROSSNAGEL, *IBM T.J. Watson Research Center*

We have been developing a device based on a 2-3 nm diameter pore between two electrolyte volumes for the transit of DNA by means of a potential gradient. The nanopore is configured with 3 electrodes, each about 3 nm thick with 2-3nm dielectric spacers. The nanopore electrodes can be used to trap DNA in-transit, and ideally measure the impedance and hence the identity of each nucleotide as it passes through the nanopore, allowing real time sequencing of the DNA. The goal is to operate at megahertz, allowing sequencing of the entire genome within a few hours at a fairly modest cost. This project has led to numerous new developments in nanoscale fabrication, particularly for nanofluidics. The nanopore devices are fabricated using a number of critical plasma processing steps, both deposition and etch, in our 200mm pilot facility.

performed in a saline environment, and current paths change as the tissue and fluid are heated. This study shows that a plasma discharge at the electrode is necessary to provide the current densities necessary to vaporize portions of the prostatic tissue in order to facilitate removal. This behavior is predicted in finite element simulations, and verified with color schlieren imaging and ex vivo bovine prostate tests.

8:30

RR1 3 Plasma-Chemical Removal of Tissue CAMERON MOORE, IL GYO KOO, GEORGE COLLINS, *Colorado State University* We report the use of plasma generated chemical species to affect a strong enhancement in removal of ex vivo tissue. The data show a demonstrable, perhaps predominant, chemical component which contributes to tissue removal. Effects expected from purely thermal processes are also observed to be limited. These initial studies have also shown the ability to create high aspect ratio regions of removed tissue, indicative of a directional process.

8:45

RR1 4 Mechanism for Ring-Opening of Aromatic Polymers by Remote Atmospheric Pressure Plasma ELEAZAR GONZALEZ, MICHAEL BARANKIN, *UCLA* PETER GUSCHL, *Surfx Technologies* ROBERT HICKS, *UCLA* A low-temperature, atmospheric pressure oxygen and helium plasma was used to treat the surfaces of polyetheretherketone, polyphenylsulfone, polyether-sulfone, and polysulfone. These aromatic polymers were exposed to the afterglow of the plasma, which contained oxygen atoms, and to a lesser extent metastable oxygen ($^1\Delta_g O_2$) and ozone. After less than 2.5 seconds treatment, the polymers were converted from a hydrophobic state with a water contact angle of $85 \pm 5[r]$ to a hydrophilic state with a water contact angle of $13 \pm 5[r]$. It was found that plasma activation increased the bond strength to adhesives by as much as 4 times. X-ray photoelectron spectroscopy revealed that between 7% and 27% of the aromatic carbon atoms on the polymer surfaces was oxidized and converted into aldehyde and carboxylic acid groups. Analysis of polyethersulfone by internal reflection infrared spectroscopy showed that a fraction of the aromatic carbon atoms were transformed into C=C double bonds, ketones, and carboxylic acids after plasma exposure. It was concluded that the oxygen atoms generated by the atmospheric pressure plasma insert into the double bonds on the aromatic rings, forming a 3-member epoxy ring, which subsequently undergoes ring opening and oxidation to yield an aldehyde and a carboxylic acid group.

SESSION RR2: CHARGED PARTICLE MOLECULE COLLISIONS

Thursday Morning, 22 October 2009; Ballroom 2, Saratoga Hilton at 8:00; Tom Kirchner, York University, presiding

Invited Papers

8:00

RR2 1 Ion induced ionization and fragmentation of biomolecules and biomolecular clusters.THOMAS SCHLATHOELTER, *Univ. Groningen*

The interaction of keV to MeV protons and heavy ions with DNA is the basis of ion therapy and risk assessment for manned space flight. The reason is, that in tissue the originally fast ions are decelerated to MeV energies and below (the Bragg peak region) where DNA damage is highest. In living cells, DNA damage always occurs in the presence of a chemical environment. The great complexity of such condensed systems rules out the investigation of fragmentation dynamics on an event by event level. For such studies, we need finite target systems still sufficiently complex to reflect relevant chemical aspects of the cell nucleus. We investigate ion collisions with isolated DNA building blocks and their neutral clusters to bridge the gap between isolated molecules and the condensed phase. In these studies, we could for instance show that intermolecular hydrogen bonds strongly affect the nucleobase fragmentation dynamics. Because of limitations of the cluster approach, we recently commissioned a novel setup interfacing an electro-spray ion source with a keV ion beamline. This allows for generation of a protonated/deprotonated beam of virtually any biomolecule. The charged biomolecules are then collected and cooled in an RF trap and subsequently collided with keV ions. Time-of-flight mass spectrometry is used to study ionization and fragmentation dynamics. First results on small protonated peptides and DNA building blocks prove the great potential of the technique.

8:30

RR2 2 Double ionization dynamics of Helium dimers investigated during charged particle impact.*MARKUS SCHOEFLER, *Lawrence Berkeley National Laboratory*

Helium dimers (He_2) are a Van-der-Waals bound system and the most extreme quantum matter in AMO physics with a binding energy below $0.1 \mu\text{eV}$ (1.1 mK). Its internuclear distance varies from 2 to several hundreds Angstrom (even larger than the DNA diameter). Their existence was predicted theoretically by Slater in 1928 and the experimental prove followed 1994 by Schöllkopf in a diffraction experiment. Singly and doubly charged projectiles with energies of 25 - 150 keV/u were used to fragment the Helium dimer into two He^+ ions. Using the COLTRIMS (COLd Target Recoil Ion Momentum Spectroscopy) imaging technique we measured the three dimensional momentum vector of all fragments (He^+ ions and emitted electrons). A detailed analysis shows different breakup channels, as a two-step-two mechanism, charge transfer and the so far only in single photon absorption observed interatomic coulombic decay (ICD), induced by the transfer of a virtual photon.

*This work was supported by the DFG, BMBF, and Roentdek Handels GmbH.

Contributed Papers

9:00

RR2 3 Positron Interactions with Biologically Important Molecules* C. MAKOCHEKANWA, W. TATTERSALL, J. SULLIVAN, A. JONES, P. CARADONNA, D. SLAUGHTER, S. BUCKMAN, CAMS, *Australian National University, Canberra* A. BANKOVIC, Z. LJ. PETROVIC, *Institute of Physics, Belgrade, Serbia* K. NIXON, M. BRUNGER, CAMS, *Flinders University, Adelaide, South Australia* Positron interactions with molecules in the body are likely to play a key role in diagnostic techniques such as Positron Emission Tomography (PET). PET scans involve the injection of a high-energy positron into the body, and the detection of the resultant gamma rays that arise on annihilation with an electron. The processes between the emission of the high-energy particle and the gamma ray production involve positron-molecule scattering, and yet there is essentially no fundamental, quantitative knowledge of these interactions. We will discuss a program of measurements that is underway to quantify such scattering processes and illustrate our first results with the water molecule and formic acid. The ultimate aim of this program is to underpin the development of positron transport studies in soft matter and a new dosimetry for PET.

*Supported by the Australian Research Council.

9:15

RR2 4 Dependence of positron-molecule binding energies on molecular parameters* J.R. DANIELSON, J.A. YOUNG, C.M. SURKO, *University of California, San Diego*

Studies of positron annihilation on many molecules show evidence of vibrational Feshbach resonances and thus provide evidence that positrons bind to these species. The downshifts in the resonances from the mode energies provide a measure of the binding energy.¹ Regression analysis on the existing data set of 30 such molecules indicates that the binding energy can be expressed as a linear combination of the molecular dipole polarizability and the permanent dipole moment with an additional term for aromatics that is proportional to the number of π bonds. This result is compared with binding energy calculations and tested with other annihilation data. Predictions of the model are discussed, including positron binding to atomic clusters, polycyclic aromatic molecules (PAHs), and other chemical species. The relationship of these positron-molecule bound states to analogous electron-molecule states is also discussed.²

*This work is supported by NSF grant PHY 07-55809.

¹J. A. Young and C. M. Surko, *Phys. Rev. A* **77**, 052704 (2008); and *Phys. Rev. A* **78**, 032702 (2008).

²H. Abdoul-Carmine and C. Desfrancios, *European Phys. J.* **2**, 149 (1998).

SESSION SR1: BIOLOGICAL AND EMERGING APPLICATIONS II

Thursday Morning, 22 October 2009; Ballroom 1, Saratoga Hilton at 10:00; Magnus Bergkvist, College of Nanscale Science and Engineering, University at Albany, presiding

Invited Papers

10:00

SR1 1 Cold atmospheric plasma sterilization: from bacteria to biomolecules.

MICHAEL KONG,* *Centre for Biological Engineering and Dept of Electronic and Electrical Engineering, Loughborough University*

Although ionized gases have been known to have biological effects for more than 100 years, their impact on the practice in healthcare service became very significant only recently. Today, plasma-based surgical tools are used for tissue reduction and blood coagulation as surgical procedures. Most significant however is the speed at which low-temperature gas plasmas are finding new applications in medicine and biology, including plasma sterilization, wound healing, and cancer therapies just to name a few. In the terminology of biotechnology, the "pipeline" is long and exciting. This presentation reviews the current status of the field with a particular emphasis on plasma inactivation of microorganisms and biomolecules, for which comprehensive scientific evidence has been obtained. Some of the early speculations of biocidal plasma species are now being confirmed through a combination of optical emission spectroscopy, laser-induced fluorescence, mass spectrometry, fluid simulation and biological sensing with mutated bacteria. Similarly, fundamental studies are being performed to examine cell components targeted by gas plasmas, from membrane, through lipid and membrane proteins, to DNA. Scientific challenge is significant, as the usual complexity of plasma dynamics and plasma chemistry is compounded by the added complication that cells are live and constantly evolving. Nevertheless, the current understanding of plasma inactivation currently provides strong momentum for plasma decontamination technologies to be realized in healthcare. We will discuss the issue of protein and tissue contaminations of surgical instruments and how cold atmospheric plasmas may be used to degrade and reduce their surface load. In the context of plasma interaction with biomolecules, we will consider recent data of plasma degradation of adhesion proteins of melanoma cells. These adhesion proteins are important for cancer cell migration and spread. If low-temperature plasmas could be used to degrade them, it could form a control strategy for cancer spread. This adds to the option of plasma-triggered programmed cell death (apoptosis). Whilst opportunities thus highlighted are significant and exciting, the underpinning science poses many open questions. The presentation will then discuss main requirements for plasma sources appropriate for their biomedical applications, in terms of the scope of up-scaling, the ability to treat uneven surfaces of varying materials, the range of plasma chemistry, and the control of plasma instabilities. Finally a perspective will be offered, in terms of both opportunities and challenges.

*In collaboration with: D. L. Bayliss, G. Shama, Z. Cao, Q. Y.Nie, J. L. Walsh, F. Iza, Loughborough University.

Contributed Papers

10:30

SR1 2 Sterilization and Mechanism of Microorganisms on A4 Paper by Dielectric Barrier Discharges Plasma at Atmospheric Pressure

JIA XIANGHONG, WAN JUN, YANG JINHUA, XU FENG, WANG SHOUGUO, INSTITUTE OF MICROELECTRONICS OF CHINESE ACADEMY OF SCIENCES TEAM, ASTRONAUT RESEARCH AND TRAINING CENTER OF CHINA TEAM, This study investigated the microorganisms' sterilization and mechanism by a DBD plasma device at atmospheric pressure. The device including a transfer system and two roller-electrodes is driven by sine-wave high voltages at frequencies of 15 kHz. Normal A4 papers were used to study the effects of the sterilization on their surfaces by analyzing the number of the living bacteria cells. The state of Escherichia coil's DNA were also measured by agarose gel electrophoresis after sterilization to analyze the inactivation mechanisms. Experimental results indicated that microorganisms on the surface of A4 Papers almost were destroyed while the papers went through the device and there was no any damage of the paper during the process. The main reason engendered bacteria death was due to the double chains of the DNA broken by the plasma.

10:45

SR1 3 Sterilization of Surfaces with a Handheld Atmospheric Pressure Plasma

ROBERT HICKS, SARA HABIB, WAI CHAN, ELEAZAR GONZALEZ, UCLA A. TIJERINA, MARK SLOAN, CMI Low temperature, atmospheric pressure plasmas have shown great promise for decontaminating the surfaces of materials and equipment. In this study, an atmospheric pressure, oxygen and argon plasma was investigated for the destruction of viruses, bacteria, and spores. The plasma was operated at an argon flow rate of 30 L/min, an oxygen flow rate of 20 mL/min, a power density of 101.0 W/cm³ (beam area = 5.1 cm²), and at a distance from the surface of 7.1 mm. An average 6log₁₀ reduction of viable spores was obtained after only 45 seconds of exposure to the reactive gas. By contrast, it takes more than 35 minutes at 121°C to sterilize anthrax in an autoclave. The plasma properties were investigated by numerical modeling and chemical titration with nitric oxide. The numerical model included a detailed reaction mechanism for the discharge as well as for the afterglow. It was predicted that at a delivered power density of 29.3 W/cm³, 30 L/min argon, and 0.01 volume% O₂, the plasma generated 1.9 x 10¹⁴ cm⁻³ O atoms, 1.6 x 10¹² cm⁻³ ozone, 9.3 x 10¹³ cm⁻³ O₂(¹Δ_g), and 2.9 x 10¹² cm⁻³ O₂(¹Σ_g⁺) at 1 cm downstream of the source. The O atom density measured by chemical titration with NO was 6.0 x 10¹⁴ cm⁻³ at the same conditions. It is believe that the oxygen atoms and the O₂(¹Δ_g) metastables were responsible for killing the anthrax and other microorganisms.

11:00

SR1 4 Characterization of a new VHF-CCP for Sterilization
KATHARINA STAPELMANN, NIKITA BIBINOV, *Ruhr-University Bochum* JOACHIM WUNDERLICH, *Fraunhofer Institute IVV Freising* PETER AWAKOWICZ, *Ruhr-University Bochum* Plasma sterilization is an upcoming alternative to common sterilization methods. Reduced process times combined with a low treatment temperature lead to proper sterilization and decontamination results even for heat-sensitive materials. The capabilities of plasma sterilization were demonstrated in several laboratory setups. Based on these experiences, a new plasma reactor was developed and realized as capacitive coupled plasma discharge with a variable frequency range between 76 and 80 MHz. The reactor concept is designed to meet industrial needs. Therefore, a specialized chamber design was developed: it is composed of PEEK, a high-performance plastic, and it is shaped like a drawer to make the sterilization process easy and uncomplicated for application. Optical Emission Spectroscopy was performed to obtain detailed information about the plasma parameters. According spectra, intensities and plasma parameters will be presented in comparison to a well established ICP laboratory setup. These data are used for optimization of sterilization efficiency. Furthermore, first microbiological tests were carried out at optimized conditions.

11:15

SR1 5 Disinfection of *E. Coli* by non-thermal microplasma electrolysis in conducting liquids TAKA AKI TOMAI, YUKINORI SAKIYAMA, DAVID GRAVES, *University of California, Berkeley* We have developed a method to inactivate microorganisms in conducting liquids by means of microplasmas. The device consists of a single powered electrode with a sharp tip and a ground electrode. Both electrodes are immersed in normal saline solution. The powered electrode is made of Titanium wire ($\sim 100 \mu\text{m}$ in diameter) covered by a glass tube with the tip exposed. We employed repetitive bipolar pulses, consisting of high-voltage (-400 V) short-duration ($10 \mu\text{s}$) negative pulses and low-voltage ($+4 \text{ V}$) long-duration ($990 \mu\text{s}$) positive pulses. On applying the voltage

waveform, microbubbles are generated at both electrodes, suggesting that electrolysis occurs. Repetitive light emission is observed in the vicinity of the sharpened tip. We employed *E. coli* as an indicator bacterium. 10^5 colony forming unit of *E. coli* in 0.4 ml saline solution was exposed to the microplasma for $0-180 \text{ s}$. The survival curve shows that more than 99% of *E. coli* is disinfected in 180 s . We believe long-lived reactive oxygen species such as HO_2 generated by microplasmas and transported by microbubbles play a key role in the inactivation process. Further details of the disinfection mechanisms will be presented at the conference.

11:30

SR1 6 Selective Encapsulation of Heterogeneous Fullerene Ions Into Single-Walled Carbon Nanotubes* TOSHIRO KANEKO, YOHEI HANABUSA, TAKATSUGU NAGAI, RIKIZO HATAKEYAMA, *Department of Electronic Engineering, Tohoku University* A plasma consisting of ionic heterogeneous fullerenes such as C_{60} negative ions and lithium endohedral fullerene positive ions ($\text{Li}@\text{C}_{60}$) is generated by means of an electron beam impact to a sublimated $\text{Li}@\text{C}_{60}/\text{C}_{60}$ composite. These C_{60} negative ions and $\text{Li}@\text{C}_{60}$ positive ions are selectively irradiated and encapsulated in single-walled carbon nanotubes (SWNTs) put on a substrate which is positively and negatively biased, respectively. It is found that the amount of $\text{Li}@\text{C}_{60}$ irradiation to SWNTs depends on the energy of the electron beam E_e which ionizes the $\text{Li}@\text{C}_{60}$, and has the maximum for $E_e \sim 200 \text{ eV}$. The electrical transport properties of the C_{60} and $\text{Li}@\text{C}_{60}$ encapsulated SWNTs are investigated by fabricating them as the channels of field-effect transistor devices. The C_{60} encapsulated SWNTs show the p-type electrical transport property. On the other hand, the $\text{Li}@\text{C}_{60}$ encapsulated SWNTs exhibit the ambipolar conduction or the n-type property. This result indicates that the electrical properties of the SWNTs can be controlled by the kinds of encapsulated fullerenes.

*This work was supported by a Grant-in-Aid for Scientific Research from the Ministry of Education, Culture, Sports, Science and Technology, Japan.

SESSION SR2: ELECTRON AND POSITRON COLLISIONS WITH ATOMS

Thursday Morning, 22 October 2009; Ballroom 2, Saratoga Hilton at 10:00; Thomas M. Miller, Boston College, presiding

Invited Papers

10:00

SR2 1 Electron impact induced light emission from zinc atoms.
DANICA CVEJANOVIC, *University of Western Australia*

Experimental studies of electron impact excitation of zinc atom are rare, primarily due to experimental difficulties. However, zinc is an interesting target because of possible applications in light sources. Also, due to its position in periodic table, zinc is an interesting case for the fundamental understanding of momentum couplings and the role of electron correlations in complex metal atoms. Recent experimental investigations have indicated the existence of highly correlated scattering mechanisms via formation of negative ion resonances and Post Collision Interaction (PCI) in the decay of autoionizing states. These can significantly modify energy dependence of the emission cross sections at low impact energies and the studies of photon emission offer a sensitive way to investigate electron correlations. Specifically, in the lowest autoionizing region of zinc, i.e. between 10 and 15 eV, both the cross sections and polarization of emitted light are affected by the formation of short lived negative ions and PCI effects. These are associated with excitation of one of the sub-valence 3d electrons and complex correlations between inner 3d and outer excited electrons in the target and also with the slow electron released into continuum, need to be included in modeling. Also the scattering of the spin polarized electrons has shown significant spin effects when excitation proceeds via negative ion resonances. Emission cross sections and comparison with theory would be discussed at the conference.

Contributed Papers

10:30

SR2 2 Benchmark calculations for electron collisions with mercury* OLEG ZATSARINNY, KLAUS BARTSCHAT, *Drake University* We have applied our recently developed fully relativistic Dirac B -spline R -matrix (DBSR) code [1] to calculate electron scattering from mercury atoms. Results from a 36-state close-coupling calculation [2] are compared with numerous experimental benchmark data for angle-integrated and angle-differential cross sections, as well as spin-asymmetry, spin-polarization, and electron-impact coherence parameters. We generally obtain much better agreement with experiment than previous distorted-wave and close-coupling attempts. The results are believed to be particularly accurate in the low-energy (below 10 eV) near-threshold regime and hence represent a significant improvement over frequently used older datasets for modeling of low-temperature plasmas containing mercury. [1] O. Zatsarinny and K. Bartschat, *Phys. Rev. A* **77**, 062701 (2008). [2] O. Zatsarinny and K. Bartschat, *Phys. Rev. A* **79**, 042713 (2009).

*Supported by the NSF under PHY-0555226 and PHY-0757755.

10:45

SR2 3 Complex q parameters for helium $L = 0, 1, 2$ autoionizing levels N.L.S. MARTIN, B.A. DEHARAK, *University of Kentucky*, K. BARTSCHAT, *Drake University* We recently reported¹ out-of-plane ($e, 2e$) experiments on He autoionization. The data were presented as angular distributions of ejected electrons from the three autoionizing levels 1S , 1D , and 1P and exhibited two well-known features, the binary and recoil peaks. It was found that the recoil peak (relative to the binary peak) could be accurately reproduced by a second order distorted wave Born calculation using the R -matrix with pseudo-states approach, but not by the equivalent first order calculation, which underestimated the size of the recoil peak. It was also found that a plane wave Born approximation calculation could reproduce the results, but only if anomalously large values of Fano q -parameters were assumed. We will present an analysis of the first and second order calculations in terms of Fano q parameters. We find that for the first order calculations the q parameters are essentially real, but for the second order calculations they are complex, quantities. The 1D_2 parameters are particularly striking in this respect. This work was supported by the U.S. NSF under Grants No. PHY-0855040 (NLSM) and PHY-0757755 (KB).

¹B.A. deHarak, K. Bartschat, and N.L.S. Martin, *Phys. Rev. Lett.* **100**, 063201 (2008).

11:00

SR2 4 Differential cross sections for modeling of noble gas plasmas ALLAN STAUFFER, *York University* ROBERT MCEACHRAN, *Australian National University* Differential cross sections are required to model the 3D diffusion of electrons in a gas under the influence of electromagnetic fields. In a low temperature plasma containing a noble gas elastic scattering from the neutral atoms is an important process governing this diffusion even at energies above the inelastic thresholds. We have calculated the phase shifts at such energies using our optical potential method

[1] which takes account of open inelastic channels. This method yields much more accurate data than potential scattering calculations using only real potentials over a wide range of scattering energies. We will present analytic fits to our results so that cross sections may be calculated for arbitrary scattering energies. [1] S. Chen, R. P. McEachran and A. D. Stauffer, *J. Phys. B* **41**, 025201 (2008).

11:15

SR2 5 Accurate atomic data for xenon: energy levels, oscillator strengths, and electron collision cross sections* KLAUS BARTSCHAT, OLEG ZATSARINNY, *Drake University* We have applied our recently developed fully relativistic Dirac B -spline R -matrix (DBSR) code [1] to calculate the atomic structure (energy levels and oscillator strengths) as well as electron scattering from xenon atoms. Results from a 31-state close-coupling model for the excitation function of the metastable ($5p^5 6s$) $J = 0, 2$ states show excellent agreement with experiment [2], thereby presenting a significant improvement over the most sophisticated previous Breit-Pauli calculations [3,4]. The same model is currently being used to calculate electron-impact excitation from the metastable $J = 2$ state. The results will be compared with recent experimental data [5] and predictions from other theoretical models [6,7]. Our dataset is an excellent basis for modeling plasma discharges containing xenon. [1] O. Zatsarinny and K. Bartschat, *Phys. Rev. A* **77** (2008) 062701. [2] S. J. Buckman *et al.*, *J. Phys. B* **16** (1983) 4219. [3] A. N. Grum-Grzhimailo and K. Bartschat, *J. Phys. B* **35** (2002) 3479. [4] M. Allan *et al.*, *Phys. Rev. A* **74** (2006) 030701(R). [5] R. O. Jung *et al.*, *Phys. Rev. A* **72** (2005) 022723. [6] R. Srivastava *et al.*, *Phys. Rev. A* **74** (2006) 012715. [7] J. Jiang *et al.*, *J. Phys. B* **41** (2008) 245204.

*Supported by the NSF under PHY-0555226 and PHY-0757755.

11:30

SR2 6 Electron excitation into the Xe($5p^5 7p$) configuration from the ground and $1s_5$ ($J=2$) metastable level* R.O. JUNG, JOHN B. BOFFARD, L.W. ANDERSON, CHUN C. LIN, *University of Wisconsin-Madison* We have measured electron excitation cross sections into the $3p_x$ (Paschen's notation for $5p^5 7p$) levels of Xe by passing an electron beam through a static gas target (for ground state excitation) or an atomic beam emerging from a hollow cathode (for excitation from metastable levels) and detecting fluorescence from the decay of excited atoms. Excitation cross sections out of the ground level, especially at high energies, exhibit moderate dependence on gas pressure due to cascades from resonant levels. For excitation out of the $1s_5$ ($J=2$) metastables into the $3p_6$, $3p_7$, $3p_8$, and $3p_9$ levels ($J=2,1,3,2$), which conform to optical selection rules, the excitation functions demonstrate a variety of shapes ranging from an expected broad maximum to a sharp peak riding on a structure of intermediate width. The cross section data for the various $3p_x$ levels are interpreted in terms of oscillator strengths as well as angular momentum coupling of the states involved. The $3p_x \rightarrow 1s_y$ emissions are prominent components of Xe plasmas, making our measured cross sections valuable for optical plasma diagnostics.

*Supported by the National Science Foundation.

11:45

SR2 7 Positron Interactions with Rare Gas Atoms* A. JONES, P. CARADONNA, C. MAKOCHEKANWA, J. SULLIVAN, D. SLAUGHTER, S. BUCKMAN, CAMS, Australian National University, Canberra D. MUELLER, University of North Texas, Denton S. BELLM, B. LOHMANN, CAMS, University of Adelaide, South Australia We present results for low energy positron scattering from the rare gas atoms He, Ne and Ar. A high resolution, trap-based positron beam has been used for these measurements which encompass absolute cross sections for total scattering, positronium formation, electronic excitation and total ionization at energies between 0.5 and 60 eV. Where possible we make comparison with previous experiments and with contemporary scattering theory for the total scattering and positronium formation cross sections. The excitation measurements have focused on the $2^1S, P$ states of helium at energies between threshold and 40 eV, and they represent the first state selective measurements of these two excited states. A key motivation of the ionization measurements is to study the near-threshold 'Wannier' regime, and we will present measurements that map the energy dependence of the ionization cross section within 2 eV of threshold.

*Supported by the Australian Research Council.

SESSION SR3: PLASMA-SURFACE INTERACTIONS

Thursday Morning, 22 October 2009; Ballroom 3, Saratoga Hilton at 10:00; Song-yun Kang, Tokyo Electron Ltd, presiding

Invited Papers

10:00

SR3 1 Plasma surface interactions in fluorocarbon systems.
MATTHEW GOECKNER, University of Texas at Dallas

Fluorocarbon plasmas have been used for close to four decades in the semiconductor industry. Because such process systems are complex, many individuals subdivided the complete system into three main subsystems, gas-phase chemistry, plasma physics and surface chemistry/physics. Using this methodology, considerable knowledge has been gained in fundamental processes found in the gas-phase chemistry and plasma physics. Despite numerous high quality studies, understanding the surface subsystem has proven to be challenging. In part this is due to the interactions of the three subsystems. In this paper we will review a model of surface interactions for fluorocarbon plasmas which is based on surface-averaged quantum mechanical processes. Using the model we arrive at a general model describing both etch and deposition. We will show how energy considerations, such as a local surface temperature, can play major roles in such processes. We will examine the basic links between the model and experimental data obtained from fluorocarbon plasmas.

Contributed Papers

10:30

SR3 2 Temperature Impact on Plasma-Surface Interactions in an FC Plasma Environment* CALEB NELSON, University of Texas at Dallas IQBAL SARAF, LAWRENCE OVERZET, MATTHEW GOECKNER, Many variables influence the nature of plasma-surface interactions. These include: radical and ion fluxes, ion energy and angle distributions, surface temperatures, and surface materials. A simplified model relates radical and ion fluxes to process rates through sticking and etch yield probability coefficients, where such coefficients are functions of particle energy, surface temperature and impact angle. Here we make use of an easily adjustable plasma system, the modified GEC reference cell, to examine the influence of temperature on sticking coefficients and etch yields. The mGEC provides the option of changing chamber dimensions, wall material, and wall temperature. The variable electrode gap permits depositing radical fluxes to be controlled almost independently of ion and etching radical fluxes, allowing

the deconvolution of the process rate model. The independent control of wall and chuck temperature can then be used to study the effect of surface temperature on plasma chemistry (changing wall recycling) and surface morphology, respectively. Increasing surface temperature decreases radical and ion-assisted deposition and alters the F/C ratio and process rate of the film as etch yields are increased.

*This work is supported by a gift from AMAT.

10:45

SR3 3 SiO₂ Film Etching Process Using Environment-Friendly New Gas C₅F₇H YUDAI MIYAWAKI, KEIGO TAKEDA, Nagoya University AZUMI ITO, MASAHIRO NAKAMURA, Zeon Corporation MAKOTO SEKINE, MASARU HORI, Nagoya University With the continuous miniaturization of semiconductor memory devices, a much precise etching process for a high aspect ratio contact hole in SiO₂ film is indispensable. Furthermore, deterioration of the SiO₂ selectivity over a fragile, thin

ArF photoresist would cause the sidewall roughness and poor pattern-width definition. In this study, we utilized a newly designed C_5F_7H gas. We compared the etch performances between the new gas and conventional C_5F_8 . Ar and O_2 were introduced with the each fluorocarbon gas to control the etching rate. A dual frequency (60 MHz / 2 MHz) capacitively coupled plasma was employed. The SiO_2 etching rate and selectivity to ArF photoresist were investigated as a function of O_2 flow rate. The maximum selectivity of only 3.7 and the SiO_2 etching rate of 416 nm/min were obtained at O_2 flow rate of 20 sccm for the $C_5F_8/O_2/Ar$ plasma. For the newly developed $C_5F_7H/O_2/Ar$ plasma, the maximum selectivity of 13.5 with the etching rate of 356 nm/min was achieved at 25-sccm O_2 flow rate. From these results, it was confirmed that almost four times higher selectivity than that of the conventional C_5F_8 gas was obtained by using the new C_5F_7H gas.

11:00

SR3 4 Plasma-surface interactions during Si etching in Cl- and Br-based plasmas: An empirical and atomistic study HIRO-TAKA TSUDA, TATSUYA NAGAOKA, HIROKI MIYATA, YOSHINORI TAKAO, KOJI ERIGUCHI, KOUICHI ONO, *Kyoto University* Nanometer-scale control of Si etching in Cl_2 - and HBr -containing plasmas is indispensable in the fabrication of gate electrodes and shallow trench isolation. There are profile anomalies of sidewalls such as tapering, bowing, footing (or corner rounding), and notching, which largely affect the critical dimension. There are also anomalies of bottom surfaces such as microtrenching and roughness (or residues), which affect the bottom uniformity, and lead to recess and damage in gate fabrication. Atomic-scale cellular model (ASCeM) based on the Monte Carlo method has been developed to simulate plasma-surface interactions and the profile evolution during etching, including passivation layer formation, and also ion reflection and penetration on feature surfaces. We have also studied atomistic plasma-surface interactions by classical molecular dynamics (MD) simulation, where an improved Stillinger-Weber interatomic potential was newly developed. The numerical results were compared with etching experiments and also with surface diagnostics including *in-situ* Fourier-transform-infrared reflection absorption spectroscopy (FTIR-RAS), to reveal the origin of profile anomalies on feature surfaces during etching, and then to achieve the precise control of etched profiles.

11:15

SR3 5 Analysis of the surface reactions of ArF photoresist during fluorocarbon plasma etching by XPS TAKUYA TAKEUCHI, MAKOTO SEKINE, HIROTAKA TOYODA, KEIGO TAKEDA, MASARU HORI, *Nagoya University* SONG-YUN KANG, IKUO SAWADA, *Tokyo Electron Ltd.* High-aspect ratio pattern etching processes with nano-scale accuracy is desired in such as a contract hole etching for the silicon dioxide that is used as a dielectric passivation layer over MOSFETs. However, photoresist used in the advanced ArF lithography is not tolerant enough for plasma etching processes, and it often causes deformations in the etched feature with bowing, distortion, twisting and so on. It is important to investigate the reaction of photoresist with fluorocarbon to overcome these problems and realize sophisticated etch processes. In this research, the modified layer of the photoresist by bombardment of CF_x^+ ions was analyzed. The ions, such as CF^+ , CF_2^+ , CF_3^+ , and F^+ , were produced from CF_4 gas by

electron impact, and selected by quadrupole mass filter. The CF_x^+ ions were bombarded to ArF photoresist as ion beam with an accelerated energy from 100 to 400 eV. The equipment system is evacuated by four turbo molecular pumps. Ultimate pressure of the equipment is lower than 10^{-9} Torr. The beam equipment and XPS analysis chamber are connected in vacuum, so we can use XPS analysis without atmospheric influence after the ion etch process. In this study, we investigated the modified layer of the photoresist by *in-situ* XPS.

11:30

SR3 6 Determination of gas phase and surface reactions in plasma polymerization DIRK HEGEMANN, *Empa, St.Gallen/Switzerland* Using macroscopic kinetics, the reactions within the gas phase are governed by the reaction parameter power input per gas flow W/F , which corresponds to a specific energy, while reactions by energetic particle bombardment at the growing film surface are rather related to power input W alone. Assuming activation reactions, the mass deposition rate per gas flow can be described by an Arrhenius-like approach:

$$R_m/F = G_{exp} \left(-E_a/W/F \right)$$

Mixtures of hydrocarbons (C_2H_4) and reactive gases (CO_2 , N_2+H_2) were examined within low pressure RF plasmas. Thus, functional a-C:H:O or a-C:H:N plasma coatings result. At increasing energy input it is found that the deposited mass shows a deviation from the above equation, commonly related to energetic particle interactions. However, using the same range of W/F with varying power input W , it was found that the observed drop in deposition rate scales solely with energy input W/F for a-C:H:O, i.e. depending on plasma chemistry. a-C:H:N films, on the other hand, show both chemical and physical influences on the film growth. Hence, gas phase reactions such as a change of film-forming species play a major role in plasma polymerization.

11:45

SR3 7 Role of plasma activation in the kinetics of CNT growth in PECVD process IRINA LEBEDEVA, *Kintech Lab Ltd* ALEXEY GAVRIKOV, ALEXEY BARANOV, MAXIM BELOV, ANDREY KNIZHNIK, BORIS POTAPKIN, *Kintech Lab Ltd* TIMOTHY SOMMERER, *GE Global Research Center* The work presents kinetic modeling of the effect of acceleration for the growth kinetics of carbon nanotubes by hydrocarbon gas mixture modification with plasma discharge. The plasma activation creates active species in hydrocarbon gas mixture, which can easily adsorb and dissociate on the catalyst surface. So plasma treatment of the gas mixture in the CVD process allows to increase the carbon supply rate by a few orders of magnitude compared to that in thermal CVD process. On the other hand, plasma can also provide etching of carbon species from the catalyst surface. To correctly reproduce both of these effects of plasma, the kinetic model of growth of carbon nanotubes is developed based on first-principles analysis of heterogeneous processes on the catalyst surface and detailed kinetics of gas phase chemistry. The model is used to compare the growth rates of carbon nanotubes in thermal and plasma-enhanced CVD processes and to determine critical gas pressures, at which CNT growth kinetics switches from the adsorption limitation to the limitation by reaction and diffusion on the catalyst.

SESSION 3R: VORPAL TUTORIAL

Thursday Noon, 22 October 2009; Whitney, Saratoga Hilton at 12:00

12:00

ED CASE, *Tech-X Corporation***SESSION TR1: MATERIALS PROCESSING**

Thursday Afternoon, 22 October 2009; Ballroom 1, Saratoga Hilton at 13:30; Jean-Paul Booth, CNRS - Ecole Polytechnique, presiding

Invited Papers

13:30

TR1 1 Reaction mechanisms in patterning complex oxide materials by plasmas.JANE P. CHANG, *University of California, Los Angeles*

The continuous down-scaling of the microelectronic and optoelectronic integrated circuits dictates the development of atomic layer deposition and high fidelity pattern transfer processes to synthesize and integrate novel materials, such as multifunctional oxides, into nanometer scaled devices. As the introduction of new gate dielectric materials in sub-32-nm metal oxide semiconductor field effect transistors (MOSFET) increases the complexity of the gate stack etch process, it is critical to formulate a comprehensive kinetics model to predict the physical and chemical effects of plasma chemistries on these complex gate dielectric materials. In this talk, I will highlight recent work on delineating the reaction mechanism in patterning complex metal oxides in halogen based plasmas. In general, the etch-rate scaled with the square-root of ion energy, and was dictated by the chemical nature of the dominant reaction ions in the plasma. The dominant metal-containing etch products were mainly MCl_x species, and their intensity and complexity increased with ion energy. A model was formulated to accurately describe the etching of composite oxide films in complex plasma chemistries involving competing deposition and etching mechanisms. This site balance-based model explains the etch-rate dependence on key plasma parameters including plasma chemistry/condition, neutral-to-ion flux ratio, and ion energy, as well as the film composition. The model fits well to a wide range of experimental data demonstrating its validity and potential application to various plasma etching processes.

Contributed Papers

14:00

TR1 2 Surface Modification of Polymer Photoresists in Fluorocarbon Plasma Etching* MINGMEI WANG, *Iowa State University*

MARK KUSHNER, *University of Michigan* In plasma etching of high aspect ratio (AR), nm sized features, erosion of polymer photoresist (PR) can perturb the feature profile (e.g., bowing). Although cross-linking of PR due to ion and VUV fluxes could make it more resistive to etching, typically the PR etch rate is too high to maintain the pattern when the AR is large (> 20). In dielectric plasma etching using fluorocarbon gases, one strategy to prevent PR erosion is to deposit a $(C_xF_y)_n$ polymer on its surface. This process may be enhanced in dc-augmented capacitively coupled plasmas (CCPs) by sputtering of Si and C_xF_y from the dc biased electrode. Dangling bonds generated on the PR surface by ion, photon or electron bombardment trap Si and C_xF_y radicals forming Si-C and C-C bonds. Sputtered Si atoms can also react with C_xF_y radicals to produce more reactive C_xF_{y-1} radicals which are more easily incorporated into the PR. In this talk we discuss scaling laws for radical production derived from a computational investigation of a dc-augmented dual frequency CCP

reactor sustained in $Ar/C_4F_8/O_2$. Fluxes of Si radicals are produced by sputtering of the dc electrode. Rates of polymer deposition on and sputtering of PR, and consequences of PR erosion (and deposition) on feature profiles will be discussed.

*Work supported by Tokyo Electron Ltd. and Semic. Res. Corp.

14:15

TR1 3 Factors Affecting the Sealing Efficiency of Low-k Dielectric Surface Pores Using Successive He and Ar/ NH_3 Plasma Treatment* JULINE SHOEB, *Iowa State University*

MARK KUSHNER, *University of Michigan* Sequential treatment of porous SiCOH by He and NH_3 plasmas is effective at sealing pores while maintaining the low-k of the dielectric. He plasmas activate surface sites to accelerate the reactions responsible for pore sealing. Additional NH_3 plasma treatment completes the sealing through formation of Si-N, C-N and N-N bonds resulting from the adsorption of NH_3 . To seal pores, sufficient He plasma exposure time is required to break Si-O bonds at SiO_2 sites and to activate pore lining CH_n groups by removal of H atoms. Sealing efficiency degrades if the pore radius is too large to link the sites of opposite pore walls by Si-N-N-C, Si-N-N-Si or C-N-N-C chains. In this talk, we discuss results from a computational investigation of the sealing efficiency of a porous carbon doped

silica films (SiOCH). The Hybrid Plasma Equipment Model provided the fluxes of ions, neutrals and photons onto the surface from He and NH₃/Ar ICPs. The sealing mechanism was implemented in the Monte Carlo Feature Profile Model with which profiles of the low-*k* pores are predicted. Factors affecting the sealing efficiency, such as treatment time, bias, average pore radius and pore radius standard deviation will be discussed.

*Work supported by Semiconductor Research Corp.

14:30

TR1 4 The influence of He plasma pretreatment on O and H atom interaction with low-*k* nanoporous materials* O.V. BRAGINSKY, A.S. KOVALEV, D.V. LOPAEV, E.M. MALYKHIN, YU. A. MANKELEVICH, T.V. RAKHIMOVA, A.T. RAKHIMOV, A.N. VASILIEVA, S.M. ZYRYANOV, *Nuclear Physics Institute, Moscow State University, Moscow, Russia* M.R. BAKLANOV, *IMEC, Leuven, Belgium* The low-*k* film damage during resist plasma processing is mainly caused by O and H atoms. Low-*k* surface modification via plasma pretreatment is capable to reduce the atom influence and therefore to minimize the damage. The effect of He plasma pretreatment both on low-*k* surface modification and interaction with O and H atoms was studied for 3 types of low-*k* SiOCH films: BDIIx, ELK 2.5, ELK 2.3 (porosity: 24, 24, 33%, pore radius: 0.8, 0.8, 1 nm). The influence of ions, VUV radiation and metastables in He low-pressure (20 mTorr) SWD 81 MHz discharge was separately investigated. The O and H surface loss probabilities were measured in the far afterglow of the

high-pressure (10 Torr) 13.56 MHz discharge. All changes occurring with low-*k* surface after treatment in both discharges were analyzed by FTIR spectroscopy. The phenomenological model, including recombination and reactions of O and H atoms on low-*k* surface, was used to analyze the obtained results.

*This research was supported by RFBR (09-02-01374-a), KSS (SS-133.2008.2) and MSU-IMEC Agreement.

14:45

TR1 5 Investigation of the etching mechanisms of Ar/Cl₂/O₂ inductively coupled plasmas on silicon by means of modelling and experiments STEFAN TINCK, *University of Antwerp* In this topic, the etching behaviour of Cl₂/O₂/Ar inductively coupled plasmas on a silicon substrate, as used in shallow trench isolation for the production of electronic devices, is investigated by means of modelling and experiments. A hybrid plasma model is applied to calculate the plasma characteristics in the reactor chamber and two additional Monte Carlo simulations are performed to predict the fluxes, angles and energy of the plasma species bombarding the silicon substrate, as well as the resulting surface processes such as etching and deposition. Experimentally, it is found that when the fraction of oxygen in the gas mixture of the plasma is too high, the deposition of oxygen species becomes superior to the etching of silicon by chlorine species, resulting in an etch rate close to zero. In the surface simulations, special attention is paid to the potential distribution and the composition of the surface layers during etching or deposition to provide a better insight in these silicon surface processes.

Invited Papers

15:00

TR1 6 Development and validation of a C5F8/Ar/O₂ mixture chemistry model using quantum chemistry methods. SONG-YUN KANG, *Tokyo Electron Ltd.*

Understanding the electron impact processes in c-C5F8 plasmas is of importance to low dielectric constant thin film deposition and etch process development. As much of radicals and excited states in c-C5F8 plasma chemistry are inaccessible by experiment, we used quantum chemistry methods, coupled with a zero-dimensional plasma kinetics model to develop an electron impact cross-section set and its associated plasma chemistry mechanism. The calculations were augmented with quadrupole mass spectrometry and actinometry measurements on a 200mm capacitively coupled plasma source. Predicted etch rates are in good agreement with experimental data examining large substrate RF bias and low pressure. The primary loss process for c-C5F8 is electron impact dissociation into isomers of C5F7 via excitation to the triplet state of c-C5F8. Electron impact dissociation of C5F7 isomers leads finally to the production of C5F5 (an isomer with two conjugate pi bonds) and C5F6 (an isomer with two pi bonds and a folded ring structure). These and other isomers characterized by a plurality of pi bonds and certain ring structures are very stable under electron impact. These "terminal" species are important from the perspective of polymer deposition. The etch precursor, atomic fluorine, is primarily produced from electron impact dissociation of the feed-gas and its degradation products. CF is produced from dissociation of CF₂. CF₃ is produced primarily from the walls.

SESSION TR2: ELECTRON AND PHOTON INTERACTIONS WITH ATOMS AND MOLECULES

Thursday Afternoon, 22 October 2009; Ballroom 2, Saratoga Hilton at 13:30; Klaus Bartschat, Drake University, presiding

Invited Papers

13:30

TR2 1 Laser-assisted electron impact autoionization of Helium.*BRUNO DEHARAK, *Illinois Wesleyan University*

We have begun to perform the first electron impact autoionization experiments in the presence of a laser field. Laser assisted electron collisions are a poorly understood process. A theoretical discussion of electron impact ionization in the presence of a laser field was published as long ago as 1988,¹ but the first experimental results were only published in 2005.² Distinct differences in the ionization process between the field free (laser off) and field assisted (laser on) cases were found. The results were in poor agreement with quantum calculations but could (oddly enough) be explained with a simple classical model. Our experiments have the advantage that autoionizing levels provides energy markers: the absorption or emission of a photon is expected to shift the resonance position in the ejected electron spectrum by the photon energy. It is easier to detect the presence of such sideband peaks than it is to observe quantitative shifts in the energy onset of traditional simultaneous electron-photon excitation (SEPE) experiments. We will provide details of our experimental apparatus, and provide a progress report on these experiments.

*This work was supported by the United States National Science Foundation under Grant No. PHY-0555541.

¹C. J. Joachain et al., *Phys. Rev. Lett.* 61, 165 (1988)

²C. Höhr et al. *Phys. Rev. Lett.* 94, 153201 (2005)

Contributed Papers

14:00

TR2 2 Super-elastic electron excitation of atoms in magnetic & optical fields

ANDREW MURRAY, *University of Manchester* WILLIAM MACGILLIVRAY, *Southern Cross University* MARTYN HUSSEY, *University of Manchester* Understanding electron impact excitation of atoms usually requires coincidence techniques to fully ascertain the interactions that occur, & to allow detailed comparison to collision theories. These experiments are slow, but have advantages since many targets can be studied. By contrast, the 'time reversed' super-elastic scattering experiment produces equivalent information thousands of times faster with higher precision, but is limited to only a few targets that can be excited by tunable lasers. Here two new techniques invented in Manchester are discussed. The first allows the cross sections to be determined over all angles using a Magnetic Angle Changer to steer electrons to & from the target [1-3]. The second adopts a resonant optical cavity around the interaction region to efficiently excite a much wider range of targets. We can then for the first time study targets of relevance to industry, including Zn (which may provide an alternative to Hg in low energy lighting), through to Au & Ag. [1] M Hussey et al *Phys Rev Lett* 99 133202 (2007) [2] A J Murray et al *Phys Rev A* 77 013409 (2008) [3] M Hussey et al *J Phys B* 41 055202 (2008)

14:15

TR2 3 (e,2e) ionization studies of diatomic & triatomic molecules

KATE NIXON, ANDREW MURRAY, CHRISTIAN KAISER, *University of Manchester* OLA AL-HAGAN, *Missouri University of Science & Technology* JAMES COLGAN, *Los Alamos National Laboratory* DON MADISON, *Missouri University of Science & Technology* (e,2e) studies yield the most detailed experimental data on electron impact ionization of atomic & molecular targets for comparison to quantum collision theories. Coincidence techniques are here used to measure the probability of ionization as a function of the incident electron scattering angle

and angle of the electron ejected from the target. In Manchester we study this process at low energies, where the ionization probability is greatest & the interaction most complex. We recently considered ionization of simple molecules (eg H₂ & H₂O) from a coplanar geometry to the perpendicular plane[1-4], and have discovered the interaction is far more complex than for ionization of atoms [5]. We here present comparisons between theory & experiment, and discuss new methods we intend to implement to study ionization from laser-aligned atoms & molecules. References. [1] J Colgan et al *Phys Rev Lett* 101 233201 (2008) [2] O Al-Hagan et al *Nature Physics* 5 59 (2009) [3] J Colgan et al *Phys Rev A* 79 052704 (2009) [4] C Kaiser et al *J Phys B* 40 2563 (2007) [5] A J Murray et al *J Phys B* 36 4875 (2003) & references therein

14:30

TR2 4 Electron Impact Ionization Cross Sections of H₂ for Low Excess Energies Ranging from 2eV to 20eV*

OLA AL-HAGAN, DON MADISON, *Missouri University of Science and Technology* JAMES COLGAN, *Los Alamos National Laboratory* CHRISTIAN KAISER, ANDREW MURRAY, *University of Manchester (UK)* We had recently investigated the nuclear structure effect for the fully differential electron impact ionization cross sections of H₂ and He measured in the perpendicular plan where the two outgoing electrons have equal energies of 10 eV (20eV excess energy). For this case we demonstrated that He had a maximum for back-to-back scattering and H₂ had a minimum due to the different nuclear configurations. We have extended our investigation for H₂ to lower excess energies down to 2eV (both final state electrons have 1eV energy). We will show that, as the excess energy decreases, the effective impact parameter increases and molecular cross sections start to look like the atomic ones as the nuclear separation becomes less important.

*Supported by NSF.

14:45

TR2 5 Accuracy of the Gamow Factor for Approximating the Post Collision Interaction (PCI) in Electron-Impact Ionization of Atoms* ADAM UPSHAW, *Missouri S&T* HARI SAHA, *University of Central Florida* DON MADISON, *Missouri S&T* Recently Kheifets et al. [1] reported a distorted wave Born (DWBA) calculation for ionization of helium, neon and argon where the post collision interaction (PCI) between the two final state electrons was approximated using the Gamow-factor (called the G-factor). For cases where there was a large difference between experiment and theory at the recoil peak, the G-factor significantly improved agreement between experiment and theory. The G-factor is an approximation for including the final state Coulomb interaction between the two continuum electrons in the final state wavefunction. The 3DW (three-body-distorted-wave) method properly includes the Coulomb interaction in the final state wavefunction without approximation. The G-factor approximation is attractive due to its computational simplicity (i.e. the effects of PCI can be determined by multiplying DWBA results by the Gamow factor). 3DW calculations, on the other hand, require a full numerical 6-dimensional integration. We will examine the accuracy of the G-factor approximation by comparing 3DW results with G-factor results for ionization of neon, argon and xenon for low, intermediate and high energy. [1] Kheifets et al., *J. Phys. B*, 41, 145201 (2008).

*Work supported by the NSF under grant 0757749.

15:00

TR2 6 Electron scattering & high resolution spectroscopy from cold atoms in an AC-MOT ANDREW MURRAY, MATTHEW HARVEY, *University of Manchester* A new revolution in atomic physics has arisen due to the ability to precisely control the external motion of atoms using laser forces. By using high resolution continuous wave lasers it is possible to reduce & compress the momentum of an atomic beam, & to trap & cool these atoms to produce a high density cloud of cold atoms in a magneto optical trap (MOT). The temperature of the atoms can be further reduced to sub-micro-Kelvin levels using a variety of techniques, so as to form a Bose Einstein Condensate (BEC). Here we discuss a new type of atom trap (the AC-MOT) which allows the magnetic fields produced by the trap to be switched off > 300 times faster than with a conventional MOT [1]. Electron scattering & high resolution laser experiments can then be performed from cold atoms with virtually no loss (apart from the normal processes associated with background gases). Results from potassium ionization will be presented, together with a discussion of new types of precision scattering experiments that can be performed using these cold targets. [1] M Harvey and A J Murray *Phys Rev Lett* 101 173201 (2008)

15:15

TR2 7 Production of Excited Atomic Hydrogen and Deuterium from H₂, D₂ and HD Photodissociation J.R. MACHACEK, *University of Nebraska-Lincoln* V.M. ANDRIANARIJAONA, *Pacific Union College* J.E. FURST, *University of Newcastle-Ourimbah* T.J. GAY, *University of Nebraska-Lincoln* A.L.D. KILCOYNE, *LBNL* A.L. LANDERS, *Auburn University* K.W. McLAUGHLIN, *Loras College* We have measured the production of Ly α and H α fluorescence from atomic H and D resulting from the photodissociation of H₂, D₂ and HD by linearly-polarized photons with energies between 20 and 65 eV. In this energy range, excited photo-fragments result primarily from the production of doubly-excited molecular species which promptly autoionize or dissociate into

two neutrals. Comparison between the relative cross sections of H₂ and D₂ and the available theory show only qualitative agreement. We will discuss the various systematic effects which affect this and other types of synchrotron-based measurements in this energy range. Support provided by the NSF (Grant PHY-0653379), DOE (LBNL/ALS) and ANSTO (Access to Major Research Facilities Programme).

SESSION TR3: PLASMA CHEMISTRY

Thursday Afternoon, 22 October 2009

Ballroom 3, Saratoga Hilton at 13:30

Robert Hicks, UCLA, presiding

Contributed Papers

13:30

TR3 1 Manipulating Plasma Surface Interaction STEPHAN REUTER, KARI NIEMI, *Queen's University Belfast* VOLKER SCHULZ-VON DER GATHEN, *Ruhr University Bochum* TIMO GANS, *Queen's University Belfast* A low temperature rf-powered atmospheric pressure plasma jet (APPJ) operated with helium and a small oxygen admixture is investigated. The study aims at a better understanding of reactive oxygen species production and annihilation processes in the APPJ's effluent. Optical emission spectroscopy (OES) measurements reveal the existence of excited atomic oxygen even at considerable distance from the jet's nozzle. In order to gain insight into energy transport mechanisms from core plasma to the effluent, (V)UV-optical emission spectroscopy measurements and chemical model calculations are performed and oxygen species densities (O, O₃, O₂(b¹ Σ_g^+)) derived from two-photon absorption laser-induced fluorescence (TALIF) spectroscopy [1], UV-absorption spectroscopy, and optical emission spectroscopy measurements are compared with the chemical model calculations, showing excellent agreement. The chemical model allows to investigate the possibility to influence the APPJ's chemistry and enhance the oxygen output – e.g. by laser radiation. The ultimate prospect is to design the properties of a plasma according to the specifications required by respective surface treatment applications. [1] S. Reuter, K. Niemi, V. Schulz-von der Gathen, and H. F. Döbele, *Plasma Sources Sci. Technol.*, **18**, 015006 (2009)

13:45

TR3 2 Comparison of mass spectra measurements and kinetic modelling* of high pressure He-Air glow discharges K.R. STALDER, *Stalder Technologies and Research, Redwood City, USA* R.J. VIDMAR, *University of Nevada, Reno, USA* W.G. GRAHAM, *Queens University Belfast, UK* Y.A. GONZALVO, *Hidden Analytical Ltd, Warrington, UK* The results of a chemistry code are compared with mass spectrometry measurements of positive and negative ion species for helium-air systems excited in the 30-50 kHz range. A 6 mm O.D. DBD with a 1.0 mm diameter inner wire electrode, operated at a flow of helium 3-10 l.min⁻¹ into air was interfaced to a Hidden Analytical HPR-60 molecular beam mass spectrometer (MBMS). This consists of a quadrupole mass spectrometer with a differentially pumped three-stage inlet system [1]. The kinetics of a parallel plate APGD, operating in static helium with 10000 ppm of air, have been modeled using a

code [3,4] which includes 461 reactions and tracks 58 species including neutral atoms and molecules, metastable species, vibrationally-excited N_2 and O_2 , electrons, positive and negative ions, and various water cluster ions. The results show interesting similarities with the main discrepancies existing in the effects of water clustering. [1] E.Stoffels et al., *Plasma Sources Sci. Technol.* 15 501 (2006) [2] Y. Aranda-Gonzalvo et al *J.Vac.Sci.Technol.A* 24 55 (2006) [3] R.J. Vidmar, *IEEE Trans. Plasma Sci.* 18, 733 (1990) [4] K.R. Stalder et al., *J.Appl. Phys.* 99, 093301 (2006).

Invited Papers

14:15

TR3 4 Effects of non-thermal plasmas and electric field on hydrocarbon/air flames.

BISWA GANGULY, *Air Force Research Laboratory*

Need to improve fuel efficiency, and reduce emission from hydrocarbon combustor in automotive and gas turbine engines have reinvigorated interest in reducing combustion instability of a lean flame. The heat generation rate in a binary reaction is $H_Q = N^2 c_1 c_2 Q \exp(-E/RT)$, where N is the density, c_1 and c_2 are mol fractions of the reactants, Q is the reaction heat release, E is the activation energy, R is the gas constant and T is the average temperature. For hydrocarbon-air reactions, the typical value of $E/R \sim 20$, so most heat release reactions are confined to a thin reaction sheet at $T \geq 1400$ K. The lean flame burning condition is susceptible to combustion instability due to a critical balance between heat generation and heat loss rates, especially at high gas flow rate. Radical injection can increase flame speed by reducing the hydrocarbon oxidation reaction activation barrier and it can improve flame stability. Advances in nonequilibrium plasma generation at high pressure have prompted its application for energy efficient radical production to enhance hydrocarbon-air combustion. Dielectric barrier discharges and short pulse excited corona discharges have been used to enhance combustion stability. Direct electron impact dissociation of hydrocarbon and O_2 produces radicals with lower fuel oxidation reaction activation barriers, initiating heat release reaction $C_n H_m + O \rightleftharpoons C_n H_{m-1} + OH$ (and other similar sets of reactions with partially dissociated fuel) below the typical cross-over temperature. Also, $N_2(A)$ produced in air discharge at a moderate E/n can dissociate O_2 leading to oxidation of fuel at lower gas temperature. Low activation energy reactions are also possible by dissociation of hydrocarbon $C_n H_m + e \rightarrow C_n H_{m-2} + H_2 + e$, where a chain propagation reaction $H_2 + O \rightleftharpoons OH + H$ can be initiated at lower gas temperature than possible under thermal equilibrium kinetics. Most of heat release comes from the reaction $CO + OH \rightarrow CO_2 + H$, nonthermal OH production seem to improve combustion stability. The effect of applied voltage in a flame below self-sustained plasma generation is known to enhance flame holding through induced turbulence. Review of recent results will be presented to show future research opportunities in quantitative measurements and modeling of hydrocarbon/air plasma enhanced combustion.

14:45

TR3 5 Ultrahigh quality amorphous silicon film deposition for solar cells employing novel plasma enhanced CVD.*

MASAHARU SHIRATANI, *Kyushu University, Japan*

Hydrogenated amorphous silicon (a-Si:H) is most widely employed as a top cell material in thin film Si tandem solar cells. The a-Si:H solar cells have three important problems to be solved: 1) a low stabilized efficiency below 10%. 2) light induced decrease in efficiency around -20% of the initial one. 3) a low deposition rate of 0.5 nm/s. In SiH_4 discharges employed for a-Si:H deposition, there coexist three deposition precursors; SiH_3 radicals, HOS radicals, and amorphous clusters [1]. SiH_3 radicals are the main deposition precursor for "good" quality films. Incorporation of clusters into a-Si:H films has been pointed out to cause the light induced degradation, whereas that of HOS radicals has not. To study effects of clusters on the light induced degradation and to control their deposition into films, we have employed a multi-hollow plasma CVD method to deposit films in which the incorporation of clusters is reduced in the upstream region with the gas flow that drive clusters toward the downstream region of the reactor [2, 3]. Films deposited in the upstream region tend to be more stable than those deposited in the downstream region; and the films deposited far from the discharges in the upstream region shows high stability, which indicates that the incorporation of clusters degrades the stability of a-Si:H films against light exposure. Our a-Si:H films deposited at 2.3 nm/s show a remarkably low stabilized defect density of $4 \times 10^{15} \text{ cm}^{-3}$. [1] M. Shiratani, et al., *Thin Solid Films* 427 (2003) 1. [2] W. M. Nakamura, et al., *J. Phys.: Conference Series* 100 (2008) 082018. [3] W. M. Nakamura, et al., *IEEE Trans. Plasma Sci.* 36 (2008) 888.

*Work supported by JSPS and NEDO.

14:00

TR3 3 Partial modeling for plasma assisted combustion – Turbine combustor application BORIS POTAPKIN, MAXIM DEMINSKY, MARINA STRELKOVA, IRINA CHERNYSHEVA, IGOR KOCHETOV, *Kintech Lab, Moscow, Russia* SEYED SADDUGHI, JOHN T. HERBON, TIMOTHY SOMMERER, *GE Global Research, Niskayuna, US* Modern gas turbine combustors have to meet increasingly stringent emissions requirements at enlarged operability at conditions of lean-premixed natural gas combustors. This work is dedicated to analysis of possible plasma effect on natural gas combustion gas turbine operation via partial modeling approach. It was shown that plasma effect has potential to enhance the stability of premixed natural gas combustion by widening the lean-blowout limit and enabling operation at lower flame temperatures thus achieving lower emissions and higher turndown capability.

Contributed Papers

15:15

TR3 6 Effect of acetylene portion on the properties of high frequency discharge in argon* IRINA SCHWEIGERT, DMITRY ARISKIN, *Institute of Theoretical and Applied Mechanics, Russian Academy of Sciences* INSTITUTE OF THEORETICAL AND APPLIED MECHANICS, RUSSIAN ACADEMY OF SCIENCES TEAM, The gas discharge in hydrocarbon mixtures is widely used for carbon film growth. These thin films are of great interest for a wide range of industrial applications due to their extraordinary material properties. Noble gases like argon and neon are often used as main background gases for hydrocarbon mixtures as their presence changes morphology of diamond like carbon films and leads to fewer crystalline defects. In this paper the numerical study of characteristics of high frequency discharge are performed with using PIC-MCC simulation for different portions of acetylene in the mixture with argon. We consider the formation of heavy ions and radicals which are precursors for nanoparticle growth in the discharge volume. The density of electrons, positive and negative ions are found to be nonmonotonic functions of the quantity of the acetylene in the mixture. The presence of the negative ions, the density of which is comparable with electron density, weakly affects the parameters of discharge.

*This work was supported by the Bilateral grant RFBR-Ukraine (08-02-90446-Uka).

SESSION URP: POSTER SESSION II

Thursday Afternoon, 22 October 2009

Hall D, Saratoga Springs City Center at 16:00

URP 1 ATOMIC AND MOLECULAR PROCESSES

URP 2 Detection limit improvement for iodine Cordes-Band based hypersonic density measurements JACK MILLS, *Old Dominion University* ROBERT BALLA, *Nasa Langley Research Center* LEPHSA VUSKOVIC, *Old Dominion University* Measurements in the wake region created by models in supersonic and hypersonic flows are required in order to understand a variety of problems in aerodynamics. In this experiment we investigated the properties of using broadband excitation, as opposed to narrowband excitation, using an ArF laser as a means for increasing the detection limit of density measurements in air. The mechanism for this involves Iodine Cordes-Band spectroscopy. Laser excitation of the Cordes bands of I_2 and the resulting emission involve a myriad of rotational, vibrational and electronic energy levels. I_2 is optically pumped to the D state where approximately 85% of the emission regardless of buffer gas pressure results from D and D' transitions. In pure I_2 McLennan-band emission dominates with the peak signal near 321nm. As the air pressure increases, collisions with air transfer the population from the D to D' state where that emission produces the 340nm band. As the air pressure increases the 321nm emission is rapidly quenched and the D' emission dominates (340nm). This provides a pressure dependent signal contribution. The goal is to improve the current detection limit by an order of magnitude by using a broadband laser beam instead of the narrowband beam. This should increase the detection limit by an order of magnitude.

URP 3 Atomic Transition Probabilities for Neutral Cerium J.E. LAWLER, E.A. DEN HARTOG, M.P. WOOD, *Univ. of Wisconsin* D.E. NITZ, *St. Olaf College* J. CHISHOLM, *Boston College* J. SOBECK, *Univ. of Chicago* The spectra of neutral cerium (Ce I) and singly ionized cerium (Ce II) are more complex than spectra of other rare earth species. The resulting high density of lines in the visible makes Ce ideal for use in metal halide (MH) High Intensity Discharge (HID) lamps. Inclusion of cerium-iodide in a lamp dose can improve both the Color Rendering Index and luminous efficacy of a MH-HID lamp. Basic spectroscopic data including absolute atomic transition probabilities for Ce I and Ce II are needed for diagnosing and modeling these MH-HID lamps. Recent work on Ce II [1] is now being augmented with similar work on Ce I. Radiative lifetimes from laser induced fluorescence measurements [2] on neutral Ce are being combined with emission branching fractions from spectra recorded using a Fourier transform spectrometer. A total of 14 high resolution spectra are being analyzed to determine branching fractions for 2000 to 3000 lines from 153 upper levels in neutral Ce. Representative data samples and progress to date will be presented. [1] J. E. Lawler, C. Sneden, J. J. Cowan, I. I. Ivans, and E. A. Den Hartog, *Astrophys. J. Suppl. Ser.* 182, 51-79 (2009). [2] E. A. Den Hartog, K. P. Buettner, and J. E. Lawler, *J. Phys. B: Atomic, Molecular & Optical Physics* 42, 085006 (7pp) (2009).

URP 4 ELECTRON AND PHOTON COLLISIONS WITH ATOMS AND MOLECULES

URP 5 The field effect on elastic electron-ion collisions in a plasma with the presence of the external field SANG-CHUL NA, YOUNG-DAE JUNG, *Department of Applied Physics, Hanyang University, Ansan, Kyunggi-Do 426-791, South Korea* The field effects on the elastic electron-ion collision are investigated in a plasma with the presence of the external field. The eikonal method and effective interaction potential including the far-field term caused by the external field is employed to obtain the eikonal phase shift and eikonal cross section as functions of the field strength, external frequency, impact parameter, collision energy, thermal energy, and Debye length. The result shows that the effect of the external field on the eikonal cross section is given by the second-order eikonal phase. In addition, the external field effects suppress the eikonal cross section as well as eikonal phase for the elastic electron-ion collision. The eikonal phase and cross section are found to be increased with an increase of the frequency of the external field. It is also shown that the eikonal cross section increases with an increase of the thermal energy and Debye length.

URP 6 Electron-helium scattering in the presence of a laser field at moderate incident energies* BRUNO DEHARAK, LUIS LADINO, *University of Kentucky* NICHOLAS MARTIN, We have begun to perform a series of experiments that examine electron-helium scattering in the presence of an Nd:YAG laser field. The goal of these experiments is to span the range of incident electron energies from 50 eV to 250 eV, and compare the results to Kroll-Watson approximation¹ (KWA) calculations. Effects of an intense laser field on the elastic scattering of electrons from argon were first reported by Andrick in 1976.² In general, KWA calculations have been adequate to describe experimental results where the photon energy is significantly less than the incident electron

energy – a major exception being the case of small scattering angles where large discrepancies have been noted.³ Our experiments will test the KWA over a range of electron incident energies that has not been previously investigated.

*This work was supported by the United States National Science Foundation under Grant No. PHY-0555541.

¹N. M. Kroll and K. M. Watson, Phys. Rev. A 8, 804 (1973)

²D. Andrick and L. Langhans, J. Phys. B 9, L459 (1976)

³e.g., B. Wallbank and J. K. Holmes, Phys. Rev. A 48, R2515 (1973)

URP 7 A Particle-in-Cell - Monte Carlo Collision (PIC-MCC) Model for Simulations of Electron Impact Collisions in Gas Mixtures* SUDHAKAR MAHALINGAM, YONGJUN CHOI, SETH VEITZER, PETER STOLTZ, *Tech-X Corporation* A PIC-MCC model has been developed to numerically model electron impact collisions with neutral gases. This model includes elastic collisions (such as scattering, and large-angle scattering), inelastic collisions (such as excitation, and ionization) and Bremsstrahlung collisions. Collision cross sections data are based on the Evaluated Electron Data Library (EEDL) dataset, obtained from the International Atomic Energy Agency Nuclear Data Services. The EEDL library contains collision cross sections and generation data for electrons and photons for atoms with $Z = 1 - 100$ for incident electron energies from 10 eV (or threshold) to 100 GeV. Additionally, we have included elastic scattering cross section for electron energies below 10 eV from other experiments so that the PIC-MCC model can be used for studying low temperature plasmas. Researchers may also specify a user-defined model of cross sections to match their own measurements. We will show results for gases and parameters relevant to the plasma processes in Hall thruster applications.

*The work is funded by the U. S. DOE under Small Business Innovation Research (SBIR) Contract No. DE-FG02-07ER84833 and by NASA under SBIR Contract No. NNX09CD11P.

URP 8 Creation, destruction, and transfer of atomic multipole moments by electron scattering: Quantum mechanical treatment* DMITRY FURSA, IGOR BRAY, *Curtin University* GEORGE CSANAK, DAVID KILCREASE, *Los Alamos National Laboratory* The rates for the creation, destruction, and transfer of atomic multipole moments by heavy-particle scattering have been studied for many years using semiclassical scattering theory along with the straight-line trajectory assumption for the scattering particle and using the multitrajectory semi-classical approximation. With the advent of plasma polarization spectroscopy the same rate-coefficients became of interest for electronic collisions also in order to model the anisotropic plasmas. In this work we give general definitions for both elastic and inelastic scattering for the creation, destruction, and transfer cross sections of atomic multipole moments via the use of pure quantum-mechanical methods with due consideration for electron-exchange and for semi-relativistic effects. In order to illustrate the order of magnitude, the sign, and the energy-dependence of these cross sections we have calculated them for electron scattering from hydrogen and barium atoms using the Convergent Close-Coupling (CCC) method.

*Supported by the Australian Research Council and the Department of Energy.

URP 9 Transport Coefficients and Cross Section Set for Electron Scattering in Mixtures CF₄, Ar and O₂ ZELJKA NIKITOVIC, VLADIMIR STOJANOVIĆ, ZORAN PETROVIĆ, *Institute of Physics, P.O.B. 68, 11080 Zemun, Belgrade, Serbia* ZVZ TEAM, We present transport coefficients for electrons in mixtures of CF₄ with Ar and O₂ for ratios of the electric field to the gas number density E/N from 1 Td to 1000 Td (1Td=10⁻²¹ Vm²). We then add a certain percentage of radicals produced by dissociation of CF₄. Our analysis of non-conservative collisions revealed a range of E/N where electron attachment introduced by radicals significantly changes electron kinetics obtained for mixtures without dissociation of CF₄ gas. Results are obtained by using a simple, two term solutions for Boltzmann's equation but are verified by Monte Carlo simulations.

URP 10 DISTRIBUTION FUNCTIONS AND TRANSPORT COEFFICIENTS FOR ELECTRONS AND IONS

URP 11 How valid is the concept of a bi-Maxwellian distribution? N.S. BRAITHWAITE, R.N. FRANKLIN, *The Open University* The sheath of a plasma with two distinct negative species was examined by Braithwaite and Allen (1988). There is no doubt of its validity to describe the situation in electronegative plasmas at low pressures when the species are electrons and negative ions, and much of the understanding of such plasmas has resulted. Though it may be convenient to describe the electron energy distribution in electropositive plasmas as if there are two distinct species, one needs to be careful in deriving such things as a modified Bohm criterion. In most situations there is but one distribution and one cannot distinguish "red" and "blue" electrons. The electrons move between different parts of the distribution by a process of "diffusion" well described by Tsendin (2009). Thus unless different parts of the total electron distribution clearly do not interact, results obtained by assuming two independent populations with different densities and temperatures lack validity.

URP 12 Non-conservative charged particle swarms in ac electric and magnetic fields* SASA DUJKO, RONALD WHITE, *School of Engineering and Physical Sciences, James Cook University* ZORAN PETROVIC, *Institute of Physics, University of Belgrade* A time-dependent multi term solution of the Boltzmann equation has been developed and used to calculate the transport properties of charged particle swarms under the influence of time-dependent electric and magnetic fields crossed at arbitrary angle. The hierarchy resulting from a spherical harmonic decomposition of the Boltzmann equation in the hydrodynamic regime is solved numerically by representing the speed dependence of the phase-space distribution function in terms of an expansion in Sonine polynomials about a Maxwellian distribution at internally determined temperature. The investigation is carried out over a wide range of electric and magnetic field amplitudes, field frequencies, field orientations and phases between the fields corresponding to various conditions operative in ICP. Values of mean energy, drift velocity, diffusion tensor and power density absorbed by the electron swarm for certain model and real gases are reported here. A multitude of new kinetic phenomena induced by temporal non-locality of electron kinetics were observed and explained using a

physical arguments. Of special note are the phenomena associated with the synergism of magnetic field and non-conservative collisions. We believe that modelling of ICP and magnetically enhanced/assisted plasma reactors can greatly benefit from this study.

*The Australian Research Council and the MNTR project 141025.

URP 13 IONIZATION OF ATOMS AND MOLECULES

URP 14 Determination of ionization cross sections and rate coefficients for C60 by electron impact* SATYENDRA PAL, ANSHU, NEERAJ KUMAR, KESHAV KUMAR, *M.M.H. College, Ghaziabad* The modified semiempirical formulation for the calculations for the partial ionization cross sections of molecules by electron impact has been extended and generalized to the calculations of the cross sections for the dissociative ionization of fullerene C60. The secondary electron energy and angle dependent cross sections for the production of various dissociative ions $C+60-2n$ ($n=1-8$) in electron dissociation of C60 are evaluated at fixed incident electron energies of 100 and 200eV. The integral partial ionization cross sections and their weighted sum i.e. total cross sections in the energy range varying from ionization threshold to 1000eV are also evaluated. The counting/total ionization cross sections along with the partial dissociative ionization cross sections are found in satisfactory agreement (within the composite error bars) with the available experimental data. The ionization rate coefficients at a function of energy are also derived using the present calculations for ionization cross sections and the Boltzmann distribution function of energy of the electron.

*Anshu is thankful to DAE for support through grant no 2007/37/13/BRNS.

URP 15 Analytical fits for electron impact ionization cross section of atomic species commonly found in material processing plasmas A. SAMOLOV, A. GODUNOV, *Department of Physics, Old Dominion University* The field of plasma modeling is in need of reliable electron impact ionization cross sections. This work aims to provide accurate analytical fits for the most common atomic species found in material processing plasmas, such as Argon and halogen elements like Fluorine and Chlorine, etc. The standard BELI formula is revisited but a few other analytical expressions are also suggested, approximating single-ionization cross sections. The preference is given to experimental data up to date covering the whole range in energies.

URP 16 Fully Differential Cross Sections for Electron Impact Ionization of Formic Acid* OLA AL-HAGAN, DON MADISON, *Missouri University of Science and Technology* BIRGIT LOHMANN, CHRISTOPHER COLYER, *University of Adelaide, Australia* CHUANGANG NING, *Tsinghua University, Beijing, China* Our recent study using the molecular three-body distorted-wave (M3DW) approximation method yielded good agreement with experimental measurements for fully differential cross sections (FDCS) for the ionization of both H₂ and N₂ by electron impact. We will present M3DW FDCS calculations for electron impact ionization of formic acid for different energies in the coplanar geometry. Theoretical results will be compared with recent unpublished measurements for formic acid from the University of Adelaide in Australia.

*Supported by NSF.

URP 17 Comparison between Experiment and Theoretical Results for (e, 2e) Ionization of the $3\sigma_g$ State of N₂* OLA AL-HAGAN, DON MADISON, *Missouri University of Science and Technology* LEIGH HARGREAVES, CHRISTOPHER COLYER, BIRGIT LOHMANN, *University of Adelaide, Australia* CHUANGANG NING, *Tsinghua University, Beijing, China* A comparison between experimental and theoretical results for (e, 2e) ionization of the $3\sigma_g$ state of N₂ will be presented. The theory presented here is the molecular three-body distorted wave (M3DW) approximation using better wave function for the molecules than we had in previous works. Results will be shown in coplanar symmetric and coplanar asymmetric geometries. We found improved agreement with experimental data using the new wave function. N₂ measurements are of particular interest due to the possibility of observing the effects of 2-center Young's-type interference terms in the cross sections. The existing experimental data suggests an interference peak but is inconclusive.

*Supported by NSF.

URP 18 Single Ionization of Molecular Hydrogen by 75 keV Proton Impact K. EGODAPITTIYA, A. LAFORGE, J. ALEXANDER, M. SCHULZ, *Dept. of Physics, Missouri University of Sci. & Tech., Rolla, MO* A. HASAN, *Dept. of Physics, UAE University, Abu Dhabi, United Arab Emirates* M. CIAPPINI, *Institute of High Performance Computing, Singapore* M. KHAKOO, *Dept. of Physics, California State University, Fullerton, CA* Triply differential cross sections (DDCS) for single ionization of molecular hydrogen by 75keV proton impact have been measured and calculated as a function of the projectile scattering angle, energy loss, and longitudinal recoil momentum. Earlier, we reported interference structures in the DDCS resulting from coherent diffraction of the incoming projectile wave from the two atomic centers in the molecule. In the experimental data these structures disappeared near $v_{el} \approx v_{proj}$. It seems plausible that this disappearance may be caused by the PCI, which is known to maximize at $v_{el} \approx v_{proj}$. In order to test this hypothesis we have measured the recoil-ion momenta in addition to the projectile momenta in a kinematically complete experiment. Indeed, in the TDCS a weak interference structure is recovered if large longitudinal recoil-ion momenta p_z^{rec} are selected, which kinematically suppress PCI. In contrast, for small p_z^{rec} , which kinematically favor PCI, no structure is observed.

URP 19 Cross-Sections and Fragmentation Pathways of Dissociative Electron Impact Ionization of 2,5-Dimethylfuran (C₆H₈O)* C.Q. JIAO, *UES Inc.* A. GARSCADDEN, S.F. ADAMS, *Air Force Research Laboratory* The possibilities offered by non-equilibrium plasma to guide parameters such as the mean electron energy provides researchers with an opportunity to change the energy branching in molecular gas plasmas from mainly gas heating and vibrational excitation to high-energy electronic excitation and ionization. The kinetics of the dissociative electron impact ionization of fuel molecules and subsequent ion-molecule reactions are important basic data needed for modeling the charged particle chemistries in plasmas. This paper presents the results of a high resolution Fourier-Transform mass spectrometry study on the electron impact ionization of 2,5-dimethylfuran (C₆H₈O), which is an important fuel additive and a possible renewable liquid fuel for the future. The total and partial ionization cross sections will be provided and the pathways of fragmentation channels forming major product ions will be discussed.

*This work supported in part by the AFOSR.

URP 20 Density functional theory calculation of ionization in antiproton-helium collisions TOM KIRCHNER, *Department of Physics and Astronomy, York University, Toronto, Ontario M3J 1P3* NILS HENKEL, *Max Planck Institute for the Physics of Complex Systems, D-01187 Dresden, Germany* MATTHIAS KEIM, HANS JURGEN LÜDDE, *Institut fuer Theoretische Physik, Goethe-Universitaet, D-60438 Frankfurt, Germany* Probabilities and total cross sections for ionization in antiproton-helium collisions are calculated in a time-dependent density functional theory approach. The Kohn-Sham potential is approximated as the sum of the Hartree-exchange potential and a correlation potential that was proposed in the context of laser-induced double ionization. Furthermore, some approaches to the problem of calculating the ionization probabilities from the density are investigated. We find that the correlation potential yields no obvious improvement of the results over the exchange-only approximation where the correlation potential is neglected. Furthermore, we find the problem of calculating the desired observables crucial, introducing errors of at least the same order of magnitude as the correlation potential. At small energies we find that trajectory effects play an important role: the ionization cross sections are enlarged significantly if curved instead of straight-line trajectories are used to describe the projectile motion.

URP 21 OTHER ATOMIC AND MOLECULAR COLLISION PHENOMENA

URP 22 Determination of collisional quenching rate coefficients of metastable nitrogen molecules by air pollutants SUSUMU SUZUKI, HARUO ITOH, *Chiba Institute of Technology* It has already been investigated on the determination of the collisional quenching rate coefficients of the metastable nitrogen molecules $N_2(A^3\Sigma_u^+)$ by some air pollutants [1] in our laboratory. In this report, we present the result on the collisional quenching rate coefficient of $N_2(A^3\Sigma_u^+)$ by formaldehyde (CH_2O) using a theoretical procedure that takes into account the reflection of metastables at the boundary. As far as we know, this report is the first result of the collisional quenching rate coefficients of $N_2(A^3\Sigma_u^+)$ by CH_2O . Formaldehyde is a colorless gas with the foul odor, and elements of the adhesive, paints, and preservative, etc. It is widely used for construction materials such as houses, because it is low cost. It is released from paint of construction materials in air, and, in that case, it is known as one of the causative agents of so-called "Sick building syndrome" to influence the human body harmfully even if it is a low concentration. The obtained collisional quenching rate coefficient of $N_2(A^3\Sigma_u^+)$ by CH_2O is $(4.7 \pm 0.4) \times 10^{-12} \text{ cm}^3/\text{s}$. Because the collisional quenching rate coefficient by CH_2O is large, it is understood that CH_2O receives energy easily from $N_2(A^3\Sigma_u^+)$. In addition, we reports on the obtained collisional quenching rate coefficient of $N_2(A^3\Sigma_u^+)$ by some air pollutants. [1] S. Suzuki, T. Suzuki and H. Itoh: Proc. of XXVIII ICPIG (Prague, Czech Republic), (2007) 1P01-40.

URP 23 PLASMA-SURFACE INTERACTIONS

URP 24 A role of low pressure plasma discharge on etch rate of SiO_2 dummy wafer VLADIMIR MILOSAVLJEVIC, *NCPST-School of Physics, DCU, Dublin, Ireland; Faculty of Physics, University of Belgrade, Serbia* ANDRJANA ZEKIC, DUSAN POPOVIC, *Faculty of Physics, University of Belgrade, Serbia* NIALL MACGEARAILT, STEPHEN DANIELS, *NCPST, DCU, Dublin, Ireland* Plasma has become indispensable for advanced materials processing, also low-k materials as SiO_2 play important role in semiconductor industry. In this work a treatment of SiO_2 single crystal by DC plasma discharge is studied in details. There are many effects occurred during plasma-surface interactions. Our work is focused on interaction between ions and dielectric surface. The etch rates, surface morphology and chemical composition of modified surface layer obtained by DC plasma etching are reported. Influence of plasma chemistry (SF_6 , O_2 , N_2 , Ar and He), discharge voltage (up to 1.2 kV), gas flow (up to 25 sccm, for each gas) and electrode-wafer geometry on etch rate of SiO_2 wafer have been studied. Offline metrology is conducted for SiO_2 wafer by SEM/EDAX technique and Raman scattering. Broad Raman peak at around 2800 cm^{-1} is observed for both, treated and original, investigated SiO_2 wafers. Effects of plasma treatment conditions on integrated intensity of this peak are reported in the paper. An analysis of this correlation could be a framework for creating virtual etches rate sensors, which might be of importance in managing of plasma etching processes.

URP 25 Manipulation of Bias Voltage Waveform to Control Bombarding Ion Energy Distribution* X. VICTOR QIN, YUK-HONG TING, AMY WENDT, *University of Wisconsin-Madison*

In materials processing applications using low pressure plasmas, positive ions are accelerated by a sheath electric field toward the substrate, where they enhance surface reactions. The amplitude of a sinusoidal bias voltage waveform applied to the substrate electrode is often used to coarsely control the average energy of bombarding ions, but generally produces a broad bimodal ion energy distribution (IED). Manipulation of the bias voltage waveform shape to produce IEDs with one or two peaks at selected energies has been previously utilized to highlight the significant role of the IED in plasma etching. Presented here are direct IED measurements made with a retarding field energy analyzer at the biased electrode. Measurements in a 10 mTorr helicon argon plasma in which ion flux and ion energy at the substrate are independently controlled clearly demonstrate the ability to predictably produce arbitrary IEDs at the substrate by tailoring the shape of the bias voltage waveform. Results for sinusoidal (500 kHz-10 MHz) and tailored (500 kHz) waveforms compare favorably with predictions based on computation of ion trajectories through the sheath electric field.

*We gratefully acknowledge support from Lam Research.

URP 26 Plasma Assisted Electron Beam Energy Boosting by Ambient Gas Pressure Optimization in Pyroelectric Crystal Accelerators JAMES BROWNRIDGE, *Binghamton Univ, Binghamton, NY* STEPHEN SHAFROTH, *Univ of NC at Chapel Hill* Pyroelectric crystal x-ray generators [1] were first reported in 1992. These crystals have a nonzero spontaneous polarization at all temperatures below their Curie temperature. A change in crystal temperature will result in a strong electric field at its surface. If the

Z- face on a Z-cut pyroelectric crystal is located in a gas at mTorr pressure the energy of electrons that are accelerated away from the crystal as it is cooled can be increased by increasing the gas pressure. As the crystal is cooled the spontaneous polarization increases, this results in an increase in the uncompensated negative charge at the surface of the crystal. The field produced by this charge is strong enough to field ionize molecules of the gas. A tentative explanation for the energy boosting of the beam follows: In this strong field these molecular ions are polarized and attracted to and stick to the surface of the crystal. Once attached to the surface of the crystal the electron cloud around the molecules is further distorted and pushed away. These polarized molecular ions increase the strength of the electric field at the surface of the crystal and increase the electron beam energy. Hence an increase in pressure boosts the beam energy. In an ultra high vacuum no energy boosting occurs. [1] J.D. Brownridge, *Nature (London)* **358,278** (1992)

URP 27 Cold-atmospheric pressure plasma polymerization of acetylene on wood flour for improved wood plastics composites WILLIAM LEKOBOU,*PATRICK PEDROW,†KARL ENGLUND,‡MARIE-PIERRE LABORIE,§ *Washington State University* Plastic composites have become a large class of construction material for exterior applications. One of the main disadvantages of wood plastic composites resides in the weak adhesion between the polar and hydrophilic surface of wood and the non-polar and hydrophobic polyolefin matrix, hindering the dispersion of the flour in the polymer matrix. To improve interfacial compatibility wood flour can be pretreated with environmentally friendly methods such as cold-atmospheric pressure plasma. The objective of this work is therefore to evaluate the potential of plasma polymerization of acetylene on wood flour to improve the compatibility with polyolefins. This presentation will describe the reactor design used to modify wood flour using acetylene plasma polymerization. The optimum conditions for plasma polymerization on wood particles will also be presented. Finally preliminary results on the wood flour surface properties and use in wood plastic composites will be discussed.

*Composite Materials and Engineering Center

†The School of Electrical Engineering and Computer Science

‡Composite Materials and Engineering Center

§Composite Materials and Engineering Center

URP 28 Evidence of production/losses of NO on a pyrex surface under and after plasma exposure. DANIIL MARINOV, OLIVIER GUAITELLA, *LPP, Ecole Polytechnique* YURY IONIKH, *State University, Saint-Petersburg* ANTOINE ROUSSEAU, *LPP, Ecole Polytechnique, France* Molecules production on plasma exposed surfaces is of great interest for plasma/catalyst coupling used in air treatment. Interaction of real surfaces with reactive plasmas is barely studied and surface-produced molecules can provide a valuable fingerprint of the underlying processes (adsorption, desorption, recombination, chemical reactions). We use CCP discharge in 60 cm pyrex tube with *in-situ* tunable laser diagnostics to monitor evolution of NO and NO₂. The tube surface is pre-treated using either Ar, O₂, N₂ or air plasma and then two types of experiments are performed i) molecules production in a pure O₂ plasma reacting with adsorbed species ii) the study of molecules losses/conversion on the surface by introducing a controlled amount of NO/NO₂ in the reactor. It was found that after N₂ plasma pre-treatment, pyrex surface is covered with nitrogen species that initiate NO production when exposed to O₂ plasma.

Assuming these species are N atoms, their density was estimated $[N_{ads}] = 3 \cdot 10^{13} \text{ cm}^{-2}$, what gives an assessment of the surface active sites density. Similarly, O₂ plasma leaves adsorbed oxygen species with $[O_{ads}] \approx 2 \cdot 10^{14} \text{ cm}^{-2}$. These species are capable of NO oxidation to NO₂ and inhibit NO₂ adsorption on pyrex (which is pronounced after N₂ and Ar plasma preparation).

URP 29 MATERIALS PROCESSING IN LOW PRESSURE PLASMAS: ETCHING, DEPOSITION, NEW MATERIALS

URP 30 Effect of resist mask roughing on the etching profile of SiO₂ trench under the presence of local charging SHINPEI INAGAKI, TAKASHI YAGISAWA, TOSHIAKI MAKABE, *Keio University* The reactive ion etching (RIE) of high-aspect ratio contact hole made of SiO₂ has been traditionally performed by fluorocarbon gas C_xF_y diluted with Ar (> 90%) in a two-frequency capacitively coupled plasma (2f-CCP) reactor. The RIE proceeds under the competition among surface protection by the deposition of C_xF_y radicals, chemical sputtering by energetic ions, and topological charging caused by the difference of velocity distribution of ions and electrons coming to the surface. In our previous work, feature profile evolution of SiO₂ trench pattern was predicted by using the level-set method considering mixing layer and C_xF_y polymer layer on SiO₂ substrate. It is experimentally known that the roughness of the photoresist mask on SiO₂ film makes large influence on the etching profile, called "faceting" or "striation" probably due to the high-energy ion impact. In this study, we develop our feature profile model in order to investigate the relation between resist mask roughing and the feature profile of SiO₂ trench. Attention will be paid to the scattering of incident ions on the faceting structure of the resist mask and local charging as functions of the flux velocity distribution of ions and radicals.

URP 31 Plasma Etching of Cu in an Ar/Cl₂ Microwave Discharge M. RASKOVIC, K. BRANNICK, S. POPOVIC, L. VUSKOVIC, *Physics Department, Old Dominion University* Copper substrates can be used for depositing superconducting material thin films, such as Nb or Nb₃Sn, lowering the cost of cavity production for linear particle accelerators based on the superconducting radiofrequency technology. To avoid contamination and mechanical damage by environmental agents, the best would be to prepare Cu surface in the same apparatus thin film deposition is performed. Low volatility of Cu halides is main difficulty for using plasma processing techniques. Standard parallel plasma etching reactor does not achieve temperature necessary for evaporation of CuCl, the most volatile Cu halide. Therefore our approach was to use a microwave glow discharge [1], characterized with higher electron and radical density as well as higher substrate temperature comparing to standard RF system. Etching rates of 300 nm/min were reached using only 3 %Vol Cl₂ reactive gas in Ar/Cl₂ mixture. Formation of CuCl during plasma etching process was monitored using emission spectroscopy techniques. Attempt to use observed CuCl rotational spectra for determining discharge gas temperature was made. Composition and morphology of Cu surface before and after exposure was investigated using scanning electron microscope. [1] M. Rašković, *et al.*, *J. Vac. Sci. Technol. A* **27**, 301 (2009).

URP 32 Spectroscopic characterization and modeling of Ar/Cl₂ microwave glow discharge* J. UPADHYAY, M. RASKOVIC, S. POPOVIC, L. VUSKOVIC, *Physics Department, Old Dominion University* Ar/Cl₂ microwave glow discharge was applied for plasma etching of niobium, metal of choice for superconducting radiofrequency accelerator technology. Etching rates were determined for different discharge parameters and results of these experiments are published elsewhere [1]. Simultaneously, plasma emission actinometry was used to estimate the absolute densities of Cl, Cl⁺ and Cl₂ in the variable plasma conditions. These results, combined with results of discharge diagnostics, were compared with results obtained through the modeling of Ar/Cl₂ discharge. We have calculated the electron-impact ionization rates of Cl₂ and its fragments for electron energy distribution present in bulk plasma. These ionization rates will be used for modeling of plasma etching process and comparing with experimentally determined etching rates. [1]. M. Rašković, et al., *J. Vac. Sci. Technol. A* **27** (2), 301 (2009).

*Supported by DOE

URP 33 Nano-block manipulation in CVD plasmas HIROSHI MIYATA, SHINYA IWASHITA, YASUYUKI YAMADA, KAZUNORI KOGA, MASAHARU SHIRATANI, *Kyushu University* We have proposed a novel nano-system construction method using plasmas [1-3]. We have succeeded in realizing size control of nano-blocks and their rapid transport towards a substrate by using pulse discharges with amplitude modulation (AM) of the discharge voltage [1-3]. We are developing a method for their three dimensional transport using a capacitively coupled RF discharge reactor having a grounded electrode with needles. During the period of AM nano-blocks are transported from their generated region near the powered electrode to the top of the needle. Such three dimensional transport needs an asymmetric electric potential profile, in other words, a large voltage drop across the sheath near the powered electrode. We will report the experimental results and discuss the mechanism of the three dimensional transport. [1] S. Nunomura, et al. *J. Appl. Phys.*, **99**, 083302 (2006). [2] K. Koga, et al. *J. Phys. D*, **40**, 2267 (2007). [3] M. Shiratani, et al. *Faraday Discuss.*, **138**, 127 (2008).

URP 34 Sputter Yield Measurement of Ferrous Metals & Alloys KIERAN DENIEFFE, C.M.O. MAHONY, P.D. MAGUIRE, *NIBEC* A. BABY, *Seagate Technology* Sputter yield measurements for bulk Co, Fe & Ni are published [1]; however no values are available for ferrous metal alloys. Here we present the results of a study of the sputter yields of thin film ferromagnetic alloys CoFe & NiFe. We also investigate the sputtering of polyamide, used for masking in microelectronics, but with no published sputter yields to our knowledge. We used a 13.56 MHz plasma ion source to bombard biased samples with 50 eV to 1k eV Ar⁺ ions. The ion flux was measured by a Faraday cup & the etch rate with a sensitive quartz crystal microbalance (QCM) modified for rf use, allowing multiple real-time measurements without breaking vacuum. The QCM was calibrated via profilometry & weight loss measurements; flux values were validated using a retarding field analyzer. A mass/energy analyser was used to measure ion energy distributions, showed the FWHM spread of beam energy to be 4eV. Measurements show that although Y values & threshold energies of the thin film alloys differ to those published for bulk ferrous metals, they do exhibit similar Y v ion energy trends. [1] Laegreid N, Wehner G. 1961 *J Appl Phys* **32** p365

URP 35 Permeation barrier coating and plasma sterilization of PET bottles and foils SIMON STEVES, MICHAEL DEILMANN, NIKITA BIBINOV, PETER AWAKOWICZ, *INSTITUTE FOR PLASMA TECHNOLOGY, RUHR UNIVERSITY BOCHUM TEAM*, Modern packaging materials such as polyethylene terephthalate (PET) offer various advantages over glass or metal containers. Beside this they only offer poor barrier properties against gas permeation. Therefore, the shelf-life of packaged food is reduced. Additionally, common sterilization methods like heat, hydrogen peroxide or peracetic acid may not be applicable due to reduced heat or chemical resistance of the plastic packaging material. For the plasma sterilization and permeation barrier coating of PET bottles and foils, a microwave driven low pressure plasma reactor is developed based on a modified Plasmaline antenna. The dependencies of important plasma parameters, such as gas mixture, process pressure, power and pulse conditions on oxygen permeation through packaging foil are investigated. A residual permeation as low as $J = 1.0 \pm 0.3 \text{ cm}^3 \text{ m}^{-2} \text{ day}^{-1} \text{ bar}^{-1}$ for 60 nm thick silicon oxide (SiO_x) coated PET foils is achieved. To discuss this residual permeation, coating defects are visualized by capacitively coupled atomic oxygen plasma etching of coated substrate. A defect density of 3000 mm⁻² is revealed responsible for permeation. For plasma sterilization, optimized plasma parameters based on fundamental research of plasma sterilization mechanisms permit short treatment times of a few seconds.

URP 36 Initial Studies of Deep Silicon Etch IQBAL SARAF, MATTHEW GOECKNER, LAWRENCE OVERZET, *University of Texas at Dallas* The kinetic behaviors of time-multiplexed deep silicon etch processes are being studied in an Oerlikon DSE II using SF₆, C₄F₈ and Ar gas flows. We have formed a model for the reactor that fits the overall pressure in time and provides insight into gas mixing during the cycle transitions. It allows one to predict cycle conditions that isolate the deposition and etch steps. Also the effect of the gas-line fill time and its correlation with residence time is studied. In addition, we have measured plasma characteristics using a diagnostic tool called a "Wise probe." Preliminary measurements of the ion current density (ICD) to the probe surface for SF₆ and C₄F₈ plasmas as a function of pressure, flow rates, power and bias power are presented and discussed. For both C₄F₈ and SF₆ plasmas the ion current density strongly depends upon the gas pressure in the range of 10 to 45 mTorr. However, the ion current density depends weakly on the ICP power at higher pressure (45mTorr) for both C₄F₈ and SF₆ plasmas. These kinetic dependencies are related to the time averaged silicon etch rate/profile, aspect ratio dependence, and photoresist selectivity in order to gain initial insights into the fundamental plasma-surface interactions controlling the etch.

URP 37 ENVIRONMENTAL APPLICATIONS

URP 38 Development of a portable greenhouse gas analyzer based on Penning ionization electron spectroscopy (PIES) in a pulsed glow discharge plasma* C. MARK DENNING, VADIM STEPANIUK, VALERY SHEVEREV, *Lenterra, Inc.* LENTERRA, INC. TEAM, A greenhouse gas (GHG) analyzer currently under development at Lenterra, Inc. is described which utilizes Penning ionization electron spectroscopy (PIES) in a glow discharge plasma. A population of helium metastable atoms (2³S, 19.8 eV) is produced in a pulsed (50 μs duration, 5 kHz rep rate)

glow discharge in helium/analyte gas mixtures. In the afterglow electrons are produced due to Penning ionization of GHG analyte molecules (including carbon dioxide and methane) by the helium metastables. These electrons possess energies equal to the energy stored in the helium metastable minus the ionization potential of the analyte molecule. Electron energy spectra are measured using the current-voltage characteristic obtained during the afterglow with a swept-voltage collector electrode. These spectra exhibit peaks that allow for the determination of the ionization potential of each analyte, and therefore selective gas detection. Experimental results are presented and components of the portable PIES device are described, including the glow discharge apparatus, as well as a carbon nanotube gas micro-concentrator and a micro gas chromatography column.

*Work Supported by DOE SBIR Grant No. DE-FG02-07ER84894.

URP 39 Improved measurement system for surface loss rate of ozone HARUO ITOH, SUSUMU SUZUKI, *Chiba Institute of Technology* ILKO MITOKOV RUSINOV, *Sofia University* In this paper, we report on application of a technique for long-term monitoring of ozone density in a cylindrical vessel, filled with ozone-containing gas mixtures, by using ultraviolet photo-absorption. An experimental system has been used in order to monitor the temporal decrease of ozone concentration in a cylindrical cell based on the HgI 254 nm photo-absorption method [1-3]. It is applied to study the dependence of effective lifetimes of ozone on the wall material at various gas pressures. Instabilities in the mercury lamp intensity, however, often cause distortion of the measured decay curves. We have attempted to build a simple setup that eliminates the effect of long-term intensity drifts. It is based on light source intensity monitoring by a separate photo-detector and data correction in software. The obtained equivalent diffusion coefficient that describes the loss rate of ozone at the inner surface of the cell is $2.0 \times 10^{-4} \text{ cm}^2/\text{s}$ at 1 Torr. Further experiments are planned to measure the coefficient and clarify the mechanism of ozone effective lifetime. [1] H.Itoh, I.M.Rusinov, T.Suzuki, S.Suzuki: *Ozone Science & Engineering*, Vol.26 (2004) 487-497. [2] H.Itoh, M.Rusinov, S.Suzuki, T.Suzuki: *Plasma Processes and Polymers*, No.2, (2005) 227-231. [3] K.Ban, S.Isegame, S.Suzuki, I.M.Rusinov and H.Itoh: *Proc. 13th Asian Conference on Electrical Discharge* (Hokkaido University, Sapporo, Japan) P-2-41 (2006).

URP 40 BIOLOGICAL AND EMERGING APPLICATIONS OF PLASMAS

URP 41 Atmospheric-Pressure Cold Plasmas Used to Embed Bioactive Compounds in Matrix Material for Active Packaging of Fruits and Vegetables SULMER FERNANDEZ, PATRICK PEDROW, *School of EECS, Washington State University* JOSEPH POWERS, *School of Food Science, Washington State University* MARVIN PITTS, *Biological Systems Engineering, Washington State University* Active thin film packaging is a technology with the potential to provide consumers with new fruit and vegetable products-if the film can be applied without deactivating bioactive compounds. Atmospheric pressure cold plasma (APCP) processing can be used to activate monomer with concomitant deposition of

an organic plasma polymerized matrix material and to immobilize a bioactive compound all at or below room temperature. Aims of this work include: 1) immobilize an antimicrobial in the matrix; 2) determine if the antimicrobial retains its functionality and 3) optimize the reactor design. The plasma zone will be obtained by increasing the voltage on an electrode structure until the electric field in the feed material (argon + monomer) yields electron avalanches. Results will be described using Red Delicious apples. Prospective matrix precursors are vanillin and cinnamic acid. A prospective bioactive compound is benzoic acid.

URP 42 Plasma needle treatment of bacteria known to cause infections of the soft tissue of the oral region and bones DEJAN MALETIC, SASA LAZOVIC, NEVENA PUAC, GORDANA MALOVIC, ZORAN LJ. PETROVIC, *Institute of Physics, Belgrade, Serbia* MAJA P. MILETIC, DUSAN B. PAVLICA, MILENA Z. JOVANOVIC, PAVLE MILENKOVIC, *Faculty of Stomatology, Belgrade, Serbia* Plasma needle can be used for non-contact disinfection of dental cavities and wounds, minimum-destructive precise treatment, as well as the removal of damaged tissue. The effect of bacterial deactivation is probably caused by reactive oxygen species while nitric oxide provided by plasma plays major role in many processes in the organism. Mass spectrometry was done to provide better insight into plasma-cell interactions. Our measurements were performed on a plasma needle that we originally used for the treatment of plant cells. Our research was done on species that are known to cause primary and secondary infections of the soft tissue of the oral region, as well as bones. The bacteria cultures used are bacterial reference culture species *Staphylococcus aureus* ATCC 25923, *Enterococcus faecalis* ATCC 29212, *Pseudomonas aeruginosa* ATCC 27853, and *Escherichia coli* ATCC 25922. We investigated the effect of the plasma needle discharge on different concentration of bacteria using several exposure times and power transmitted to the plasma. It was found that excellent removal of this and other bacteria may be achieved by the plasma needle treatment.

URP 43 Modeling and experiment of ring-shaped emission profile in plasma bullet YUKINORI SAKIYAMA, DAVID GRAVES, *University of California at Berkeley* JULIEN JARRIGE, MOUNIR LAROSSI, *Old Dominion University* Our recent measurement demonstrated that a plasma "bullet" at atmospheric pressure shows ring-shaped emission profile. In this study, we focus on the mechanisms of the ring-shaped profile by means of finite element method and spectroscopic measurement. Our model is based on a fluid model with the local field approximation in 1D cylindrical coordinates, corresponding to a cross section of a plasma bullet. An expected concentration gradient of humid air is assumed to be present due to diffusion of air. Pulse-like electric field is given perpendicular to the simulation domain. Our simulation results show that the major ionization reaction is Penning ionization between nitrogen (air) and helium metastables. The density of electrons and positive nitrogen ions show the peaks near the outer boundary due to the higher concentration of air there. Accordingly, the emission peak appears near the outer boundary, corresponding to a ring-shaped emission profile. Experiments were performed with a dielectric barrier discharge reactor driven by high voltage short rise time pulses. Radial profile and time-resolved OES of radiative species were compared to simulation results.

URP 44 Treatment of Second Order Structures of Protein on Medical Equipments Using Oxygen Plasma NOBUYA HAYASHI, SATOSHI KITAZAKI, MASAOKI GOTO, *Saga University* YOSHIHITO YAGYU, *Sasebo National College of Technology* AKIRA YONESU, *University of Ryukyus* Removal of proteins from the surface of medical equipments are attempted using an RF plasma. Oxygen gas is introduced into a vacuum chamber with dimensions of 450 mm in length, 200 mm in diameter and 20L of capacity. When an RF power (13.56 MHz, 60W) is applied to an ICP type antenna, oxygen radicals (atomic oxygen and excited oxygen molecule) are produced below the antenna. The characteristics of removing protein from the medical equipments was investigated using casein and heat-resistant keratin proteins. Initial concentration of the proteins on a CaF₂ substrate is several mg/cm². The treatment effect of proteins is determined by the peak height of chemical bonds in amide and second order structures appeared on FTIR spectra. The second order structure of a protein such as alpha-helix and beta-sheet are decomposed with the treatment period. Complete treatment of proteins including the second order structure requires several hours avoiding the damage to medical equipments.

URP 45 Sterilization of Long Tube Inner Surface Using Oxygen and Water Vapor Plasmas Produced by AC HV Discharge SATOSHI KITAZAKI, NOBUYA HAYASHI, *Saga University* Oxygen and water vapor plasmas inside a narrow long tube were produced using an AC HV glow discharge at low pressure in order to sterilize the inner surface of a tube. In order to produce plasma inside a narrow tube, an AC high voltage was adopted. The material of the tube used in this experiment was silicon rubber. The length and diameter of the tubes ranged from 300 to 1,000 mm and from 1 to 4 mm, respectively. The tube was placed in a stainless steel vacuum chamber and was evacuated to 10 Pa using a rotary pump. The material gas for plasma and radical productions was pure oxygen or water vapor, which was introduced to the chamber from a gas cylinder or water reservoir. Light emission spectral lines of oxygen and OH radicals were observed at 777 nm and 306 nm, respectively. The chemical indicator was inserted into the tube and turned to a yellowish color (from the original red) after a treatment, which indicates the generation of sufficient oxygen on OH radicals for sterilization. A tube with the length of 500 mm and diameter of 4 mm is sterilized using oxygen plasma by 10 minutes treatment. Also a tube with the length of 300 mm and diameter of 2 mm is sterilized using water vapor plasma by 5 minutes treatment.

URP 46 Pulsed plasma polymerization of Ethylene Glycol for development of ultra thin biocompatible interfaces G. PADRON-WELLS, I.C. ESTRADA-RAYGOZA, L.J. OVERZET, M.J. GOECKNER, *The University of Texas at Dallas* An investigation of the gas phase and surface phase behavior for Ethylene Glycol (EG) pulsed discharges is presented. Infrared spectroscopy was utilized to study the effect of plasma average power and its correlation to monomer selective fragmentation. This allows one to predict the proper average power range to maximize preservation of monomer functionality in film deposition processes. The main daughter species detected in the gas phase were identified as formaldehyde (CH₂O), carbon monoxide (CO), carbon dioxide (CO₂), and water (H₂O). This data allowed for the construction of a dissociative model of the EG molecule in the gas phase during discharge conditions. From this it was observed that neutral byproduct formation is the result of complex recycling

processes occurring at the reactor walls. This is similar to previously reported results with a related compound: Di-ethylene glycol vinyl-ether.¹ In addition to gas-phase chemistry and surface reactions; we will also report on the analysis of the films grown under such conditions. This will be linked to the processes deduced from the gas-phase chemistry.

¹G. Padron-Wells, et al., *Colloids Surf. B: Biointerfaces* (2008)

URP 47 FTIR Analysis of Process Effluent Generated From Tissue Removed By Plasma-Chemical Process IL GYO KOO, MYEONG CHOI, CAMERON MOORE, GEORGE COLLINS, *Colorado State University* We present analysis of the effluent produced during a tissue removal process driven by a RF excited plasma which generates chemical species. We collected and analyzed the process by-product gas, small particles trapped by fine-pore filtration, and the post-process tissue surface using FTIR absorption and ATR-FTIR. From these data we make initial estimates for the kinetic pathways that are accessed by the plasma-based tissue removal process.

URP 48 Analysis of Plasma Based Tissue Removal versus Standard Electrosurgery ARLEN WARD, *Covidien Energy-based Devices* IL GYO KOO, MYEONG YEOL CHOI, GEORGE COLLINS, *Colorado State University* This study compared and contrasted biological tissue removal via plasma chemistry compared and contrasted with standard electrosurgery. With high speed image capture of the tissue division, the mechanism differences between the two methods are evident. While standard electrosurgery removes tissues with thermal vaporization during arc events, the plasma application modifies the tissue structure during plasma exposure. The thermal damage zones in the remaining tissue are also compared between techniques.

URP 49 Comparative Histology of Plasma Treated Tissue KYLE RICK, *Covidien Energy-based Devices* Atmospheric plasmas applied in surgical settings have unique characteristics found in histological results from animal tissue studies. This is evident in both ex vivo bench tissue tests and in vivo fresh tissue. Examples of these histological features are presented as results of a comparative study between plasma treated, common medical argon coagulation, and electrosurgery.

URP 50 Fabrication of two types of atmospheric pressure microplasma jet sources: A capillary electrode and a single pin electrode surrounded by tapered insulator with eight holes TAE HUN CHUNG, SUN JA KIM, HYE SUN PARK, SE HWAN BAE, *Dong-A University* Atmospheric pressure microplasma jet sources driven by radio-frequency wave and by low frequency pulsed wave of several kilohertz were specially fabricated and characterized. Two different types of jet were developed. The first one consists of a sharpened metal pin which is covered with a cone type Teflon layer confined in an acrylic tube. This structure allows an efficient ignition since the electrical field is concentrated at the end of electrode. The second one is a jet with a capillary electrode in which the working gas, helium or argon, and the additive gas, oxygen, are fed into the tube. The electrical properties of the discharges have been studied by means of voltage and current probes. The neutral-gas temperature and the electron temperature are measured by optical emission spectroscopy. The neutral gas temperature is compared with the results obtained by

optical fiber thermometer. To study the effect of pulsed discharges, we utilized a pulsed high voltage source with the variable frequency of 10-60 kHz and the voltage of 1-10 kV_{pp}. The effects of various design configurations and operation parameters were investigated. The cultured mammalian cells were treated using the plasma jet sources. The effects of plasma jet treatment were observed with a special focus on the cell apoptosis.

URP 51 Absolute ozone measurements for a low-energy pulsed plasma needle* CHUNQI JIANG, *University of Southern California* VINCENT PUECH, LIONEL MAGNE, PASCAL JEANNEY, *Université Paris-Sud* USC TEAM, UNIVERSITÉ PARIS-SUD TEAM, Applications of an atmospheric-pressure, nanosecond pulsed plasma jet for biomedical and dental disinfections have motivated numerous diagnostic studies in understanding of the underlying physics and chemistry during the plasma bactericidal processes. In this work, we present spectroscopic studies of a 3 cm long needle-like He-O₂ plasma jet. Rotational temperature of the plasma jet was measured to be about 300 K with optical emission spectroscopy. Ozone, as a typical bactericidal species, was detected in the plasma. Optical absorption spectroscopy identifies the absolute concentration ozone to be 10¹⁵ cm⁻³ when the plasma was powered with 140 ns, 6 kV pulses at 1.5 kHz. The production of ozone increases with pulse voltage and pulse repetition rate. O₂ concentration in He was also found affecting the ozone generation. In addition, two-photon laser induced fluorescence radially resolves an ozone profile in a diameter of 1 mm produced by the plasma needle.

*This work is partly supported the Air Force Office of Scientific Research and a Los Angeles Basin Clinical and Translational Science Institute Pilot and Feasibility Grant.

URP 52 Study of structural modification of sugarcane bagasse employing hydrothermal treatment followed by atmospheric pressure plasmas treatment JAYR AMORIM, MARIA TERESA PIMENTA, *Centro de Ciencia e Tecnologia do Bioetanol* LEANDRO GURGEL, *IQSC, Universidade de Sao Paulo* FABIO SQUINA, JORGE SOUZA-CORREA, *Centro de Ciencia e Tecnologia do Bioetanol* ANTONIO CURVELO, *IQSC, Universidade de Sao Paulo* CTBE TEAM, USP SC COLLABORATION, Nowadays, the cellulosic ethanol is an important alternative way to many liquid biofuels using renewable biomass rich in polysaccharides. To be used as feedstock for ethanol production, the bagasse needs to be pretreated in order to expose its main constitutive. The present work proposes the use of different pretreatment processes to better expose the cellulose for hydrolysis and fermentation. In the present paper the sugarcane bagasse was submitted to a hydrothermal pretreatment followed by atmospheric pressure plasmas (APPs). An RF microplasma torch was employed as APPs in Ar and Ar/O₂ mixing. The bagasse was treated in discharge and post-discharge regions. The position and time of treatment was varied as well as the gas mixture. The quantity of polysaccharides was determined by using high performance liquid chromatography. It was observed the release of a fraction of the hemicelluloses in the sugarcane bagasse. Modifications in the surface of the sugarcane fibers were monitored by employing scanning electron microscopy.

URP 53 PLASMA DIAGNOSTICS: OPTICAL, ELECTRICAL, OTHERS

URP 54 Diagnostic of N₂(A) concentration in high velocity nitrogen afterglow at atmospheric pressure ANNE-MARIE POINTU, EVGENY MINTUSOV, *Paris-South University-CNRS* An optical emission diagnostic was used to measure N₂(A) concentration in a high velocity (1000 cm/s) N₂ flowing afterglow of corona discharge at atmospheric pressure, used for biological decontamination. Introducing impurities of NO (< 1e-5) we used two well separated and relatively intense lines of NO gamma and beta bands (248nm and 321 nm), easily studied with a low resolution spectrometer. Based on a simplified transport kinetics, the technique is validated using a variation of lines intensity ratios used as coordinates, for numerous experimental points, measured at different axial distances and for different values of NO injected flow. Moreover, it has been demonstrated that N₂(A) creation comes from N+N+N₂ atom recombination with a global rate around 2e-33 cm⁶/s, a result which agrees with literature, as well as N₂(A) loss mechanisms were confirmed to go via quenching with O and N atoms. The order of magnitude of obtained N₂(A) concentration, about 1e11 cm⁻³, coincides with the results of direct measurement (by Vegard-Kaplan band), using a spectrometer of better resolution.

URP 55 Spatial variation of O⁻ Energy distribution in an RF magnetron plasma* H. TOYODA, K. GOTO, T. ISHIJIMA, *Nagoya University* N. OHSHIMA, K. KINOSHITA, *NEC Corporation* Magnetron plasmas are one of the most important tools for sputter deposition of thin films. However, energetic particles from the sputtered target sometimes induce physical and chemical damages to the deposited film surface during the sputtering processes. For example, magnetic and/or electrical properties of magnetic recording films or magnetic tunneling junction for magnetoresistive random access memory (MRAM) are sensitively changed with sputtering condition, suggesting the damage to the deposited film interface. Therefore, measurement of energetic particles in the magnetron plasma is indispensable to improve the deposition process. So far, we have investigated behavior of high energy Ar atoms backscattered from the sputter target, using a quadrupole mass analyzer (QMA) with an energy analyzer. As another possible energetic species in magnetron plasma, oxygen negative ions in oxide targets is known and existence of O⁻ ions up to a few hundred eV has been reported in YBCO magnetron sputter plasma. In this paper, energy distribution of O⁻ and their spatial variation in an RF magnetron plasma is measured using a QMA with the energy analyzer. An equivalent circuit model which explains the spatial variation of O⁻ energy distribution is proposed.

*The authors would like to thank Mr. T. Morita, ULVAC, Inc. for supporting the magnetron plasma source.

URP 56 Sheath Effects on Electron Density Measurements in Frequency Shift Probe and their Application to Electron Temperature Measurements KEIJI NAKAMURA, QI ZHANG, HIDEO SUGAI, *Chubu University* Technologies of plasma monitoring are important for accurate plasma control. We have developed a frequency shift probe, and the probe enables us to measure an electron density from variation of resonance frequency of the

probe head similarly to the hairpin probe. A plane structure of the probe head make it possible to minimize disturbance to the processing plasma, and the probe is applicable to a reactive polymer-deposition plasmas since the polymer has no significant effects on the resonance frequency. The electron density is usually obtained from a plasma-induced shift of the probe resonance frequency, however influences of a sheath around the probe should be considered for more precise density measurements. In this work, sheath effects on the frequency shift probe were investigated, and the frequency shift probe was applied to measure a electron temperature using the sheath effects. As the sheath thickness increased, the resonance frequency decreased, and the sheath effect is enhanced depending on probe structure. Since the sheath width is proportional to Debye length, the probe resonance frequency depends on electron density and electron temperature, suggesting that resonance frequencies obtained in two probes having different sheath dependence gives an unique solution of the density and temperature of electrons.

URP 57 Electromagnetic treatment of the multipole resonance probe* MARTIN LAPKE, THOMAS MUSSENBROCK, RALF PETER BRINKMANN, *Institute for Theoretical Electrical Engineering, Ruhr University Bochum* We present an electromagnetic model of the "multipole resonance probe" (MRP) – a diagnostic concept which enables the simultaneous determination of plasma density, electron temperature, and collision rate in low-pressure gas discharges. The MRP is a radio-frequency driven probe of particular spherical design. In an idealized version the probe consists of two dielectrically shielded, conducting hemispheres. Driven by a radio-frequency source, the hemispheres are powered symmetrically. An analysis of the absorption spectrum shows a multitude of resonances, which allows for an analytical evaluation of the measured signal. The signal provides information on the distribution of the plasma in the probe's vicinity, from which the values of electron density, electron temperature and collision rate can be inferred. In this contribution the MRP will be modeled electromagnetically. Based on a comparison between full electromagnetic and electrostatic treatment, we show that a previously presented electrostatic treatment [1] was well justified. [1] M.Lapke et al., *Appl. Phys. Lett.* **93**, 051502 (2008)

*The authors acknowledge the support by the Deutsche Forschungsgemeinschaft and the Ruhr-University Research School.

URP 58 Determination of Ar($3p^54s$) number densities in an inductively coupled plasma* R.O. JUNG, JOHN B. BOFFARD, CHUN C. LIN, A.E. WENDT, *University of Wisconsin-Madison* Metastable and resonance level atoms can build to substantial number densities in laboratory plasmas and play an important role in various dynamical processes within the plasma. We have measured number densities of the four Ar($3p^54s$) levels using two independent optical techniques for a range of source pressures (1-25 mTorr) in an Ar inductively coupled plasma (ICP). In the first technique, radiation from a Xe arc lamp is passed through the plasma and the resulting (white light) absorption dips yield number densities. The second method employs a simplified radiation trapping model (based on a photon escape factor) to exploit changes in observed branching fractions of optical emissions corresponding to an array of $3p^54p \rightarrow 3p^54s$ transitions, which are sensitive to number densities of the $3p^54s$ levels via reabsorption. Results of these two methods and a related method developed by

Schulze *et al.*¹ are shown to be consistent, validating use of the emission technique for measuring number densities of excited species. We also present similar measurements of the four levels of the Ne($2p^53s$) configuration in a pure Ne plasma.

*Supported by NSF (Grant # CBET-0714600).

¹M Schulze *et al.*, *J Phys. D: Appl. Phys.* **41**, 065206 (2008)

URP 59 OES-Measurement on the spatial distribution of the Ar($1s5$) population density in a 2f-CCP KAZUKI TAKAHASHI, TOMIHITO OHBA, TOSHIKI MAKABE, *Capacitively coupled plasmas (CCPs) are generally used for SiO₂ etching processes. The application of RF-power to both electrodes of a CCP (2f-CCP) provides advantages for the operation. Optical emission spectroscopy (OES) is widely used as noncontact method to determine plasma parameter. Ar metastables play an important role for the characteristics as a probe of active dissociated molecules (radicals). Since metastables are non-emissive species, their population density can not be directly evaluated from OES. In the present study we measured Ar($1s5$) population densities by using the combinations of line intensity ratios emitted from upper states and the escape factor of radiation trapping, following Schulze *et al.* [*J. Phys. D: Appl. Phys.* **41** (2008), 065206]. Abel inversion is used to resolve the spatial distribution. Due to diffusion, the spatial distribution of the Ar metastable density is different from the density of the short-lived resonance states. We show that there exists a density of Ar($1s5$) in front of the side wall as expected. We focus on the spatial distribution of the Ar($1s5$) density and discuss its behavior compared with Ar($2p2$).*

URP 60 Optical emission spectroscopy of a dynamic E-H transition in an inductively coupled plasma in Ar SATOSHI MORISHITA, Keio University YUICHIRO HAYASHI, TOSHIKI MAKABE, *Inductively coupled plasmas (ICPs) are used as a high density plasma source in various applications. It is well-known that an ICP has two operating modes, E and H mode. The transition between both modes shows strong hysteresis behaviors in various characteristics. In our series of experiments, we have studied the E-H transition in Ar for 100 and 300 mTorr in an ICP driven by a single-turn coil around a quartz tube. In our recent research we investigate the dynamic optical characteristics of the E-H transition, in the form of the integrated signal along the axial direction, by using an ICCD camera. In the present study, the net excitation rate of Ar($2p9$) mainly caused by two-step collisions of electrons with energy comparable to 1.5 eV is observed. The temporal change in the transition of Ar($2p9$) is compared with that of previous measured Ar($2p1$) caused by electrons with energy greater than 13.6 eV. Discussion will be focused on the influence of high- and low-energy electrons on the dynamic transition. This work is partly supported by Global COE program operated in Keio University.*

URP 61 Time of Flight Ion Mass Spectrometry for Plasma Doping JOHN (BON-WOONG) KOO, ZIWEI FANG, LUDOVIC GODET, JAMES BUFF, DEVEN RAJ, TIMOTHY MILLER, *Varian Semiconductor Equipment Associates* Plasma doping provides cost effective dopant implantation in semiconductor device fabrication. Unlike conventional beamline implantation, plasma doping is not mass-analyzed, making control of the ion species in the low temperature plasma very important. It is also a pulsed system, making time resolution important. We have developed a

time of flight (TOF) ion mass spectrometer that can provide in-situ, time-resolved plasma monitoring. The composition of the plasma determines the ions implanted into the wafer and these experiments also provide insight into the electron-radical interactions. We report Particle in Cell (PIC) modeling of our TOF sensor and experimental results from various chemistries. For BF_3 plasma process, we report time-resolved measurements during and after the high voltage pulse and also qualitative comparison with a commercial (Hiden Analytical) ion mass spectrometer. For B_2H_6 plasma process, we report a correlation between TOF data and processed wafer data. For AsH_3 plasma process, we report the ion composition changes with respect to several plasma parameters. This has led to better understanding of the gas phase phenomena and an optimization of the low temperature plasma processes.

URP 62 Electron Density Measurements in a Supersonic Flowing Ar/ H_2 /Air Discharge M. NIKOLIC, D.J. DRAKE, P. LAURIN, S. POPOVIC, L. VUSKOVIC, *Department of Physics, Old Dominion University*

Local measurements of the electron density in high pressure discharges have commonly been performed through use of an electrical probe, such as a Langmuir probe, or by the Stark broadening of the hydrogen lines. However in supersonic flowing discharges electrical probes can cause shocks to form, which is unwanted. In addition, these types of discharges do not often contain the hydrogen needed to determine the electron density through Stark broadening where the measurements are hampered by the lack of intensity and breadth of the hydrogen Balmer lines. An alternative approach is to use the intensity of the rotational bands of the N_2 second positive system. We performed detailed measurements of the population densities of the N_2 $\text{C}^3\Pi_u$ - $\text{B}^3\Pi_g$ system and the hydrogen Balmer lines in a supersonic flow of weakly ionized Ar/ H_2 /Air. Gases were premixed in the stagnation chamber at room temperature by adding up to 10% hydrogen and up to 45% air to pure argon. A cylindrical cavity was used to sustain a discharge in the pressure range of 100-700 Pa. Absolute emission spectroscopy was used to determine the gas temperature in the flow from the N_2 system. Comparison was made between the results obtained from the N_2 band intensity technique and Stark broadening of the hydrogen Balmer lines.

URP 63 On the floating harmonics method in non-Maxwellian plasmas ARAM KIM, JIN YOUNG BANG, CHIN WOOK CHUNG, *Hanyang University*

The floating harmonics method applicable to measure electron temperature and ion density in processing plasmas assumes that electrons are in a Maxwellian distribution [1]. To investigate the effect of non-Maxwellian electron distributions to the floating harmonics method, the electron energy distribution functions (EEDFs) were measured. The electron temperatures from the EEDFs at floating potentials were compared with that from the floating harmonics method. Slight discrepancies between them were observed. A new approach to address this was proposed using the second harmonics and third harmonics of the probe current and was compared. This method was not affected by the displacement current due to the stray capacitance of the measure system. The results were in good agreement with the electron temperature from the EEDFs at floating potentials. [1] M. H. Lee, S. H. Jang and C. W. Chung, *J. Appl. Phys.*, 101, 033305 (2007)

URP 64 Spectroscopic studies of the primary-to-secondary streamer transition in short air gap YURI SHCHERBAKOV, *High-Voltage Research Center*

LEONID NEKHAMKIN, REIDAR SIGMOND, *Norwegian University of Science and Technology (NTNU)* We present results on synchronous spectroscopic and electrical studies of the filamentary streamer discharge in short air gap in stage of primary-to-secondary streamer transition. This study continues our previous studies of the high-stable DC positive streamer corona by measurement of absolute intensities of the second positive (SPS) and first negative (FNS) systems of molecular nitrogen. Special attention was paid to measurement of the luminosity intensities just at the moment of arrival of the primary streamer at the cathode followed by the stage of very fast redistribution of the electric field as well as by the stage of the relatively low-speed neutralization of the primary streamer channel to transform finally to the secondary streamer in resistive stage of the residual streamer channel. Spectroscopic data have been supplemented with synchronous electric current waveforms. Some preliminary theoretical analysis has been done for the very fast stages of streamer dynamics near the cathode.

URP 65 Real time two-dimensional spatial distribution measurement method of electron temperature and plasma density YOUNG CHEOL KIM, SUNG HO JANG, GUN HO KIM, CHIN WOOK CHUNG, *Hanyang University*

Real time two-dimensional spatial distribution measurement method of electron temperature and plasma density was developed. It is based on a floating probe method [1], because the floating probe has high time resolution. Two-dimensional array of sensors on a 300 mm diameter wafer-shaped printed circuit board (PCB) and a high speed multiplexer circuit were used for real time distribution measurement. The method was tested at various powers and pressures, spatial distributions of the electron temperature and the plasma density could be obtained. And in the measurement results, asymmetric plasma density distributions caused by pumping port effect could be observed. This method can measure spatial distribution of plasma parameters on the wafer in real time without plasma perturbation, therefore it will be expected to improve the uniformity of processing plasmas such as etching and deposition. [1] M. H. Lee, S. H. Jang, C. W. Chung, *J. Appl. Phys.* 101, 033305 (2007).

URP 66 Measurements of electron energy distributions in short DC discharges* J.M. WILLIAMSON, *Innovative Scientific Solutions, Inc., Dayton, OH 45440* S.F. ADAMS, *Air Force Research Laboratory, Wright-Patterson AFB, OH 45433* J. BLESSINGTON, V.I. DEMIDOV, *West Virginia University, Morgantown, WV 26506*

The energetic portion of the electron energy distribution function (EEDF) in short DC discharge plasmas was investigated. For this experiment, a short DC discharge with a conducting radial wall and cold cathode was used. The conducting wall was electrically isolated and used as a large electric probe. The probe surface area was much larger than a typical cylindrical Langmuir probe. The application of the wall as an electric probe for plasma measurements was possible under the condition of nonlocality of the EEDF. Nonlocality is related to the dimension of the plasma volume and the gas pressure. Increasing the probe surface area results in an increase in probe sensitivity. Since the wall probe was nearly flat, the resulting contribution of the ion current to the measurements was also dramatically reduced. The measured EEDFs had clear signatures of the creation of energetic electrons in the plasma from atomic and molecular volume processes. Plasma particle densities were estimated from the probe measurement.

*This work supported in part by AFOSR.

URP 67 ABSTRACT WITHDRAWN

URP 68 Electronic Temperature Measurements in a Micro-Cathode Sustained Discharge in Neon* VERONICA MURPHY, ERICA BARDEN, KEVIN MARTUS, *William Paterson University* Optical emission spectroscopy of plasmas produced from a Micro-Hollow-Cathode-Discharge (MHCD), with a Neon feedstock gas are reported. The properties that have been analyzed in these plasmas include the composition, electronic temperature of and the excited state neutral gases in the discharge. The MHCD consists of two Molybdenum plates sandwiched around a Mica insulator with an axial hole through the three layers. The feedstock gas is driven through the discharge reactor and a high voltage applied across the discharge plates produces the plasma. The plasma was generated at gas pressures ranging from 150 to 500 Torr, voltages ranging from 250 to 500V, and flow rates between 10 and 60 sccm. The Neon spectrum included a set of emission features that terminate at the same energy level from which a Boltzmann Plot was generated. The variation in the electronic temperature as a function of gas pressure, gas flow rate and driving voltage will be presented and discussed. Also to be presented is preliminary data for a discharge generated using a feedstock gas consisting of a combination of Neon and Methane.

*Work Supported by the WPUNJ ART Program and the WPUNJ College of Science and Health Student Worker Funds.

URP 69 Retarding field analysis of the time resolved ion energy distribution at a biased electrode DAVID GAHAN, *Dublin City University* BORISLAV DOLINAJ, *Impedans Ltd.* MIKE HOPKINS, *Dublin City University* Retarding field energy analyzers (RFEAs) are commonly used to measure the ion energy distribution function (IEDF) at grounded and driven electrodes in plasma reactors. At the grounded surface the RFEA operation is easier to implement due to the absence of large voltages. At the driven electrode the RFEA design is more complex. Filtering techniques are used to ensure the entire RFEA floats at the electrode bias potential. If the discharge, or the substrate electrode, is driven with a pulsed signal the time resolved IEDFs through the pulse cycle are desirable. RFEAs and mass spectrometers have been used to make time resolved measurements of the IEDF at grounded surfaces in discharges pulsed in the tens/hundreds of kHz range. Time resolved measurements made at a pulsed bias surface are more complicated, mainly because of the need to incorporate low pass filters to allow the RFEA to float at the bias potential. Here, we present time resolved IEDF measurements at a pulsed/rf driven electrode in the kHz range. The RFEA body is allowed to float at the bias potential while the internal components are rf grounded. The ion retarding potential is always determined relative to the instantaneous RFEA body potential. Time resolved IEDFs are presented for various square pulse and sinusoidal bias waveforms.

URP 70 Electrical and emission spectroscopic investigation of a self-pulsing micro hollow cathode discharge BEILEI DU, SEBASTIAN MOHR, DIRK LUGGENHOELSCHER, UWE CZARNETZKI, *Institute for Plasma and Atomic Physics, Ruhr-Universität Bochum* Micro hollow cathode discharges (MHCD) consist of two electrodes separated by a thin dielectric (here: 100 μm). The discharge develops in a hole penetrating all three foils (200 μm diameter). When powered by a DC voltage of several 100 V, the discharge shows self-pulsing operation. Voltage and

current measurements, optical emission measurements by an ICCD camera equipped with a microscope lens as well as the determination of electron density from the Stark broadening of the H_{β} -line are performed in argon at pressure from several 1000 Pa to atmospheric pressure. The voltage-current characteristic during self-pulsing indicates a transition from abnormal mode to spark mode as in a DC glow discharge. The pulse frequency can range from kHz up to about 1 MHz and depends on the capacitance of the discharge setup. The pulse width can be as short as several 10 ns and the current peaks can be as high as 1 A. With the appearance of the self-pulsing the electron density increases from the order of 10^{15} cm^{-3} during the non self-pulsing operation to the order of 10^{16} cm^{-3} . A comparison of the plasma conductivity obtained from the performed measurements with the electrical measurements shows excellent quantitative agreement.

URP 71 X-Ray Induced Breakdown in Air at High Reduced Electric Field: Experimental Details* ROBERT VIDMAR, ANUSHA UPPALURI, *University of Nevada, Reno* Breakdown of laboratory air in parallel plate geometry was triggered by an X-ray pulse originating from an electron beam source. The electron beam operates at 100 keV and a few mA for a few hundred ns to several ms. The source is shielded with stainless steel and lead from the breakdown device. Theory is presented relating the X-ray count rate in a NaI(Tl) crystal to the volumetric ionization rate in air. Measurements quantify the X-ray count rate in a detector and provide an estimate of the volumetric ionization rate during an X-ray pulse. An air-chemistry code provides a time history of electrons and air species leading up to breakdown in air subject to high reduced electric field. Measurements are made with a parallel plate geometry biased to near breakdown. X-ray emissions serve as the source of ionization resulting in breakdown. Details of the method and measurements are discussed.

*This material is based on research sponsored by the Air Force Research Laboratory, under agreement numbers FA9550-05-1-0087 and FA9550-07-1-0021.

URP 72 RF Measurement Techniques and Improvements CARL ALMGREN, SCOTT HERES, CAMERON MOORE, GEORGE COLLINS, *Colorado State University* Measurements of RF voltage, current, and phase at the plasma load (after the matching network) requires a careful implementation, especially for plasmas at atmospheric pressure with small electrode surface areas and excitation volumes. We present a comparison of measurements produced by two commercial instruments and conclude that to achieve accuracy with minimal perturbation requires an understanding of the equivalent circuit for the sensing method used. Finally we discuss how impedance match characteristics and a chosen measurement method need both be considered as a system when making these measurements.

URP 73 Modeling of Optical Emission Spectra in an Ar Pulsed Discharge to Determine Absolute Metastable Density* S.F. ADAMS, J.A. MILES, A.C. LABER, *Air Force Research Laboratory* J.M. WILLIAMSON, *Innovative Scientific Solutions Inc.* Optical emission measurements of relative intensities of violet spectral lines in an Ar pulsed discharge have been combined with available electron-impact cross sections to yield absolute Ar metastable species concentration. An enabling factor of this analysis is that the electron excitation pattern from the Ar singlet ground state and the triplet metastable state (1s in Paschen's notation) is quite

different between the 10 levels of the resonant 3p state ($3p_1...3p_{10}$). The result of this pattern is that the emission spectrum of 3p-1s transitions will display a unique intensity distribution depending on whether the 3p state is generated by direct excitation from the ground state, or by stepwise excitation from one of the 1s metastable states. Data is shown for a model that accurately simulated experimental spectra using the metastable state density and the E/N as fitting parameters.

*This work supported in part by the AFOSR.

URP 74 High accuracy identification of microwave hairpin resonances MARK BOWDEN, VLADIMIR SAMARA, NICHOLAS BRAITHWAITE, *The Open University* The quarter-wave hairpin resonator is a useful density diagnostic in low pressure plasmas. Among its advantages are the immediacy and potential accuracy of the determination of electron density by a microwave frequency measurement. One difficulty in making high precision measurements has been the identification of the precise resonant frequency because of the shape of the resonance and the background signal on which it is superimposed. In a development of the hairpin method the mean potential of the hairpin is directly modulated at a few kHz while a separate, inductively coupled microwave signal is swept through the range of resonance. When immersed in a plasma the low frequency modulation perturbs the electron density in the immediate vicinity of the hairpin, impressing a modulation on the resonant frequency. At resonance there is a sharp phase change in the modulated microwave reflection (referenced to the modulation input). This aids identification of the resonance since all other structure in the microwave signal reflected from the hairpin is unaffected. This provides a simple determination of the resonance that can be readily implemented in software for automated measurements, with time resolution restricted only by the modulation period. The method has been demonstrated in a GEC reference cell with pulsed and steady CCP excitation at 13.56 MHz.

URP 75 The electron temperature measurement by using an optical emission spectroscopy in inductive Ar/O₂ mixture discharge YU SIN KIM, YOUNG-KWANG LEE, CHIN-WOOK CHUNG, *Hanyang University* Electron temperatures (Te) were measured by using an optical emission spectrometer (OES) method in Ar/O₂ mixture inductively coupled plasma. The OES method is based on the simple collisional-radiative model with relative intensities from the light emission of the argon 4p level [1]. The OES measurements were compared with the floating harmonics method [2]. At a pure argon discharge of 5 mTorr, the measured Te from the OES method was 3.6 eV. As O₂ flow rates increase, the Te increased gradually from 4.1 eV to 4.7 eV. However, the Te from the OES method was slightly higher than that of the floating harmonics method. These differences caused by changed metastable densities which can affect the light intensity ratio of the 4p lines and the error of rate coefficient(K) values. Although there are a little difference of the Te, note that trends of the measured Te with the O₂ addition were good agreement with that from the floating harmonics method. These results show that our OES method is applicable to the plasma diagnostics in the mixture gas discharges such as an industrial plasma process monitoring because this noninvasive OES method does not perturb the plasmas. [1] Y.K. Lee, K.T. Hwang, M.H. Lee and C.W. Chung, *J. Korean Phys. Soc.* 52, 6(2008) [2] M.H. Lee, S.H. Jang, and C.W. Chung, *J. Appl. Phys.* 101, 033305 (2007)

URP 76 Simple in situ method for real time measurement of dielectric film thickness in plasmas SUNG-HO JANG, GUN-HO KIM, CHIN-WOOK CHUNG, *HanYang University* An in situ thickness measurement method of dielectric films (Dual frequency method) was developed, and the thickness was measured in an inductively coupled plasma. This method uses a small AC bias voltage which has two frequencies for the thickness measurement. The dielectric thickness is obtained from measuring amplitudes of two frequency ac current through a sensor and using an equivalent circuit model describing impedance of the dielectric film and the plasma sheath. In the experiment, thicknesses of Al₂O₃ film could be accurately measured in real time. To check the measurement reliability, the dual frequency method was compared with Reflection spectrophotometry as a kind of optical thickness diagnostics, and it was found that the dual frequency method agrees closely with reflection Spectrophotometry at various rf powers and pressures. In addition, this method is very simple and able to install at anywhere in plasma reactors in contrasted with optical methods, therefore it is expected to be applied to in situ surface diagnostics for various processing plasmas.

URP 77 Rotational CARS Temperature Measurements in Nanosecond Pulse Discharge Plasmas YVETTE ZUZEEK, KEISUKE TAKASHIMA, IGOR ADAMOVICH, WALTER LEMPERT, *Ohio State University* Time-resolved and spatially resolved temperatures in repetitively pulsed nanosecond discharges in air and ethylene-air mixtures have been measured by purely rotational Coherent Anti-Stokes Raman Spectroscopy (CARS). The experiments have been done in a capacitively coupled plane-to-plane discharge and in an atmospheric pressure near-surface Dielectric Barrier Discharge (DBD), both powered by repetitive nanosecond duration voltage pulses. Gated ICCD camera images demonstrated that the capacitively coupled discharge plasma remains diffuse and stable, with no sign of arc filaments. Comparison of the experimental results with plasma chemical kinetic modeling calculations shows good agreement. The results demonstrate that the rate of heating in the fuel-air plasma is significantly more rapid compared to the one in the air plasma. Kinetic model analysis shows that this occurs due to exothermic reactions of fuel with radical species generated in the plasma, such as O atoms. The present results provide additional insight into kinetics of hydrocarbon fuel oxidation in low-temperature plasmas and into the mechanism of localized heating of air flows by nanosecond DBD discharges.

URP 78 Properties of a hairpin probe in a strongly magnetized plasma* S.K. KARKARI, *National Center for Plasma Science and Technology, Dublin City University, Collins Avenue, Dublin 9, Ireland* G.S. GOGNA, *National Center for Plasma Science and Technology, Dublin City University, Dublin 9, Ireland* D. BOILSON, *Department CEA/DSM/DRFC, CEA-Cadarache, 13108 ST PAUL-LEZ-DURANCE France* Understanding of the physics in the filter field region of a neutral beam injection source for ITER under development is very important, as this region is where the negative ions are generated and extracted. For accurately determining electron densities in this complex plasma, a floating hairpin probe is applied on the KAMABOKO III ion source, at the MANTIS test bed at CEA Cadarache. The technique is based on measuring the probes resonance frequency (few GHz) shift in plasma with respect to that obtained in vacuum. The resonance

frequency is proportional to the permittivity of the medium filling the space between the wires of the hairpin resonator. Using this technique we obtained the electron density variation as function of discharge power and on the external grid bias in front of the plasma grid.

*This project is funded by the Enterprise Ireland grant TD/07/335 and EURATOM Association DCU Fusion grant FU07-CT-2007-00052.

URP 79 PLASMA CHEMISTRY: ATMOSPHERIC, GAS PHASE, SURFACE

URP 80 Developing a Consistent Chemical Kinetic Model for Electron Beam Irradiation of Humid Air* THEODORE DIBBLE, KAREN SCHMITT, DAVID-ANTHONY MURRAY, *SUNY-Environmental Science and Forestry* A chemical kinetic model has been assembled to assist in better understanding the mechanisms underlying hydroxyl radical production via electron beam irradiation of humid air. Thermodynamic determination of the feasibility of particular product sets was used to eliminate certain reactions proposed previously, dynamical models were used to guide the choice of product sets, and updated rate constants were obtained from the current literature. Tracers were also used to determine the major reactions producing and destroying hydroxyl radical, because of its role in removing pollutants from irradiated air. Modeling results for selected species have been presented for 1 atmosphere of air at 298.15 K and 50% relative humidity, at doses of 1, 5, 10, 25, and 50 kGy delivered over 0.8 seconds to a static sample. The concentrations of the most abundant ions, radicals, and stable reaction products are reported, and the major reactions producing and destroying hydroxyl radical are quantified.

*This research was supported by grant CTS-0626302 from the National Science Foundation.

URP 81 Influence of the pulse-periodic discharge on ignition and laminar flame propagation of methane and ethylene BORIS POTAPKIN, MAXIM DEMINSKY, MARINA STRELKOVA, IRINA CHERNYSHEVA, IGOR KOCHETOV, *Kintech Lab, Moscow, Russia* ANATOLII NAPARTOVICH, *TRINITI, Troizck, Russia* SEYED SADDUGHI, JOHN T. HERBON, TIMOTHY SOMMERER, *GE Global Research, Niskayuna, US* Influence of non-equilibrium plasma on ignition and combustion of hydrocarbons are investigated theoretically and experimentally now intensively. In our previous work [1] we have shown that the problem of correct description of influence of non-equilibrium plasma on hydrocarbon combustion can be solved taking into account the effect of active species of plasma on initiation of low-temperature branch of hydrocarbons oxidation. Therefore the development of model where plasma and chemical processes are closely coupled is the key for predictive modeling of such phenomena. The model of pulse-periodic barrier discharge was elaborated and demonstrated reasonable agreement with experiments [2] of ignition of methane and ethylene. Advantages of the non-thermal plasma initiation of combustion over the pure thermal acceleration are discussed. [1] M. Deminsky et al, ISPC 18, 2009, Bochum, Mechanism of influence of the pulse-periodic discharge on low temperature oxidation of hydrocarbons [2] E. Mintusov et al, 46th AIAA Aerospace Sciences Meeting, 7 - 10 January 2008, Reno, Nevada, 7, 26, (2009).

URP 82 Electron-Beam Generated Air Plasma Measurement Details: I/Q Detector and Effect of Reduced Electric Field*

ROBERT VIDMAR, ANUSHA UPPALURI, *University of Nevada, Reno* KENNETH STALDER, *Stalder Technologies and Research* An in-phase (I) and quadrature (Q) microwave detector operating at 10 GHz is used to measure the electron number density and momentum-transfer collision rate of air plasma as a function of pressure from 1 mT to 636 T and reduced electric field. Raw measurements from the I/Q detector and the method to convert such measurement into electron number density and momentum transfer, collision rate, are discussed. Optical emissions at 391.4 nm from N_2^+ are used to quantify the volumetric ionization profile along the microwave propagation path. At low pressure a MAGIC code calculation provides the relative ionization profile. Results of electron number density and momentum-transfer collision rate are shown as a function of reduced electric field and pressure.

*This material is based on research sponsored by the Air Force Research Laboratory, under agreement numbers FA9550-05-1-0087 and FA9550-07-1-0021.

URP 83 Mechanism of methane dry reforming using an arc-jet plasma reactor

HWANG NA KYUNG, *Dept. of Environmental-System Engineering, University of Science and Technology* CHA MIN SUK, HUR MIN, SONG YOUNG-HOON, *Eco-Machinery Research Division, Korea Institute of Machinery and Materials* The characteristics of plasma reaction for dry reforming of methane have been studied using an arc-jet plasma reactor with AC power supply. The effects of the operating parameters, which are input power, CO_2/CH_4 ratio, added O_2 ratio, and the portion of $CH_4 + CO_2$ amount in reactants, were investigated by product analysis. As results, the decompositions of CH_4 and CO_2 were enhanced by input electrical power. The amount of produced hydrogen was affected by the supplied power and the portion of $CH_4 + CO_2$ in the reactants, demonstrating increasing behavior with increasing supplied power and the volume of CH_4 and CO_2 . For fuel based energy efficiency, the effect of the supplied power was neutral, while the CO_2/CH_4 ratio and the portion of $CH_4 + CO_2$ amount gave a positive impact to the efficiency. Moreover, we could get various H_2/CO ratio ranged 0.8 - 2.5 by controlling the CO_2/CH_4 ratio. Detailed mechanism and characteristics of the dry reforming of methane will be discussed also.

URP 84 Optical and electrical characterization of atmospheric pressure microplasma for $CH_3OH/H_2O/Ar$ mixtures

JIN HOON CHO, *Research Institute of Basic Sciences, Ajou University* YOUNG DONG PARK, MYEONG YEOL CHOI, WOONG MOO LEE, *Dept. of Chemistry, Ajou University* Atmospheric pressure, non-equilibrium microplasmas have become powerful experimental tools for many applications including microfabrications in microelectronics, surface modifications, environmental processing and many other areas. We investigated that comparative study of atmospheric pressure microdischarge generated in different nonequilibrium discharge with respect to observation optical and electrical characteristics at $CH_3OH/H_2O/Ar$ mixtures. This paper focuses on plasma chemical reactions from methanol and water vapor mixture and the effects of plasma generation methods in the perspective of hydrogen generation. The microplasmas were generated by resorting to discharge modes such as some variations of glow dielectric barrier discharge (DBD) and also a variation of corona discharge called a microdischarge inside

a porous ceramic (MIPC). Plasma chemical reactions were monitored using optical emission spectroscopy to gather information on the degree of non-equilibrium, electron density, uniformity of plasma reaction and concentrations of transient species.

URP 85 Analysis of Optical Spectra Measured in Plasma-Based Tissue Removal System MYEONG CHOI, IL GYO KOO, CAMERON MOORE, GEORGE COLLINS, *Colorado State University* An atmospheric pressure plasma used for tissue removal is characterized based on emission spectroscopy. This type of plasma system, which produces large concentrations of reactive chemical species, demonstrates potential application to tissue processing. The plasma is generated using radio frequency (RF) power that is delivered through the dielectric barrier of a quartz tube. In particular we identify gas phase species and estimate their relative concentrations with varying amounts of delivered power, chemical flow, and amount of tissue removal.

**URP 86 PLASMA BOUNDARIES:
SHEATHS, BOUNDARY LAYERS, OTHERS**

URP 87 A simulation of a capacitively coupled oxygen discharge using the oopd1 particle-in-cell Monte Carlo code J.T. GUDMUNDSSON, *University of Iceland* M.A. LIEBERMAN, YING WANG, J.P. VERBONCOEUR, *University of California at Berkeley* The oopd1 particle-in-cell Monte Carlo (PIC-MC) code is used to simulate a capacitively coupled discharge in oxygen. oopd1 is a one-dimensional object-oriented PIC-MC code [1] in which the model system has one spatial dimension and three velocity components. It contains models for planar, cylindrical, and spherical geometries and replaces the XPDx1 series [2], which is not object-oriented. The revised oxygen model includes, in addition to electrons, the oxygen molecule in ground state, the oxygen atom in ground state, the negative ion O^- , and the positive ions O^+ and O_2^+ . The cross sections for the collisions among the oxygen species have been significantly revised from earlier work using the xpdp1 code [3]. Here we explore the electron energy distribution function (EEDF), the ion energy distribution function (IEDF) and the density profiles for various pressures and driving frequencies. In particular we investigate the influence of the O^+ ion on the IEDF, we explore the influence of multiple driving frequencies, and we do comparisons to the previous xpdx1 codes. [1] J. P. Verboncoeur, A. B. Langdon, and N. T. Gladd, *Comp. Phys. Comm.* 87 (1995) 199 [2] J. P. Verboncoeur, M. V. Alves, V. Vahedi, and C. K. Birdsall, *J. Comp. Physics* 104 (1993) 321 [2] V. Vahedi and M. Surendra, *Comp. Phys. Comm.* 87 (1995) 179

URP 88 Studies and comparison of currently utilized models for ablation in Electrothermal-chemical guns SHENLI JIA, RUI LI, XINGWEN LI, Wall ablation is a key process taking place in the capillary plasma generator in Electrothermal-Chemical (ETC) guns, whose characteristic directly decides the generator's performance. In the present article, this ablation process is theoretically studied. Currently widely used mathematical models designed to describe such process are analyzed and compared, including a recently developed kinetic model which takes into account the unsteady state in plasma-wall transition region by dividing it into two sub-layers, a Knudsen layer and a collision

dominated non-equilibrium Hydrodynamic layer, a model based on Langmuir Law, as well as a simplified model widely used in arc-wall interaction process in circuit breakers, which assumes a proportional factor and an ablation enthalpy obtained empirically. Bulk plasma state and parameters are assumed to be consistent while analyzing and comparing each model, in order to take into consideration only the difference caused by model itself. Finally ablation rate is calculated in each method respectively and differences are discussed.

URP 89 Comparison of sheath thickness obtained from the theories of ion correction in the floating potential HYEONG SIK HAN, KWANG TAE HWANG, IK JIN CHOE, CHIN WOOK CHUNG, *Hanyang University* In the cold plasmas, when the cylindrical probe is used to measure the ion density, an expansion of the sheath thickness related to the sheath voltage increases the ion current. The expansion of the sheath thickness results in an incorrect measurement of ion current. To measure ion density correctly, the sheath thickness should be considered. In the collisionless sheath, the sheath thickness can be calculated by the Child-Langmuir (CL) theory or the Allen-Boyd-Reynolds (ABR) theory. We measured the sheath thicknesses using the floating harmonics method [1] and the cut-off method by the microwave [2], and the results compared with the CL theory [3] and ABR theory [4] in the floating potential. The sheath thicknesses obtained from the ABR theory were in good agreement with the experimental results. [1] M. H. Lee, S. H. Jang and C. W. Chung, *J. Appl. Phys.*, 101, 033305 (2007) [2] J.H. Kim, S.C. Choi, Y.H. Shin, and K. H. Chung, *Rev. Sci. Instrum.* 75, 2706 (2004) [4] F. F. Chen and D. Arnush, *Phys. Plasmas* 8, 5051 (2001)

URP 90 Experimental observation of multiple reflections of highly energetic electron beams by the boundary sheaths in capacitive discharges* EDMUND SCHÜNGEL, JULIAN SCHULZE, UWE CZARNETZKI, *Ruhr-University Bochum* In capacitively coupled radio frequency (CCRF) discharges operated at low pressures stochastic electron heating is dominant. It leads to the acceleration of highly energetic electron beams by the expanding plasma boundary sheaths. Such beams can propagate through the entire plasma bulk at low enough pressure and low enough electron-neutral collision frequencies. In 1991 Wood et al. [1] demonstrated by a PIC simulation that under certain conditions such electron beams can be reflected several times between the opposing boundary sheaths. This effect leads to an enhanced confinement of highly energetic electrons in the discharge. Here these reflections are observed experimentally in CCRF discharges of different geometries including the case that the plasma is in contact with a floating wall and that it is confined between two electrodes (powered and grounded) of equal surface areas by a glass cylinder. Phase resolved optical emission spectroscopy is verifying the previously obtained simulation results. [1] Wood B. P. PhD thesis, University of California at Berkeley, 1991

*Funding: DFG (GRK1051)

URP 91 Are there double layers in unmagnetized electronegative plasmas?* CHI-SHUNG YIP, NOAH HERSHKOWITZ, *University of Wisconsin - Madison* Bounded electronegative plasmas are predicted to have electropositive halos. A recent experiment [1] showed that for a negative ion to electron concentration ratio of $\alpha=0.43$ for an Argon-Oxygen plasma a positive halo was a consequence of negative ion satisfying a Boltzmann relation.

When Te/T_e is greater than $5 + \sqrt{24}$ [2] and that α is greater than Te/T_e [3], the negative ions are predicted to be confined by a double layer. Experiments are reported in Ar-SF₆ and Ar-Cl₂ plasmas aimed at finding the double layer by varying the gas concentrations. Experiments are carried out in a filament discharge in a multi-dipole chamber, with no magnetic field on the end walls. An unmagnetized boundary of the plasma is set by a bias plate along the axial direction of the chamber. Negative ion concentrations are determined from the phase velocity of C.W. Ion Acoustic Waves. Electron temperature and density are determined using Langmuir probes. Plasma potentials are determined by emissive probes. Argon drift velocities are determined by Laser Induced Fluorescence. [1] Ghim, YC and Hershkowitz, N, Applied Physics Letters. **94**, 15, 151503 (2009) [2] N. Braithwaite and J. E. Allen, J. Phys. D: Appl. Phys. **21**, 1733 (1988) [3] R. N. Franklin, Plasma Sources Sci. Technol. **11**, A31, (2002)

*Work supported by the DoE grant no. DE-FG02-97ER54437.

URP 92 PLASMA TOPICS

URP 93 Plasma Assisted Combustion in a Supersonic Flow* HYUNGROK DO, SEONG-KYUN IM, MARK CAPPELLI, MARK MUNGAL, *Stanford University* A nanosecond pulsed plasma discharge is used to ignite jet (hydrocarbon and hydrogen) flames in supersonic air cross flows ($Ma = 1.7$ to 3.0). The flow pattern and shockwaves induced by the fuel jets and flow disturbances are characterized by Schlieren imaging. Planar laser induced fluorescence and emission spectroscopy are employed for imaging the distribution of OH radicals. Two common test model flow configurations (cavity and flat wall) are used with integration electrodes for plasma excitation. Cavity flames are found to be readily enhanced by plasma excitation, with a clear reduction in ignition delay time. However, flame propagation beyond the cavity is limited. A flat wall configuration combining an upstream subsonic oblique fuel jet and a downstream sonic transverse fuel jet is shown to provide a more favorable flow condition for jet flame ignition and propagation. The OH distribution in the vicinity of the discharge confirms jet flame ignition by the plasma. Experimental results are validated using a simple theoretical/numerical model. The reduction in the ignition delay and other qualitative features are validated by the model.

*Sponsored by AFOSR/MURI program.

URP 94 Arc plasma assisted purification of metallic silicon for solar cells: numerical modeling and real time process monitoring JUNGHOON JOO, WONKYUN YANG, *Department of Materials Science and Engineering, Kunsan National University* BO-YUN JANG, YOUNG SOO AHN, *Korean Institute of Energy Research* For achieving the grid parity in solar cell business, cheaper materials and processing technology are necessary. Thin film solar cell could be a strong candidate. Ribbon type polycrystalline solar cell may be a low cost solution with much simpler equipments: melting and specialized casting devices. For further reduction of the manufacturing cost, device grade of silicon starting material (99.99999%) should be replaced with cheaper substitute without degrading the solar conversion efficiency. To reduce the complicated chloride based purification steps, simple vacuum arc melting and purification are considered. It is using small

amount of reactive gases (hydrogen or water vapor) under certain plasma conditions to remove B and P through formation of highly volatile oxides and hydrides. Due to the low electrical conductivity of metallic grade silicon, non-transferable arc operation mode was selected. We used 3D CFD based numerical modeling to optimize the process conditions; arc to silicon pool distance, plasma power input and reactive gas mixing ratio. As a real time monitoring technique, QMS and OES were used to detect any volatile species related with impurities during melting and purification steps.

URP 95 INNOVATIVE PLASMA APPLICATIONS

URP 96 Application of pulsed plasma thruster to materials processing* TAKASHI KIMURA, MASAYASU IIDA, AKI-NORI ODA, *Nagoya Institute of Technology* An electrothermal pulsed plasma thruster with a discharge room in an insulator rod is used as the pulsed plasma for ablation of insulator (PPA), and the material of the insulator rod is polytetrafluoroethylene (PTFE). The PPA has an anode at the end of the room and a cathode of divergent nozzle at the exit of the room. Both the anode and the cathode are made of aluminum. The distance of 13 mm between the anode and the cathode is equal to the plasma length. The diameter of the insulator rod is 4 mm. The pulsed plasma is generated by the stored energy in the capacitor connected to the electrodes. Electrical and optical measurements of PPA are carried out. From the measured waveforms of the voltage applied between the electrodes and the current, the maximum of the instantaneous power is on the order of MW and the maximum of current is on the order of kA during a short time of 5-10 μ s. On the other hand, the optical emission intensities emitted from the excited carbon and fluorine atoms are predominant. This fact should indicate the possibilities of diamond-like-carbon coating or Si etching without a parent gas such as hydrocarbon gas and fluorocarbon gas.

*This work is partially supported by Grant-in-Aid from the Japan Society for the Promotion of Science.

URP 97 Industrial Applications to the Inertial Electrostatic Confinement Configuration* ELIJAH MARTIN, STEVE SHANNON, MOHAMED BOURHAM, *NCSU* Since Fransworth's observation of inertial electrostatic confinement in the 1930's several applications have been proposed and studied with fusion being the main focus. Inertial electrostatic confinement is a scheme in which ions are focused and confined by means of either an electrostatic field or a combination of electrostatic and magnetic fields to produce an effective spherical potential well. Due to the spherical symmetric configuration and the convergent non-Maxwellian ion beams IEC presents a unique energy spectrum that could enhance or enable a variety of industrial plasma applications from material processing to light sources. This work will present the possible industrial applications of the IEC configuration and initial characterization of an IEC source for these applications. The current industrial applications under consideration include materials synthesis, processing, and light production.

*This project is supported by UFNRC, Applied Materials, and North Carolina State.

URP 98 AC Excited Si Microplasma Channel Devices: Photon amplification through microchannels TAEK-LIM KIM, EUNG SOO KIM, EFRAIN MEJIA, SUNG-JIN PARK, JAMES GARY EDEN, *Optical Physics and Engineering Laboratory* In this presentation, we report the design and performance of ac-excited Si micro-plasma "V-grooved" channel devices. These Si channels have been fabricated by anisotropic etching and the width of the channels ranges from 50 to 100 microns and the length ranges from 2 to 5 cm. The V-grooved microchannel generates and confines stable microdischarge in Ne or Ar gas pressures above 400 Torr with the ac excitation of 20 kHz. Radiative intensity from the microplasma is dependent on the channel length, gas pressure and direction. The ratio of photon flux at the transverse and the vertical direction is about 10:1. Furthermore, strong infrared wavelength transitions from Ne or Ar/Xe gas mixtures were also observed at the transverse direction through the microchannel. The optical amplification and radiative efficiency through these devices are characterized with the function of microchannel geometry and dimension.

URP 99 COMPUTATIONAL METHODS FOR PLASMAS

URP 100 Simulation of Chemical Reactions of an Atmospheric Pressure DBD using Graphics Processing Unit PHILIPP MERTMANN, PRIYADARSHINI RAJASEKARAN, NIKITA BIBINOV, PETER AWAKOWICZ, *AAPT THOMAS MUSSEN-BROCK, MARKUS GEBHARDT, TET INSTITUTE FOR PLASMA TECHNOLOGY TEAM, INSTITUTE FOR THEORETICAL ELECTRICAL ENGINEERING TEAM*, A dielectric barrier discharge in air for biomedical applications is characterized by numerical simulations. Plasma in air produces species like NO or O₃, which are of special interest for medical application due to their potential of reacting on surfaces. Optimisation of plasma conditions to produce required density of these species is simulated using different experimental parameters. Input values for the simulation are obtained by optical emission spectroscopy, current-voltage measurements and micro-photography. Solving diffusion equation considering the gain and loss of particles by plasma-chemical reactions in a transient differential equation can be parallelized very efficiently. The use of a graphics processing unit (GPU, graphics card) for calculations allows for quick solutions of this problem. Performance tests showed that the run-time could be decreased by a factor of about 240, compared to a conventional CPU and thereby from a couple of days to 25 minutes.

URP 101 Feature Profile Simulator Algorithm Utilizing Finite Penetration Depth PAUL MOROZ, *TEL US Holdings* Fast particles, such as ions or fast neutrals, coming to the material surfaces in plasma etch systems typically possess enough energy to penetrate many mono-layers into materials, leading to the volume-type reactions. This is very different from typical low-energy gaseous species that could interact only with the upper mono-layer. Our feature profile algorithm represents materials as consisting of cells. The cell size could vary from the smallest (containing a single atom) to a very large one containing many mono-layers of atoms. The penetration depth and energy loss in mono-layers is calculated for each fast incoming particle and is used in calculation of its fate and the following reaction mechanisms. Results obtained with the corresponding feature profile simulator FPS, currently, for 2D3V cases (two-dimensional in space with three velocity components of incoming particles) will be presented.

URP 102 Modelling of Low Pressure Breakdown by a Monte Carlo Technique MARIJA SAVIC, MARIJA RADMILOVIC-RADJENOVIC, ZORAN PETROVIC, *Institute of Physics, Belgrade-Serbia* INSTITUTE OF PHYSICS TEAM, It was recently shown that the basic assumption of Townsend's theory that ions produce the secondary electrons is correct only in a very narrow range of conditions [1]. According to the revised Townsend's theory [1] secondary electrons required to maintain the discharge are produced in collisions of ions, fast atoms, metastable atoms and photons with the cathode or by gas phase ionization mainly by fast neutrals. In this paper, we have tried to build up a procedure for obtaining the secondary electron yields from the gas breakdown data motivated by the fact that published results for the secondary electron yields from ion beam experiments and gas discharges are systematically in serious disagreement. For that purpose, we use a Monte Carlo code that is not limited by assumptions of the energy distribution function and that includes gas phase and surface collisions in arbitrary number and degree of complexity of representation. The results provide partial contributions of different processes and are in general, if not in all detail in agreement with [1]. Argon as a test was the first obvious target of study with calculations being extended to other gases. [1] A.V. Phelps and Z.Lj. Petrović, *Plasma Sources Sci. Technol.* **8** (1999).

URP 103 3D simulations of surface roughness in nanotechnologies MARIJA RADMILOVIC-RADJENOVIC, BRANISLAV RADJENOVIC, *Institute of Physics* Plasma etching represents one of the basic steps used in semiconductor processing for the fabrication of electronic devices. One of the limiting factors in applications of plasma etching in new generations of plasma technologies is controlling of plasma induced roughness or surface roughness by plasma etching. Decreasing the roughness of a surface will usually increase exponentially its manufacturing costs. This often results in a trade-off between the manufacturing cost of a component and its performance in application. In this paper we have studied roughening of nanocomposite materials during plasma etching for by using a level set method [1]. It was found that the presence of two phases with different etch rates affects the evolution of the surface roughness. The obtained results apart from their theoretical relevance, have practical implications for surface treatment of nanocomposite materials. [1] M. Radmilović-Radjenović, B. Radjenović and Z.Lj. Petrović, *Thin Solid Films* **517** (2009) 3954.

URP 104 Three dimensional simulations of the anisotropic wet etching of silicon MARIJA RADMILOVIC-RADJENOVIC, BRANISLAV RADJENOVIC, *Institute of Physics* In this paper we have shown that profile evolution during anisotropic wet etching of silicon can be described by the non-convex Hamiltonian arising from the Hamilton-Jacobi equation for the level set function. Angular dependence of the etching rate is calculated on the base of the silicon symmetry properties, by means of the interpolation technique using experimentally obtained values of the principal [100], [110], [111] directions in KOH solutions. Some examples illustrating developed methodology are presented. The obtained simulation results indicate that inclusion of additional directions for which the etching rates are known, would lead to the better quantitative agreement with the measured data.

URP 105 Modeling of self organization in Xe micro hollow cathode discharges HARUAKI AKASHI, *National Defense Academy* Recently, self organization discharges in Xe micro hollow cathode discharges (MHCDs) have been obtained. The discharge is sustainable in DC, not like dielectric barrier discharge (DBD). Stollenwerk et al [1] reported the self organized pattern in DBD is related to the accumulated charge on the dielectric. In DBD, self organized patterns are significantly affected by dielectric, however, it is not known yet in MHCD. To clarify the mechanism, the simulation has been started. Cylindrical symmetric two dimensional fluid model is taken. The fluid model is adapted from the Ref. [2]. The electrodes configuration is similar to Ref. [3]. Negative voltage is applied to cathode. In this condition, the self organization pattern is not shown, but the discharge becomes glow like discharge as written in Ref. [3]. The peak of electron density is obtained slightly above the hole, but the excimer and ions density peaks are obtained in the hole. [1] L. Stollenwerk et al. *Phys.Rev.Lett.*,96,255001(2006) [2] H.Akashi et al, *IEEE Trans.Plasma Sci.*,33,2,308(2005) [3] W.Zhu et al, *J.Phys.D: Appl.Phys.*,40,3896(2007)

URP 106 Particle-In-Cell simulations of high pressure plasmas using graphics processing units* MARKUS GEBHARDT, FRANK ATTELN, RALF PETER BRINKMANN, THOMAS MUSSENBROCK, PHILIPP MERTMANN, PETER AWAKOWICZ, *Ruhr University Bochum* Particle-In-Cell (PIC) simulations are widely used to understand the fundamental phenomena in low-temperature plasmas. Particularly plasmas at very low gas pressures are studied using PIC methods. The inherent drawback of these methods is that they are very time consuming – certain stability conditions has to be satisfied. This holds even more for the PIC simulation of high pressure plasmas due to the very high collision rates. The simulations take up to very much time to run on standard computers and require the help of computer clusters or super computers. Recent advances in the field of graphics processing units (GPUs) provides every personal computer with a highly parallel multi processor architecture for very little money. This architecture is freely programmable and can be used to implement a wide class of problems. In this paper we present the concepts of a fully parallel PIC simulation of high pressure plasmas using the benefits of GPU programming.

*This work is supported by the Research Group FOR 1123 “Physics of Microplasmas” founded by the German Research Foundation DFG.

URP 107 Numerical Simulation of Cold Dense Plasma Sputtering with VORPAL CHUANDONG ZHOU, PETER STOLTZ, SETH VEITZER, *Tech-X Corporation* Sputtering is an evaporation process that physically removes atoms from a solid target material. This process takes place under bombardment of the target surface by energetic ions. Sputtering is widely applied in material processing and coating, such as etching and thin film deposition. Numerical simulation of sputtering process requires both accurate models of nuclear stopping in materials, particle dynamics and consistent electromagnetic fields. The particle in cell code VORPAL can simulate cold dense plasma under many different electromagnetic configurations. The dynamics of both incident particles and sputtered neutral atoms are simulated in VORPAL, and the sputtering yield is calculated from a standalone numerical library for a variety of materials that are commonly used in industrial applications. Numerical simulation of the spatial distribution of sputtering resulting from a cold dense plasma under externally applied magnetic field and self-consistent electric field is presented.

URP 108 Benefits of Higher-Order Particles in Simulating an Overdense Plasma Using a Particle-in-Cell Code CHRISTINE M. ROARK, PAUL MULLOWNEY, KEVIN PAUL, DAVID SMITHE, PETER H. STOLTZ, *Tech-X Corporation* TECH-X CORPORATION TEAM, Researchers often would like to apply Particle-in-Cell (PIC) methods to model cold, high pressure plasmas in order to discern any kinetic, nonlinear or space charge effects. However, the PIC method typically does not perform well at low temperatures and high densities due to limitations on time and space scales for numerical and practical reasons. One of these limitations is the requirement to resolve the Debye length. Failure to resolve the Debye length in a PIC simulation typically results in artificial heating of the plasma known as grid heating. For applications such as plasma processing, the rate of plasma production is a sensitive function of the electron temperature, so grid heating can make simulation results entirely unreliable. The use of higher-order particle algorithms that smooth out the particle current and charge can help to eliminate this unphysical heating and allow cold, dense plasmas to be simulated using PIC. We present results of using higher-order particles for modeling an overdense plasma sustained by microwaves and we compare to results using standard first-order particles. Specifically, we compare the electron temperature, sheath size, and rate of plasma formation for simulations with an argon gas of 0.05 Torr pressure with an applied microwave power of 1000 Watts at 2.45 GHz.

SESSION VR: BANQUET

Thursday Evening, 22 October 2009; Ballroom 1-2-3, Saratoga Hilton at 19:00; Bill Graham, Queen's University Belfast, presiding

19:00

VR 1 Dinner

20:30

Banquet Talk: Irving Langmuir: Inventing Industrial Research
GEORGE WISE, *GE Historian*

SESSION WF1: PLASMAS AND LIQUIDS
 Friday Morning, 23 October 2009
 Ballroom 1, Saratoga Hilton at 8:00
 Eric Eisenbraun, College of Nanoscale Science and
 Engineering, the University at Albany-SUNY, presiding

8:00

WF1 1 Efficient bacterial inactivation in aqueous solution by low-temperature atmospheric pressure plasma application with a reduction of the solution pH KATSUHISA KITANO, *Osaka Univ.* SATOSHI IKAWA, *TRI Osaka* ATSUSHI TANI, *Osaka Univ.* NAOFUMI OHNISHI, *Tohoku Univ.* SATOSHI HAMAGUCHI, *Osaka Univ.* With some medical applications in mind, bacterial inactivation experiments in aqueous solution have been performed with the use of low-temperature atmospheric pressure plasmas. We have successfully found that efficient bactericidal activity can be achieved if the solution is sufficiently acidic. It is interesting to note that there is a critical pH value of about 4.7 for the bactericidal effects, below which the bacteria are efficiently inactivated and above which the bacteria are hardly affected by the plasma application. When the plasmas were exposed to *E. coli* suspensions at pH 5.2, 4.7, 4.2 and 3.7, D values were found to be 1.92, 0.96, 0.59, and 0.21 min., respectively, under our experimental conditions. It has been also found experimentally that the presence of superoxide anion radicals O_2^- bullet in the solution is essential for bacterial inactivation by the plasma application. The critical pH value may be associated with pKa of the dissociation equilibrium between O_2^- bullet and hydroperoxy radicals HO_2 bullet, which is known to be approximately 4.8. The formation of radicals in solution by such plasma has been confirmed from ESR (Electron Spin Resonance) with spin trapping agents. The ambient gas has been found to influence the radical formation in liquid significantly.

8:15

WF1 2 Properties of Ion Irradiation to Plasma-Ionic Liquid Interface Relating to Metals Nanoparticle Synthesis* TAKASHI HARADA, KAZUHIKO BABA, TOSHIRO KANEKO, RIKIZO HATAKEYAMA, *Department of Electronic Engineering, Tohoku University* We investigate basic physics of gas-liquid interfacial discharge plasmas under low gas pressures and effects of ion irradiation to ionic liquids as an electrode on the gold (Au) and platinum (Pt) nanoparticle synthesis by a plasma-reduction method. We successfully measure the Paschen curves using the ionic liquid as a cathode and an anode. We also measure electrostatic potentials in the ionic liquid and the gas phase plasma, and investigate a change of the potential formation which determines the ion irradiation energy E_i . The Au or Pt nanoparticles can be synthesized using the ionic liquids as a cathode, i.e., ion irradiation on the ionic liquids. It is found that the larger E_i enhances the amount of the synthesized Au nanoparticles. In addition, the nanoparticles can be synthesized in a shorter time compared with the case using the ionic liquid as the anode. The Pt nanoparticles are synthesized only by the ion irradiation. Based on these results, it is suggested that the ion irradiation to the ionic liquid is essential to synthesize the metal nanoparticles.

*This work was supported by a Grant-in-Aid for Scientific Research from the Ministry of Education, Cultures, Sports, Science and Technology, Japan.

8:30

WF1 3 DC Corona Discharges in Liquids for Thin Film Deposition BAKHTIER FAROUK, DION ANTAO, ALEXANDER FRIDMAN, *Drexel University* Non-thermal plasma discharges have been extensively studied in gaseous media for various applications in sterilization and materials processing. The study of electrical breakdown in both conducting and dielectric liquids has gained interest due to various applications. Most studies on plasma discharges in liquids were done for applications in switching circuits, capacitors and film deposition. The discharges are unsuitable for many applications due to their thermal nature. Non-thermal discharges in liquids are relatively unexplored. In this study we investigate dc plasma discharges in liquids for a negative pin-to-plate electrode configuration. The discharge is characterized by voltage-current characteristics and visualization. The corona discharge is observed to deposit films on the anode surface when operated in tetraethyl orthosilicate (TEOS). The deposition of films and particles on the anode surface by the proposed method has introduced the possibility of using corona discharges as a novel method of materials deposition or surface modification directly in liquid phase. The proposed PECVD technique is encouraging because it is both simple and effective in depositing films without damaging the substrate material.

8:45

WF1 4 Characterization of DBD Plasma Jet JOHN FOSTER, *University of Michigan* DBD plasma jet operation underwater was characterized. In this case, the entire discharge operated as a jet submerged underwater. The jet was operated on dry air, nitrogen, argon, and steam. Current-voltage profiles for each gas was obtained. Plasma jet gas temperature dependence on gas type and dissipated discharge power was also characterized. Self-organization of the plasma jet at high argon flow rates was observed. The effect such self organization on observed emission spectra, gas temperature, and water chemistry was investigated using thermocouple, pH, and peroxide measurements. The dependence of gas species type on water chemistry was assessed using an oxidation-reduction dye.

9:00

WF1 5 Effect of polarity and electric field uniformity on streamer propagation inside bubbles immersed in liquids* NATALIA BABAEVA, MARK KUSHNER, *University of Michigan* Streamers propagating in bubbles immersed in liquids are of interest for the generation of radicals. Streamers often propagate along the surface of a bubble immersed in a liquid instead of propagating along the axis of the bubble. In this talk, we discuss results from a 2-d computational investigation of the propagation of streamers inside bubbles immersed in liquids. We show that dielectric constant and conductivity of the liquid, streamer polarity, degree of electric field non-uniformity and bubble size determine the axial or surface mode of streamer propagation. A bubble of humid air at atmospheric pressure is placed at the tip of corona discharge or near the opposite plane electrode. The bubble is immersed in a liquid of conductivity, σ , and permittivity, ϵ/ϵ_0 with radii up to 0.9 mm. For weakly-conducting liquids, the steamer propagates along the axis for low ϵ/ϵ_0 and along the surface for large ϵ/ϵ_0 . The transition occurs at $4 < \epsilon/\epsilon_0 < 8$ for positive streamers and at $2 < \epsilon/\epsilon_0 < 4$ for negative, depending on the size

of the bubble and voltage. For large values of σ and ϵ/ϵ_0 , the streamer propagates along the surface for both positive and negative polarities. Streamers in bubbles in uniform fields develop from the equator of the bubble where the electric field is enhanced by bubble polarization.

*Work supported by the Department of Energy.

9:15

WF1 6 Plasma parameter variations during liquid droplet injection into low pressure plasmas DAISUKE OGAWA, LAWRENCE OVERZET, MATTHEW GOECKNER, *The University of Texas at Dallas* The direct injection of liquid droplets into low pressure plasmas results in a complex interaction between the evaporating gas, liquid droplets and plasma species. While

similar to dusty plasmas, the fact that the droplets are liquid allows their (potentially fast) evaporation in time. This difference can cause wide variations in the reactor state as a function of time after the injection. In this presentation, we show some of those variations and investigate how the liquid evaporation and gas chemistry change affects the plasma parameters. In order to better understand the effects of fast injections at low pressures, we injected argon (gas), nitrogen (gas), hexane (gas), and hexane liquid droplets into the same argon plasma. We will show in-situ measurements of the plasma parameters, (electron density, electron temperature), RF power and optical emission intensity. Specifically, we see that the injection of droplets can very quickly decrease the electron density in the glow even though charging of the droplets could not possibly be the reason and the RF power to the glow is not decreasing commensurately. The injection of gases, even hexane gas, does not result in such a dramatic reduction.

SESSION WF2: ELECTRON MOLECULE COLLISIONS

Friday Morning, 23 October 2009; Ballroom 2, Saratoga Hilton at 8:00; Don Madison, Missouri University of Science and Technology, presiding

Invited Papers

8:00

WF2 1 Spin-Dependent Effects in Electron-Molecule Scattering.*

TIMOTHY GAY, *University of Nebraska*

This talk will review the study of electron-molecule collisions that use electron polarization as a probe of the collision dynamics. Compared with atoms, early experiments with molecular targets seemed to indicate a "quenching" of spin-dependent effects. Measurements by the Rice [1] and Muenster [2] groups showed that exchange cross sections for electron-molecule scattering were much smaller than those for atoms. These discrepancies were never adequately explained. More recently, measurements by our group and at Muenster have given similar results when collision-induced fluorescence is observed. We will discuss these latter fluorescence measurements with H_2 and N_2 targets in detail, and show how rotational resolution of the electron-impact excited states can resolve, at least partially, the "quenching" puzzle. [1] G.H. Rutherford et alii, *Rev. Sci. Instrum.* **61**, 1460 (1990). [2] T. Hegemann *et al*, *J.Phys.B* **26**, 4607 (1993).

*Work supported by NSF Grant PHY-0653379.

8:30

WF2 2 Electron-driven excitation and dissociation of molecules.*

ANN OREL, *University of California, Davis*

Due to the large difference in mass between the electron and the nuclei, when an electron collides with a molecule or molecular ion, there is inefficient transfer of energy from the electron into the motion of the nuclei, leading to little vibrational excitation or dissociation. However, in certain special cases, the electron can temporarily attach to the molecule and change the forces felt between its atoms for a period of time comparable to a vibrational period. This can lead to resonant vibrational excitation and dissociative attachment, for neutral targets, or dissociative recombination in the case of ions. Studies of dissociative recombination and attachment in several polyatomic systems have shown that simple one-dimensional models can fail to capture the correct dissociation dynamics. In our treatment of these processes we first carry out *ab initio* electron scattering calculations at fixed internuclear geometries to determine the resonant energy surfaces and the corresponding surface of autoionization widths using the Complex Kohn variational method. These resonance positions and widths are then used as input to a dynamics study to determine the cross-section and product distributions for the dissociation or excitation process. We will present results on a number of systems, including HCCH, HCN/HNC and HCCCN as examples of dissociative attachment and N_2H^+ and H_2O^+ for dissociative recombination.

*Work supported by the NSF, Grant No.PHY-05-55401 and the U. S. DOE Office of Basic Energy Science, Division of Chemical Science. Work done in collaboration with S. Chourou, V. Ngassam, UC Davis and A. Larson Stockholm University, Sweden

Contributed Papers

9:00

WF2 3 Electron attachment to halomethanes at high temperatures T.M. MILLER, J.F. FRIEDMAN, L.C. SCHAFFER, A.A. VIGGIANO, *Air Force Research Laboratory* We have modified our high-temperature flowing-afterglow apparatus to include a movable Langmuir probe, a 4-needle reactant gas inlet, and a microwave discharge plasma source for the purpose of measuring electron attachment rate constants at high temperatures. We have focused initially on molecules which have very small attachment rate constants, k_a , at room temperature to see if their behavior at high temperatures can be described in Arrhenius fashion. We have reported k_a for CH_3Cl , but only above 600 K, because the value at 600 K was quite small: $5.8 \times 10^{-12} \text{ cm}^3 \text{ s}^{-1}$. The Arrhenius plot for these data imply $k_a = 10^{-17} \text{ cm}^3 \text{ s}^{-1}$ at 300 K, a value that is so small as to be immeasurable with any current apparatus. We now have k_a for other halomethanes, CF_3Cl , CF_2Cl_2 , and CH_2Cl_2 . The halomethane data cover seven orders-of-magnitude in k_a . Electron attachment to CF_3Cl is endothermic by 143 meV at 300 K, but our measurements indicate that there is a barrier of about 400 meV, probably related to the energy at which the anion surface crosses that of the neutral. The reactions for CH_3Cl , CF_2Cl_2 , and CH_2Cl_2 are exothermic, but our data again indicate large barriers to attachment which accounts for the extremely slow attachment at 300 K. From these data and literature measurements at 300 K, one can make educated guesses as to the behavior of k_a for other halomethanes.

9:15

WF2 4 Dissociative Electron Attachment to Polyatomic Systems* S.T. CHOUROU, A.E. OREL, *UC Davis* We have performed a multi-dimensional computational treatment of the dissociative electron attachment (DEA) dynamics of 3 polyatomic systems; HCCH , HCN/HNC and HCCCN to investigate predicted inherent polyatomic effects. We have considered the following reaction channels: $\text{C}_2\text{H}_2 (X^1\Sigma_g^+, \nu) + e^-(E) \rightarrow (\text{C}_2\text{H}_2)^{-*} ({}^2\Pi_g) \rightarrow \text{C}_2\text{H}^-(1^1\Sigma^+, \nu') + \text{H}(2^2S)$, $\text{HCN/HNC} (X^1\Sigma^+, \nu) + e^-(E) \rightarrow (\text{HCN/HNC})^{-*} ({}^2\Pi_g) \rightarrow \text{CN}^-(1^1\Sigma, \nu') + \text{H}(2^2S)$ and $\text{HCCCN} (X^1\Sigma^+, \nu) + e^-(E) \rightarrow \text{HCCCN}^{-*} \rightarrow \{\text{CCCN}-(2\Sigma^+, \nu'I-)+\text{H}(2S):(I); \text{CN}^-(1\Sigma^+, \nu'II-)+\text{HCC}(2\Sigma^+, \nu'III):(II); \text{HCC}^-(1\Sigma^+, \nu'III-)+\text{CN}(2\Sigma^+, \nu'III):(III); \text{CC}^-(2\Sigma^+, \nu'IV-)+\text{HCN}(1\Sigma^+, \nu'IV):(IV)\}$. We carried out electron scattering calculations using the Complex Kohn Variational Method with respect to a suitable internal coordinate system to obtain the complex resonant energy surfaces. We use this as input to a dynamics calculation using the Multiconfiguration Time-Dependent Hartree approach. We then compare our DEA cross sections and branching ratios to available experimental results.

*We acknowledge support from the National Science Foundation under Grant No. PHY-05-55401 and the U.S. DOE Office of Basic Energy Science, Division of Chemical Science.

SESSION XF1: MICROPLASMAS

Friday Morning, 23 October 2009; Ballroom 1, Saratoga Hilton at 10:00; Paul Maguire, University of Ulster, presiding

Invited Papers

10:00

XF1 1 Large Arrays of Microplasmas: Science, Applications, and the Road Ahead.J. GARY EDEN, *University of Illinois at Urbana-Champaign*

The science and technology of microcavity plasma devices has advanced rapidly over the past 5 years. Large arrays, comprising $> 10^5$ devices, have been realized and electron number densities as large as $> 10^{17} \text{ cm}^{-3}$ have been generated reproducibly on a pulsed basis. This presentation will review briefly the characteristics of microplasmas generated within cavities as small as $10 \mu\text{m}$. A view of future scientific opportunities will be offered and the recent discovery of a hybrid plasma/semiconductor device, based upon coupling of electron-hole and gas phase plasmas, will be reported.

Contributed Papers

10:30

XF1 2 Comparison of Silicon- and Polymer-based Microstructured Atmospheric Pressure Plasma Arrays HENRIK BOETTNER, ARTHUR GREB, VOLKER SCHULZ-VON DER GATHEN, JÖRG WINTER, *Ruhr-Universität Bochum* We report on phase, space and spectrally resolved optical emission spectroscopic combined with electrical measurements on microstructured atmospheric pressure plasma arrays. These arrays have confining structures in the range of several $10 \mu\text{m}$ and consist of typically 50×50 single discharges. Two different types of arrays are investigated. One is made up of a Ni-grid and inverse pyramidal structures etched in a Si-wafer as electrodes, separated by

an insulator and each coated with Si-Ni. The second type consists of small capillaries etched in a polymer arranged as a grid. The polymer is coated with ITO electrodes. Both types are typically operated in rare gas at atmospheric pressure and frequencies in the range of several kHz. The devices are compared in their individual and collective discharge behavior. We study the influence of excitation function shape and frequency on the development of pulse bursts. This determines the on-time and hence the emission efficiency of the devices. Furthermore, excitation waves running across the arrays are observed, indicating cross-talk between individual pixels. First measurements on basic energy transport systems and excitation dynamics leading to this phenomenon have been performed. This work is funded by DFG project SCHU-2353/1.

10:45

XF1 3 Electrical characterization of Direct Current atmospheric pressure micro discharges using Radio frequency signal in Argon MONALI MANDRA, LAWRENCE OVERZET, MATTHEW GOECKNER, *The University of Texas at Dallas* THIERRY DUFOUR, REMI DUSSART, PHILIPPE LEFAUCHEUX, *GREMI Polytech d'Orleans* Parallel Micro Hollow Cathode discharges (MHCD) are fabricated in a sandwich structure as Nickel-Alumina-Nickel. 500 μm thick, 3.5 inch alumina wafers are used as the dielectric between the 8 μm thick Nickel films. A single micro cavity of 180 μm diameter is laser drilled. An L-C tank circuit along with a matching network is used to super impose a small RF signal on the DC ignited micro discharge as a diagnostic tool. A simple equivalent circuit is used for analyzing the various key plasma parameters such as electron density, cathode sheath thickness, cathode sheath area and ion current density in the sheath by measuring the RF-impedance and capacitance of the micro-plasma. Reasonable results were obtained for argon DC micro-plasmas over a wide pressure range from 300 Torr to 1000 Torr and varying DC current. The sheath widths are found to vary slowly with pressure and are constant with DC current, while the electron density and sheath area both increase with current. These along with the IV characteristic of single hole MHCD are all consistent with what is expected for normal glow discharge regime. The technique and analysis results for argon micro-plasmas will be presented.

11:00

XF1 4 Modeling cathode boundary layer discharges E. MUNOZ-SERRANO, *Univ Cordoba* J.P. BOEUF, L.C. PITCHFORD, *CNRS and Univ Toulouse* A Cathode Boundary Layer Discharge or CBL (Schoenbach, et al *Plasma Sources Sci. Technol.* 13, 177, 2004) is an electrode/dielectric/electrode sandwich with a central hole pierced through the dielectric and one of the electrodes (the anode). Thus, the cathode surface area available to the discharge is limited by the annular dielectric, and the discharge operates in an abnormal glow mode with a positive V-I characteristic at higher current. Using a two-dimensional fluid model, we have studied the electrical properties of CBLs in argon at 100 and 400 torr pressure. The spatial profiles of charged particle and metastable densities, potential, and gas temperature, as well as calculated V-I characteristics will be shown for a range of conditions for a 800 micron hole diameter. One interesting result (anticipated in the work of Belostotskiy, et al, *Plasma Sources Sci. Technol.* 17, 045018, 2008) is that there is a sharp increase in the slope of the V-I characteristic when gas heating is taken into account. This current limiting effect is not observed when the discharge is able to expand on the outer surface of the cathode as in the case of the MicroHollow Cathode Discharge (MHCD) configuration, for example.

11:15

XF1 5 Coupled Mode Theory: A Path to Stable Microplasma Arrays* JEFFREY HOPWOOD, ZHIBO ZHANG, *Tufts University* Atmospheric plasmas are challenging to generate across large dimensions due to a plethora of instabilities. Recently, however, microplasmas have been generated with electron densities approaching that of a plasma torch, but with gas temperatures near room temperature. The possibility of treating large areas of low-temperature material with dense, atmospheric pressure plasma is attractive, but requires that microplasma concepts be dimensionally scaled. In this work we demonstrate that strong coupling among arrays of microwave resonators allows for the production

of 1-dimensional arrays of microplasmas. Each microplasma is sustained at the tip of a quarter-wave microstrip resonator which is driven at 400 MHz. This individual resonator stabilizes the 200 micron plasma against the glow-to-arc transition. Linear arrays of identical quarter-wave resonators naturally redistribute energy among each other according to coupled mode theory. This redistribution of energy allows us to sustain multiple microplasmas by simply supplying power to just one resonator in an array. In the paper, we show that coupled mode theory, 3-D electromagnetic simulations, and experimental optical emission from microplasma arrays of 5 and 16 resonators are in close agreement.

*This work was funded by the Wittich Family Fund for Sustainable Energy.

11:30

XF1 6 Properties of Dielectric-Barrier-Free Atmospheric Pressure Micro Plasma Driven by Sub-Micro Second DC Pulse Voltage HAE JUNE LEE, CHANG SEUNG HA, HO-JUN LEE, DONG-HYUN KIM, *Pusan National University* PLASMA APPLICATION GROUP TEAM, An atmospheric pressure micro-plasma driven by a DC pulse has been developed. This device consists of He flowing two dielectric-free metal electrodes with a voltage pulse shorter than 500 ns, thus it maintains a glow discharge. Spatio-temporal measurements by the optical emission spectroscopy show that the change of partial pressure ratio between He and N_2 is one of the most important factors affecting the discharge properties. The enhancement of the oxygen emissions for higher He flow rate mainly comes during afterglow, which suggests that the dissociative excitation of O_2 by He metastable states is critical process for effective generation of oxygen radicals. As an alternative of atmospheric pressure micro plasma jet based on the dielectric barrier discharge or rf-driven micro plasma, dc pulse driven dielectric barrier-free configuration discharge can be used as an efficient and cost effective source for bio-medical and material processing applications.

11:45

XF1 7 Atmospheric pressure direct current micro glow discharge simulation: Effects of the external circuit TANVIR FAROUK, *Princeton University* BAKHTIER FAROUK, *Drexel University* The effect of the external circuit on discharge conditions are not explicitly considered in most modeling studies of thermal and non-thermal plasma discharges. In this study, we investigate the effects of including the external circuit on simulation results of atmospheric pressure micro discharges. Two-dimensional simulations of DC atmospheric pressure micro glow discharges were conducted using a hybrid model. The discharge model is coupled to an external circuit model enabling to study the effect of the external circuit parameter. Simulation results were first obtained by excluding the external circuit. When included, the external circuit consisted of a ballast resistance and a parasitic capacitance connected in series and parallel in respect to the discharge. Simulations were conducted over a broad discharge current range (varying ballast resistance) and also for varying parasitic capacitance. For large ballast resistance the discharge was found to operate in the Townsend regime as a dark discharge. At smaller ballast resistance the discharge showed 'normal' glow like characteristics. The simulations further indicated that for higher values of the parasitic capacitance the discharge even with a DC power supply was self oscillatory; indicating some unstable regime. The predicted results were found to be in agreement with experimental observations.

**SESSION XF2: CAPACITIVELY-COUPLED
PLASMAS II**

Friday Morning, 23 October 2009

Ballroom 2, Saratoga Hilton at 10:00

Pascal Chabert, CNRS - Ecole Polytechnique, presiding

10:00

XF2 1 High Frequency Capacitively Coupled Plasmas: Implicit Electron Momentum Transport with a Full-wave Maxwell Solver* YANG YANG, *Iowa State University* MARK KUSHNER, *University of Michigan* Excitation frequencies for capacitively coupled plasmas (CCPs) are increasing to hundreds of MHz. At these high frequencies electrons may not be in equilibrium with the local electric field. Modeling electron transport in high frequency CCP tools requires solving the electron momentum equation to address inertia; and the full set of Maxwell's equations to address wave effects. In this talk, we discuss results from a 2-dimensional modeling study of the plasma properties in 300 mm and 450 mm dual frequency CCP (DF-CCPs) tools. Algorithms for electron transport are improved by integrating the electron momentum equation into the full-wave Maxwell equation solver. To capture the high frequency heating, excitation rates are provided by spatially dependent electron energy distributions generated by a Monte Carlo simulation. Results will be discussed for plasma properties in DF-CCPs for low frequencies of ≤ 10 MHz and high frequencies up to 200 MHz, and gas pressure of < 10 s mTorr in argon. Comparisons of plasma properties will be made to those obtained using drift-diffusion formulations.

*Work supported by Tokyo Electron Ltd., Applied Materials Inc. and Semiconductor Research Corp.

10:15

XF2 2 Space- and Time-dependent electron velocity distribution in VHF-CCP in CF_4/Ar TAKASHI YAGISAWA, *Keio University* TOSHIAKI MAKABE, The electron velocity distribution (EVD) is fundamentally important for all aspects in plasma electronics. EVD given as a solution of the Boltzmann equation provides the swarm parameter as functions of external E/N and B/N utilized for a plasma simulation. Two-term expansion was traditionally employed for solving the Boltzmann equation. This method, however, cannot give EVD in a large E/N appearing in the ion sheath region in front of a wall surface. Particle simulation (PIC/MC) was also used to estimate EVD, but heavy computational load prohibits the sample of a large number of particles in order to eliminate the statistical fluctuation. A solution of the Boltzmann equation in phase space (velocity, position-space, and time) intrinsically involves numerical diffusion resulting from the differentiation of the advection terms. In this study, we develop the numerical procedure for predicting space- and time-dependent EVD. That is, the Boltzmann equation is solved in velocity space by using our direct numerical procedure (DNP) under the presence of 2D-t electric field distribution in VHF-CCP, calculated by the RCT model. Nonlinear behavior of EVD in the bulk plasma during one cycle of VHF (100 MHz) is discussed depending on the collisional relaxation time for energy and momentum of electrons. Also, we will investigate the temporal change of EVD in the sheath region under a large E/N.

10:30

XF2 3 A scalable, VHF/UHF, capacitively coupled plasma source for large-area applications at high frequencies* BERT ELLINGBOE, *Dublin City University* DAVID O'FARRELL, CEZAR GAMAN, *Dublin City University* FIACHRA GREEN, NEAL O'HARA, TOMASZ MICHNA, *Phive Plasma Technologies* Process results are driving both plasma etch and CVD to higher frequencies; This is incompatible with increases in wafer size to 450mm and beyond. No where is the evidence more clear than in PECVD of amorphous and microcrystalline Silicon for the photo-active layer in thin-film photovoltaic devices. Growth rates for these layers, while maintaining the necessary mechanical and electrical properties, can increase with increasing rf frequency, and in some cases yield superior film properties at the higher deposition rates (P.G. Hugger, et al, MRS 2008). However, in this industry substrate sizes are very large, exceeding 1m characteristic lengths, which puts substantial limits for a conventional plasma diode topology on using frequency as a control vector to increase deposition rate, thus increasing factory through-put and decreasing cost. In this talk we will introduce a novel plasma source topology that enables increased rf frequencies on arbitrary size plasma source without causing wavelength effects. The concept is to segment the powered electrode into discrete tiles; For example as a checkerboard. Adjacent tiles can be powered out of phase with each other. In this way the displacement current coupled by one electrode is balance by and equal and opposite current of the adjacent electrode. Thus zero net current is coupled into the plasma, zero net current is coupled through the sheath above the substrate, and no wavelength effects occur even for substrates large in comparison to the rf wavelength. Highlights of recent results in the operation and application of the plasma source to PECVD of silicon will be presented.

*Funded by Enterprise Ireland

10:45

XF2 4 Selective Influence of Magnetic Field Direction on Plasma Uniformity WENLI COLLISON, VLADIMIR KUDRIAVTSEV, MICHAEL BARNES, *Intevac* MARK KUSHNER, *University of Michigan* In this study we have investigated computationally hybrid ICP/CCP plasma reactor, with static magnets located under RF electrode. Plasma system is designed for discrete track recording magnetic disk etch applications. Effect of the orientation of magnetic field direction (radial or axial) is studied for Ar plasma using HPEM model [1]. Results show that for both radial and axial magnetic field orientations there is optimal magnet strength which provides maximum uniformity. Axial magnetic field orientation allows simultaneous reversal of both ion flux and plasma density radial distributions (when compared to similar plasma conditions without magnetic field present). Radial magnetic field orientation allows selective reversal of radial distribution of the ion flux, but without affecting radial distribution of plasma density Ne. This can be utilized as an independent knob for selective plasma control. Above described effects are explained by the changes in radial distributions of axial E field and of ion velocity. Finding optimal magnetic strength for both considered field orientations allowed reducing radial uniformity of the ion flux and plasma density across the disk from 7 to 3% (axial) and from 10 to 2.5% (radial). The effects of inclined magnetic field on the ion flux and plasma density have also been investigated. [1] Y. Yang and M. J. Kushner, *J. Vac. Sci. Technol. A* **25**, 1420 (2007).

11:00

XF2 5 Experimental and theoretical studies of the electrode impedance effect in capacitive discharges DENNIS ZIEGLER, THOMAS MUSSENBRÖCK, RALF PETER BRINKMANN, *Ruhr University Bochum* YOHEI YAMAZAWA, *Tokyo Electron AT LTD* It is widely acknowledged that one can observe a strong harmonics content in the current of an asymmetric capacitive discharge, even in case of a strongly sinusoidal driving voltage. This particular phenomenon is directly connected to the heating of electrons.¹ It has been shown by means of careful measurements that the increase of certain harmonics indicates an increase of the electron density.² In this paper we revisit these experiments. We also propose a model to study the possibility of controlling the excitation of current harmonics using an external circuit and its effect on the electron density (which is often referred to as the electrode impedance effect).

¹T. Mussenbrock et al., *Phys. Rev. Lett* **101**, 085004 (2008).

²Y. Yamazawa et al., *Jpn. J. Appl. Phys.* **46**, 7453 (2007).

11:15

XF2 6 Influence of collisions on spatial damping of electrostatic electron waves in a low-pressure plasma JENS OBERRATH, RALF PETER BRINKMANN, *Theoretical Electrical Engineering, Ruhr-Universität Bochum* Electrostatic electron waves in a plasma can be excited in several ways. One possibility is a resonance effect, if any rf frequency is locally equal to the electron plasma frequency. In this region the energy of the electric field increases and has to disperse into the plasma. Therefore, a transport mechanism is needed which is given by electrostatic waves. These waves can be damped in time and space domain. After a short time period waves with temporal damping do not exist in the plasma anymore. Thus, we are interested in waves with spatial damping to describe the resonance effect for any length of time. This damping depends on collisions between the electrons and the neutral background gas. To investigate the influence of collisions on the damping we formulate a kinetic model for the electron behavior in the high frequency range of weakly ionized low-pressure plasmas with elastic collisions. We assume an isotropic collision term with a constant collision frequency because of the huge mass difference between electrons and neutrals. This allows the derivation of a dispersion relation from the linearized Boltzmann-Poisson system for homogeneous longitudinal waves, which is able to describe the influence of collisions on the wave propagation of electrons. In addition we find the relation for a Vlasov plasma as a special case which shows the spatial Landau damping.

11:30

XF2 7 Intermediate frequency breakdown DEREK MONAHAN, MILES TURNER, *Dublin City University* The mechanisms underlying low-frequency/dc and high-frequency breakdown differ greatly due to the contrasting nature of the charged particle trajectories. At low-frequencies charged particle trajectories are open, terminating at the electrodes, and secondary electron production at the cathode plays a central role in the breakdown process. At high-frequencies, and typical discharge dimensions, charged particle oscillations are closed. In this limit trajectories have a diffusive nature and ionization via field heated bulk electrons plays a central role in breakdown. Between these two frequency extremes one may envisage a regime in which electron trajectories are open and ion trajectories are closed. While experiments confirm breakdown may be achieved in such a regime, a plausible breakdown mechanism does not appear to have been identified. In this paper we investigate breakdown in this regime using a kinetic simulation and propose a breakdown mechanism in which secondary electron production via fast neutral bombardment of the electrodes plays a significant role.

11:45

XF2 8 Atmospheric Pressure RF Plasma Electrical and Optical Characteristics ALI GULEC, *Suleyman Demirel University Turkey* LUTFI OKSUZ, NOAH HERSHKOWITZ, *University of Wisconsin Madison* An atmospheric pressure 13.56 MHz RF source is used for plasma polymerization, nanocomposite deposition and for sterilization purposes. The air discharge electrical and optical characteristics are measured using monochromator and electrical probes. The addition of helium flow to the RF discharge system allows production of stable glow plasma discharge. The electron temperature and plasma densities are estimated using the emission lines of HeI and double probes. Emission of the He+air atmospheric pressure plasma is observed from the OH radical, several lines of the N₂, N₂⁺ and atomic O, H and He lines. He flow rate and applied rf voltage affect on these emission spectra are investigated and the spectral lines are used for calculation of plasma parameters. Plasma electron temperature is calculated using HeI lines and compared with double probe data. The OI 777 and H_α 656 lines are also investigated by varying the applied voltage and He flow rate. The calculated electron temperature was approximately 0.2 eV and dependent on the He flow rate and applied power.

A

Aanesland, Ane **KTP 50, LW1 3**
 Abe, Yusuke **GT3 6**
 Adamek, Petr **KTP 49**
 Adamovich, Igor **KTP 101, URP 77**
 Adams, S.F. **URP 19, URP 66, URP 73**
 Adams, Steve **KTP 14**
 Agarwal, Pulkit **LW1 1**
 Ahn, Young Soo **URP 94**
 Akashi, Haruaki **URP 105**
 Al-Hagan, Ola **TR2 3, TR2 4, URP 16, URP 17**
 Alcouffe, G. **KTP 29**
 Alexander, J. **GT3 2, URP 18**
 Alexander, Jason **PW2 3**
 Algwari, Qais Th. **KTP 69**
 Almgren, Carl **JT2 4, KTP 32, RR1 2, URP 72**
 Alvarez, R. **KTP 65**
 Alves, L.L. **KTP 4, KTP 29, KTP 62, KTP 63, KTP 65**
 Amatucci, W.E. **KTP 18**
 Amirov, Ravil **KTP 23**
 Amorim, Jayr **URP 52**
 Anderson, L.W. **SR2 6**
 Andrianarijaona, V.M. **TR2 7**
 Anshu **URP 14**
 Antao, Dion **PW3 6, WF1 3**
 Aoyama, Naoki **KTP 83**
 Ariskin, Dmitry **TR3 6**
 Arnold, John **QW 2**
 Astapenko, Valerii **LW3 4**
 Atis, Skudra **HT1 6**
 Ateln, Frank **URP 106**
 Avtaeva, Svetlana **KTP 80, KTP 84**
 Awakowicz, Peter **HT2 7, KTP 25, KTP 87, LW3 2, SR1 4, URP 35, URP 100, URP 106**
 Azooz, Aasim A. **KTP 15**

B

Baalrud, Scott **DM 3, JT1 2**
 Baba, Kazuhiko **WF1 2**
 Babaeva, Natalia **LW3 6, WF1 5**
 Babou, Yacine **GT2 2**
 Baby, A. **URP 34**
 Bae, Se Hwan **URP 50**
 Baeva, Margarita **KTP 76**

Bains, Amandeep Singh **KTP 103**
 Baklanov, M.R. **TR1 4**
 Balla, Robert **URP 2**
 Bandyopadhyay, M. **KTP 104**
 Bang, Jin Young **KTP 38, URP 63**
 Bankovic, A. **RR2 3**
 Barankin, Michael **RR1 4**
 Baranov, Alexey **SR3 7**
 Barden, Erica **URP 68**
 Barnat, Edward **HT3 2, SR2 3**
 Barnes, Michael **HT2 4, KTP 33, XF2 4**
 Bartschat, Klaus **PW1 5, SR2 2, SR2 5**
 Bauville, Gerard **KTP 60, KTP 85, RR1 1**
 Becker, Markus M. **KTP 3, KTP 61**
 Begum, Asma **JT3 4**
 Bellm, S. **SR2 7**
 Belov, Maxim **SR3 7**
 Benova, Evgenia **KTP 77**
 Bentaleb, Sabrina **KTP 22**
 Berger, A.G. **JT3 2**
 Bergkvist, Magnus **QW 3**
 Bergner, Andre **KTP 86**
 Bibinov, Nikita **SR1 4, URP 35, URP 100**
 Bienholz, Stefan **KTP 25**
 Bisek, Nicholas **JT2 3**
 Blessington, J. **URP 66**
 Boerner, J.J. **KTP 17**
 Boettner, Henrik **XF1 2**
 Boeuf, J.P. **XF1 4**
 Boffard, John B. **PW1 6, SR2 6, URP 58**
 Bogaerts, Annemie **BM 3**
 Bogdanov, Eugene **KTP 64**
 Bogdanov, Yevgeny **KTP 14**
 Boilson, D. **URP 78**
 Boisse-Laporte, C. **KTP 62, KTP 63**
 Booth, Jean-Paul **FT1 3, HT3 3**
 Bourham, Mohamed **URP 97**
 Bowden, Mark **URP 74**
 Boyd, Iain **JT2 3**
 Bradley, James **LW1 6**
 Braginsky, O.V. **TR1 4**
 Braithwaite, N.S. **URP 11**
 Braithwaite, Nicholas **KTP 70, URP 74**
 Brannick, K. **URP 31**
 Brates, Nanu **LW3 6**

Bravenec, Ron **HT2 3**
 Bray, Igor **URP 8**
 Breden, Doug **GT2 4**
 Bredin, Jerome **FT1 3, HT3 3**
 Brinkmann, Ralf Peter **BM 4, KTP 27, KTP 30, KTP 34, KTP 36, URP 57, URP 106, XF2 5, XF2 6**
 Brown, Daniel **KTP 39, PW3 2**
 Brownridge, James **URP 26**
 Brunger, Michael **LW2 1, RR2 3**
 Bryant, Paul **LW1 6**
 Buckman, Stephen **CM 1, RR2 3, SR2 7**
 Buff, James **URP 61**

C

Cada, Martin **KTP 49**
 Calixto-Rodriguez, Manuela **KTP 13**
 Callen, J.D. **JT1 2**
 Cappelli, Mark **KTP 48, KTP 54, KTP 95, URP 93**
 Caradonna, P. **RR2 3, SR2 7**
 Case, Ed **3R 1**
 Cernak, Mirko **PW3 5**
 Cernogora, G. **KTP 29**
 Chabert, Pascal **FT1 3, HT1 3, KTP 50, KTP 51, KTP 52, KTP 72, LW1 3**
 Chan, Wai **SR1 3**
 Chang, Jane P. **TR1 1**
 Chen, Lee **FT1 5, HT2 3**
 Chen, Maolin **KTP 59**
 Chernysheva, Irina **KTP 89, LW3 3, LW3 4, TR3 3, URP 81**
 Chirtsov, Alexander **KTP 64**
 Chisholm, J. **URP 3**
 Chitre, Aditya **KTP 71**
 Cho, Jin Hoon **URP 84**
 Choe, Ik Jin **URP 89**
 Choe, Jae-Myung **KTP 11**
 Choi, Da-Hae **KTP 5**
 Choi, Joon-Young **FT3 1**
 Choi, Myeong **URP 47, URP 85**
 Choi, Myeong Yeol **URP 48, URP 84**
 Choi, Yongjun **URP 7**
 Chourou, S.T. **WF2 4**

Chowdhury, Uttam **PW2 2**
 Chu, Paul K. **GT1 5**
 Chung, Brian P. **JT3 3**
 Chung, Chin-Wook **GT3 1, HT1 5, KTP 38, KTP 40, KTP 41, KTP 42, URP 63, URP 65, URP 75, URP 76, URP 89**
 Chung, Kyung-Jae **KTP 5**
 Chung, Tae Hun **URP 50**
 Ciappini, M. **PW2 3, URP 18**
 Colgan, James **TR2 3, TR2 4**
 Collins, George **JT2 4, KTP 32, PW1 3, RR1 2, RR1 3, URP 47, URP 48, URP 72, URP 85**
 Collision, Wenli **KTP 33, XF2 4**
 Colyer, Christopher **URP 16, URP 17**
 Cothran, C.D. **KTP 18**
 Cotrino, J. **KTP 4**
 Crintea, D.L. **PW1 7**
 Crozier, P.S. **KTP 17**
 Csanak, George **URP 8**
 Cupoli, Edward M. **QW 5**
 Curley, Garrett **FT1 3**
 Curry, J.J. **LW3 5**
 Curvelo, Antonio **URP 52**
 Cvejanovic, Danica **SR2 1**
 Czarnetzki, Uwe **FT1 1, FT1 2, FT3 2, KTP 26, KTP 28, PW1 7, URP 70, URP 90**

D

Dalton, Timothy J. **QW 7**
 Daniels, Stephen **PW1 1, URP 24**
 Danielson, J.R. **RR2 4**
 deHarak, Bruno **SR2 3, TR2 1, URP 6**
 Deilmann, Michael **HT2 7, URP 35**
 Demidov, V.I. **URP 66**
 Demidov, Vladimir **KTP 8, KTP 14**
 Deminsky, Maxim **KTP 88, KTP 89, LW3 3, LW3 4, TR3 3, URP 81**
 Den, Shoji **GT3 4**
 Den Hartog, E.A. **URP 3**
 Denieffe, Kieran **URP 34**
 Denisova, Natalia **GT3 7, HT1 6**
 Denning, C. Mark **URP 38**

- Despiau-Pujo, Emilie
HT1 3
- Dias, F.M. **KTP 78**
- Dias, Francisco **KTP 16**
- Dias, Fransisco **KTP 77**
- Dibble, Theodore **FT3 5,**
URP 80
- Dinklage, Andreas **PW1 5**
- Ditmire, Todd **PW3 1**
- Do, Hyungrok **URP 93**
- Dodd, Robert **LW1 6**
- Dotd, Dirk **PW1 5**
- Dolinaj, Borislav **URP 69**
- Donko, Zoltan **FT1 2,**
KTP 26, KTP 28
- Dorf, Leonid **KTP 99**
- Drake, Dereth **KTP 66,**
URP 62
- Du, Beilei **URP 70**
- Duffey, Thomas **PW3 2**
- Dufour, Thierry **XF1 3**
- Dujko, S. **KTP 110**
- Dujko, Sasa **AM 4,**
URP 12
- Dussart, Remi **XF1 3**
- Dyatko, Nicolai **HT2 6**
- E**
- Eden, J.G. **JT3 2, JT3 3,**
QW 4, URP 98, XF1 1
- Egodapitiya, K. **PW2 3,**
URP 18
- Eisenbarth, Thomas
KTP 36
- Eismann, B. **JT1 4**
- El Saghir, A. **GT3 2**
- Eletskii, Alexander **KTP 89**
- Eletskii, Alexaner **LW3 4**
- Ellingboe, Albert R. **PW1 1**
- Ellingboe, Bert **KTP 31,**
XF2 3
- Englund, Karl **URP 27**
- Eriguchi, Koji **FT2 1,**
KTP 97, SR3 4
- Ernie, Douglas **GT2 3,**
GT2 5, GT2 6
- Estrada-Raygoza, I.C.
URP 46
- F**
- Fang, Ziwei **GT1 4,**
URP 61
- Farouk, Bakhtier **PW3 6,**
WF1 3, XF1 7
- Farouk, Tanvir **XF1 7**
- Felizardo, Edgar **KTP 16,**
KTP 77
- Feng, Xu **SR1 2**
- Fernandez, Sulmer **URP 41**
- Fernsler, R.F. **KTP 18**
- Ferreira, C.M. **KTP 78**
- Ferreira, Carlos **KTP 16**
- Fisch, Nathaniel J. **FT2 3,**
KTP 99
- Fontes, Christopher **LW2 3**
- Foster, John **WF1 4**
- Franklin, R.N. **URP 11**
- Frederickson, Kraig **HT3 2**
- Fridman, Alexander **PW3 6,**
WF1 3
- Friedman, J.F. **WF2 3**
- Fujita, Masao **KTP 82**
- Fukumasa, Osamu **KTP 83**
- Funk, Merritt **FT1 5,**
HT2 3
- Fursa, Dmitry **URP 8**
- Furst, J.E. **TR2 7**
- G**
- Gahan, David **URP 69**
- Galli, Federico **LW1 2**
- Gaman, Cezar **KTP 31,**
XF2 3
- Ganguly, Biswa **KTP 56,**
TR3 4
- Gans, Timo **FT1 4, HT2 2,**
HT3 5, TR3 1
- Garcia-Cosio, Gerardo
KTP 13
- Garcia-Perez, Manuel
PW3 7
- Garscadden, A. **URP 19**
- Gavrikov, Alexey **SR3 7**
- Gay, Timothy **TR2 7,**
WF2 1
- Gebhardt, Markus
URP 100, URP 106
- Gekelman, Walter **HT2 4**
- Genba, Yuki **KTP 81**
- General, Andrij **KTP 80**
- Gianchandani, Yogesh
JT3 1
- Gill, Tarsem Singh
KTP 103
- Girshick, Steven **LW1 1**
- Gita, Revalde **HT1 6**
- Gnybida, Mykhaylo **KTP 6**
- Godet, Ludovic **GT1 4,**
URP 61
- Godunov, A. **URP 15**
- Goeckner, Matthew **SR3 1,**
SR3 2, URP 36,
URP 46, WF1 6, XF1 3
- Gogna, G.S. **URP 78**
- Gong, W. **JT3 5**
- Gonzalez, Eleazar **RR1 4,**
SR1 3
- Gonzalvo, Y.A. **TR3 2**
- Gordiets, Boris **KTP 16**
- Goto, K. **URP 55**
- Goto, Masaaki **URP 44**
- Govinda Raju, Gorur **CM 2**
- Graham, Lucy M. **HT3 5**
- Graham, W.G. **HT2 2,**
TR3 2
- Graves, David **KTP 37,**
MW 1, SR1 5, URP 43
- Greb, Arthur **XF1 2**
- Green, Fiachra **XF2 3**
- Greenan, J. **HT2 2,**
KTP 68
- Gregorio, J. **KTP 62,**
KTP 63
- Grubert, Gordon K.
KTP 3, KTP 108
- Gu, J.P. **PW2 5**
- Guaitella, Olivier **URP 28**
- Gudmundson, Jesse
KTP 98
- Gudmundsson, J.T. **LW1 4,**
URP 87
- Guerra, V. **KTP 4**
- Gulec, Ali **XF2 8**
- Guo, Song **GT2 1, GT2 5**
- Gurgel, Leandro **URP 52**
- Guschl, Peter **RR1 4**
- H**
- Ha, Chang Seung **XF1 6**
- Ha, Su **PW3 7**
- Habib, Sara **SR1 3**
- Hagelaar, Gerjan **HT1 1**
- Hakel, Peter **HT3 4**
- Hamaguchi, Satoshi **FT3 2,**
WF1 1
- Han, Hyeong Sik **URP 89**
- Hanabusa, Yohei **SR1 6**
- Harada, Takashi **WF1 2**
- Hargreaves, Leigh **URP 17**
- Harris, Allison **PW2 1**
- Harrison, Stephen **KTP 39**
- Harvey, Matthew **TR2 6**
- Hasan, A. **PW2 3, URP 18**
- Hatakeyama, Rikizo **QW 6,**
SR1 6, WF1 2
- Hayashi, Nobuya **URP 44,**
URP 45
- Hayashi, Yuichiro **URP 60**
- Heering, Wolfgang **LW3 1**
- Hegemann, Dirk **SR3 6**
- Hegna, C.C. **JT1 2**
- Hemke, Torben **KTP 27**
- Heneral, Andrij **KTP 84**
- Henkel, Nils **URP 20**
- Henriques, J. **KTP 78**
- Herbon, John T. **TR3 3,**
URP 81
- Heres, Scott **JT2 4,**
KTP 32, URP 72
- Hershkowitz, Noah **JT1 3,**
KTP 98, KTP 100,
URP 91, XF2 8
- Hicks, Robert **RR1 4,**
SR1 3
- Higashijima, Yasuhiro
GT3 4
- Hopkins, M.M. **KTP 17**
- Hopkins, Mike **URP 69**
- Hopwood, Jeffrey **FT3 3,**
XF1 5
- Hori, Masaru **GT3 4,**
GT3 6, SR3 3, SR3 5
- Horioka, Kazuhiko **KTP 75**
- Hosokai, Tomonao **KTP 75**
- Hotta, Eiki **KTP 75**
- Hu, J. **JT3 5**
- Huang, George **KTP 56**
- Hubicka, Zdenek **KTP 49**
- Hughes, T.P. **KTP 17**
- Huo, Xintao **JT2 6**
- Hussey, Martyn **TR2 2**
- Hwang, Kwang Tae
URP 89
- Hwang, Yong-Seok **KTP 5**
- Hyakuta, Yasuhisa **FT3 6**
- I**
- Iida, Masayasu **URP 96**
- Ikawa, Satoshi **WF1 1**
- Im, Seong-kyun **URP 93**
- Inagaki, Shinpei **URP 30**
- Inoue, Mari **GT3 4**
- Ionikh, Yury **URP 28**
- Ionin, Andrei **HT3 6**
- Ionin, Andrey **HT2 8**
- Iordanova, S. **PW1 7**
- Iqbal, Muhammad M.
KTP 67
- Ishijima, T. **HT2 1,**
URP 55
- Ito, Azumi **SR3 3**
- Ito, Masafumi **GT3 4**
- Ito, Tsuyohito **FT3 2,**
KTP 48
- Ito, Yosuke **FT3 1**
- Itoh, Haruo **URP 22,**
URP 39
- Iwashita, Shinya **URP 33**

- J**
 Jang, Bo-Yun URP 94
 Jang, Sung-Ho URP 65, URP 76
 Jarrige, Julien JT3 4, URP 43
 Jeanney, Pascal KTP 60, URP 51
 Jia, Shenli JT2 5, JT2 6, KTP 74, URP 88
 Jiang, Chunqi URP 51
 Jiang, Naibo KTP 101
 Jiang, Z. JT3 5
 Jiao, C.Q. URP 19
 Jinhua, Yang SR1 2
 Johnsen, Rainer PW2 7
 Johnson, Paul LW2 2
 Johnson, Peter KTP 70
 Jones, A. RR2 3, SR2 7
 Joo, Junghoon URP 94
 Jorand, Francois KTP 22
 Joseph, D.C. PW2 5
 Jovanovic, Milena Z. URP 42
 Jugroot, Manish KTP 9
 Jun, Wan SR1 2
 Jung, Jae-Chul KTP 43, KTP 91
 Jung, R.O. PW1 6, SR2 6, URP 58
 Jung, Young-Dae URP 5
- K**
 Kabala, Michael KTP 32
 Kaganovich, Igor BM 2, KTP 8, KTP 99
 Kaiser, Christian TR2 3, TR2 4
 Kakati, B. KTP 104
 Kakehashi, Hidenori KTP 82
 Kalra, Chiranjeev GT2 7
 Kanda, Takashi KTP 81
 Kaneko, Toshiro SR1 6, WF1 2
 Kang, Song-Yun SR3 5, TR1 6
 Kano, Hiroyuki GT3 4
 Kapustin, Kirill KTP 64
 Karakas, Erdinc JT3 4
 Karkari, S.K. URP 78
 Karkari, Shantanu KTP 12
 Kausik, S.S. KTP 104
 Kawamura, Emi KTP 37, KTP 47
 Kawashima, Sho GT3 6
 Keim, Matthias URP 20
 Kennedy, C. GT3 2
 Kerlo, Anna-Elodie GT2 2
 Kettlitz, Manfred KTP 90
 Keville, Bernard HT1 4, KTP 45
 Khakoo, M. PW2 3, URP 18
 Kharchenko, Nadiia KTP 2
 Khrabrov, Alex V. KTP 8
 Kilcoyne, A.L.D. TR2 7
 Kilcrease, David URP 8
 Kim, Aram URP 63
 Kim, Dong-Hyun XF1 6
 Kim, Eung Soo URP 98
 Kim, Gon-Ho KTP 11
 Kim, Gun-Ho URP 65, URP 76
 Kim, Sun Ja URP 50
 Kim, Taek Lim URP 98
 Kim, Wan Soo KTP 43
 Kim, Young Cheol URP 65
 Kim, Yu Sin URP 75
 Kimura, Takashi URP 96
 Kinoshita, K. URP 55
 Kirchner, Tom PW2 6, URP 20
 Kishi, Nozomu KTP 75
 Kitanishi, Shunsuke FT2 1
 Kitano, Katsuhisa WF1 1
 Kitazaki, Satoshi URP 44, URP 45
 Klick, Michael KTP 34
 Klimachev, Yurii HT2 8, HT3 6
 Kment, Stepan KTP 49
 Knake, Nikolas FT3 4
 Knizhnik, Andrey SR3 7
 Knoll, Aaron KTP 95
 Kobayashi, Kazunobu FT3 2
 Kochetov, Igor HT2 6, HT2 8, KTP 89, TR3 3, URP 81
 Koga, Kazunori URP 33
 Kohler, Brian KTP 106
 Koleva, I. PW1 7
 Kolobov, Vladimir BM 1
 Kong, Michael SR1 1
 Kono, Akihiro HT3 1
 Koo, Il Gyo PW1 3, RR1 3, URP 47, URP 48, URP 85
 Koo, John (Bon-Woong) URP 61
 Kortshagen, Uwe GT2 1, GT2 3, GT2 5, GT2 6, LW1 2, QW 1
 Kotkov, Andrei HT3 6
 Kovacic, Dusan PW3 5
 Koval, Veronika KTP 20
 Kovalev, A.S. TR1 4
 Kozlov, Andrei HT3 6
 Ku, Ju-Hwan KTP 41, KTP 42
 Kubincova, Jana PW3 5
 Kudriavtsev, Vladimir KTP 33, XF2 4
 Kudryavtsev, Anatoly KTP 14, KTP 64
 Kumar, Keshav URP 14
 Kumar, Neeraj URP 14
 Kushner, Mark AM 2, GT1 2, JT2 3, KTP 33, LW3 6, PW3 2, TR1 2, TR1 3, WF1 5, XF2 1, XF2 4
 Kwok, Dixon T.K. GT1 5
- L**
 Laber, A.C. URP 73
 Laborie, Marie-Pierre URP 27
 Lacoste, Deanna JT2 1
 Lacour, Bernard KTP 60, KTP 85, RR1 1
 Ladino, Luis URP 6
 LaForge, A. PW2 3, URP 18
 Lahr, David GT3 5
 Landers, A.L. TR2 7
 Lapke, Martin KTP 34, KTP 36, URP 57
 Laroussi, Mounir JT3 4, URP 43
 Laurin, P. URP 62
 Laux, Christophe JT2 1
 Lawler, J.E. URP 3
 Lazovic, Sasa URP 42
 Lazzaroni, Claudia KTP 72
 Lebedeva, Irina SR3 7
 Lee, H.C. JT3 2
 Lee, Hae June FT2 2, XF1 6
 Lee, Ho-Jun XF1 6
 Lee, Hyo-Chang HT1 5, KTP 40
 Lee, Min-Hyong HT1 5, KTP 40
 Lee, Woong Moo URP 84
 Lee, Yeong-Kwang KTP 42
 Lee, Young-Kwang KTP 41, URP 75
 Lefauchaux, Philippe XF1 3
 Lekobou, William URP 27
 Lempert, Walter KTP 101, URP 77
 Leprince, P. KTP 63
 Leray, Gary KTP 52
 Leroy, O. KTP 63
 Li, Chao DM 2
 Li, Rui URP 88
 Li, Xingwen URP 88
 Liard, Laurent KTP 50, KTP 51
 Lichtenberg, Allan KTP 47, KTP 52
 Lieberman, Michael GT1 1, KTP 37, KTP 47, KTP 52, KTP 109, URP 87
 Lin, Chun C. PW1 6, SR2 6, URP 58
 Linnane, Shane KTP 31
 Lino da Silva, M KTP 16
 Lisovski, Valeriy KTP 2, KTP 20
 Liu, Feng KTP 56
 Liu, J. JT3 5
 Liu, Ke JT2 5
 Loffhagen, Detlef CM 4, KTP 3, KTP 6, KTP 61, KTP 76, KTP 90, KTP 108
 Lohmann, Birgit SR2 7, URP 16, URP 17
 Lopaev, D.V. TR1 4
 Lopez, C. KTP 4
 Lu, XinPei JT3 5
 Luedde, Hans Juergen PW2 6, URP 20
 Luggenhoelscher, Dirk FT1 2, FT3 2, PW1 7, URP 70
- M**
 Macek, Joseph PW2 4
 Macgearailt, Niall URP 24
 MacGillivray, William TR2 2
 Machacek, J.R. TR2 7
 Macheret, Sergey KTP 96
 Madison, Don PW2 2, TR2 3, TR2 4, TR2 5, URP 16, URP 17
 Magne, Lionel KTP 60, URP 51
 Maguire, P.D. HT2 2, KTP 68, URP 34
 Mahadevan, Shankar FT2 4
 Mahalingam, Sudhakar URP 7

- Mahony, C.M.O. HT2 2,
KTP 68, URP 34
- Makabe, Toshiaki AM 3,
PW1 2, URP 30,
URP 59, URP 60, XF2 2
- Makochekanwa, C. RR2 3,
SR2 7
- Maletic, Dejan URP 42
- Malovic, Gordana KTP 7,
KTP 110, URP 42
- Malykhin, E.M. TR1 4
- Mamunuru, Meenakshi
GT2 3, GT2 6
- Mandra, Monali XF1 3
- Mankelevich, Yu.A. TR1 4
- Mao, Genwang KTP 59,
KTP 94
- Maric, Dragana FT1 3,
KTP 7, KTP 68,
KTP 110
- Marin-Flores, Oscar PW3 7
- Marinov, Daniil URP 28
- Marques, L. KTP 29,
KTP 65
- Martin, Elijah URP 97
- Martin, Nicholas SR2 3,
URP 6
- Martin, Virginie KTP 85
- Martinez, Horacio KTP 13
- Martus, Kevin URP 68
- Mazouffre, Stephane
KTP 50
- McCurdy, William E.
HT2 5
- McEachran, Robert SR2 4
- McLaughlin, K.W. TR2 7
- Meger, R.A. KTP 18
- Meisser, Michael LW3 1
- Mejia, Efrain URP 98
- Mentel, Juergen KTP 86,
KTP 87, LW3 2
- Mertmann, Philipp
URP 100, URP 106
- Michael, Darryl KTP 88,
KTP 89, LW3 3
- Michna, Tomasz XF2 3
- Milenkovic, Pavle URP 42
- Miles, J.A. URP 73
- Miles, Richard GT2 7,
KTP 96, PW3 3
- Miletic, Maja P. URP 42
- Miller, T.M. WF2 3
- Miller, Timothy GT1 4,
URP 61
- Mills, Jack URP 2
- Milosavljevic, Vladimir
PW1 1, URP 24
- Min, Hur URP 83
- Min Suk, Cha URP 83
- Mintusov, Evgeny URP 54
- Miura, Naoto FT3 3
- Miyata, Hiroki SR3 4
- Miyata, Hiroshi URP 33
- Miyawaki, Yudai SR3 3
- Mizuno, Bunji GT1 3
- Mohr, Sebastian URP 70
- Monahan, Derek LW1 5,
XF2 7
- Moon, Yeon Joon JT3 3
- Moore, Cameron JT2 4,
KTP 32, RR1 3,
URP 47, URP 72,
URP 85
- Moore, Jon KTP 70
- Moreau, Nicolas KTP 22
- Morishita, Satoshi URP 60
- Moroz, Paul URP 101
- Mueller, D. SR2 7
- Mueller, Sarah FT3 2
- Mujawar, Mubarak KTP 12
- Mullowney, Paul URP 108
- Mungal, Mark URP 93
- Munoz-Serrano, E. XF1 4
- Munro, James KTP 39
- Murphy, Veronica URP 68
- Murray, Andrew TR2 2,
TR2 3, TR2 4, TR2 6
- Murray, David-Anthony
URP 80
- Mussenbrock, Thomas
KTP 27, KTP 30,
KTP 34, KTP 36,
URP 57, URP 100,
URP 106, XF2 5
- N**
- Na, Sang-Chul URP 5
- Na Kyung, Hwang URP 83
- Nagai, Takatsugu SR1 6
- Nagaoka, Tatsuya SR3 4
- Naggary, Schabnam
KTP 34
- Naidis, George KTP 70
- Nakamura, Keiji URP 56
- Nakamura, Masahiro SR3 3
- Napartovich, Anatolii
HT2 6, URP 81
- Napartovich, Anatoly
HT2 8
- Nekhamkin, Leonid
URP 64
- Nelson, Caleb SR3 2
- Nguyen, Huong KTP 33
- Niemi, Kari HT3 5, TR3 1
- Nikitovic, Zeljka GT1 6,
KTP 110, URP 9
- Nikolic, M. URP 62
- Ning, Chuangang URP 16,
URP 17
- Nishihara, Munetake
KTP 101
- Nitz, D.E. URP 3
- Nixon, K. RR2 3
- Nixon, Kate TR2 3
- Nordheden, K. GT3 2
- Noro, Koji LW3 6
- Nourgostar, Cyrus
KTP 100
- Nozawa, Toshihisa HT2 3
- O**
- O'Connell, Deborah HT2 2,
KTP 69
- O'Farrell, David KTP 31,
XF2 3
- O'Hara, Neal XF2 3
- O'Neill, Colm KTP 69
- Oberrath, Jens XF2 6
- Oda, Akinori URP 96
- Ogawa, Daisuke WF1 6
- Oh, Byung Joo KTP 91
- Oh, Seung-Ju KTP 41
- Ohara, Kota FT3 6
- Ohba, Tomihito URP 59
- Ohnishi, Naofumi WF1 1
- Ohshima, N. URP 55
- Ohta, Takayuki GT3 4
- Okino, Akitoshi KTP 75
- Oksuz, Lutfi KTP 98,
KTP 100, XF2 8
- Ono, Kouich FT2 1,
KTP 97
- Ono, Kouichi SR3 4
- Opaitis, Dmitry KTP 96
- Orel, Ann WF2 2, WF2 4
- Overzet, Lawrence SR3 2,
URP 36, URP 46,
WF1 6, XF1 3
- P**
- Padron-Wells, G. URP 46
- Pai, David JT2 1
- Pal, Satyendra URP 14
- Pan, Y. JT3 5
- Papasouliotis, G.D. GT1 4
- Paravia, Mark LW3 1
- Paris, Sebastien GT2 2
- Park, Hye Sun URP 50
- Park, S.J. JT3 2
- Park, Sung-Jin JT3 3,
URP 98
- Park, Yeong-Shin KTP 5
- Park, Young Dong URP 84
- Parker, Jeffrey B. FT2 3
- Pasquiers, Stephane
KTP 22
- Pathak, B. GT3 2
- Paul, Kevin URP 108
- Pavlica, Dusan B. URP 42
- Pedrow, Patrick PW3 7,
URP 27, URP 41
- Pencheva, Mariana KTP 77
- Peters, Silke KTP 90
- Petrov, Alexey KTP 23
- Petrovic, Zoran GT1 6,
KTP 7, KTP 110,
RR2 3, URP 9, URP 12,
URP 42, URP 102
- Phelps, A.V. JT1 4,
KTP 10
- Pimenta, Maria Teresa
URP 52
- Pintassilgo, C.D. KTP 29
- Pitchford, L.C. JT1 4,
XF1 4
- Pitts, Marvin PW3 7,
URP 41
- Podder, Nirmol HT2 5
- Poggie, Jonathan JT2 3
- Pointu, Anne-Marie
URP 54
- Popelier, Lara LW1 3
- Popovic, Dusan URP 24
- Popovic, S. KTP 66,
URP 31, URP 32,
URP 62
- Postel, Christian KTP 22
- Potapkin, Boris KTP 88,
KTP 89, LW3 3, LW3 4,
SR3 7, TR3 3, URP 81
- Powers, Joseph URP 41
- Pribyl, Patrick HT2 4
- Pu, Yi-Kang PW1 4
- Puac, Nevena URP 42
- Puech, Vincent KTP 60,
KTP 85, RR1 1, URP 51
- Q**
- Qin, Shu GT1 4
- Qin, X. Victor URP 25
- Quintero, M.C. KTP 65
- R**
- Radjenovic, Branislav
KTP 21, URP 103,
URP 104
- Radmilovic-Radjenovic,
Marija KTP 21,
URP 102, URP 103,
URP 104
- Radovanov, Svetlana
GT1 4, GT1 6

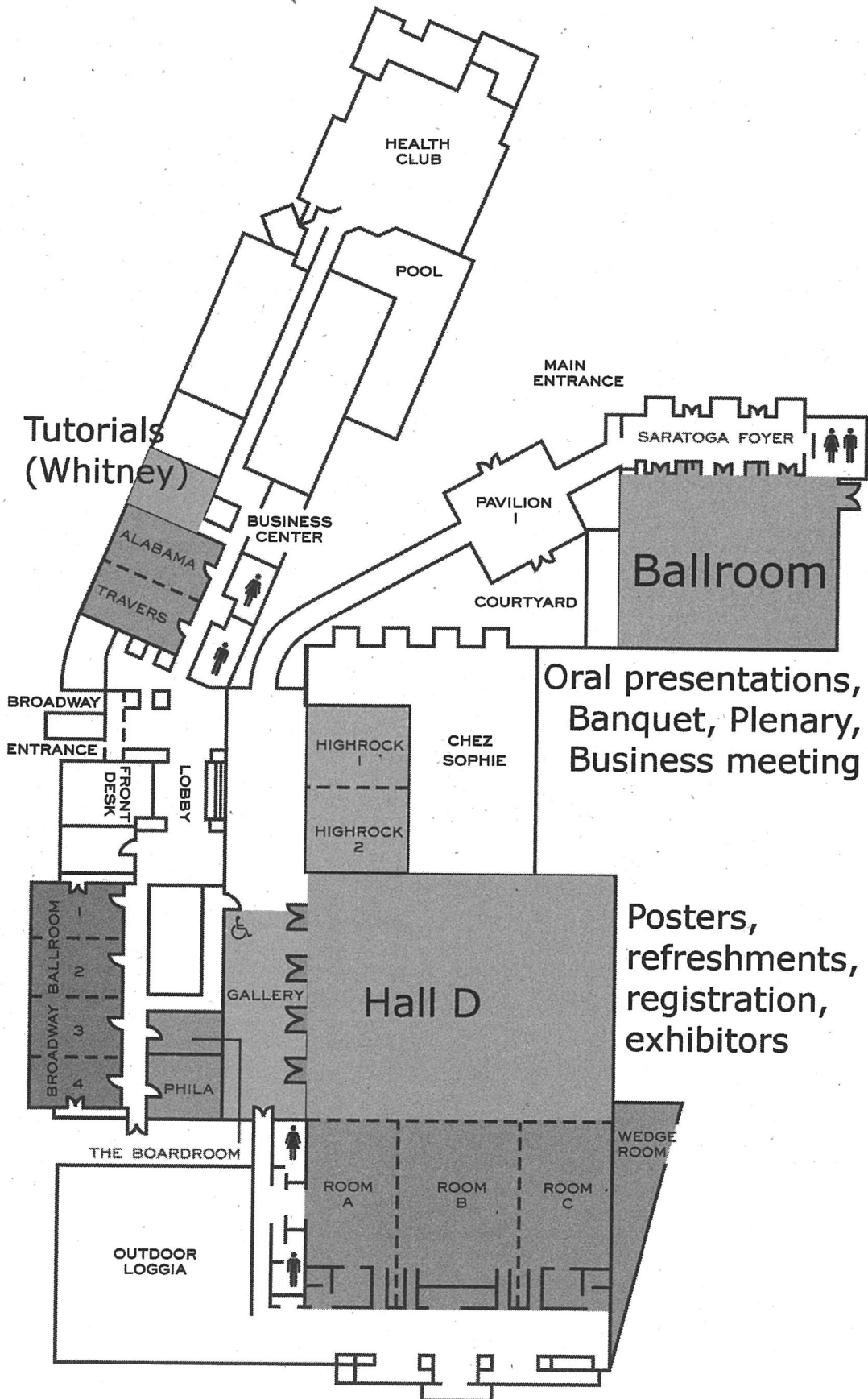
- Rahel, Jozef PW3 5
 Raimbault, Jean-Luc
 KTP 50, KTP 51
 Raitses, Yevgeny FT2 3,
 KTP 8, **KTP 99**
 Raj, Deven URP 61
 Raja, Laxminarayan CM 3,
 FT2 4, **FT2 5**, GT2 4
 Rajasekaran, Priyadarshini
 URP 100
 Rakhimov, A.T. TR1 4
 Rakhimova, T.V. TR1 4
 Raskovic, M. **URP 31**,
 URP 32
 Raspopovic, Zoran GT1 6
 Ravanat, Jean-Luc RR1 1
 Reinelt, Jens KTP 87,
 LW3 2
 Reuter, Stephan **HT3 5**,
TR3 1
 Rich, J. William KTP 101
 Rick, Kyle **URP 49**
 Riemann, Karl-Ulrich
JT1 1
 Roark, Christine M.
URP 108
 Robson, R.E. KTP 110
 Rodero, A. KTP 65
 Rossnagel, S.M. **RR1 5**
 Rousseau, Antoine KTP 72,
 URP 28
 Rubio, S.J. KTP 65
 Ruhmann, Cornelia
KTP 87, LW3 2
 Rulev, Oleg HT2 8
 Rusinov, Ilko Mitokov
 URP 39
- S**
 Saddoughi, Seyed TR3 3,
 URP 81
 Sadeghi, Nader KTP 72
 Saha, B.C. PW2 5
 Saha, Hari TR2 5
 Saikia, Bipul Kumar
KTP 104
 Saimi, Motohiro KTP 82
 Sakai, Osamu FT3 1
 Sakiyama, Yukinori SR1 5,
URP 43
 Samara, Vladimir URP 74
 Samolov, A. **URP 15**
 Samoylov, Igor KTP 23
 Santos Sousa, Joao
KTP 60, **RR1 1**
 Saraf, Iqbal SR3 2,
URP 36
 Sartor, Joe RR1 2
- Sasic, Olivera GT1 6
 Sato, Ayumu LW3 6
 Savic, Marija **URP 102**
 Sawada, Ikuo SR3 5
 Schaffer, L.C. WF2 3
 Scharf, Frank KTP 86
 Scharwitz, Christian
PW1 2
 Schlathoelter, Thomas
RR2 1
 Schmitt, Karen URP 80
 Schoeffler, Markus **RR2 2**
 Schroeder, Daniel FT3 4
 Schuengel, Edmund FT1 2,
 KTP 26, KTP 28,
URP 90
 Schulz, M. PW2 2, PW2 3,
 URP 18
 Schulz-von der Gathen,
 Volker FT3 4, TR3 1,
 XF1 2
 Schulze, Julian **FT1 2**,
 KTP 26, **KTP 28**,
 URP 90
 Schweigert, Irina **JT1 5**,
TR3 6
 Sekin, Makoto GT3 6
 Sekine, Makoto SR3 3,
 SR3 5
 Seleznev, Leonid HT2 8
 Semmler, Egmont KTP 25
 Seo, In Woo **KTP 91**
 Setsuhara, Yuichi **HT1 2**
 Shafroth, Stephen URP 26
 Shannon, S. **DM 1**, GT3 2,
 URP 97
 Sharp, David KTP 70
 Shcherbakov, Yuri **URP 64**
 Sheverev, Valery URP 38
 Shi, Shi HT2 5
 Shi, Zongqian JT2 5,
JT2 6, **KTP 74**
 Shiratani, Masaharu **TR3 5**,
 URP 33
 Shneider, Mikhail GT2 7,
 KTP 96, **PW3 3**
 Shoeb, Juline **TR1 3**
 Shouguo, Wang SR1 2
 Sigmond, Reidar URP 64
 Simon, Terry GT2 3,
 GT2 5, GT2 6
 Singh, Vikram GT1 4
 Sinitsyn, Dmitry HT2 8
 Skoro, Nikola **KTP 7**
 Slaughter, D. RR2 3,
 SR2 7
 Sloan, Mark SR1 3
 Sloneker, Kenneth **HT2 5**
- Smarandache, Florentin
KTP 111
 Smith, Andrew **KTP 54**
 Smith, David KTP 88,
 KTP 89, **KTP 92**,
 LW3 3
 Smithe, David URP 108
 Sobock, J. URP 3
 Sobolewski, Mark **GT3 5**
 Sommerer, Tim KTP 92
 Sommerer, Timothy HT2 6,
 KTP 88, KTP 89,
 LW3 3, SR3 7, TR3 3,
 URP 81
 Song, Jae Hyun KTP 43
 Song, Xiaochuan JT2 6
 Souza-Correa, Jorge
 URP 52
 Spranger, Tobias PW2 6
 Squina, Fabio URP 52
 Srivastava, Nimisha FT3 5
 Staack, David **KTP 71**
 Stalder, K.R. **TR3 2**
 Stalder, Kenneth JT2 2,
 URP 82
 Stamate, Eugen **JT1 6**
 Stapelmann, Katharina
SR1 4
 Stauffer, Allan **SR2 4**
 Stepaniuk, Vadim URP 38
 Steves, Simon **HT2 7**,
URP 35
 Stojanovic, Vladimir
 GT1 6, URP 9
 Stoltz, Peter URP 7,
 URP 107, URP 108
 Strelkova, Marina TR3 3,
 URP 81
 Sugai, Hideo URP 56
 Sullivan, J. RR2 3, SR2 7
 Sung, S.H. **JT3 2**
 Surko, C.M. **RR2 4**
 Sutton, Yvonne **KTP 70**
 Suzuki, Susumu **URP 22**,
 URP 39
 Sydorenko, Dmytro KTP 8,
 KTP 99
- T**
 Tachibana, Kunihide FT3 1
 Takahashi, Kazuki **URP 59**
 Takahashi, Takeshi FT2 1
 Takao, Yoshinori **FT2 1**,
KTP 97, SR3 4
 Takashima, Keisuke
 KTP 101, URP 77
 Takeda, Keigo GT3 6,
 SR3 3, SR3 5
- Takeda, Yuji KTP 83
 Takeuchi, Takuya **SR3 5**
 Takota, Naoki GT3 4
 Tani, Atsushi WF1 1
 Tardiveau, Pierre KTP 22
 Tatarova, Elena KTP 16,
 KTP 77, **KTP 78**
 Tattersall, W. **RR2 3**
 Tennyson, Jonathan
 KTP 39
 Thorsteinsson, Eythor Gisli
 LW1 4
 Tijerina, A. SR1 3
 Tinck, Stefan **TR1 5**
 Ting, Yuk-Hong URP 25
 Tomai, Takaaki **SR1 5**
 Tomita, Kentaro **FT3 6**
 Touzeau, Michel RR1 1
 Toyoda, H. **HT2 1**, SR3 5,
URP 55
 Trieschmann, Jan KTP 30
 Tsuda, Hirotaka **SR3 4**
 Tudorovskaia, Maria
 LW3 3
 Turner, Miles HT1 4,
 KTP 45, **KTP 67**,
 LW1 5, XF2 7
- U**
 Uchino, Kiichiro FT3 6
 Uetsuki, Tadao **KTP 81**,
KTP 82, **KTP 83**
 Uhrandt, Dirk KTP 6,
 KTP 76
 Umanski, Stanislav
 KTP 88
 Upadhyay, J. **URP 32**
 Uppaluri, Anusha JT2 2,
 PW3 4, URP 71,
 URP 82
 Upshaw, Adam **TR2 5**
 Urabe, Keiichiro **FT3 1**
- V**
 Vasilieva, A.N. TR1 4
 Veitzer, Seth URP 7,
 URP 107
 Verboncoeur, John
 KTP 109, URP 87
 Vidmar, Robert **JT2 2**,
PW3 4, TR3 2, **URP 71**,
URP 82
 Viehland, Larry PW2 7
 Viggiano, A.A. WF2 3
 Vincena, Steven HT2 4
 Virostko, Petr KTP 49
 Vuskovic, L. KTP 66,

- URP 2, URP 31,
URP 32, URP 62
- W**
Wais, Sabah I. KTP 15
Walton, S.G. **KTP 18**
Wang, Chuji **FT3 5**
Wang, Lijun **JT2 5, JT2 6,**
KTP 74
Wang, Liuhou **JT2 5**
Wang, Liuhuo **KTP 74**
Wang, Mingmei **TR1 2**
Wang, Ying **KTP 109,**
URP 87
Ward, Arlen **PW1 3,**
RR1 2, URP 48
Ward, Pat **KTP 33**
Waskoenig, Jochen **FT1 4,**
HT3 5
Watanabe, Masato **KTP 75**
Wemlinger, Erik **PW3 7**
Wendt, A.E. **PW1 6,**
URP 58
Wendt, Amy **URP 25**
Wendt, Martin **KTP 90**
- Westermeier, Michael
KTP 87, **LW3 2**
Whang, Ki-Woong **KTP 43,**
KTP 91
White, R.D. **KTP 110**
White, Ronald **URP 12**
Williamson, J.M. **URP 66,**
URP 73
Winter, Joerg **FT3 4,**
XF1 2
Wise, George **VR 2**
Wood, M.P. **URP 3**
Wright, Scott **JT3 1**
Wright, Timothy **PW2 7**
Wunderlich, Joachim **SR1 4**
- X**
Xia, Guangqing **KTP 59,**
KTP 94
Xian, Y. **JT3 5**
Xianghong, Jia **SR1 2**
Xiong, Q. **JT3 5**
Xiong, Z. **JT3 5**
Xiong, Zhongmin **PW3 2**
Xu, Lin **FT1 5**
- Xue, Jun **FT3 3**
- Y**
Yagisawa, Takashi **URP 30,**
XF2 2
Yagyu, Yoshihito **URP 44**
Yamada, Junzaburo **KTP 75**
Yamada, Yasuyuki **URP 33**
Yamakawa, Koji **GT3 4**
Yamazawa, Yohei **GT3 3,**
XF2 5
Yang, Dingge **JT2 5,**
KTP 74
Yang, Haipeng **HT2 1**
Yang, Wonkyun **URP 94**
Yang, Yang **XF2 1**
Yano, Hidetoshi **KTP 83**
Yasar, Tug **2W 1**
Yegorenkov, Vladimir
KTP 2, **KTP 20**
Yip, Chi-Shung **JT1 3,**
URP 91
Yonesu, Akira **URP 44**
Yoon, Je Kwon **JT3 3**
You, ShaoDon **LW1 6**
- Young, J.A. **RR2 4**
Young-Hoon, Song **URP 83**
Yu, Zeng-Qi **PW1 3,**
RR1 2
- Z**
Zahoranova, Anna **PW3 5**
Zaidi, Sohail **GT2 7**
Zaitsevskii, Alexander
KTP 88
Zaitsevskii, Andrei **KTP 89**
Zatsarinny, Oleg **PW1 5,**
SR2 2, SR2 5
Zekic, Andriana **URP 24**
Zhang, Qi **URP 56**
Zhang, Zhibo **XF1 5**
Zhao, Jianping **HT2 3**
Zhou, Chuandong
URP 107
Zhu, Qiushi **KTP 75**
Ziegler, Dennis **KTP 30,**
KTP 34, **XF2 5**
Zou, C. **JT3 5**
Zou, F. **JT3 5**
Zuzeek, Yvette **URP 77**
Zyryanov, S.M. **TR1 4**

NOTES

[The text in this section is extremely faint and illegible. It appears to be a list of notes or a table with multiple columns, but the specific content cannot be discerned.]

Saratoga City Center



16:00 THURSDAY AFTERNOON
22 OCTOBER 2009

URP **Poster Session II (4:00-6:00PM)**
Hall D, Saratoga Springs City Center

19:00 THURSDAY EVENING
22 OCTOBER 2009

VR **Banquet**
George Wise
Ballroom 1-2-3, Saratoga Hilton

8:00 FRIDAY MORNING
23 OCTOBER 2009

WF1 **Plasmas and Liquids**
Ballroom 1, Saratoga Hilton

WF2 **Electron Molecule Collisions**
Timothy Gay, Ann Orel
Ballroom 2, Saratoga Hilton

10:00 FRIDAY MORNING
23 OCTOBER 2009

XF1 **Microplasmas**
J. Gary Eden
Ballroom 1, Saratoga Hilton

XF2 **Capacitively-Coupled Plasmas II**
Ballroom 2, Saratoga Hilton

On the Cover: Intense plasma waves are locally excited at the $\omega = \omega_p$ resonance condition near a slot-pair antenna in the RLSA microwave Surface Wave Plasma. Results courtesy of Ron Bravenec, Tokyo Electron America. Simulation performed on a 32-processor version of VORPALTM.

Epitome of the 62nd Gaseous Electronics Conference of the American Physical Society

**7:45 MONDAY MORNING
19 OCTOBER 2009**

AM Kinetics Workshop: Opening Session, Role of Electron Kinetics, Swarms
Mark Kushner, Toshiaki Makabe, Sasa Dujko
Ballroom 1, Saratoga Hilton

**10:00 MONDAY MORNING
19 OCTOBER 2009**

BM Kinetics Workshop: General Kinetic Models
Vladimir Kolobov, Igor Kaganovich, Annemie Bogaerts, Ralf Peter Brinkmann
Ballroom 1, Saratoga Hilton

**13:30 MONDAY AFTERNOON
19 OCTOBER 2009**

CM Kinetics Workshop: Data for Modeling and Modeling Example
Stephen Buckman, Gorur Govinda Raju, Laxminarayan Raja, Detlef Loffhagen
Ballroom 1, Saratoga Hilton

**16:00 MONDAY AFTERNOON
19 OCTOBER 2009**

DM Kinetics Workshop: Electron Kinetics
Steven Shannon, Chao Li, Scott Baalrud
Ballroom 1, Saratoga Hilton

**18:00 MONDAY EVENING
19 OCTOBER 2009**

EM Reception
Gallery, Saratoga Hilton

**8:00 TUESDAY MORNING
20 OCTOBER 2009**

FT1 Capacitively-Coupled Plasmas I
Uwe Czarnetzki
Ballroom 1, Saratoga Hilton

FT2 Plasma Thrusters
Laxminarayan Raja
Ballroom 2, Saratoga Hilton

FT3 Laser Based Diagnostics at High Pressure
Ballroom 3, Saratoga Hilton

**10:00 TUESDAY MORNING
20 OCTOBER 2009**

GT1 Plasma Aided Implantation
Michael A. Lieberman, Mark Kushner
Ballroom 1, Saratoga Hilton

GT2 Actuators and Flow Control
Ballroom 2, Saratoga Hilton

GT3 Low Pressure Plasma Diagnostics
ChinWook Chung
Ballroom 3, Saratoga Hilton

**13:30 TUESDAY AFTERNOON
20 OCTOBER 2009**

HT1 Inductively Coupled Plasmas
Gerjan Hagelaar, Yuichi Setsuhara
Ballroom 1, Saratoga Hilton

HT2 DC, Pulsed, RF and Microwave Glows
Ballroom 2, Saratoga Hilton

HT3 Optical Diagnostics I
Akihiro Kono, Peter Hakel
Ballroom 3, Saratoga Hilton

**16:00 TUESDAY AFTERNOON
20 OCTOBER 2009**

JT1 Sheaths
Ballroom 1, Saratoga Hilton

JT2 High Pressure Cold Plasmas and Arcs
Ballroom 2, Saratoga Hilton

JT3 Microplasmas and Jets
Ballroom 3, Saratoga Hilton

**19:00 TUESDAY EVENING
20 OCTOBER 2009**

KTP Poster Session I (7:00-9:00PM)
Hall D, Saratoga Springs City Center

**8:00 WEDNESDAY MORNING
21 OCTOBER 2009**

LW1 Dusty and Negative Ion Plasmas
Ballroom 1, Saratoga Hilton

LW2 Atomic Data for Modeling
Michael Brunger, Paul Johnson, Christopher Fontes
Ballroom 2, Saratoga Hilton

LW3 Lamps
Ballroom 3, Saratoga Hilton

**10:00 WEDNESDAY MORNING
21 OCTOBER 2009**

MW GEC Foundation Talk
David Graves
Ballroom 1-2-3, Saratoga Hilton

**11:00 WEDNESDAY MORNING
21 OCTOBER 2009**

NW Business Meeting
Ballroom 1-2-3, Saratoga Hilton

**12:00 WEDNESDAY NOON
21 OCTOBER 2009**

2W Intellectual Property Tutorial
Tug Yasar
Whitney, Saratoga Hilton

**13:30 WEDNESDAY AFTERNOON
21 OCTOBER 2009**

PW1 Optical Diagnostics II
Yi-Kang Pu
Ballroom 1, Saratoga Hilton

PW2 Heavy Particle Collisions with Atoms and Molecules
Allison Harris
Ballroom 2, Saratoga Hilton

PW3 Laser Produced Plasmas Induced Breakdown and Applications of High Pressure Plasmas
Todd Dimire
Ballroom 3, Saratoga Hilton

**19:00 WEDNESDAY EVENING
21 OCTOBER 2009**

QW Joint GEC/CNSE Session following CNSE Visit
Uwe Kortshagen, John Arnold, Magnus Bergkvist, J. Gary Eden, Edward M. Cupoli, Rikizo Hatakeyama, Timothy J. Dalton
NFS Auditorium, College of Nanoscale Science and Engineering

**8:00 THURSDAY MORNING
22 OCTOBER 2009**

RR1 Biological and Emerging Applications of Plasma I
S.M. Rosnagel
Ballroom 1, Saratoga Hilton

RR2 Charged Particle Molecule Collisions
Thomas Schlathoelter, Markus Schoeffler
Ballroom 2, Saratoga Hilton

**10:00 THURSDAY MORNING
22 OCTOBER 2009**

SR1 Biological and Emerging Applications II
Michael Kong
Ballroom 1, Saratoga Hilton

SR2 Electron and Positron Collisions with Atoms
Danica Cvejanovic
Ballroom 2, Saratoga Hilton

SR3 Plasma-Surface Interactions
Matthew Goeckner
Ballroom 3, Saratoga Hilton

**12:00 THURSDAY NOON
22 OCTOBER 2009**

3R VORPAL Tutorial
Ed Case
Whitney, Saratoga Hilton

**13:30 THURSDAY AFTERNOON
22 OCTOBER 2009**

TR1 Materials Processing
Jane P. Chang, Song-Yun Kang
Ballroom 1, Saratoga Hilton

TR2 Electron and Photon Interactions with Atoms and Molecules
Bruno deHarak
Ballroom 2, Saratoga Hilton

TR3 Plasma Chemistry
Biswa Ganguly, Masaharu Shiratani
Ballroom 3, Saratoga Hilton



0003-0503(200910)54:12;1-K